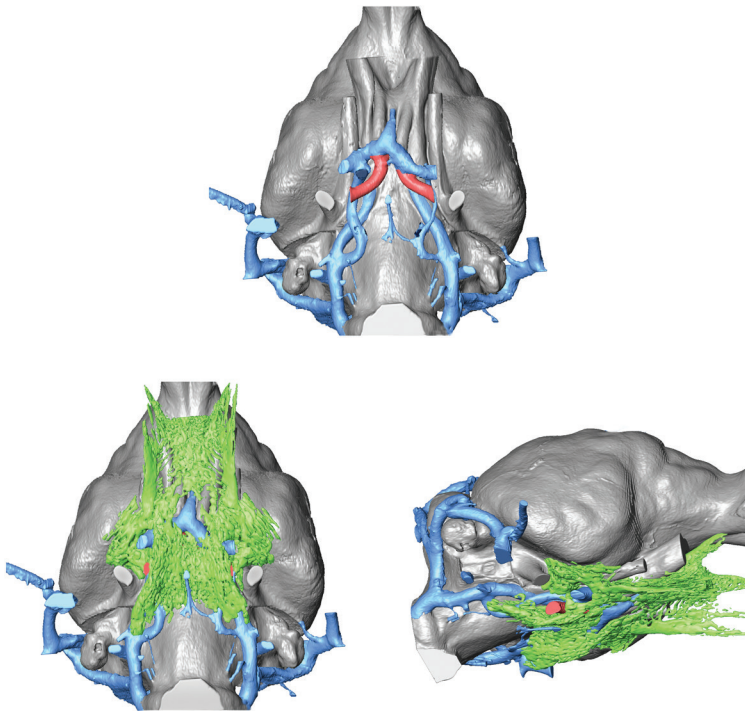


---

# TRANSVERSE CANAL FORAMEN AND PERICAROTID VENOUS NETWORK IN METATHERIA AND OTHER MAMMALS

---

R.D.E. MACPHEE, C. GAILLARD, A.M. FORASIEPI,  
AND R.B. SULSER



# TRANSVERSE CANAL FORAMEN AND PERICAROTID VENOUS NETWORK IN METATHERIA AND OTHER MAMMALS

ROSS D.E. MACPHEE

*Division of Vertebrate Zoology, Department of Mammalogy,  
American Museum of Natural History*

CHARLÈNE GAILLARD

*Instituto Argentino de Nivología, Glaciología, y Ciencias Ambientales,  
CCT-CONICET, Mendoza, Argentina*

ANALÍA M. FORASIEPI

*Instituto Argentino de Nivología, Glaciología, y Ciencias Ambientales,  
CCT-CONICET, Mendoza, Argentina*

R. BENJAMIN SULSER

*Division of Vertebrate Zoology, Department of Mammalogy,  
American Museum of Natural History;  
Division of Evolutionary Ecology, Institute of Ecology and Evolution,  
University of Bern, Bern, Switzerland*

BULLETIN OF THE AMERICAN MUSEUM OF NATURAL HISTORY

Number 462, 122 pp., 42 figures, 5 tables

Issued June 21, 2023

## CONTENTS

Abstract.....	3
Introduction.....	4
Materials and Methods.....	5
Specimens and Comparative Set.....	5
Illustrations.....	6
Techniques of Preparation.....	7
Anatomical Structures.....	9
Anatomical Acronyms Used in Text.....	11
Institutional Abbreviations.....	11
Anatomy of the Pericarotid Venous Network.....	12
Mesocranial Osteology and Context.....	12
Network Components.....	13
Homologies of Mesocranial Distributaries.....	21
Mesocranial Pattern Features.....	24
Junctions and Other Connections.....	24
Patterns.....	24
Systematic Description of Pericarotid Venous Networks in Extant Therians.....	26
Marsupialia.....	26
Didelphimorphia.....	26
Paucituberculata.....	32
Microbiotheria.....	33
Diprotodontia.....	35
Dasyuromorphia.....	41
Peramelemorphia.....	53
Notoryctemorphia.....	55
Placentalia.....	59
Rodentia.....	59
Primates.....	63
Macroscelidea.....	63
Other Placentals.....	63
Reconstructing Pericarotid Venous Networks in Extinct Sparassodontan Metatherians.....	65
<i>Sipalocyon</i> (Hathliacynidae).....	65
<i>Prothylacynus</i> (Borhyaenoidea).....	69
Discussion.....	71
Morphological Summary and Conclusions.....	71
Character Analysis and Phylogeny.....	77
Phylogenetic Implications.....	93
Functional Considerations.....	101
Acknowledgments.....	107
References.....	108
Appendix 1. Components of the Pericarotid Venous Network and Related Structures.....	115

## ABSTRACT

Although few nondental features of the osteocranium consistently discriminate marsupials from placentals, the transverse canal foramen (TCF) has been repeatedly offered as a potential synapomorphy of crown-group Marsupialia and their closest allies. To explore this contention appropriately, the TCF needs to be evaluated in relation to the morphofunctional complex of which it is a part, something never previously undertaken in a systematic fashion. This complex, here defined as the pericarotid venous network (PCVN), is assessed using osteological, histological, and ontogenetic information.

Although the TCF is usually thought of as a marsupial attribute, some living placentals also express it. What do these clades actually share in regard to this feature, and how do they differ? Our leading hypothesis is that the chief components of the PCVN begin development in the same way in both Marsupialia and Placentalia, but they follow different ontogenetic trajectories in terms of persistence, size, and connections with other elements of the cephalic venous vasculature. Similarities include shared presence of specific emissary and emissarylike veins in the mesocranial region that connect part of the endocranial dural vasculature (cavernous sinus or CS) to the systemic circulation (external and internal jugular veins plus the cerebrospinal venous system). In marsupials the principal pericarotid vessels are the transverse canal vein (TCV) and internal carotid vein (ICV). These veins almost always attain relatively large size during marsupial ontogeny. By contrast, in most placentals their apparent homologs (among others, emissary vein of the sphenoidal foramen and internal carotid venous plexus) evidently slow down or terminate their growth relatively early, and for this reason they play only a proportionally minor role in cephalic drainage in later life. In both clades, these vessels (informally grouped with others in the same region as pericarotid mesocranial distributaries, or PMDs) play a variable role in draining the CS in conjunction with the much larger petrosal sinuses.

A pneumatic space within the basisphenoid—called the sphenoid sinus in placentals, transverse basisphenoid sinus (TBS) in marsupials—communicates with PCVN vasculature and should be considered an integral part of the network. The TBS contains red marrow tissues that are active centers of extramedullary hematopoiesis in young stages of some species, although how widespread this function may be in marsupial clades is not yet known.

Previous explorations of the marsupial PCVN have been largely limited to determining whether, in any given taxon, a continuous passageway linking the right and left TCFs could be demonstrated running through the basisphenoid (“intramural” condition). It has long been known that a number of species apparently lack this particular passageway, and that the TCFs instead open into the braincase (“endocranial” condition). Puzzlingly, some species appear to have both passageways, others one or the other, and a few none at all, thus inviting questions about their equivalency and the circumstances under which the CS is actually drained by the TCV.

Morphologically, these uncertainties can be resolved by viewing the full TCV as a tripartite entity, consisting of a trunk and rostral and caudal branches. The trunk, or the part that leaves the TCF for the external jugular system, receives the rostral and caudal branches, if both are present, within the body of the basisphenoid. The rostral or intramural branch has little or no direct communication with the endocranium in most investigated species. By contrast, the caudal or endocranial branch is an ordinary emissarium, in that it connects a part of the endocranial system of dural veins with the extracranial circulation.

Determining branch routing alone does not adequately capture the scale of morphological variety and function encountered in marsupial PCVN organization. We distinguish five patterns of association between TCVs and other PCVN components. These patterns, based on both histological and osteological criteria, are defined as follows: **(1) Simple:** only rostral passageway present, caudal passageway absent or reduced to a thread; rostral branch veins form midline confluence within TBS in advance of hypophysis; minimal interaction with CS and its distributaries; rostral and caudal

portions of TBS discontinuous. (2) **Complex**: mostly as in (1), except both rostral and caudal branches present and functional; caudal branches communicate with CS/ICV and do not form a confluence; TBS more extensive. (3) **Compound**: mostly as in (2), except TBS greatly expanded, incorporating most of rostral branch canals, which are correspondingly short. (4) **Hybrid**: differs from others in that only the pathways for enlarged caudal branches are significant; they originate from the CS/ICV caudal to the position of the hypophysis; rostral branches absent or highly reduced. (5) **Indeterminate**: transverse foramina, canals, and branches absent or unidentifiable as such, presumably due to vascular involution early in ontogeny.

In light of TCV composition, the trunk of the TCV can be considered a mixed-origin vein, maximally receiving both a quasisystemic or emissarylike vessel (rostral branch) that does not originate from endocranial dural vessels, and a true emissarial vessel (caudal branch) that does. Some extant geomyoid rodents and strepsirrhine primates exhibit enlarged venous structures in the mesocranial region; these are briefly surveyed for comparative purposes, but resemblances to conditions in marsupials are superficial and unmistakably interpretable as convergences. Members of the extinct marsupial sister group Sparassodonta sometimes lack detectable TCFs, as do other non-marsupial metatherians in the fossil record. Evidence for the transverse canal and other PCVN components in other therians is briefly outlined.

In summary, the development of mesocranial vasculature as outlined in this paper is hypothesized to be basal for therians, but Marsupialia and Placentalia radically differ in the end expression of PMDs in the adult stage. In prenatal stages of both clades, initial differentiation of these distributaries is presumably similar, but, compared to marsupials, in almost all placental groups these vessels are retained in an undeveloped or neotenic state. By contrast, enhanced expression of the TCV trunk and its branches seems to be a genuine novelty characterizing Marsupialia, although one probably present in some other metatherian groups. Accordingly, the transverse foramen, canal, and related features are probably best regarded as an innovation occurring in the marsupial stem, not a synapomorphy of the crown group as previously suggested by some authors.

There is no overstatement in Mall's picturesque comment that the 'history of the arteries is simple when compared with the gyrations the veins undergo.'

—Dorcas H. Padget (1957: 81)

## INTRODUCTION

Few discrete features of the therian osteocranium consistently distinguish marsupials from placentals. Ones that do may be important systematically, especially if they are apparent in fossil material and therefore available for character definition and analysis. The best-known example of an infraclass-level distinction of this kind is the separate optic foramen, found on almost all placental osteocrania but lacking in marsupials because the optic nerve passes instead through the sphenoorbital fissure (De Beer, 1937). Less regarded, but also sharply restricted in distribu-

tion, is the transverse canal foramen, which has been proposed as a potential synapomorphy of crown-group Marsupialia (Sánchez-Villagra and Wible, 2002; Horovitz and Sánchez-Villagra, 2003; see also Aplin, 1990). However, apart from presence/absence data collected on dry skulls to complete character matrices, the foramen and the vessel it conducts (trunk of the transverse canal vein and its chief branches) remain underinvestigated in terms of ontogeny, homology, and function. This mirrors the general paucity of information on cranial venation in marsupials (but see, as basic references, Cords, 1915; Shindo, 1915; Dom et al., 1970; Archer, 1976; Wible, 1984; Aplin, 1990).

In this survey we show that the complex of veins that pass through the mesocranial region should be considered a specialized vascular suite, here identified as the pericarotid venous network. This network is responsible not only for helping to

drain endocranial structures through linkages with dural vasculature, but also for transporting new blood cells from extramedullary hematopoietic tissues located in basicranial pneumatic sinuses. It may have other functions as well, but at present information concerning these alternative possibilities is too limited for determination.

The seemingly sharp contrasts between the major therian subclades for features of the pericarotid network may be related to the effects of relative growth rather than absolute differences. We hypothesize that, in almost all placentals, potential equivalents of the marsupial transverse canal vein and internal carotid vein are present but cease to develop beyond a certain point, thus appearing to be vestigial or otherwise less important in the adult. The very few instances of hypertrophy or additional functions related to these vessels in extant placentals are obviously in a different category, but apart from their morphological interest they surely represent independent innovations, developed on an ancient ontogenetic substrate within Theria.

To analyze the development and expression of the marsupial pericarotid network we provide original observations on a range of New World and Sahulian taxa representing the seven extant marsupial orders (*Didelphimorphia*, *Paucituberculata*, *Microbiotheria*, *Peramelemorphia*, *Dasyuromorphia*, *Diprotodontia*, and *Notooryctemorphia*), using combinations of stained sections, tomography, and osteology (table 1). *Yalkaparidontia*, an eighth order (Beck et al., 2022), is wholly extinct. Its pericarotid circulation has not yet been investigated using modern methods, but Beck et al. (2014) report features consistent with the presence of at least some PCVN features.

Representatives of the extinct nonmarsupial metatherian order *Sparassodonta* are also briefly reviewed, as are taxa from three placental orders (*Rodentia*, *Primates*, and *Macroscelidea*), in order to provide a broader comparative perspective for exploration of some issues in homology determination and character analysis. Monotremes are known to

possess some aspects of pericarotid venation, as are some now-extinct nontherian mammals according to osteological indicators described in the literature. In the Discussion we evaluate possible functional attributes of the pericarotid network, as well as point to several unsettled questions concerning the network's origin and configuration in different metatherian taxa. The transverse canal foramen is not unique to *Marsupialia* even within *Metatheria*, but other features of mesocranial circulation, described here for the first time, are of great interest for their bearing on cephalic vascular organization in this clade.

## MATERIALS AND METHODS

### SPECIMENS AND COMPARATIVE SET

Original information on mesocranial vasculature presented in this paper comes chiefly from sectioned and stained perinatal stages of extant taxa (referenced as “whole specimens” in the text and tables). Other sources of information are based on dry skulls and CT segmental data, including virtual endocast reconstructions (isosurfaces) of selected taxa (see Illustrations). These specimens constitute our comparative set (table 1) and form the basis for most of the observations reported in the systematic descriptions. We gratefully recognize investigators and individuals at institutions who made scans of certain specimens critical for this study freely available (see Acknowledgments).

Although there was considerable interest in cranial development in marsupials during the classical period of comparative embryology during the late 19th and early 20th centuries (see Matthes, 1921; De Beer, 1937), very little of this literature concerns vascular development and still less includes observations on the vessels of chief interest here. Placentalia is not a focus of this paper, as few species possess well-developed pericarotid vasculature. However, a few examples of those that do are showcased to illustrate convergent aspects of

mesocranial organization in this major clade. Nor are fossil taxa given much attention, apart from evaluations of conditions in recently extinct *Thylacinus* and two Miocene sparassodontans, *Sipalocyon* and *Prothylacynus*. This was intentional: before the PCVN can play much of a role in systematic interpretation of fossil metatherians, its anatomy and physiological correlates need to be better understood in extant taxa. This paper is meant as a beginning in that direction. Details for all specimens used for original descriptions may be found in tables 1 and 2.

Species designations are those provided by the institutions holding the specimens unless there are revisionary changes that are simply nomenclatural. In the case of specimens previously assigned to *Macropus eugenii* and *M. robustus*, we follow Celik et al. (2019) in assigning them, respectively, to *Notamacropus eugenii* and *Osphranter robustus*. The older literature consulted for this study does not generally provide sufficient information to allow revision of species-level nomenclature, and for the most part the names used in those papers concerned have been retained. In the case of sectioned whole specimens, measurements and relative developmental age are given, if known, along with brief remarks on the degree of basicranial ossification. Dry skulls and fossils that are obviously postperinatal are designated as juvenile or adult based on general impressions, including tooth eruption status when available (see Anders et al. [2011], Díaz and Flores [2008], Cook et al. [2021] for discussion of issues related to ontogenetic staging of marsupial specimens). The order in which taxa are presented in the systematic descriptions does not adhere to any particular hypothesis of relationships, although our higher-level systematic terminology generally follows Beck et al. (2022). Our understanding of phylogenetic relationships among major clades of marsupials has greatly improved in recent years as new information (particularly molecular information) has become readily available (Eldridge

et al., 2019; Beck et al., 2022). This includes recent proposals for reorganizing Phalangeriformes (restricted to Petauroidea + Phalangeridae + Burramyidae) and formally recognizing other higher-level clades, including Agreodontia (Dasyuromorphia + Peramelemorphia + Notoryctemorphia) and a reconstituted Australidelphia (Microbiotheria + Agreodontia + Diprotodontia). As this is primarily a morphological study, systematic controversies are mentioned where relevant to character analysis but are not our primary focus.

When available, other relevant data (such as row and position number of stained sections on slides) are provided in figure legends. Azan is the recorded histological stain for the MPIH and ZIUT specimens described here. For additional information on this material, see MacPhee (1981) and Sánchez-Villagra and Forasiepi (2017). Many relevant osteological features of Sahulian taxa not covered here are illustrated in papers by Archer (1976), Beck et al. (2022), and references cited therein.

#### ILLUSTRATIONS

In the figures, anatomical identifications concentrate on features associated with the pericardotid network, but certain additional structures are recurrently labelled in order to provide context and orientation. The italicized word *to* before an acronym means “in this direction,” and it is used to locate the general position of features hidden by other structures in a given view. In the main text, first occurrences of key anatomical terms are highlighted in **bold**. Frequently cited terms are denoted by acronyms (see Anatomical Acronyms Used in Text) after first use, and where appropriate are given additional morphological treatment (see appendix 1).

Detailed endocranial reconstructions (*Didelphis*, fig. 4, *Caenolestes*, fig. 13; *Dromiciops*, fig. 15; *Trichosurus*, fig. 21; *Thylacinus*, fig. 30; *Sipalocyon*, fig. 38; *Prothylacynus*, fig. 40) are intended to provide comprehensive visualizations of the mesocranial area in representatives of selected

major taxa, but a few conventions need mentioning. There are usually five panels to each reconstruction. In part A, the endocranial surface of the braincase is reproduced in ventral perspective, with certain vascular trackways indicated. In panels B and C, the transverse basisphenoid sinus is shown as a digital extraction laid beneath the brain endocast, in order to reveal trabeculation, canaliculi, and the sinus's relations with other components. The subject matter of panel D varies from figure to figure, but usually illustrates points not adequately depicted in the other parts. In panel E the external surface of the intact skull is usually rendered in ventral view as an aid to visualizing placement and orientation of relevant structures. In making reconstructions we adopted the convention of rendering sulci and similar osteological features as tubes, so that they better resembled actual channels. In some cases the complexity of interconnected features produced visually misleading results, and for this reason additional interpretation is also presented (e.g., *Thylacinus*, fig. 30F).

In addition to full reconstructions, segment series in rostrocaudal order can be very useful for interpretation and are utilized throughout (*Didelphis*, fig. 5; *Monodelphis*, fig. 12; *Caenolestes*, fig. 14; *Dromiciops*, fig. 17; *Osphranter*, fig. 20; *Trichosurus*, fig. 22; *Vombatus*, fig. 25; *Dasyurus*, fig. 27; *Thylacinus*, fig. 31; *Notoryctes*, fig. 35; *Sipalocyon*, fig. 39; *Prothylacynus*, fig. 41). Apart from CT files hosted by other facilities, surface meshes of the endocasts of specimens scanned for this paper are available for download (see Acknowledgments and online supplement: <https://doi.org/10.5531/sd.sp.58>).

**COLOR CONVENTIONS.** In general, indicia directly associated with selected veins are colored blue (e.g., foramina, canals, sulci). Red is reserved for the carotid canal to differentiate it from other structures, but we emphasize that it contains two vascular entities, the internal carotid artery as well as the internal carotid vein. Carotid and transverse canals are always shown as extracted and superimposed on the endocast in the same way as the transverse basisphenoid sinus (colored green). Other venous trackways

are partially reconstructed as needed and where indicia permit. As far as we are aware, our virtual reconstructions of the transverse basisphenoid sinus are the first detailed depictions of the actual conformation of this feature in metatherians.

#### TECHNIQUES OF PREPARATION

Source materials useful for studying cephalic venation are highly disparate, and for this reason a few comments on preparation methods are warranted. In the past, a hair probe was often employed to ascertain, by proxy, whether the transverse canal vein passed from side to side through the basisphenoid or went directly into the endocranium. Blind probing, however, can be hampered by various kinds of impediments along the way, which may lead to incorrect conclusions about the presence or absence of canal connectivity. X-ray venograms, ink injections, and corrosion casts have also been extensively used to visualize vascular structures. Single-viewpoint X-ray venograms using an injected contrast medium are simple to acquire but are of limited value for the present purposes because of inevitable overlapping of vessels at different levels in the plane of observation. Ink injection works as long as there is good control over seepage, but as the result is not readily dissectible it is suitable only for young or cleared specimens. A better alternative is the corrosion cast, which can be produced in a variety of ways (Reinhard et al., 1962; Bugge, 1974; Archer, 1976; Verli et al., 2007; Cornillie et al., 2019), most commonly by injecting vessels with latex or a similarly resistant material such as methyl methacrylate and hardening the result. All surrounding tissues, including bone if desired, are typically macerated or chemically digested to reveal the vascular tree. The infilling, unaffected by this treatment, replicates the network at natural scale in three dimensions. However, if the skull is fully digested, bony landmarks such as foramina will be lost, which may lead to misidentifications. A disadvantage of all such methods is that, depending on the vis-

TABLE 1

## Specimens Referenced in Systematic Descriptions

See Material and Methods. Material: **DS**, dry skull; **Fo**, fossil; **Wh**, whole specimen. Age Class: **A**, adult; **F**, fetus; **J**, juvenile; **P**, perinatal. Data Sources: **D**, digital; **H**, histological; **O**, osteological. For digital parameters on scanned specimens, see table 2.

Order	Family	Genus	Species	Institution	ID Number	Material	Age Class	Data Sources	Figure Reference
Didelphimorphia	Didelphidae	<i>Didelphis</i>	<i>virginiana</i>	AMNH	M-217731	DS	A	O	2
	Didelphidae	<i>Didelphis</i>	<i>virginiana</i>	TMM	M-2517	DS	A	D	4, 5
	Didelphidae	<i>Philander</i>	<i>opossum</i>	AMNH	M-266385	DS	A	O	6
	Didelphidae	<i>Philander</i>	sp.	ZIUT	HL 32 mm	Wh	P	H	7
	Didelphidae	<i>Caluromys</i>	<i>derbianus</i>	AMNH	M-18910	DS	A	O	8
	Didelphidae	<i>Caluromys</i>	<i>derbianus</i>	AMNH	M-164491	DS	A	O	
	Didelphidae	<i>Caluromys</i>	<i>derbianus</i>	AMNH	M18911	DS	A	O	
	Didelphidae	<i>Caluromys</i>	sp.	AMNH	M-184599	DS	A	O	8
	Didelphidae	<i>Caluromys</i>	sp.	ZIUT	PND 77	Wh	P	H	9
	Didelphidae	<i>Monodelphis</i>	<i>domestica</i>	AMNH	M-133247	DS	A	O	10
	Didelphidae	<i>Monodelphis</i>	<i>domestica</i>	ZIUT	PND 12, HL 8.5 mm	Wh	P	H	11
	Didelphidae	<i>Monodelphis</i>	<i>domestica</i>	NMB	c. III.777	DS	A	D	12
Paucituberculata	Caenolestidae	<i>Caenolestes</i>	sp.	IANIGLA	uncat.	DS	A	D	13, 14
	Caenolestidae	<i>Caenolestes</i>	<i>convelatus</i>	AMNH	M-64457	DS	A	O	
	Caenolestidae	<i>Caenolestes</i>	<i>fuliginosus</i>	AMNH	M-64455	DS	A	O	
Microbiotheria	Microbiotheriidae	<i>Dromiciops</i>	<i>gliroides</i>	MACN	Ma-23607	DS	A	D	15, 17
	Microbiotheriidae	<i>Dromiciops</i>	<i>gliroides</i>	ZIUT	HL 19 mm	Wh	J	H	16
Diprotodontia	Macropodidae	<i>Notamacropus</i>	<i>eugenii</i>	AMNH	197003	DS	J	O	18
	Macropodidae	<i>Notamacropus</i>	<i>eugenii</i>	ZIUT	HL 29	Wh	P	H	19
	Macropodidae	<i>Osphranter</i>	<i>robustus</i>	AMNH	M-80171	DS	J	D, O	18, 20
	Phalangeridae	<i>Trichosurus</i>	<i>vulpecula</i>	TMM	M-849	DS	A	D	21, 22
	Phalangeridae	<i>Distoechurus</i>	<i>pennatus</i>	AMNH	M-105938	DS	A	O	23
	Vombatidae	<i>Vombatus</i>	<i>ursinus</i>	AMNH	M-176103	DS	A	O	24
	Vombatidae	<i>Vombatus</i>	<i>ursinus</i>	TMM	M-2953	DS	A	D	25
	Dasyuromorphia	Dasyuridae	<i>Dasyurus</i>	<i>hallucatus</i>	AMNH	M-16033	DS	A	O
Dasyuridae		<i>Dasyurus</i>	<i>hallucatus</i>	TMM	M-6921	DS	A	D	27
Dasyuridae		<i>Sarcophilus</i>	<i>lanarius</i>	AMNH	M-65673	DS	A	O	28
Thylacinidae		<i>Thylacinus</i>	<i>cynocephalus</i>	AMNH	M-144316	DS	A	O	29
Thylacinidae		<i>Thylacinus</i>	<i>cynocephalus</i>	NMB	c.2526	DS	A	D	30, 31

TABLE 1 *continued*

Order	Family	Genus	Species	Institution	ID Number	Material	Age Class	Data Sources	Figure Reference
Permelemorphia	Peramelidae	<i>Perameles</i>	<i>nasuata</i>	AMNH	M-160199	DS	A	O	32
	Peramelidae	<i>Perameles</i>	<i>nasuta</i>	AMNH	M-154403	DS	A	O	32
	Peramelidae	<i>Perameles</i>	sp.	ZIUT	HL 17.5 mm	DS	P	H	33
Notoryctemorphia	Notoryctidae	<i>Notoryctes</i>	<i>typhlops</i>	AMNH	M-202103	DS	A	O	34, 35
Sparassodonta	Hathlicynidae	<i>Sipalocyon</i>	<i>gracilis</i>	AMNH	VP-9254	Fo	A	D	38, 39
	Borhyaenidae	<i>Prothylacynus</i>	<i>patagonicus</i>	YPM	VPPU-15700	Fo	A	D	40, 41
Rodentia	Heteromyidae	<i>Dipodomys</i>	<i>deserti</i>	AMNH	M-182081	DS	A	D	36
Primates	Galagidae	<i>Galago</i>	<i>demidovii</i>	AMNH	M-89605	DS	A	O	36
	Galagidae	<i>Galago</i>	<i>demidovii</i>	MPIH	120	Wh	F	H	37
	Cheirogaleidae	<i>Microcebus</i>	<i>murinus</i>	MPIH	1964/41	Wh	F	H	37
Macroscelidea	Macroscelididae	<i>Elephantulus</i>	<i>fuscipes</i>	MPIH	305E	Wh	F	H	37

cosity of the injection mass and related factors, small or thin-walled vessels may be distorted or fail to fill adequately.

These preparations do not provide the level of contextual detail possible with soft-tissue dissection or serial sectioning. The advantage of serially sectioned whole specimens is that all tissues are preserved in their original anatomical environments. The disadvantage is that structures must be reconstructed from physical thin sections, something that is rarely undertaken these days. Digital scanning of whole specimens can greatly facilitate reconstruction efforts because slices are automatically acquired and aligned. The disadvantage is that X-rays do not visualize untreated soft-tissue structures such as blood vessels. This problem can be overcome to some extent with dyes such as iodine (e.g., Gignac et al., 2016), although studies of marsupial venous vasculature using this approach have yet to appear.

For our study, we selected specimens from the MPIH and ZIUT collections that had been prepared and stained previously using conventional histological techniques (MacPhee, 1981; Sánchez-Villagra and Forasiepi 2017). In the case of ZIUT specimens, individual sections were

photographically recorded with a Leica DFC 420 C digital camera mounted on a Leica MZ 16 stereoscopic microscope. Image contrast was enhanced with Adobe Photoshop. In the case of MPIH specimens, similar apparatus was used to produce physical black and white negatives that were then printed as hard copy.

#### ANATOMICAL STRUCTURES

Unless indicated otherwise, anatomical names used in this paper are English equivalents of terms listed in the *Nomina Anatomica Veterinaria*, 6th ed. (hereafter, NAV) and published online by the International Committee on Veterinary Gross Anatomical Nomenclature (2017). As noted in subsequent sections, some structures important for this study are not included in the NAV or are identified in the specialized literature by obscure or poorly defined synonyms. Appendix 1 covers these to the extent necessary. For this paper we utilize most of the common terms for mesocranial structures used in marsupial morphology, but where necessary we define additional terms for features and conditions not previously described or adequately named. We

TABLE 2

## Comparative Set: CT Scanning Parameters

Abbreviations: **ST**, Slice thickness; **Vol**, Voltage; **Amp**, Amperage; **SR**, Slice resolution; **TS**, Total slice; **BW**, Body weight. Data for extant species: Animal Diversity Web (<https://animaldiversity.org>). Estimates for *Sipalocyon* and *Prothylacynus*: Ercoli and Prevosti (2011).

Taxon	Specimen	ST [mm]	Vol [kV]	Amp [ $\mu$ A]	SR [pxl]	TS	BW range [kg]
<i>Sipalocyon gracilis</i>	AMNH VP-9254	0.069	170	190	1037 $\times$ 593	1648	2.11
<i>Prothylacynus patagonicus</i>	YPM VPPU-157000	0.072	200	200	1710 $\times$ 1700	1950	31.8
<i>Caenolestes</i> sp.	IANI-GLA uncat.	0.01	70	114	2048 $\times$ 2048	1436	0.030-0.040
<i>Dromiciops gliroides</i>	MACN Ma-23607	0.012	90	140	1152 $\times$ 1075	1800	0.016-0.042
<i>Didelphis virginiana</i>	TMM M-2517	0.132	180	133	1024 $\times$ 1024	859	1.9-6.0
<i>Monodelphis domestica</i>	NMB c.III.777	0.021	79	251	2000 $\times$ 2000	2000	0.090-0.155
<i>Thylacinus cynocephalus</i>	NMB c.2526	0.072	180	90	3052 $\times$ 3058	3612	15.0-30.0
<i>Dasyurus hallucatus</i>	TMM M-6921	0.078	180	133	1024 $\times$ 1024	781	0.30-0.90
<i>Trichosurus vulpecula</i>	TMM M-849	0.116	180	133	1024 $\times$ 1024	675	1.2-4.5
<i>Vombatus ursinus</i>	TMM M-2953	0.5	420	1800	1024 $\times$ 1024	399	20.0-35.0
<i>Osphranter robustus</i>	AMNH M-80171	0.0470	180	150	1598 $\times$ 1649	1869	18.0-42.0
<i>Notoryctes typhlops</i>	AMNH M-202103	0.0189	130	110	1592 $\times$ 1085	2017	0.030-0.060
<i>Dipodomys deserti</i>	AMNH M-182081	0.037	145	130	865 $\times$ 561	937	0.083-0.148

also introduce a few pertinent terms from comparative embryology (see table 3).

Human anatomy, fetal and adult, is frequently relied on in comparative studies not only for the obvious reason that conditions in *Homo sapiens* have been abundantly explored, but also because a feature recorded as an anomaly in humans may turn out to be the typical condition in another mammal. Whether this kind of information is useful for making primary homological determinations depends on relevancy, but it often helps.

For general background on mesocranial venation the reader is referred to works by Padgett (1956, 1957) and Tubbs et al. (2020). Although devoted to cephalic vascular development and expression in the human, they are profusely illustrated and contain much information useful to the

comparative anatomist. For this paper, the availability of well-illustrated online sources makes extensive citation of hardcopy anatomical texts unnecessary. Brief definitions of cephalic features not provided here can be found in Kielan-Jaworowska et al. (1986), Wible (2003 and other listed papers), and MacPhee et al. (2021).

In regard to previous investigations directly pertinent to this paper, we especially wish to acknowledge the work of Archer (1976) and Aplin (1990). For his investigation, Archer double-injected representatives of Dasyuridae (*Antechinus*, *Sminthopsis*, *Planigale*) and Peramelidae (*Isoodon*), and dissected dry skulls of several others, mostly focusing on dasyuromorphians and didelphimorphians (*Thylacinus*, *Sarcophilus*, *Dasyercus*, *Dasyuroides*, *Myrmecobius*, *Didelphis*, *Marmosa*, *Monodelphis*). In addition to

descriptions, he provided diagrammatic line drawings of the cephalic vasculature of the injected dasyurids, although these can be hard to interpret because of vessel overlaps. Aplin's (1990) study, which is his unpublished dissertation, focused on the cranial anatomy of possums and gliders, but also included descriptions of dry skulls and serially sectioned young specimens of other marsupial taxa as well as resin casts and radiographs of the cephalic venous anatomy of selected macropodids. Much of this information was never reported in published papers, and for that reason his contributions are heavily referenced here. Another paper of importance is the study of Sánchez-Villagra and Wible (2002): these authors collected information on the osteological transverse canal system using large samples of marsupial taxa, and their incidence data are referenced throughout.

Finally, most of our inferences about TCV anatomy are based on dry skulls, not on the veins themselves. For that reason we distinguish pathways based on bony indicia from those based on dissection, sectioned heads, and other kinds of empirical preparations (injected specimens, venograms). In particular, we distinguish the osteological rostral and caudal pathways of the transverse canal branches from the venological rostral and caudal veins that occupy these pathways during life.

#### ANATOMICAL ACRONYMS USED IN TEXT

BVP	basicranial venous plexus
CBF	caudal branch foramen
CBV	caudal branch vein of the transverse canal vein
CBTC	caudal branch of the transverse canal (osteological pathway)
ch.	chapter
char.	character
CS	cavernous sinus
CSVS	cerebrospinal venous system
EJV	external jugular vein
EJVS	external jugular venous system

EVPS	extracranial continuation of ventral petrosal sinus
ICV	internal carotid vein
IJV	internal jugular vein
IJVS	internal jugular venous system
PCVN	pericarotid venous network
PGLV	postglenoid vein
PGLVN	postglenoid venous network
PMDs	pericarotid mesocranial distributaries
PVP	pterygoid venous plexus
RBV	rostral branch vein of transverse canal vein
RBTC	rostral branch of the transverse canal (osteological pathway)
rev.	side reversed (stained section or segment)
SS	sigmoid sinus
TBS	transverse basisphenoid sinus (= transverse canal sinus, pterygoid sinus)
TCF	transverse canal foramen
TCV	transverse canal vein
v. e.	vena emissaria
VPS	ventral petrosal sinus
VV	vertebral vein

#### INSTITUTIONAL ABBREVIATIONS

AMNH M	American Museum of Natural History (Mammalogy)
AMNH VP	American Museum of Natural History (Vertebrate Paleontology)
MACN Ma	Museo Argentino de Ciencias Naturales "Bernardino Rivadavia" (Mammalogy), Buenos Aires, Argentina
MHNC	Museum national d'Histoire naturelle, Paris, France
MPIH	Max Planck Institute für Hirnforschung (ex Anatomisches Abteilung, "Primatologie"), Frankfurt am Main, Germany
NMB	Naturhistorisches Museum Basel (Mammalogy)
TMM	Texas Memorial Museum, Austin (Mammalogy)

- YPM VPPU Yale Peabody Museum (Vertebrate Paleontology, ex collection of Princeton University), New Haven, CT
- ZIUT Zoologisches Institut, University of Tübingen, Germany

#### ANATOMY OF THE PERICAROTID VENOUS NETWORK

In keeping with the overall emphasis of this paper, this general introduction is devoted to conditions in extant marsupials. In this section we introduce anatomical features on the basis of their appearance and location in *Didelphis virginiana* (fig. 2), because this species is widely available in collections and comparatively well investigated. However, no single taxon can cover the range of disparities encountered in a large natural group like Marsupialia. Major differences by taxon are noted in this section where appropriate as well as in the systematic descriptions.

Interpretative appeals to ontogeny are made throughout this paper, either as a device for asserting homologies or for making inferences about the origin of certain character states. Scenarios of this kind are easy to propose but difficult to test in a meaningful way. The danger is that overreliance on ontogeny to explain morphological similarities and differences may result in true innovations being missed or at least misconstrued. This is important, but the proper approach is to exhaust simpler explanations first—and most of the time, this implicates development. This is especially relevant to the interpretation of venous systems, where variation in relative speed of vessel development, programmed involution, prevalence of certain anastomoses, and other factors may result in very different final architectures in both individuals and species (Padget, 1957).

“Presence” in anatomical descriptions usually means that there is evidence of a positive kind for a structure’s existence or position. “Absence” should mean that a structure’s non-presence is based on confirmatory evidence as

well, but this is often impossible to provide given the kinds of specimens utilized for studies such as this. In the ontogenetic context, both “presence” and “absence” may be contingent, varying with age or developmental stage. In our descriptions we try to acknowledge gray areas where certainty is not possible.

#### MESOCRANIAL OSTEOLOGY AND CONTEXT

As defined here, the **mesocranium**, or rostral basicranial region of the mammalian skull, is formed by the basisphenoid, presphenoid, and parasphenoid. On each side it is externally bordered by the pterygoid and alisphenoid ventral to the infratemporal fossa (fig. 2A–C). In most extant marsupials the ventral aspect of the mesocranium is roughly trapezoidal, its rostral border slightly to markedly shorter than the caudal. In life, intervals bounding the elements making up the **basicranial keel** (i.e., midline bones from vomer to basioccipital) are filled with synchondrosial cartilage, which may persist late into maturity unless finally replaced by bone (Moore, 1981). The traditional embryological term for the chondrocranial precursor of the keel is **central stem**. In advanced prenatal specimens the stem consists of a more or less continuous block of cartilage, extending from the nasal cavity to the foramen magnum, in which the ossification centers for basicranial replacement bones eventually appear.

Chief features of the mesocranial region that are visible ventrally or ventrolaterally include the **foramen rotundum**, **foramen ovale** (often incompletely separate from the **piriform fenestra**), trackways or foramina for components of the **nerve of the pterygoid canal**, and the **exocranial carotid foramen** (i.e., external basicranial aperture of the carotid canal). In metatherians this last feature is always situated near the rear edge of the basisphenoid, although the artery’s trackway may excavate a longer **exocranial carotid sulcus** that begins in the rostral part of the basioccipital. Incidentally, to reduce confusion when referring to apertures for the internal carotid neurovascular bundle as

depicted in CT segments, we recommend adding “exocranial” or “endocranial” to their anatomical names, however styled (see synonyms listed by Beck et al., 2022: 62).

The **transverse canal foramen (TCF)** is usually situated lateral or rostralateral to the exocranial carotid foramen. It is normally separate from, but occasionally continuous with the latter (or, more rarely, with the piriform fenestra, fide Archer [1976]). The **transverse canal** is the medial continuation of the TCF within the basisphenoid. As a tube its length varies widely, and in small-bodied taxa it may be very short to essentially nonexistent. Vessels associated with the transverse foramen and canal are treated separately below (see Network Components).

Within the braincase, a deep, pitlike **endocranial carotid groove** (Wible, 2022: fig. 17) is a distinctive feature of the marsupial endocranial floor that always lies on either side of the hypophyseal fossa (e.g., *Didelphis*, fig. 2C; *Osphranter*, fig. 18C; *Vombatus*, fig. 24C; *Perameles*, fig. 32C, D). It is much larger than the **endocranial carotid foramen**, the major aperture opening onto the groove’s caudolateral aspect that transmits the internal carotid neurovascular bundle. Unlike placentals, which exhibit an aperture for the same bundle in the same topographical position (MacPhee and Forasiepi, 2022), other vessels regularly share this space in marsupials. It is reasonable to infer that, during the development of the marsupial endocranial floor, the size of the vessels passing through the carotid grooves influences the latter’s form and depth as ossification proceeds (see below). Other markings seen in the middle cranial fossa, representing the trackways of major vessels and nerves (**maxillary nerve**, **ophthalmic nerve**, **ophthalmic veins**) are consistently present but not always as well marked as they are in *Didelphis* (fig. 2C). Among these structures are the **hypophyseal fossa** for reception of the **pituitary body (hypophysis)** and the **cavernous sinus**.

Major vessels related to the mesocranium and basicranial keel are diagrammed in figure

1A for a hypothetical marsupial. In mammals, blood is principally returned from the head of the organism to the systemic circulation via the **external jugular venous system (EJVS)**, the **internal jugular venous system (IJVS)**, and the **vertebral veins (VVs)** of the **cerebrospinal (CSVS) venous system** (Arnautovic et al., 1997; Tobinick and Vega, 2006; Nathoo et al., 2011; Tubbs et al., 2020). Redundancy is a key feature of cephalic venation, as it helps to ensure adequate physiological performance even when flow in one or another streamline is reduced or blocked by disease, posture, or other contingencies (e.g., vascular pressure gradients) (Tubbs et al., 2020). Dural channels lack valves; because of that, the direction of encephalic venous blood flow is potentially bidirectional. However, inherent or extrinsic factors—including gravity—result in unidirectional dominance in most postures (fig. 1B). In the descriptions we follow the sense of direction implied by the veins themselves, which usually means from inside the head to the outside, where the systematic circulation is encountered. In some reconstructions the direction of flow is implied by arrows, but this should not be interpreted literally.

Venous systems may be further divided into subsystems or networks responsible for drainage of specific areas or organs, such as the **postglenoid venous network (PGLVN)** and its major outlets, the **postglenoid vein** and **suprameatal vein**. Another is the **pericarotid venous network (PCVN)**, which functionally impinges on all of the major cephalic systems and is the main subject of this paper. Ignoring overlaps shared with the foregoing, the PCVN may be defined for present purposes as having four chief components: **transverse canal vein (TCV)**, **cavernous sinus (CS)**, **internal carotid vein (ICV)**, and **transverse basisphenoid sinus (TBS)** (fig. 1A, B; tables 3, 4; appendix 1).

#### NETWORK COMPONENTS

TRANSVERSE CANAL VEIN AND ITS MAJOR BRANCHES. “Transverse canal vein” is the tra-

ditional name for the major vessel that departs the skull through the TCF. Use of the singular makes it sound as though there is only one entity involved, but, as Archer (1976) was the first to show, the TCV is branched in specific ways in different marsupials. These vessels are rarely described as separate entities, but as they are fundamental to a proper understanding of PCVN organization (see below), it is important to clarify their roles and how they may be distinguished.

The **trunk of the TCV** is the simplest to describe: it is the portion that departs the mesocranium via the TCF and enters the pharyngeal region where it immediately anastomoses with local tributaries of the **external jugular vein (EJV)**, especially the **pterygoid venous plexus (PVP)** (fig. 1A). Inside the mesocranium the trunk may receive one or two distinctively different branches, depending on the species involved. The branch that is usually, but incorrectly, regarded as “the” TCV travels in a bony canal to the middle of the body of the basisphenoid, where it meets its antimere (Sánchez-Villagra and Wible, 2002). This vein is here called the **rostral branch vein (RBV)** and its pathway is the **rostral branch of the transverse canal (RBTC)** (*Didelphis*, fig. 4B, D; *Perameles*, fig. 33A). The other pathway, often a groove rather than a canal, is the **caudal branch of the transverse canal (CBTC)**; its vein is the **caudal branch vein (CBV)** (*Caenolestes*, fig. 13D; *Vombatus*, fig. 25). In the text we refer to both veins as **source vessels**, to emphasize that both contribute to the TCV when present.

Early investigators (e.g., Wortman, 1901–1903) implicitly assumed that the transverse canals were unbranched and primarily functioned to drain the CS. Although terminology differs from study to study, more recent investigations (e.g., Archer, 1976; Aplin, 1990; Sánchez-Villagra and Wible, 2002) have shown that TCV branching is the rule rather than the exception in most marsupial clades. In particular, Archer (1976) noticed that although many taxa showed evidence of both rostral and caudal branches, some exhibited only the

one or the other. However, he did not comment on what these differences might mean homologically. Sánchez-Villagra and Wible (2002: 29, char. 2) made a similar observation, but, like Archer (1976), they did not view the two branches as essentially different entities.

Recognizing that there are two source vessels for the trunk helps to make sense of apparently contradictory or incompatible observations in the literature relating to the TCV. To ensure consistency in identifications, whenever possible we distinguish the trunk portion of the TCV from the sources that join it. We maintain the use of rostral and caudal modifiers even when only one branch is demonstrably present in a taxon (e.g., *Didelphis*, fig. 4).

**ROSTRAL BRANCH OF THE TRANSVERSE CANAL.** The RBTC route is the familiar “intramural,” or continuous, pathway of previous authors. Although the RBV has been called an emissarium (e.g., Aplin, 1990), and contrary to the notion that it drains the CS, the rostral vein usually passes through the mesocranium without receiving any dural input at all, apart from relatively tiny hypophyseal canaliculi (e.g., *Trichosurus*, fig. 21A–D). The function of this vessel is uncertain (see Discussion), but one unusual role may be mentioned here. RBVs converge on, and presumably drain, a structure—the TBS—that is ontogenetically programmed to produce erythrocytes in young stages of at least some species (see below). This arrangement recalls the drainage of red marrow by vena diploica, which are characteristically situated in cranial cancellous tissues (see Warwick and Williams, 1973; Cline and Maronpot, 1985; García-González et al., 2009; MacPhee et al., 2021). Most diploic veins discharge endocranially into dural channels, but in some taxa, including *Homo* and *Canis*, certain veins designated as vena diploica connect directly to external vasculature (e.g., occipital or asterional diploic vein; Evans and Christensen, 1979: 793). Whether any functional insight is to be gained by designating RBVs as remarkably large diploic veins is arguable, but as they clearly differ from

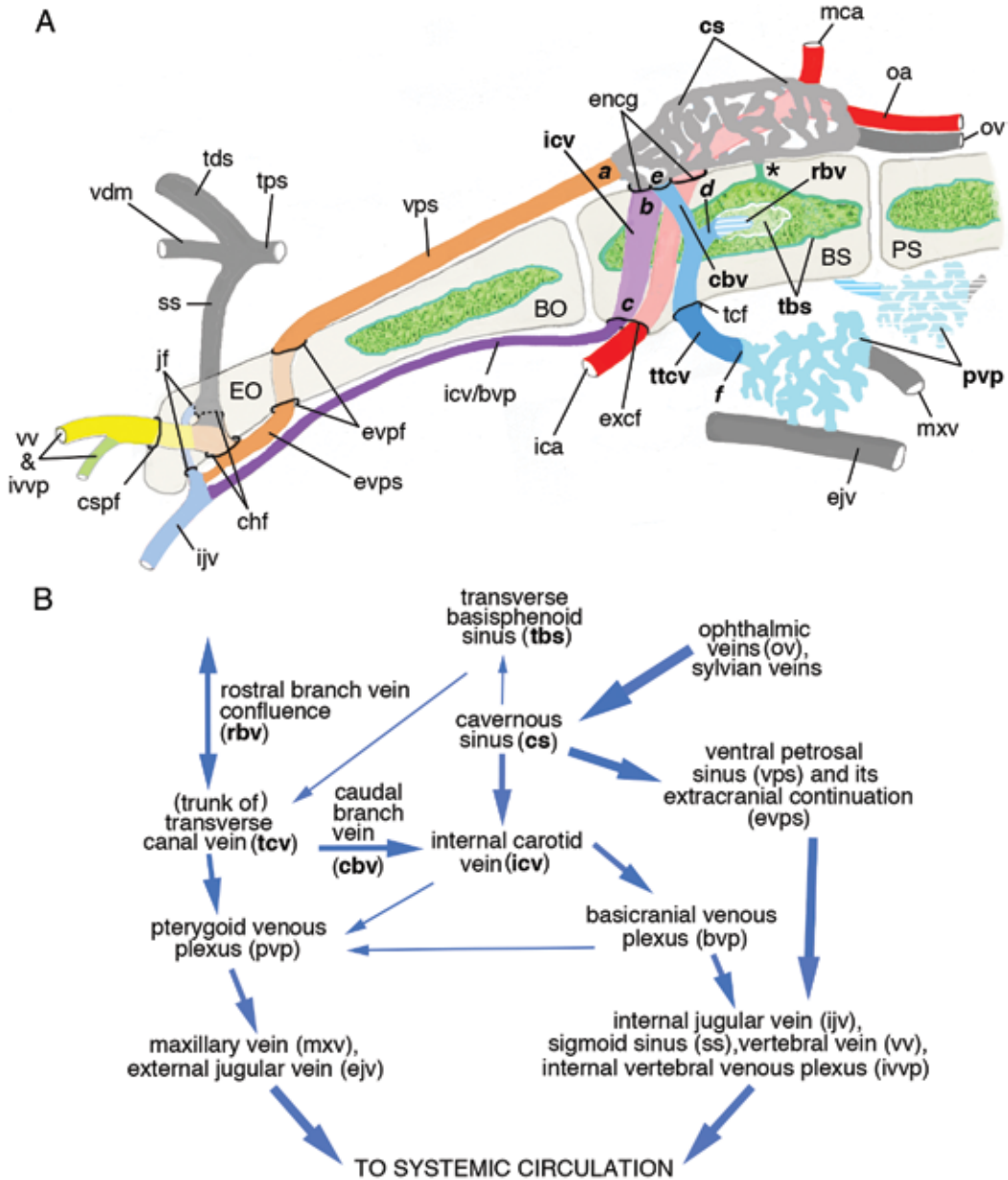
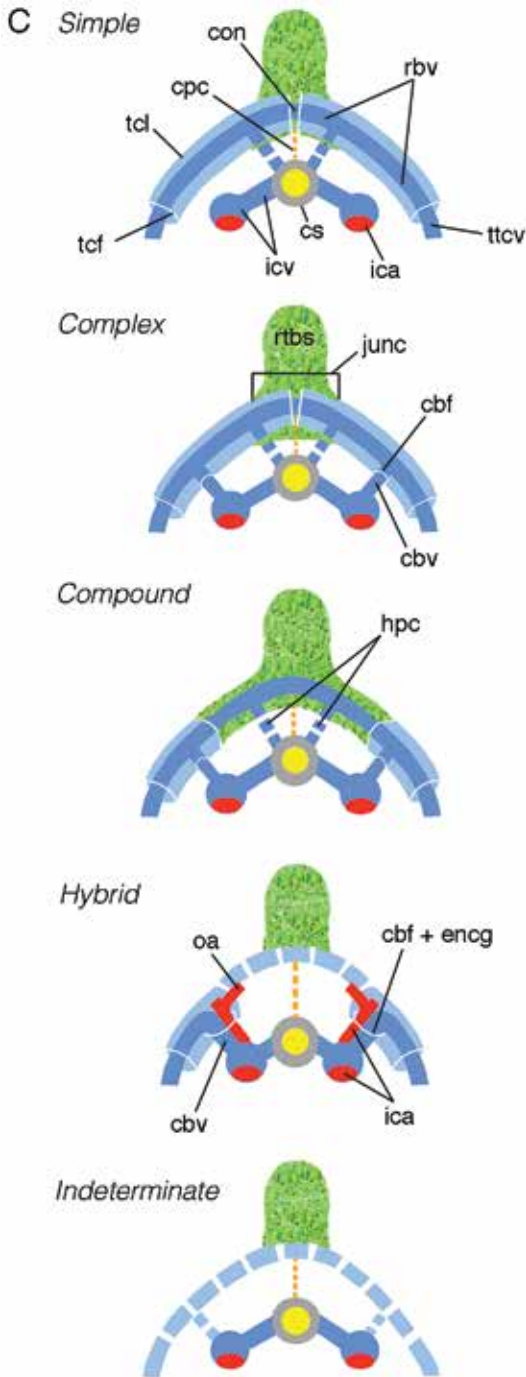


FIG. 1. **A.** Cartoon of pericarotid venous network (PCVN) in a hypothetical marsupial in lateral aspect, with chief components of network in bold type (color scheme also in fig. 3). In addition to transverse basisphenoid sinus, pneumatic sinuses (not separately named) in presphenoid and basioccipital are also frequently present. Six major venous connections involving PCVN components occur in most investigated marsupials at some stage of development and are indicated by italicized letters: *a*, cs → vps (e.g., *Osphranter*, fig. 20C); *b*, cs → icv (e.g., *Perameles*, fig. 33D); *c*, icv → bvp (e.g., *Monodelphis*, fig. 11C); *d*, rbv → rbv (confluence of antimeres) (e.g., *Dromiciops*, fig. 16B, C); *e*, icv → tcv via cbv (e.g., *Caenolestes*, fig. 13D); *f*, tcv → pvp (e.g., *Caluromys*, fig. 9E). Smaller accessory connections (e.g., hypophysial and interstitial canaliculi), not separately illustrated, vary considerably among taxa or individuals. Asterisk, craniopharyngeal canal, frequently patent in adult but



not certainly vascular. **B.** Simplified streamline model, illustrating PCVN-systemic connections. Arrows indicate inferred predominant direction of flow, which is potentially bidirectional in intracranial vessels as they lack valves. Relative proportions and spatial relationships of specific features exaggerated or rearranged for clarity. No attempt made to show all connections, especially ones lacking significant association with bony indicia. **C.** Transverse canal junction patterns, in schematic horizontal aspect in marsupials and sparassodontans (see text). Patterns are based on presence/absence of critical osteological and venological features, as follows. Rostral or “intramural” branch trackways include bony canals (light blue) that extend between transverse canal foramina and transverse basicranial sinus (green). Merger of canals and sinus, called a junction, may take various forms in different taxa. In life each canal conducts a rostral branch vein (RBV, dark blue); RBVs meet in a midline anastomosis or confluence, which creates a circuit linking trunks of transverse canal veins and, ultimately, right and left external jugular systems. RBVs are emissarylike veins, not typically in significant communication with dural circulation. By contrast, caudal or “endocranial” branch trackways may or may not include discrete canals or sulci. Each caudal branch vein (CBV, also dark blue) arises directly from cavernous sinus/internal carotid vein within endocranial carotid groove; it immediately passes through caudal branch foramen to terminate in ipsilateral trunk of transverse canal vein. CBVs are emissarial by definition; they do not meet or form a confluent like RBVs. In simple and hybrid patterns, only one set of veins (RBVs or CBCs, respectively) is predominantly present; other set reduced or absent. In complex and compound patterns, both sets are fully represented; in indeterminate pattern, neither is present. In cartoons of individual patterns, solid structures are present in adult stage, while dashed structures are variable, involute in young stages, or are inferred for ancestor. Only rostral portion of transverse basi-sphenoid sinus is indicated, caudal portion omitted for clarity. Yellow circle represents pituitary body, surrounded by cavernous sinus (gray). Internal carotid artery route and furcation shown indicated for hybrid pattern only. Frequency and relations of patent craniopharyngeal canal (orange dashed line) not known for individual patterns. Hypophyseal canaliculi are merely suggested as they are thought to be too variable for separate depiction. Interstitial

canaliculi are not shown. **Key:** **BO**, basioccipital; **BS**, basisphenoid; **bvp**, basicranial venous plexus; **cbf**, caudal branch foramen; **cbf + encg**, caudal branch foramen + endocranial carotid groove; **cbv**, caudal branch vein; **chf**, condylohypoglossal foramen (nonspecific); **con**, confluence of transverse canal veins (rostral branches), **cpc**, craniopharyngeal canal; **cs**, cavernous sinus; **cspf**, craniospinal foramen; **ejv**, external jugular vein; **encg**, endocranial carotid groove; **EO**, exoccipital; **evpf**, foramen for extracranial continuation of ventral petrosal sinus; **evps**, extracranial continuation of ventral petrosal sinus; **excf**, ectocranial carotid foramen; **hpc**, hypophyseal canaliculus; **ica**, internal carotid artery; **icv**, internal carotid vein; **icv/bvp**, anastomosis of internal carotid vein and basicranial venous plexus; **ijv**, internal jugular vein; **jf**, jugular foramen; **ivvp**, internal vertebral venous plexus; **junc**, junction of transverse canals; **mca**, middle cerebral artery; **mxv**, maxillary vein; **oa**, ophthalmic artery; **ov**, ophthalmic vein; **PS**, presphenoid; **pvp**, pterygoid venous plexus; **rbv**, rostral branch vein; **rtbs**, rostral portion of transverse basicranial sinus; **ss**, sigmoid sinus; **tbs**, transverse basisphenoid sinus with vacuity, rostral and caudal portions not discriminated; **tcf**, transverse canal foramen; **tcl**, transverse canal (nonspecific portion); **t ds**, transverse dural sinus; **tps**, temporal sinus; **ttcv**, trunk of transverse canal vein; **vdm**, vena diploetica magna; **vps**, ventral petrosal sinus; **vv** & **ivvp**, vertebral vein and internal vertebral venous plexus.

ordinary endocranial or true emissarial vessels, we distinguish them as **emissarylike veins**.

Two other anatomical distinctions concerning the intramural pathway are worth making. One is osteological and has already been introduced. In marsupials possessing recognizable RBVs in the adult stage, the right and left RBTC pathways meet at the midline in a junction that also involves the rostral part of the TBS (into which they open). The **RBTC junction** thus always lies immediately rostral to the hypophyseal fossa. The other distinction is venological. Within the osseous junction, right and left RBVs anastomose to form a vascular **mesocranial confluence** (e.g., *Didelphis*, fig. 5B–D; *Dromiciops*, fig. 16B; *Perameles*, figs. 32C, D; 33A). Actual confluence has been directly observed in *Didelphis* (Dom et al., 1970) and *Monodelphis* (Sánchez-Villagra and Wible, 2002: 29); it presumably occurs in all

other taxa in which RBTC pathways are functionally present.

A low, bow-shaped **transverse canal eminence** may define the rostral border of the hypophyseal fossa (e.g., *Didelphis*, fig. 2C). In small species with wafer-thin basisphenoids, the RBTCs may be sharply projecting, allowing their entire endocranial routes to be traced (e.g., *Caenolestes*, figs. 13D, 14B). Their prominence may be reduced when the associated TBS is strongly pneumatized. Note that an **eminence of the transverse basisphenoid sinus** may also be distinguished, so mere presence of a prehypophyseal swelling is not necessarily indicative of RBTC presence. The TBS eminence usually involves the presphenoid bone as well.

**CAUDAL BRANCH OF THE TRANSVERSE CANAL.** In the past the RBTC and CBTC pathways were not consistently differentiated, or were simply regarded as alternative expressions of the same thing. A characteristic attribute of the CBTC pathway is its brevity, as it runs only from the endocranial carotid groove to the ipsilateral TCV trunk lying within the transverse canal, and may thus be easily overlooked (e.g., *Perameles*, fig. 33A–D, H).

The pathway's chief marker is the **caudal branch foramen (CBF)**, usually found, when present, on the rostral wall of the endocranial carotid groove (e.g., *Monodelphis*, fig. 10C; *Vombatus*, fig. 24C; see also Wible, 2022). In taxa with large CBVs but reduced or absent RBVs, such as macropodids, the transverse canal foramen and the CBF are essentially the same size and appear as opposite ends of the same tube (e.g., *Osphranter*, fig. 18C). As noted, a key venological difference is that CBVs do not form a mutual anastomosis or confluence in the sense that RBVs do.

**MORPHOLOGICAL STATUS OF TRANSVERSE CANAL VEIN.** Aplin (1990) categorized the TCV as an emissarium, but in light of the distinctions made above, it is best considered a mixed-origin vessel, neither systemic nor emissarial exclusively. Apart from upsetting tidy morphological classification, this duality is of no consequence: many other cephalic veins (e.g., occipital vein, vertebral

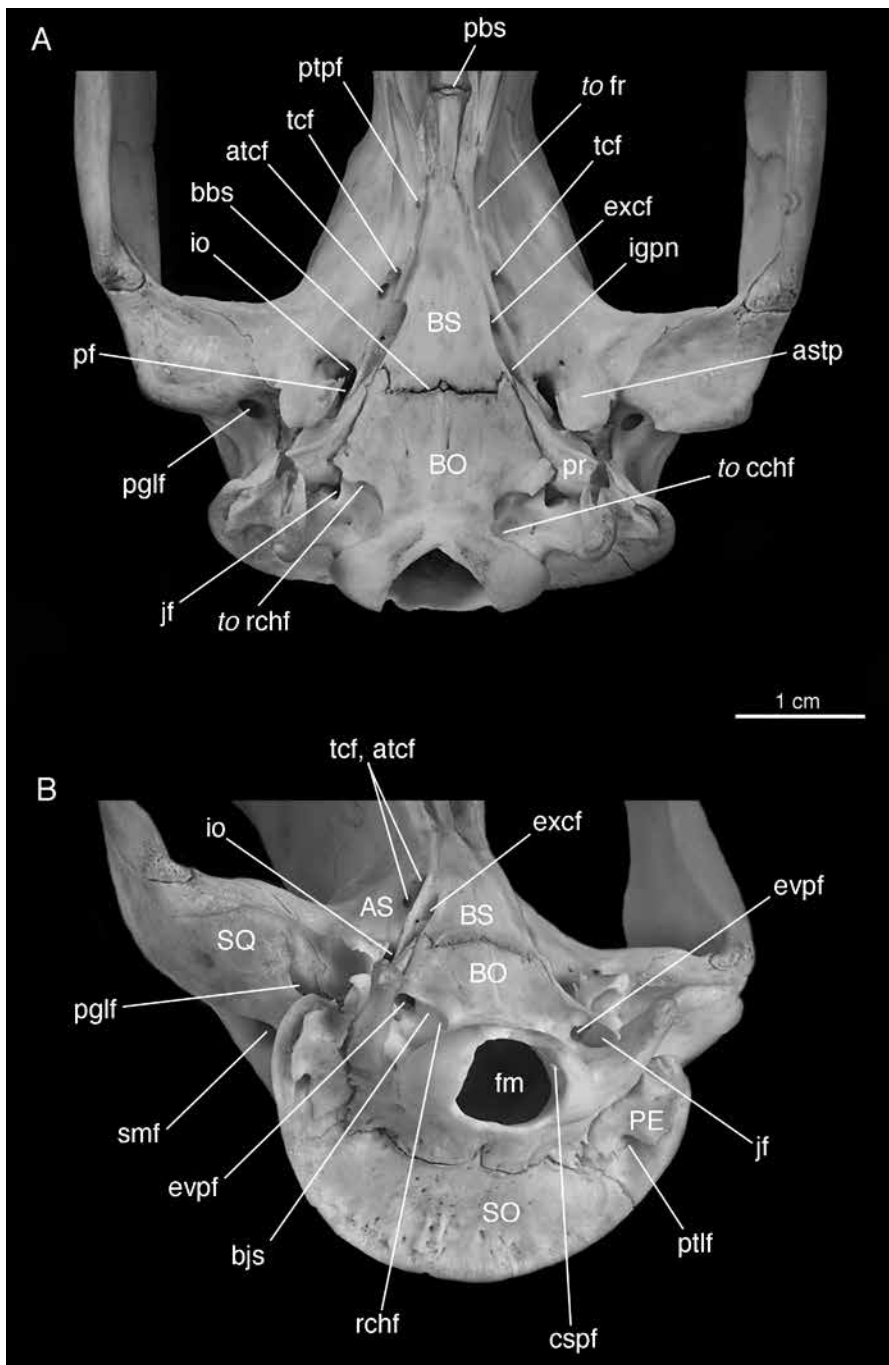
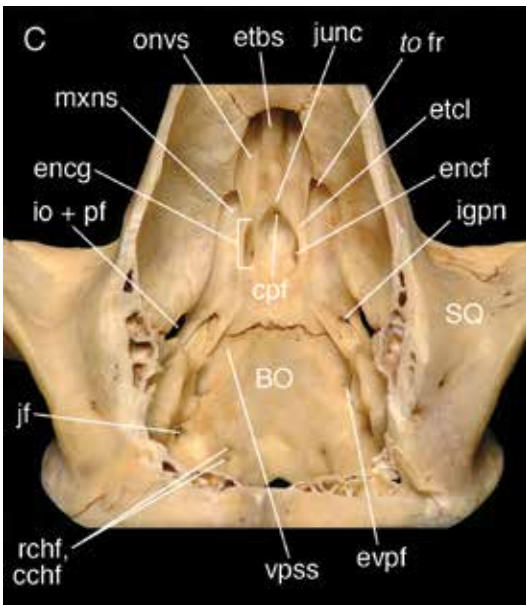


FIG. 2. *Didelphis virginiana* AMNH M-217731 (Didelphidae, Didelphimorphia), caudal cranium in **A**, ventral; **B**, oblique caudal, and **C**, endocranial views. In **C**, only one foramen (for internal carotid neurovascular bundle) opens into endocranial carotid groove, because caudal branch of transverse canal vein and its foramen are not present. Small aperture opening in rostral wall of hypophyseal fossa is cranio-



pharyngeal foramen (remnant of hypophyseal end of Rathke's pouch, not confirmably vascular in adult). **Key:** AS, alisphenoid; **astp**, tympanic process of alisphenoid; **atcf**, accessory transverse canal foramen; **bbs**, basisphenoid-basioccipital synchondrosis; **bjs**, basijugular sulcus; **BO**, basioccipital; **BS**, basisphenoid; **cchf**, caudal condylohyoglossal foramen; **cpt**, craniopharyngeal foramen; **csptf**, craniospinal foramen; **encf**, endocranial carotid foramen; **encg**, endocranial carotid groove; **etbs**, eminence of transverse basisphenoid sinus; **etcl**, eminence of transverse canal; **evpf**, foramen for extracranial continuation of ventral petrosal sinus; **excf**, exocranial carotid foramen; **fm**, foramen magnum; **fr**, foramen rotundum; **igpn**, incisura for greater petrosal nerve; **io**, incisura ovalis; **io + pf**, incisura ovalis indenting piriform fenestra; **jf**, jugular foramen; **junc**, junction of transverse canals; **mxns**, sulcus for maxillary nerve; **onvs**, sulcus for ophthalmic neurovascular array; **pbs**, presphenoid-basisphenoid synchondrosis; **PE**, petrosal; **pf**, piriform fenestra; **pglf**, postglenoid foramen; **pr**, promontorium of petrosal; **ptpf**, pterygopalatine fissure; **ptlf**, posttemporal foramen; **rchf**, rostral condylohyoglossal foramen; **smf**, suprameatal foramen; **SO**, supraoccipital; **smf**, suprameatal foramen; **SO**, supraoccipital; **tcf**, transverse canal foramen; **vpss**, sulcus for ventral petrosal sinus.

vein) are composite in the same descriptive sense, the product of multiple anastomoses between extracranial and intracranial channels. Apart from the transverse canal foramen, the TCV trunk does not generally leave external evidence of its passage in the infratemporal fossa or pterygoid region, but in some taxa (e.g., many phalangeriforms; *Distoechurus*, fig. 23) a short sulcus for it may crease the mesocranial sidewall.

**CAVERNOUS SINUS AND ITS TRIBUTARIES.** Morphologically, the CS consists of a pair of venous compartments situated between the periosteal and meningeal layers of the dura in the middle cranial fossa. Blood delivered to the CS by the dorsal and ventral **ophthalmic veins** (not individually distinguished in figures), as well as by other veins serving the forebrain area, may be passed to the systemic circulation along several routes, which vary in turn in their relative importance (Prince et al., 1960). In the text, the convention **CS/ICV (cavernous sinus + internal carotid vein)** is used to jointly refer to the cavernous sinus and its daughter branch, especially in the area of the hypophyseal fossa and endocranial carotid groove.

We do not attempt to identify or model morphological divisions of the CS because there is virtually no useful comparative marsupial data available for this purpose. Archer's (1976: figs. 2–4) portrayals of cavernous sinuses in injected specimens of the dasyuromorphians *Sminthopsis*, *Planigale*, and *Antechinus* are highly schematic and difficult to harmonize with visualizations using other media, such as venograms (e.g., *Sarcophilus*, fig. 28D) and corrosion casts (*Didelphis*, fig. 3). The structures that he identified as anterior and posterior intercavernous sinuses, for example, are positioned transversely under the presphenoid and (roughly) the basisphenoid-basioccipital synchondrosis. In our dry specimens there are no osteological correlates for such features in the locations indicated, and they are therefore effectively untraceable.

In therians the chief route for CS return is generally the **ventral petrosal sinus (VPS)**, which in marsupials connects endocranially with

one or more of the **sigmoid sinus (SS)**, **internal jugular vein (IJV)**, and **vertebral vein (VV)** (fig. 1A). The VPS may be assisted by the **dorsal petrosal sinus** and **basilar plexus**, although these are not always present as morphologically distinguishable structures and are not discriminated as such here. In most marsupials the VPS exhibits a large **extracranial continuation of the ventral petrosal sinus (EVPS)**, which lies on the external surface of the exoccipital within a prominent groove (**basijugular sulcus**) (*Dasyurus*, fig. 28). The extracranial extension is categorized as an emissarium by Aplin (1990: 198); no details are available on its ontogeny in marsupials. This vessel is also present in placentals, but it is rarely as well marked as it is in metatherians (see Forasiepi et al., 2019).

**INTERNAL CAROTID VEIN AND BASICRANIAL VENOUS PLEXUS.** Although the petrosal sinuses and their dependencies are the chief routes for CS drainage in mammals, there is also another pathway that is rarely mentioned, the ICV. Originating from the caudolateral side of the CS, the vein enters the carotid canal and travels in company with the internal carotid artery and nerve. In the sectioned and stained material, the proximal part of the ICV, which lies within the carotid groove, is clearly enlarged relative to the vein's caliber in the pharyngeal region (e.g., *Dromiciops*, fig. 16D, E). On leaving the exocranial carotid foramen the ICV tends to diminish rapidly in size, anastomosing with nearby veins and terminating anatomically in the **basicranial venous plexus (BVP)**. This union often takes the form of a plexiform trunk (identified as the **ICV/BVP** to signify its dual morphological origin) that communicates with local vessels and usually ends in the IJV or VV, or both (e.g., *Caluromys*, fig. 9F; *Perameles*, fig. 33E). The BVP was briefly noted by Aplin (1990: 199) as consisting of "a number of small veins" in *Macropus*, but was not otherwise characterized in this or the other specimens he examined. Despite its relatively large size at its origin in marsupials, the ICV pathway does not usually leave a separate trace on

the walls of the carotid canal. The BVP may be quite extensive in both marsupials and placentals because it receives inputs from multiple veins along its route (see below and MacPhee et al., 2021). In some placentals the BVP may groove the external basicranial surface or lie within the petrooccipital suture; a similar indicium has not been reported for marsupials.

**TRANSVERSE BASISPHENOID SINUS AND ITS RELATIONS.** For reasons provided in subsequent sections, the TBS is regarded as a functionally integral part of the PCVN. In earlier literature, TBS presence was usually not scored as such unless a macroscopic vacuity ("pterygoid sinus" of some authors) could be identified in a specimen. This is too restrictive, for the sinus's interior is often diffusely trabeculated, and thus may grade into diploe without presenting a large void (e.g., *Didelphis*, figs. 4D; 5A, B; *Dromiciops*, fig. 15D; *Thylacinus*, fig. 31C, D). Although there is no doubt that the sinus contains blood during life, the reason for this has not been previously examined. We argue that the TBS, whatever its form, develops as a site of hematopoiesis in young stages of at least some marsupials, although this needs to be confirmed on suitable material of more species (see Functional Considerations). In this regard the marsupial TBS resembles similar erythrocyte-forming areas in cranial bones of perinatal placentals, but whether this function is maintained into adulthood has not been established.

In making virtual reconstructions we tried to distinguish the general form of the TBS by grouping together small continuous channels while excluding less organized diploe, recognizing at the same time that tissue boundaries will be arbitrary in some instances. Morphologically, the sinus usually presents two portions (**rostral TBS**, **caudal TBS**) that are linked by **lateral extensions**. The hypophyseal fossa is a convenient landmark for defining their shared border. If the width of the endocranial floor is narrow, the transverse canals may be incorporated into the lateral extensions (e.g., *Caenolestes*, fig. 13B, D). The TBS is frequently continuous with a similar vacuity in the pre-

sphenoid, reflecting origin in both cases from pneumatic fronts expanding caudally from the nasal cavity. Whether the presphenoid sinus participates in hematopoiesis has not been separately studied but seems probable.

**OTHER FEATURES.** In addition to joining the TCV trunk, the branches of the transverse canals communicate with the contents of the hypophyseal fossa by means of small channels called **hypophyseal canaliculi** (e.g., *Caenolestes*, fig. 13D). CT scanning reveals that such connections are pervasive, although they are frequently tiny and therefore difficult to separately detect in dry skulls (see also Wible et al., 2021).

Beck et al. (2022: char. 50) question whether the aperture they designate as the anterior pterygoid foramen in certain petauroids (e.g., *Dactylopsila*) might be an alternate route for a vein functioning as a TCV. A foramen in roughly the same position occurs in *Dromiciops* (fig. 15E), a taxon that sometimes lacks a transverse canal foramen in the usual place according to some authors. The relations of this foramen have not been adequately studied in any metatherian, but considering how complicated mesocranial pathways may be (see *Prothylacynus*, fig. 40F), the possibility that it transmits another PMD should be seriously considered.

Other small channels communicating with the endocranial circulation can be found within or immediately peripheral to the TBS. **Interstitial canaliculi** are generally small, branch irregularly, and presumably have nutritive or maintenance functions, such as transporting maturing blood cells from the TBS. Both the RBV and CBV, or their tributaries, may communicate with the TBS in this way (e.g., *Didelphis*, fig. 4D; *Thylacinus*, fig. 30D). Hypophysial and interstitial canaliculi are only briefly referenced in the text as they are likely to vary significantly among individuals as well as among species.

The unpaired **craniopharyngeal canal** and **notochord canal** require brief mention because their endocranial openings, when present, are located near or in the hypophyseal fossa (*Caluromys*, fig. 8B; *Vombatus*, fig. 24C). Whether these

developmentally relictual channels have any function related to either the hypophysis or the PCVN in adult therians is uncertain. When present in the adult human, the craniopharyngeal canal runs from the deepest part of the hypophyseal fossa to emerge on the pharyngeal roof near the vomerosphenoidal junction (Arey, 1950: figs. 1, 2; Lang, 1983: 136). In marsupials, the canal's endocranial foramen is usually found on the rostral slope of the hypophyseal fossa rather than its base, and its canaliculus disappears into the rostral TBS or, in at least one case, into the junction of the transverse canals (*Didelphis*, fig. 2C, 5B, C). The endocranial foramen for the notochord, if present, usually appears in marsupials (and humans; Frazer, 1911) immediately caudal to the basisphenoid-basioccipital synchondrosis, and thus further away from the hypophyseal fossa (e.g., *Thylacinus*, fig. 30D). Its exocranial opening may be obliterated in adults even though the endocranial foramen is patent, and conversely.

The protracted debate (see Arey, 1950; Moore, 1981; Lang, 1983) concerning whether these canals function as vascular channels in later ontogeny is not of immediate interest here, because neither of them has a demonstrated participatory role in the PCVN. However, it is nonetheless striking that in *Vombatus* (fig. 24C), for example, the craniopharyngeal foramen is as large as the CBF, which implies functionality of some sort. If this is correct, given its relations the only likely role for the craniopharyngeal canal would indeed be venous drainage, either of the pituitary itself or tissues in the rostral TBS. In *Homo* patent canals are almost always considered pathological or pathology related (e.g., Abele et al., 2014), but this view cannot be generalized to apply to species in which such features are probably universal and clearly nonteratological.

#### HOMOLOGIES OF MESOCRANIAL DISTRIBUTARIES

The scanty comparative literature on the anatomy of emissaries and emissarylike vasculature is

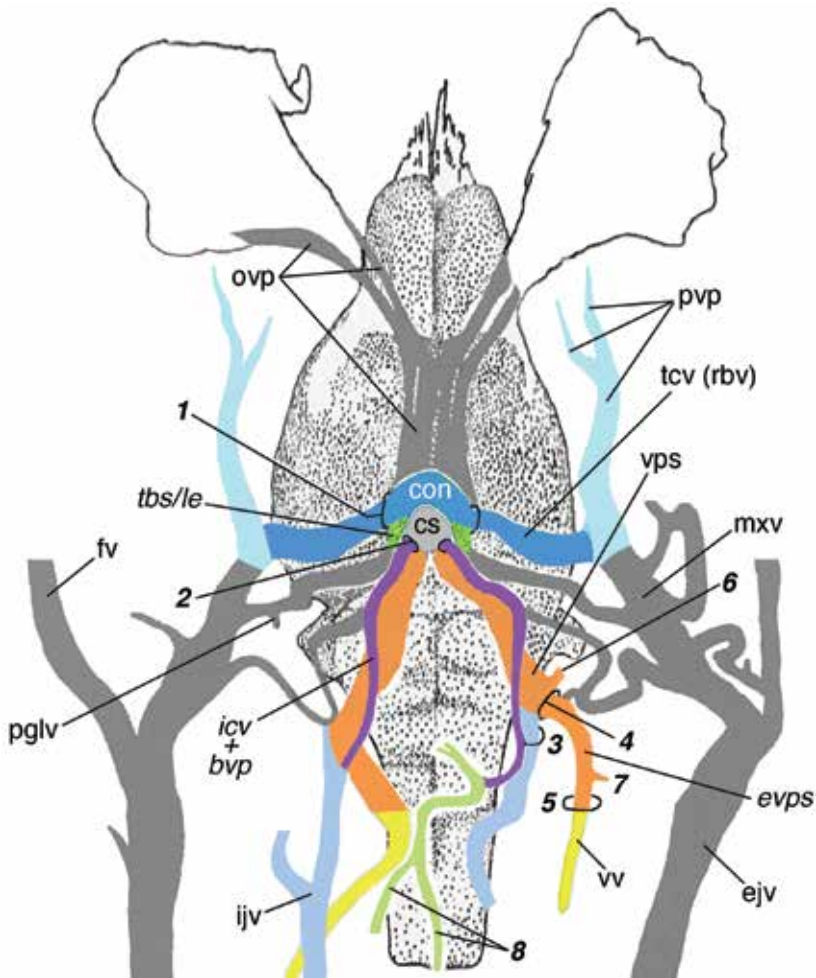


FIG. 3. *Didelphis virginiana* (Didelphidae, Didelphimorphia), representation of adult cephalic venous tree in ventral aspect, based on corrosion cast illustrations and descriptions by Dom et al. (1970: figs. 4, 5). Original authors' verified identifications (altered as necessary to conform to our terminology) are in regular type; italicized type and bold numbers represent additional identifications made for this paper (see key; color scheme as in fig. 1). Dorsal petrosal sinus, said to be present in this species (but see Shindo, 1915), is omitted. Craniopharyngeal canal, whatever its function, not depicted (foramen is present in *Didelphis* AMNH M-217731, fig. 2C). Right/left differences in vessel calibers probably represent natural variation or possibly distortions caused by latex injection. Dom et al. (1970: 494) state that "Plexus vertebralis internus ventralis appears to be the major pathway for drainage of the dural venous sinuses," but in our terminology this description should apply to vertebral vein per se, draining to craniospinal venous system. Internal plexus may instead be represented by relatively small vessels beneath brain stem. **Key:** **con**, confluence of transverse canal veins (rostral branches) (dark blue); **cs**, cavernous sinus (light gray); **ejv**, external jugular vein (dark gray); **evps**, extracranial continuation of vertebral petrosal sinus (orange, here inferred to directly anastomose with vertebral vein; **fv**, facial vein (dark grey); **icv + bvp**, internal carotid vein and basicranial venous plexus (purple); **ijv**, internal jugular vein (light blue); **mxv**, maxillary vein (dark grey); **ovp**, ophthalmic venous plexus, including ophthalmic vein (dark grey); **pglv**, postglenoid (emissary) vein (dark grey); **pvp**, pterygoid venous plexus (aquamarine); **tbs/le**, rostral portion of transverse basicranial sinus and lateral extension (mottled green); **tcv (rbv)**,

almost exclusively devoted to *Homo* and a handful of other taxa (e.g., Sisson and Grossman, 1953; Padget, 1956; Butler, 1957, 1967; Warwick and Williams, 1973; Lang, 1983; Evans and Christensen, 1979; James et al., 1980; Mortazavi et al., 2011; NAV, 2017; Tubbs et al., 2020; Campos Leonel et al., 2020). However, it is reasonable to assume that emissarial development in mammals is broadly similar enough to allow some generalizations. Emissaries begin as tiny capillaries budding from the primary head vein and its tributaries surrounding the brain. These eventually anastomose, mostly with branches of the EJVS situated in the developing face and jaws, to create transcranial channels (Butler, 1957; Barnett et al., 1958; Tubbs et al., 2020). This is not a random process: in the fetus, veins definable as emissaries tend to develop in places where ontogenetically programmed gaps, such as foramina or other dehiscences, are situated in the developing chondrocranium. This is important, because the relative position of emissaries to other features may be the only available guide to their homologies—especially in cases in which their surroundings are highly modified compared with the probable basal condition. This Bauplan argument is prescriptive in the sense that it infers homology from location, but it is not meant to be completely restrictive. Like other vessels, emissaries can also appear de novo, given the right concentration of molecular factors and tissue interactions (see Towbin et al., 1999). The possibility of novelty must be acknowledged, as in any homological determination, but there is no fundamental reason why sorting out homologies should be more difficult in the case of emissaria than elsewhere.

Emissaria are generally named after the apertures through which they pass, although this convention is inconsistently applied. Unsurprisingly, naming schemes are based on conditions in *Homo*, the default pla-

cental. In *Homo*, it is well established that emissaries in the mesocranial area act as connectors between the CS, IJV, and pterygoid and pharyngeal venous plexuses (Warwick and Williams, 1973: 698). The emissaries and emissarylike veins of greatest comparative interest in the present context are the **emissary of the sphenoidal foramen** (= vena emissaria sphenoidalis; vesalian emissary) and **emissary of the foramen ovale** (= v.e. foraminis ovalis). Another relevant emissary, joining the IJV and other caudally positioned systemic veins, is the **emissary of the carotid canal** (= v.e. foraminis carotidis), often called in human anatomies the **internal carotid venous plexus** (= veins of Rektorzik; Cironi et al., 2022). For simplicity of reference we call all mesocranial venous channels (including mixed-origin veins) **pericarotid mesocranial distributaries** (PMDs) (see appendix 1 for additional details).

To summarize our current views, the probable homolog of the marsupial ICV is the internal carotid venous plexus of *Homo* and other placentals. The placental homolog of the marsupial TCV is less obvious, because the latter is not a conventional emissarium, but the likeliest candidate in human anatomy is the emissary of the sphenoidal foramen (see appendix 1). This requires the assumption that the TCV has lost a primitive function related to dural irrigation, although a vestige of it may exist in the connections of the CBV or the hypophyseal canaliculi. In the case of *Homo*, Lang (1983: 136) distinguishes a lateral craniopharyngeal foramen and vessel that may communicate with the sphenoid sinus, but whether this poorly known feature is identical to any of the emissaria just mentioned is uninvestigated.

Mesocranial emissarial connections in marsupials need not be limited to the ones so far mentioned, although different routings imply

---

← transverse canal vein (rostral branch) (dark blue); **vps**, ventral petrosal sinus (orange); **vv**, vertebral vein (yellow); **1**, transverse canal foramen; **2**, exocranial carotid foramen; **3**, jugular foramen; **4**, foramen for extracranial continuation of ventral petrosal sinus; **5**, craniospinal foramen; **6**, ?sigmoid sinus (truncated; orange); **7**, ?condylar emissarium (truncated; orange); **8**, ?internal vertebral venous plexus (mint green).

different homologies. For example, emissaria are known to pass through foramen ovale or the piriform fenestra in a number of dasyuromorphians (e.g., *Planigale*) according to Archer's (1976) data (see also *Perameles*, fig. 33H). These channels cannot be the same homologically as the TCV trunk, especially if the latter is also present. Likewise, the emissarium passing through the carotid canal in phalangiforms that lack a TCV should not be regarded as a repositioned TCV (cf. Aplin, 1990) but instead as the normally-present ICV.

#### MESOCRANIAL PATTERN FEATURES

Although the osteology of mesocranial vascular relationships is fairly uniform across Marsupialia, there are a few significant contrasts. These chiefly concern how the transverse canals and their branches communicate with the TBS, carotid canal, endocranium, and/or each other. These several variations on basically the same theme are categorized as **junction patterns** (see table 4).

#### Junctions and Other Connections

Most previous assessments of transverse canal morphology have centered on whether the canals form a continuous intramural passageway in different species. However, a simple presence/absence dichotomy does not adequately capture the nature or scale of variation actually encountered. In this section we describe our approach, which is to assess patterns of association between transverse canal branches and other PCVN components. The chief basis for discriminating transverse canal junctions at present is osteological, as sufficiently detailed venological anatomies do not exist for most marsupials. In addition to focusing on RBTC and CBTC pathways, junction patterns also consider the relationship of the TBS to the transverse canals and the degree of amalgamation of the latter with the carotid canals (e.g., *Dromiciops*, figs. 15, 17; see also Archer, 1976: 252).

Beck et al. (2022: 66) noted that, in extant marsupials, hypophyseal canaliculi and other small endocranial channels form "a continuous range of intermediate morphologies (sometimes within a single taxon)." Part of the problem in interpreting their significance is that minor channels servicing the area of the hypophyseal fossa and CS have not been well investigated in any nonexperimental mammal, apart from a few notes on *Homo* (e.g., James et al., 1980; Schnitzlein et al., 1985; see also Wible et al., 2021). One possibility for making some sense of their origin, and perhaps their homologies, is location: their foramina tend to lie along the chondrocranial margin of the processus alaris, a lateral projection of the central stem (e.g., *Monodelphis*, fig. 11B; *Perameles*, fig. 33A) that adjoins the ala temporalis of the developing alisphenoid bone and helps mark the boundary between the latter and the basisphenoid (Starck, 1967; Maier, 1987). With ossification, these gaps progressively narrow, creating the small fissures and foramina seen on dry skulls. This might account for apparent variability in apertural size, frequency, and position as noted by Beck et al. (2022), as well as their connection with the transverse canal. Their abundance indicates that, unsurprisingly, the several components of the PCVN are normally in some degree of mutual contact. At present, hypophyseal and interstitial canaliculi (indicated by dashed lines in fig. 1C) play only a marginal role in defining junction patterns and are not considered as part of their definitions.

#### Patterns

The following classification of patterns covers the diversity seen in our material (fig. 1C). It is recognized that, for this classification to be considered minimally adequate, more data are needed from underinvestigated clades. Some of the distinctions among patterns made here may turn out to be less sharp when more specimens are evaluated, while others may prove substantial enough to warrant their own category. Also, endocranial examination is indispensable to the

assignment of pattern, whether that is conducted by dissection of dry skulls or, better, by CT scanning of whole specimens.

In all patterns except the indeterminate, the trunk of the TCV is assumed to be universal in the adult stage, allowing for minor individual differences as well as involution in some species. By contrast, the incidence and size relationships of the rostral and caudal branches varies across marsupial clades, which provides one basis for making discriminations among patterns. Interstitial communications between TCVs and the TBS may be more extensive than shown in the reconstructions; linkages not routed through bone are obviously not detectable in dry skulls and fossils.

**SIMPLE** (e.g., *Didelphis*, fig. 4): The RBTC pathways meet at the midline rostral to the hypophyseal fossa. The transverse canals open into the rostral TBS, but are distinct from it. Communication with the hypophyseal fossa is very restricted (e.g., ?vascular craniopharyngeal canal, seen from dorsal perspective in fig. 4D). Pathways for CBTCs absent or not recognizable. The TBS is not as extensive as in other patterns, and rostral and caudal portions do not broadly communicate.

**COMPLEX** (e.g., *Caenolestes*, fig. 13; *Vombatus*, fig. 25): This resembles the simple pattern, but with the addition of well-developed CBTC pathways and separate CBFs within the carotid grooves. The degree of communication between the RBTCs and the TBS is variable, but does not involve strong incorporation of the canals into the sinus as in the compound pattern. There may or may not be a large vacuity within the rostral TBS, depending partly on the thickness of the basisphenoid body. Small apertures in the endocranial floor, for TCV communication with the hypophyseal fossa, are frequently present.

**COMPOUND** (e.g., *Dromiciops*, figs. 15D, 17A; *Perameles*, fig. 33A): In the most diagnostic arrangement, the expanded rostral TBS almost completely incorporates the RBTCs, creating a large bony envelope around a major midline space ("pterygoid sinus" of many descriptions).

This is unlike the situation in the simple and complex patterns in which the canals remain distinct. Endocranially, expansion results in a single swollen eminence rostral to the hypophyseal fossa (e.g., contrast *Perameles* [fig. 33C] and *Caenolestes* [fig. 13D]). RBVs pass through this space, meeting at the midline to form a confluence. CBTC pathways are generally narrower than RBTC pathways. Gaps in the endocranial floor allow hypophyseal canalicular communication with the CS, as in the complex pattern.

**HYBRID** (e.g., *Osphranter*, fig. 20; *Thylacinus*, fig. 30): Compared to the patterns just defined, the hybrid is chiefly distinguished by its lack of significant intramural pathways. RBTCs are absent or highly reduced relative to CBTCs, and either no union of osseous pathways occurs rostral to the hypophyseal fossa or it is negligible in size. Right and left CBVs arise directly from the CS/ICV and pass out of the endocranium as the trunk of the TCV without forming a confluence. Compared to caudal branch pathways in other patterns, in the hybrid pattern the CBTCs and their associated foramina are relatively larger (e.g., *Osphranter*, fig. 18C vs. *Vombatus*, fig. 24C). Although the exocranial apertures of the transverse and carotid canals remain separate in macropodids, as seen osteologically their canals almost immediately coalesce into a single volume corresponding to the endocranial carotid groove. Osteological merger is more extreme in *Thylacinus* (fig. 31C), as right and left canals also briefly unite across the midline. This union, however, is not homologous with the junction formed by rostral branch canals. Communication with the TBS is minor. Separate hypophyseal canaliculi may be absent.

**INDETERMINATE** (e.g., *Caluromys*, fig. 8A; *Sipalocyon*, fig. 38A, E). Both branches of the transverse canal are absent in the adult. Therefore there is no TCF, midline junction in advance of the hypophyseal fossa, or CBF foramen in the endocranial carotid groove. It is not known, but probable, that the TCVs begin to form in fetal life but, if so, quickly involute—hence the ancestral condition is unknown or indeterminate. The

TBS is present, but communication is restricted to interstitial canaliculi. The craniopharyngeal canal is present in *Caluromys*.

**OTHER CONSIDERATIONS.** Some members of the comparative set are not easy to categorize. For example, conditions in *Thylacinus* are quite different, as far as is now known, from those in other taxa in its order. Phalangeriforms are particularly troublesome because of conflicting or unverified observations regarding presence/absence of the TCV and its route through the mesocranium. According to Aplin (1990), the TCF is very small or missing altogether in a number of phalangeriform species, and branching patterns are uncertain. By contrast, Beck et al. (2022) found that the only taxon in the group (s.l.) that consistently lacked a TCF was *Tarsipes*, although the aperture was sometimes absent in the petauroids *Pseudochirops archeri*, *Dactylopsila trivirgata*, and *Gymnobelideus leadbeateri*.

Osteological investigations cannot account for what happened to the TCV trunk in such cases: is it actually absent, or does it connect with the endocranium via a different emissarium issuing from a different foramen? One possibility for an exit aperture for the trunk when the TCF is absent is the exocranial carotid foramen (Aplin, 1990). In macropodids this arrangement could be achieved by taking conditions found in *Macropus* and *Osphranter* one step further, so that the exocranial ports for the carotid canal and transverse canal are completely merged. In another variation in TCV connectivity, *Trichosurus* (figs. 21, 22) exhibits links between the location of the hypophyseal fossa and the TBS via the accessory transverse canal. In this case the connecting channels could be functionally regarded as hypophyseal canaliculi, even though they lie outside the endocranial carotid grooves. Patterns inferred for the sparassodontans *Sipalocyon* and *Prothylacynus* resemble the indeterminate and complex patterns, respectively (figs. 1B, 42). However, they differ in numerous details from marsupials in these same categories, as noted in the systematic descriptions.

## SYSTEMATIC DESCRIPTIONS OF PERICAROTID VENOUS NETWORKS IN EXTANT THERIANS

### Marsupialia

#### DIDELPHIMORPHIA

*DIDELPHIS* (DIDELPHIDAE) (figs. 2–5). Compared with other marsupials, the cephalic vasculature of the Virginia opossum (*D. virginiana*) may be considered relatively well explored, but most investigations cover major vessels only and provide little information on PCVN components (see literature summaries by Aplin, 1990). Shindo's (1915) comparative investigation of the cavernous sinus in mammals may be considered a landmark because it includes the first detailed study of cephalic venation in marsupials (young specimens of *D. virginiana* and *Acrobates* sp.). The ICV is described, but not named, as arising from the caudal aspect of the CS and passing through the carotid foramen to join the "vein of the roof of the nasopharynx" (Shindo, 1915: 398 [trans.]). The identity of this last vessel is not apparent from Shindo's text; it may represent one of the pharyngeal components of the PVP or even the TCV (also not recognizably identified). The BVP is not distinguished as such, although a "v. thyreoidea" has the expected relations for this vessel as it runs lateral to the larynx and thyroid gland to discharge into the IJV (Shindo, 1915: 395). The VPS (= sinus petrosalis) is described as leaving the chondrocranium through the jugular foramen to unite with the IJV, although these vessels have separate exit foramina in adult *Didelphis* (fig. 2B). Connections of these vessels with the condylar veins, lateral head vein, and internal vertebral venous plexus are also briefly mentioned or illustrated.

Toeplitz (1920) described some aspects of cephalic venation in the closely related species *D. marsupialis*, but most of her relevant text concerns carotid canal homology, not content, in different vertebrates (see MacPhee and Forasiepi, 2022). She illustrated the ICV (= "Sin. intercavern. post.") as separating from the CS within the

TABLE 3

**Major osteological features associated with features of pericarotid venous network**  
Vessels in same streamline are separated by commas; those in different streamlines, by semicolons.

Osteological Feature	Contents (veins in bold)	Streamline (major vessels only)
Sulcus (canal) for ophthalmic neurovascular array	<b>ophthalmic vein</b> , artery, nerve	cavernous sinus
Hypophyseal fossa	<b>cavernous sinus</b> , hypophysis	internal carotid vein, hypophyseal canaliculi; ventral petrosal sinus. If present: caudal branch vein of transverse canal vein; dorsal petrosal sinus, basilar venous plexus
Carotid canal (foramen)	<b>internal carotid vein</b> , artery, nerve	basicranial venous plexus; pterygoid venous plexus, internal jugular vein
Transverse canal foramen	<b>trunk of transverse canal vein</b>	pterygoid venous plexus; maxillary vein, other tributaries of external jugular vein
Rostral branch of transverse canal	<b>rostral branch vein of transverse canal vein</b>	If present: antimere (confluent); trunk of transverse canal vein
Caudal branch of transverse canal	<b>caudal branch vein of transverse canal vein</b>	If present: trunk of transverse canal vein
Transverse basisphenoid sinus	<b>interstitial canalicular veins</b> erythroid tissue	diploe; transverse canal vein; ventral petrosal sinus; external jugular vein
Interstitial canaliculus	<b>innominate channels within transverse basisphenoid sinus</b>	external jugular vein; diploic channels; transiting transverse canal vein
Piriform fenestra/foramen ovale	<b>emissary of foramen ovale</b> mandibular nerve; other structures	maxillary vein, pterygoid venous plexus
Basicapsular fenestra, caudal portion	<b>ventral petrosal sinus, internal jugular vein</b> , caudal cranial nerves	extracranial ventral petrosal sinus; sigmoid sinus, internal jugular vein, vertebral vein
Foramen (canal) for extracranial extension of ventral petrosal sinus	<b>extracranial ventral petrosal sinus</b>	rostral and caudal condylar emissary veins, internal jugular vein, vertebral vein (often via separate foramen)
Basijugular sulcus	<b>extracranial ventral petrosal sinus</b>	rostral and caudal condylar emissary veins; suboccipital plexus
Condylahypoglossal foramina (canals)	<b>rostral and caudal condylar emissary veins</b>	vertebral vein, suboccipital plexus
Craniospinal foramen (canal, sulcus)	<b>vertebral vein</b>	internal vertebral venous plexus, occipital vein

carotid canal, but did not describe or otherwise comment on it (Toeplitz, 1920: fig. 18).

Of greater significance is the work of Dom et al. (1970), which describes the cephalic venous vasculature of adult *D. virginiana* in considerable detail, chiefly on the basis of corrosion casts of injected specimens from which all hard and soft tissues had been removed. Their line

drawing of the venation tree for *Didelphis*—surprisingly, still the only such representation available for this taxon—is reproduced here as figure 3, to which we have added color coding and other modifications to improve intelligibility. Their depiction is difficult to interpret in places because it completely lacks foraminal landmarks; some of these have been drawn in

by us, but they are only approximations. Additionally, some vessels inevitably overlap, obscuring their relations. Dom et al. (1970) limited themselves to identifications of major vessels that could be readily harmonized with names in the then current edition of the NAV. As a result their figure is rather minimally labelled. Nevertheless, major PCVN components can be plausibly identified based on vascular relations and position. In the following paragraphs we attempt to clarify the anatomy of the PCVN and associated vasculature, based on segmental data from the scan of TMM M-2517 and checked against adult dry skulls (see figs. 2, 4, 5).

Dom et al. (1970: 488) were aware that the feature that they named the “pterygoid sinus” or “plexus pterygoideus with emissary vein and anastomosis” was not part of the CS, which they separately identified, but was instead a different structure (the TBS of this paper) lying in the midline immediately adjacent to the CS. The identification of the TCV as an “emissary vein and anastomosis” is nonspecific, but it is unambiguously present on each side of the basisphenoid sinus and as expected joins the maxillary vein and PVP.

The parasagittally oriented channels departing from the caudal border of the CS represent not only the VPSSs, which Dom et al. (1970) labelled, but also the much smaller ICV/BVPs, which they did not. In the perspective chosen for the original figure the two channels overlap almost completely, unfortunately giving the impression that they are closely appressed. As depicted, the right and left sides of the venation tree differ, especially caudally, due either to individual variability or possibly insufficient infilling. The ICV/BVP is not shown as plexiform, probably because infilling was inadequate or small branches were clipped to improve visualization. Their text (p. 494) indicates that the ICV/BVP is connected to the IJV and CSVS, which is shown on the specimen's right side but not the left (fig. 3). Importantly, Dom et al. (1970) emphasized that the IJV is relatively small and mostly concerned with draining the deep structures of the neck and

muscles of the larynx and pharynx rather than the endocranium, but they did not refer explicitly to the extracranial VPS or its relations with the emissaria of the condylohypoglossal foramina. Other matters concerning identification are noted in the legend of figure 3.

The most relevant osteological features of *Didelphis* have already been mentioned. The confluence of RBVs occurs within the rostral TBS (fig. 5A, B). The fact that the TBS is represented at all in the corrosion cast specimen indicates that the injection mass probably entered it from the RBVs. The lateral extensions of the TBS trail off into regular diploe and do not connect the sinus's rostral and caudal portions, although the existence of very fine connections between the two portions of the TBS cannot be excluded.

Archer (1976: 283) noted that the “transverse canal of *Didelphis* differs [from that of *Marmosa*] in that, in no specimen observed, does any branch of this canal penetrate entocarotid canal” (i.e., no CBF in endocranial carotid groove). This corresponds to our observations on our material. Assuming that the absence of the caudal branch is invariant in the genus (but see *Sarcophilus*, fig. 28C), this character serves to distinguish *Didelphis* from all other didelphids examined to date. The craniopharyngeal canal is not identifiable on the venation tree; this may indicate that, despite its location, it may be nonvascular in the opossum (fig. 5I).

In the adult skull the foramen for the EVPS (fig. 2A, B) is larger than the jugular foramen, although this is not obvious in our ventral illustration because the former is obscured by a bony lip. The basijugular sulcus deeply scores the exoccipital surface and continues caudally to intersect sulci associated with the condylohypoglossal canals.

*PHILANDER* (DIDELPHIDAE) (figs. 6, 7). The specimen of the gray four-eyed opossum, *P. opossum* ZIUT HL 32 mm, is developmentally somewhat younger than the perinatal specimen of *Monodelphis* described below, from which it

TABLE 4

**Transverse Canal Junction Patterns in Some Marsupials**

In bold, taxa investigated in this paper; in roman, taxa described in sufficient detail in literature to allow determination of junction pattern. Taxa in parentheses provisionally included; see text. Sources: Aplin, 1990; Archer, 1976; Beck et al., 2022; Sánchez-Villagra and Wible, 2002; Wible, 2022; Wible et al., 2021.

PATTERN	Simple	Complex	Compound	Hybrid	Indeterminate
TAXON	<i>Didelphis</i>	<i>Philander</i>	<i>Dromiciops</i>	<i>Notamacropus</i>	<i>Caluromys</i>
		<i>Monodelphis</i>	<i>Perameles</i>	<i>Osphranter</i>	<i>Caluromysiops</i>
		<i>Marmosa</i>	<i>Notoryctes</i>	( <i>Trichosurus</i> )	<i>Tarsipes</i>
		<i>Dasyurus</i>		( <i>Distoechurus</i> )	
		<i>Caenolestes</i>		<i>Thylacinus</i>	
		<i>Vombatus</i>			
		<i>Phascolarctos</i>			

otherwise differs little for the features of interest. The auditory capsule is completely cartilaginous, and central stem ossification is at an early stage. Wible et al. (2021) provide a detailed, CT-based osteological description of the ear region of this didelphid.

The TCFs are rather small (fig. 6A, B), despite this species's intermediate body size (400 g; Amador and Giannini, 2016). On the right side of AMNH M-28329, two TCFs are found, situated close together, but only one occurs on the left (fig. 6A: asterisk). In *P. opossum* ZIUT HL 32 mm there is an anastomotic link between the presumptive ICV and a channel emanating from the body of the basisphenoid (fig. 7A), presumably representing the TCV trunk. In the adult, the rostral branches are typically placed and form a junction, as a probe can be passed through the TCFs (Sánchez-Villagra and Wible, 2002: table 2; J. Wible, personal commun.). In the sectioned specimen the CBF cannot be discriminated, but one is present in the mature stage, as shown by Wible et al. (2021: TCF in their fig. 3). These observations confirm that *Philander* differs from *Didelphis* in having both TCV branches present in the adult, which means that Didelphini is polymorphic for this character.

The diameter of the ICV is large at its point of exit from the skull, but the vein rapidly trans-

forms into a leash of smaller-diameter vessels representing the BVP. The VPS is either very small or possibly collapsed in this specimen (fig. 7B). The IJV (not illustrated) is also small, which if true of the adult as well would be consistent with most encephalic return passing through the PGLVN rather than the IJVS, as noted for *Didelphis* by Dom et al. (1970). Foramina for the IJV and EVPS are incompletely separated (see also Wible et al., 2021). As in most marsupials, the large basijugular sulcus is notched by prominent gutters for condylohyoglossal emissaria.

*CALUROMYS* (DIDELPHIDAE) (figs. 8, 9). The rostral part of the head of *Caluromys* sp. ZIUT PND 77, a juvenile specimen, was well prepared, but the caudal part is less satisfactory. Ossification of the petrosal and central stem is far advanced.

The woolly opossum typically lacks the TCF (Archer, 1976; Voss and Jansa, 2003, 2009)—a feature also recorded by Sánchez-Villagra and Wible (2002) for closely related *Caluromysiops* and as an occasional individual variation in some other didelphid taxa. On both sides of the skull of adult *Caluromys derbianus* AMNH M-18910 (fig. 8) there is a tiny dimple located immediately lateral to the extracranial opening of the carotid canal. Its position is arguably typical for a TCF, although there is no certainty that the feature is correlated with initial TCV presence. If there was

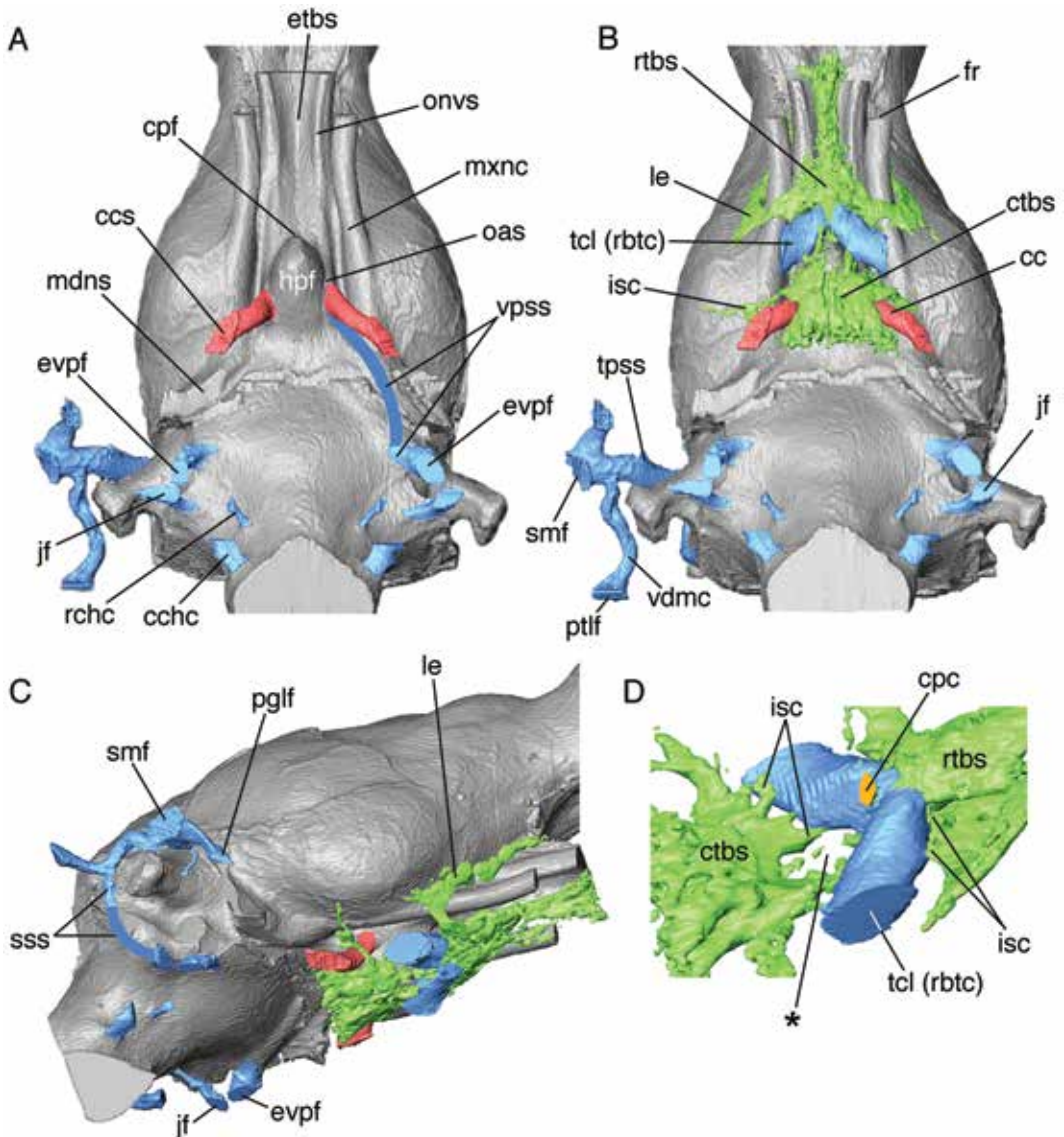
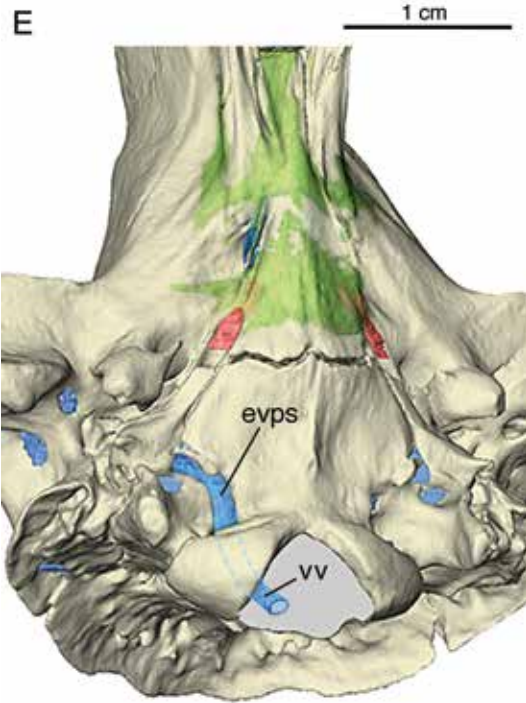


FIG. 4. *Didelphis virginiana* TMM M-2517 (Didelphidae, Didelphimorphia), adult specimen, endocast reconstruction showing osteological features associated with pericarotid venous network and related vasculature (data source, table 2). In this and all other figures depicting endocasts, unless indicated otherwise red-colored structures are casts of carotid canal, and thus represent both internal carotid artery and internal carotid vein. Blue-colored structures mostly represent venous conduits. Isolated portions of certain trackways have been reconnected to restore continuity of ventral petrosal sinus, extracranial continuation of ventral petrosal sinus, and sigmoid sinus. Views: **A**, ventral; **B**, same, with transverse basisphenoid sinus (in green) superimposed; **C**, oblique right lateral; **D**, oblique dorsal closeup of transverse canal junction (simple pattern); **E**, oblique caudoventral surface of intact caudal cranium. In **D**, note craniopharyngeal canal and interstitial canaliculi communicating with transverse canal along different planes. Canals actually open into transverse basisphenoid sinus, although this is not obvious because of color coding. Gap (asterisk) locates positions of cavernous sinus and pituitary. In **E**, extracranial continuation of ventral petrosal sinus reconstructed and shown passing, suc-



cessively, through basijugular sulcus, caudal condylohyoglossal canal, and craniospinal foramen (to emerge as vertebral vein). **Key:** **cc**, carotid canal; **cchc**, caudal condylohyoglossal canal; **ccs**, sulcus leading to carotid canal; **cpc**, craniopharyngeal canal; **cpf**, craniopharyngeal foramen; **ctbs**, caudal portion of transverse basicranial sinus; **etbs**, eminence of transverse basicranial sinus; **evpf**, foramen for extracranial continuation of ventral petrosal sinus; **evps**, extracranial continuation of ventral petrosal sinus (recon.); **fr**, foramen rotundum; **hpf**, hypophyseal fossa; **isc**, interstitial canaliculus examples; **jf**, jugular foramen; **le**, lateral extension of transverse basicranial sinus; **mdns**, sulcus for mandibular nerve; **mxnc**, canal for maxillary nerve; **oas**, sulcus for ophthalmic artery; **onvs**, sulcus for ophthalmic neurovascular array; **pglf**, postglenoid foramen; **ptlf**, posttemporal foramen; **rchc**, rostral condylohyoglossal canal; **rtbs**, rostral portion of transverse basicranial sinus; **smf**, suprameatal foramen; **sss**, sulcus for sigmoid sinus (reconstructed); **tcl (rbtc)**, transverse canal (rostral branch of transverse canal); **tpss**, sulcus for temporal sinus; **vdmc**, canal for vasa diploetica magna; **vpss**, ventral petrosal sinus (reconstructed); **vv**, vertebral vein.

a relationship between the two, then the vessel must have involuted after differentiation, with the consequence that its aperture was later mostly obliterated by remodeling. The sectioned specimen gives no indication that another emissarium might have stood in for the trunk of the TCV (see Discussion). From these considerations, it may be reasonably concluded that, among potential PMDs, only the ICV plays a substantial role in CS drainage in *Caluromys*.

Together, the ICV/BVP and PVP form a plexus directly below the carotid foramen, surrounding the internal carotid artery (fig. 9C). As the caudal portion of the head of this specimen is not well preserved, it was not possible to determine whether the ICV/BVP terminated as usual in the IJV and CSVS, although this is likely. In *C. derbianus* AMNH M-18910, the apertures for the EVPS and IJV are recessed within a single large opening (fig. 8A). The basijugular sulcus as such is absent, because the EVPS at its origin passes almost immediately into a canal that joins the craniospinal foramen in the interior of the exoccipital. This character state is also present in *C. derbianus* AMNH M-18911 and 164491. Conditions in other woolly opossum species were not investigated.

**MONODELPHIS (DIDELPHIDAE)** (figs.10–12). In *M. domestica* ZIUT PND 12, a pouch young of the short-tailed opossum, the auditory capsule is still completely cartilaginous, although small ossification centers in the central stem are evident. By this stage of development, the trunk of the TCV had apparently differentiated and participated in an anastomosis with the ICV (fig. 11A), but the TBS as a distinct space is not yet evident. The ICV/BVP is plexiform for most of its length and receives several branches through the basicapsular fenestra at the presumptive site of the foramen for the EVPS (fig. 11D). Also identifiable is the distal section of the lateral head vein, at a point close to its anastomosis with the IJV (fig. 11F). The VPS is large; its extracranial continuation anastomoses with the IJV and condylar emissaria (see also Wible, 2003). These proportions are carried into the adult stage: in *Monodelphis domestica* AMNH M-133247 the

foramen for the EVPS is notably larger than the jugular foramen (fig. 10B). Sánchez-Villagra and Wible (2002: fig. 2) present a micrograph of a sectioned pouch young in which the transverse canal vein (i.e., RBV) is indicated, but the magnification is low and no details of the intramural passageway can be made out.

In the adult, the intramural conduits for the RBTCs are low but prominent on the basisphenoid's endocranial surface (fig. 10C, 12B–F). The endocranial carotid grooves bear foramina for the CBVs; they are notably large in *M. domestica* AMNH M-133247 and NMB c. III.777 (fig. 10C; 12D: arrow; see also Wible, 2022: fig. 17b). The transverse canal junction is well defined, as in *Caenolestes*, and incorporates somewhat more of the rostral TBS than is the case in *Didelphis*. The result is consistent with the complex junction pattern, but differs from the compound version in which TBS involvement is much greater.

**OTHER DIDELPHIDS.** Rostral and caudal branches of the transverse canal also occur in the mouse opossum *Marmosa* (Archer, 1976; Sánchez-Villagra and Wible, 2002: table 2), as in *Monodelphis*. However, Sánchez-Villagra and Wible, 2002: 29) state that in “*Marmosops noctivagus*, *Gracilinanus* sp., and some specimens of *Thylamys elegans*, the transverse canal foramen simply opens endocranially,” which implies that only the CBTC is present. If Thylamyini lack the RBTC, which seems unlikely, then they would differ substantially from other Didelphinae. This can be resolved with CT scanning.

It would be of interest to know what kind of pattern is present in the largest known extinct didelphid, the Late Pliocene *Thylophoros lorenzini* (estimated body mass, 4.6–7.4 kg; see Goin et al., 2009), assuming that body size influences pattern expression to some extent.

#### PAUCITUBERCULATA

**CAENOLESTES** (CAENOLESTIDAE) (figs. 13, 14). Despite much early interest in the morphology and relationships of *Caenolestes* (e.g., Dederer, 1909; Gregory, 1910; Broom, 1911), a thorough

investigation of its mesocranial anatomy has never been undertaken. Osgood's (1921) monograph provides some information on the carotid and transverse canal foramina, but he did not investigate vascular contents or intracranial connections. Herrick's (1921) complementary study of the external morphology of the brain in *Caenolestes* provides a few helpful observations, such as the size and position of the hypophysis.

As whole specimens of shrew opossums were not available for this study, our analysis is based on a scanned skull (*Caenolestes* sp. IANIGLA uncataloged) supplemented by specimens in the AMNH Mammalogy collection. Within the endocranium, the eminences of the canals for the rostral branches of the TCVs and the rostral TBS form low but very distinct mounds on the endocranial surface of the basisphenoid (figs. 13D; 14A–C). The mesocranium of *Caenolestes* appears to differ little from that of non-*Didelphis* didelphids. In junction pattern *Caenolestes* seems more similar to *Monodelphis* (fig. 12A) than to *Dromiciops* (fig. 15D, 17A–D), in part because the TBS does not surround the RBTC canals.

In figure 13D, the CBF can be seen at the rostral end of the carotid groove; it opens into a short sulcus that communicates with the endocranial carotid foramen and thus the CS/ICV (fig. 12D). In the scanned specimen the CBF is separate from the carotid canal, but in some of the other material examined (e.g., *Caenolestes convelatus* AMNH M-64457) these apertures appear to be continuous. Hypophyseal canaliculi on the periphery of the hypophyseal fossa presumably transmitted small veins to/from the CS (figs. 13D; 14C: feature 1). Similar apertures are lacking in *Didelphis* (fig. 2C).

Sánchez-Villagra and Wible (2002: 28) considered the intramural character state to be absent in *Caenolestes* because a hair probe simply went straight into the endocranium. This illustrates the limits of the probe approach: although the rostral canals are clearly present, probing failed to find them because of the sharp turns that would have been required to manipulate the probe in the proper direction.

Other features of interest are the large apertures situated along the flanks of the rostral TBS well in advance of the junction (fig. 13D: asterisks). These are positioned too rostrally to be morphologically part of the transverse canal apparatus, but they might be related to the ophthalmic veins in some way. Similar foramina were also encountered in dry specimens of *C. fuliginosus* (e.g., AMNH-M 64455).

The basicapsular fenestra is widely open for most of the length of the petrosal-basioccipital interface, but foramina for the EVPS and IJV are distinct and separate. The paired tubes that pass through the lateral margins of the basioccipital (fig. 14E–G: asterisks) communicate with the sulci for the VPS and are doubtless vascular, but their significance is otherwise uncertain. Terminating in the condylohypoglossal foramina, these accessory canals diminish rather than increase in size caudally, indicating that they receive few or no additional vascular inputs.

#### MICROBIOTHERIA

*DROMICIOPS* (MICROBIOTHERIIDAE) (figs. 15–17). *Dromiciops gliroides* ZIUT HL 19 mm was probably an advanced pouch young at the time of its collection, judging from the degree of cranial ossification. The slide set, although adequate for morphological interpretation, exhibits shrinkage artifacts incurred during histological preparation. A slightly damaged near-adult skull of the monito del monte, *Dromiciops gliroides* MACN Ma-23607, was used for endocast reconstruction and segment illustration.

Making allowance for tissue shrinkage in the ZIUT specimen, the ICV and internal carotid artery would have filled the carotid groove (fig. 16D). Presence of the CBV within the groove could not be verified histologically, although its foramen in the scanned specimen confirms its normal presence (figs. 15C, 17C). The ICV at its point of origin from the CS is at least twice as wide as the internal carotid artery (fig. 16E), assuming consistent shrinkage. After leaving the carotid foramen the ICV's caliber rapidly

decreases (fig. 16D) before it becomes continuous with the BVP. Because of the specimen's condition the ICV/BVP could not be satisfactorily traced to the jugular area. Exit points for the EVPS and IJV on the basicranium are quite distinct (fig. 15A).

Although not obvious in the ventral reconstruction (fig. 15E), the basicranial keel of *Dromiciops* is well pneumatized. Pneumatization occurs in the parasphenoid as well as the central and lateral parts of the basisphenoid and presphenoid (figs. 16A, B; 17A–D). The transverse canals (RBTCs) are fully continuous with the rostral TBS, forming a single vacuity with a minor amount of internal subdivision. Their broad continuity is consistent with the compound junction pattern (table 4). The medial aspect of the petrosal is also extensively pneumatized, although it could not be determined whether this was due to, or independent of, middle ear expansion. Sánchez-Villagra and Wible (2002: 30) record the TCF of *Dromiciops* as technically polymorphic (i.e., one known case of absence, in AMNH M-92147, which we confirm). Absence must be rare, however, because Beck et al. (2022: 65) report the TCF as present in every *Dromiciops* specimen they examined that preserved this region (N = 22 specimens).

On either side of the midline a large discontinuity interrupts the lateral margin of the presphenoid, here identified as the pterygopalatine fissure in recognition of its size (fig. 15E; see also D'Elia et al., 2016: fig. 7). This is not the TCF, which lies in its expected place on the basisphenoid or in the basisphenoid-alisphenoid interface, lateral to the carotid foramen (Beck et al., 2022). In the sectioned juvenile the pterygopalatine fissure transmits only the nerve of the pterygoid canal (fig. 16A: asterisk), despite the aperture's size and the nearby presence of large vessels like the ophthalmic veins. Large fissures in this location occur in some other marsupials (e.g., *Perameles*, fig. 32A), presumably with the same content. In cases in which the fissure is small or subdivided, it might be better labelled the rostral foramen for the nerve of the pterygoid

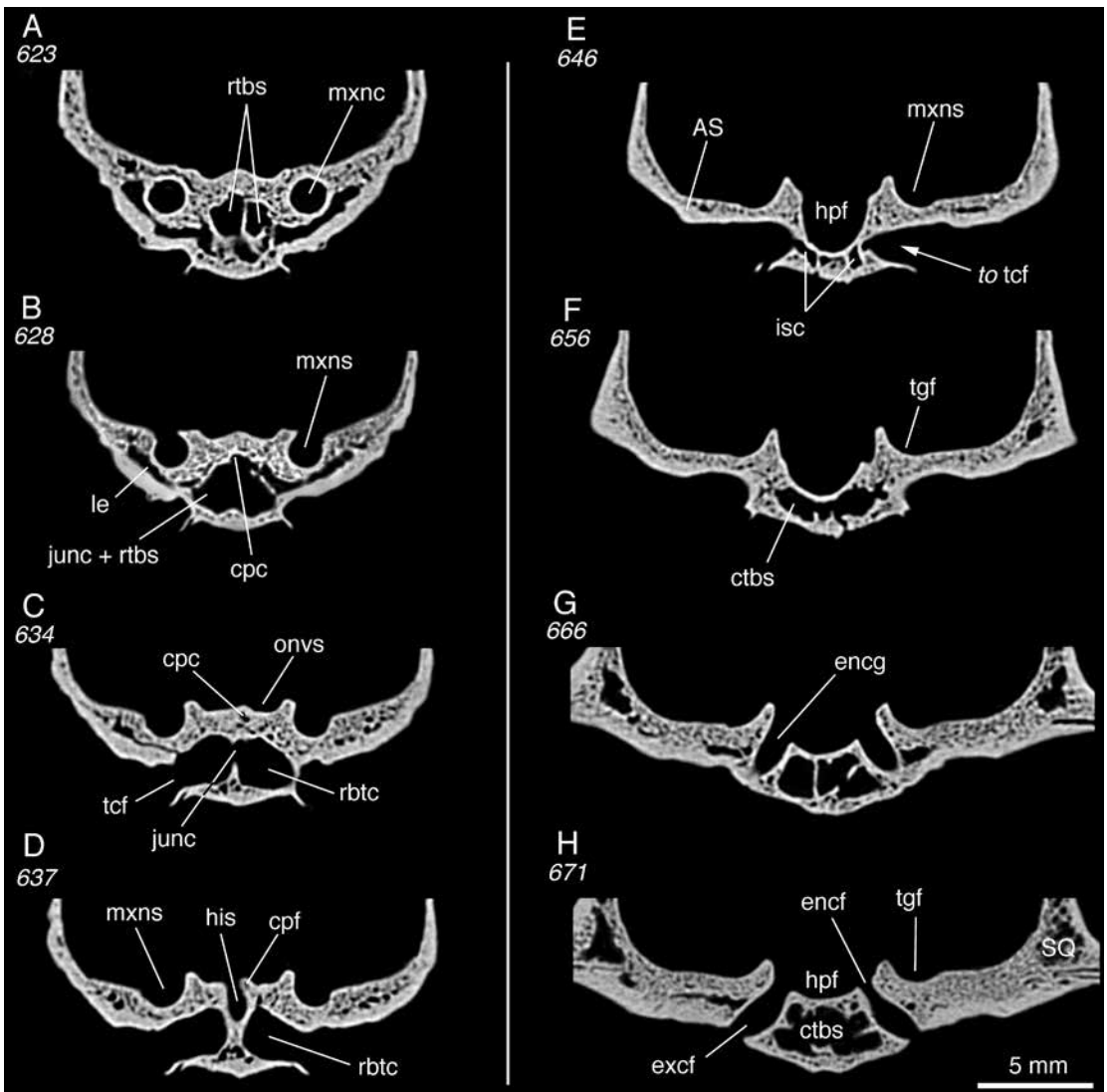
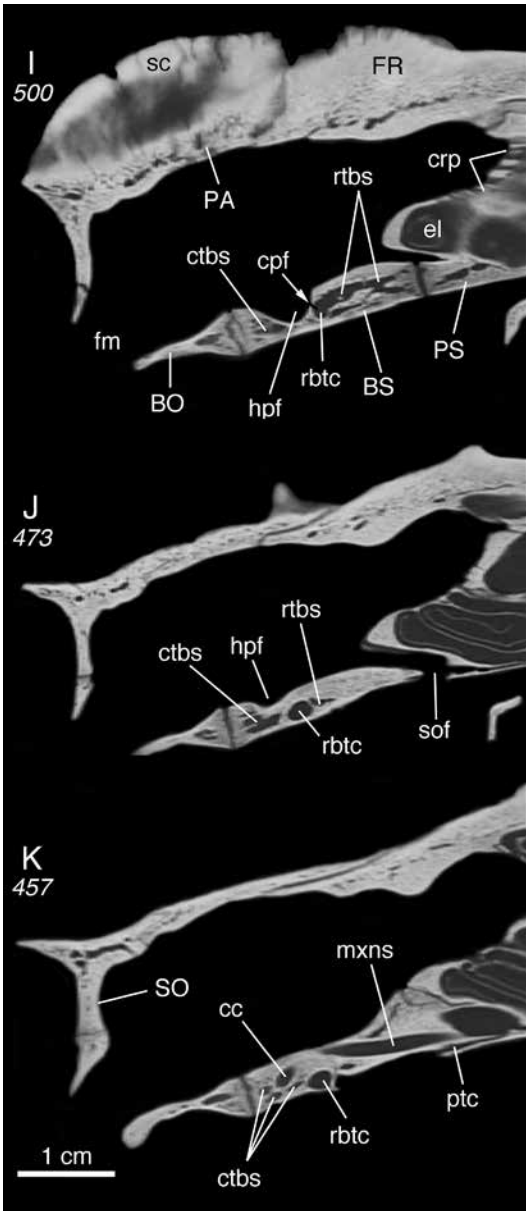


FIG. 5. *Didelphis virginiana* TMM M-2517 (Didelphidae, Didelphimorphia), adult caudal cranium, selected coronal (A–H) and parasagittal (I–K) segments (data source, table 2). In A and B, note junction of rostral branches of transverse canals, communicating with but not enveloped by transverse basisphenoid sinus. Boundary between transverse basisphenoid sinus and regular diploe is gradational. In B–D, craniopharyngeal canal, of uncertain function, connects transverse canal junction with hypophyseal infundibular sulcus (see also I). In E, true caudal branches of transverse canals are absent; only short interstitial canaliculi represented. In J and K, pneumatized areas (possible additional sites of hematopoiesis) also seen in basioccipital and presphenoid). **Key:** AS, alisphenoid; BO, basioccipital; BS, basisphenoid; cc, carotid canal; cpc, craniopharyngeal canal; cpf, craniopharyngeal foramen; crp, cribriform plate; ctbs, caudal portion of transverse basisphenoid sinus; el, ethmoid labyrinth; encf, endocranial carotid foramen; encg, endocranial carotid groove; excf, exocranial carotid foramen; fm, foramen magnum; FR, frontal; his, hypophyseal infundibular sulcus; hpf, hypophyseal fossa; isc, interstitial canaliculus; unc, junction of transverse canals; unc + rtbs, combined junction and rostral transverse basisphenoid sinus; le, lateral extension of transverse basisphenoid



sinus; **mxnc**, maxillary nerve canal; **mxns**, maxillary nerve sulcus; **onvs**, sulcus for ophthalmic neurovascular array; **PA**, parietal; **PS**, presphenoid; **ptc**, pterygoid canal; **rbtc**, rostral branch of transverse canal; **rtbs**, rostral portion of transverse basisphenoid sinus; **sc**, sagittal crest; **SO**, supraoccipital; **sof**, sphenoorbital fissure; **SQ**, squamosal; **tcf**, transverse canal foramen; **tgf**, trigeminal ganglion fossa.

canal, to distinguish it from the foramen at the canal's tympanic end (i.e., caudal foramen for the nerve of the pterygoid canal).

#### DIPROTODONTIA

**NOTAMACROPUS AND OSPHRANTER** (MACROPODIFORMES, MACROPODIDAE) (figs. 18–20). This large family is represented in the comparative set by several specimens, including a serially sectioned perinatal specimen of *Notamacropus* (= *Macropus*) *eugenii* ZIUT HL 29 mm (fig. 19). The specimen's head was divided midsagittally prior to histological preparation, and only the right half was available for study. As a result, structures on or near the midline are not well represented. Aplin (1990) described another specimen of the same species, of known age (28-day pouch young). Judging from his micrographs, the degree of ossification of the auditory capsule (fully cartilaginous except in the region of the fenestra cochleae) is similar to that of the ZIUT specimen. Our macropodid material also includes juveniles of *N. eugenii* AMNH M-197003 (fig. 18A, B), the tamar wallaby, and *Osphranter* (= *Macropus*) *robustus* AMNH M-80171 (fig. 18C), the common wallaroo.

In the sectioned *N. eugenii*, the vein identified by the red pointer in figure 19A is interpreted as the presumptive TCV because it is the only external channel that joins the ICV within the mesocranium. The TCV, ICV, and CS freely communicate around the site of the developing carotid canal in this specimen. Figure 20 illustrates the probable organization of the large vessels that would have passed through the mesocranium in *O. robustus* during life, although no claim for accuracy in their shapes is made. A diagnostic feature of the hybrid pattern is the absence or great reduction of the intramural RBTC pathway. Instead, only the CBTC pathway is clearly present, indicated by the very large CBF. The importance of the CBV is underlined by the fact that its foramen is equivalent in width to the canal for the TCV trunk, which makes

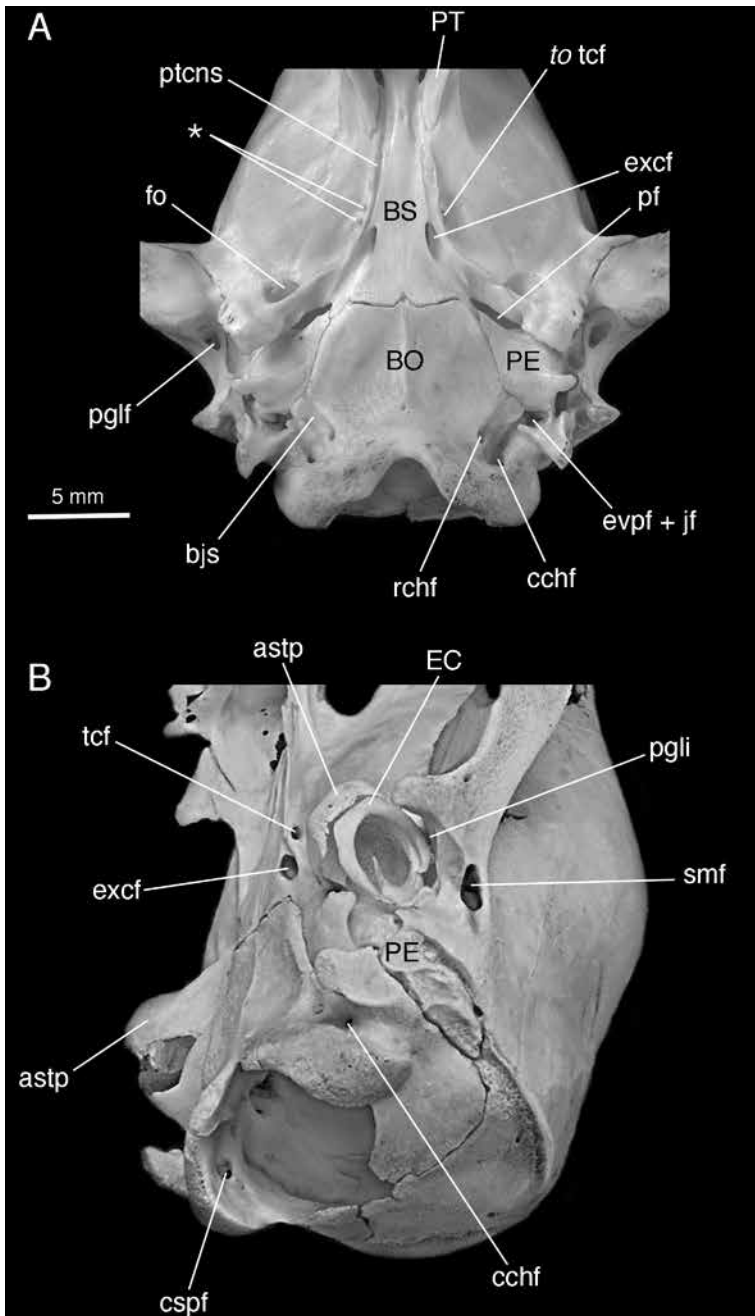


FIG. 6. In **A**, *Philander opossum* AMNH M-28329 (Didelphidae, Didelphimorphia), adult specimen, ventral view. In **B**, *P. opossum* AMNH M-266385, juvenile specimen, caudal cranium in oblique caudolateral view. Note relatively small size of transverse canal foramina in both specimens compared with exocranial carotid foramen (double foramina on right side in A, asterisk). Note also joint foramen for external continuation of ventral petrosal sinus and internal jugular vein. **Key:** *astp*, tympanic process of alisphenoid; *bjs*, basijugular sulcus; *BO*, basioccipital; *BS*, basisphenoid; *cchf*, caudal condylohyopoglossal foramen; *cspf*, craniospinal

sense because it is the latter's only major tributary (fig. 18C).

The fact that the CBTC pathway passes immediately into the braincase is consistent with Sánchez-Villagra and Wible's (2002: 30) probe-based observation that "in no case in our study was an intramural bilateral connection found" in any macropodiform. It is also consistent with Aplin's (1990: 185) observation that in macropodids the connection with the CS "is made via one or more transverse canal foramina: they are usually located in the most deeply excavated region of the medial pterygoid fossa and open directly into the lateral wall of the hypophyseal fossa" (see figs. 18C, 20A–C). Aplin (1990: 184) also noted that the ICV (= pericarotid vein) was "sizeable" in his wallaby specimen and that it was "connected with the prevertebral plexus [= BVP, pharyngeal plexus] and with the posterior emissary vein [= ?EVPS] via the posterior lacerate foramen."

Aplin (1990: 191) tried to trace the formation of the TCF and its associated canal by comparing perinatal stages of several different macropodid species: "A transverse canal emissary foramen is first observed at Stage 3; ... the late appearance of this emissary vein suggests that it forms as a direct consequence of the progressive excavation of the medial surface of the pterygoid fossa, perhaps through the annexation of an existing intraosseous vascular component." Stage 3, of a total of 5 stages, is defined as representing "more advanced pouch-young" (Aplin, 1990: 150), although the only criterion for staging mentioned in Aplin's table 3.1 is premolar/molar eruption status. How "progressive excavation" and "annexation of an existing vascular component" might lead to the formation of the TCV is insufficiently explained. Aplin's observations might alternatively concern the developing TBS and onset of blood cell production, but this has not yet been demonstrated to occur in macropo-

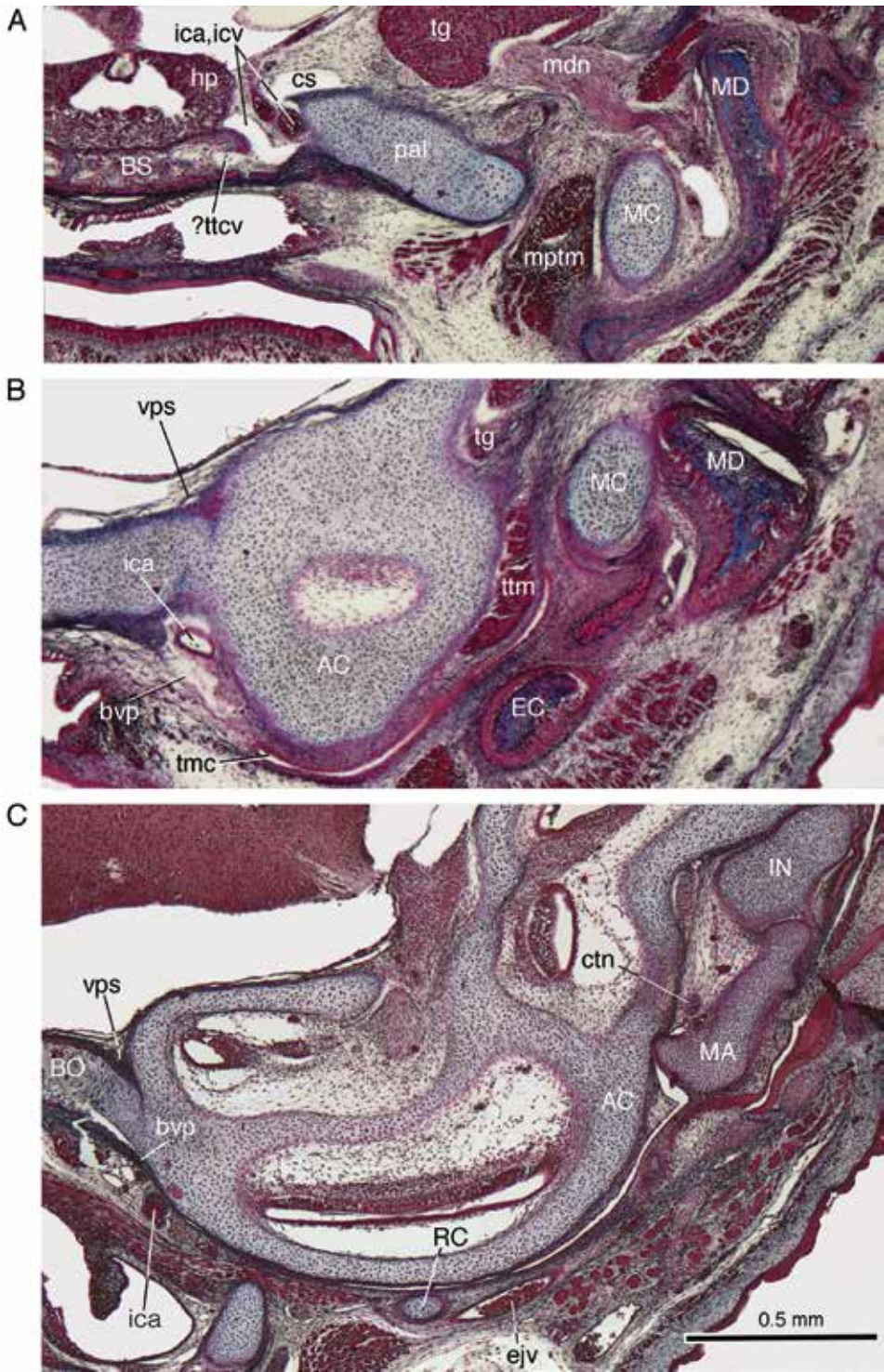
did. Also, the number of transverse canals is variable: in *O. robustus* AMNH M-80171 there are accessory transverse canals (fig. 20A; see also *Trichosurus*, fig. 22B).

Aplin's (1990: fig. 3.6b) venogram of an ?adult *Potorous tridactylus* is of interest because he identified a remarkably large ICV/BVP (= pericarotid vein) in this specimen. Because of vessel overlaps, his identification is difficult to verify. Although ICV/BVP hypertrophy cannot be excluded in this species, nothing similar has been reported for other taxa. For example, in the perinatal ZIUT specimen of *Notamacropus* the VPS is not especially large, but neither is the ICV, and as usual the plexiform ICV/BVP rapidly diminishes caudally (fig. 19C). If relative vessel size were similar in the adult, venous return from the ICV/BVP to the IJV would be limited, also as expected. By contrast, according to its venogram the EJV is massive in *Potorous*, indicating a dural drainage pattern apparently dominated by the PGLVN, which is also the case in *Macropus* (sensu Aplin, 1990).

*TRICHOSURUS* (PHALANGERIFORMES, PHALANGERIDAE) (figs. 21, 22). On each side of the scanned specimen of the brushtail possum, *Trichosurus vulpecula* TMM M-849, a primary and a smaller accessory TCF occur in close proximity (figs. 21B, 22B–F). Their suggested homologies as branches of the TCV trunk are indicated in the figures, but verification is still required (see below). Their canals open directly into the compound vacuity shared with the rostral TBS. On the endocranial floor, two large, partly overlapping apertures perforate the TBS eminence at the presumptive location of the pituitary body and CS (fig. 21A; asterisk, fig. 22B–D). In the dry skull of another specimen, *T. vulpecula* AMNH 48055, conditions are similar except that the apertures are much smaller and can be interpreted as a group of

---

venous foramen; **EC**, ectotympanic; **excf**, exocranial carotid foramen; **evpf + jf**, external continuation of ventral petrosal sinus and jugular foramen; **fo**, foramen ovale; **PE**, petrosal; **pf**, piriform fenestra; **pgli**, postglenoid incisure; **pglf**, postglenoid foramen; **PT**, pterygoid; **ptcns**, sulcus for nerve of pterygoid canal; **rchf**, rostral condylohyoglossal foramen; **smf**, suprameatal foramen; **tcf**, transverse canal foramen.



hypophyseal canaliculi (fig. 21D). Aplin (1990: 326) made no mention of large apertures on the eminence of the TBS of *Trichosurus*, but did say that “the primary canal is connected intraosseously with the carotid canal [?in the carotid groove], and thus has no direct communication with the cavernous sinus.” These remarks may be contradictory, as CBFs are represented on the endocast of *Trichosurus vulpecula* TMM M-849 and therefore direct communication with the CS does occur in this taxon (figs. 21C, D; 22E, F).

Clearly, additional investigation will be needed to clear up apparent discrepancies before anything definitive can be said about PCVN organization in bush-tail possums (or phalangeriforms generally). At present the available evidence for *Trichosurus* is consistent with the interpretation that the main transverse canal represents the CBTC rather than the RBTC. This is supported by the observation that CBFs can be identified in the carotid grooves, even though Aplin’s (1990) text as written seems to exclude contact with the CS/ICV. In this scenario the accessory transverse canal could be a reduced or perhaps defunct RBTC, which is the interpretation favored in figure 42. A similar issue affects interpretation of *Osphranter* (fig. 20A). Rather than propose yet another junction pattern at this time, we provisionally conclude that the architecture seen in *Trichosurus* conforms better to the hybrid pattern than the compound pattern, and include this taxon under the former heading in table 4 (but in parentheses) and in figure 42.

With regard to other points of interest, the jugular foramen is larger on the left side of the scanned specimen than on the right (fig. 21C, E). Such asymmetries are evident in other specimens in the comparative set (e.g., *Didelphis*, fig. 3; *Thylacinus*, fig. 30) and may be a common variation in certain species. Both rostral and caudal condylohypoglossal foramina are present (fig. 21A), but the basijugular sulcus is either not evident or noncontinuous along its usual pathway. Aplin (1990: 324) found a small foramen on the medial side of the foramen ovale in specimens of *Trichosurus*. He attributed the additional aperture to the passage of the ramus medialis of the mandibular nerve, but another possibility is that it transmitted an emissary (in this case, v.e. foraminis ovalis). TMM M-849 exhibits a foramen in apparently the same location (fig. 21E: double asterisks).

**OTHER PHALANGERIFORMS.** According to Aplin (1990: 326), the TCF is either very small or altogether absent in several taxa, including most species of the phalangerids *Phalanger* and *Spilocuscus*, the petaurid *Petaurus*, as well as the burramyid *Cercartetus lepidus* and the related tarsipedid *Tarsipes rostratus*. However, there is a difference between “small” and “absent.” According to Beck et al. (2022), who checked Aplin’s results in their survey, the only “possum” taxon in which the TCF is consistently completely absent is *Tarsipes*, although sporadic absence occurs in others.

How PMD drainage is conducted in marsupials that lack a designated TCF is of interest. In a sectioned and stained specimen of *Acrobates pygmaeus*, Aplin (1990: 326) noted that a “major

FIG. 7. *Philander* sp. ZIUT HL 32 mm (Didelphidae, Didelphimorphia), perinatal specimen, stained coronal sections in rostrocaudal order. **A**, section through hypophysis, with presumptive transverse canal vein (?trunk or branch) adjacent to internal carotid vein (s. 28.04.01); **B** and **C**, rostral and middle portions of auditory capsule, showing multiply branched basicranial venous plexus and (in this specimen) relatively small ventral petrosal sinus (ss. 30.03.02, 35.04.03). Developmentally this is youngest specimen in comparative set. **Key:** **AC**, auditory capsule; **BO**, basioccipital; **BS**, basisphenoid; **bvp**, basicranial venous plexus; **cs**, cavernous sinus; **ctn**, chorda tympani nerve; **EC**, ectotympanic; **eju**, external jugular vein; **hp**, hypophysis; **ica**, internal carotid artery; **icv**, internal carotid vein; **IN**, incus; **MA**, malleus; **MC**, meckelian cartilage; **MD**, mandible; **mdn**, mandibular nerve; **mptm**, medial pterygoid muscle; **pal**, processus alaris; **RC**, reichertian cartilage; **tg**, trigeminal ganglion; **tmc**, tympanic cavity; **?ttcv**, trunk of transverse canal vein or branch; **ttm**, tensor tympani muscle; **vps**, ventral petrosal sinus.

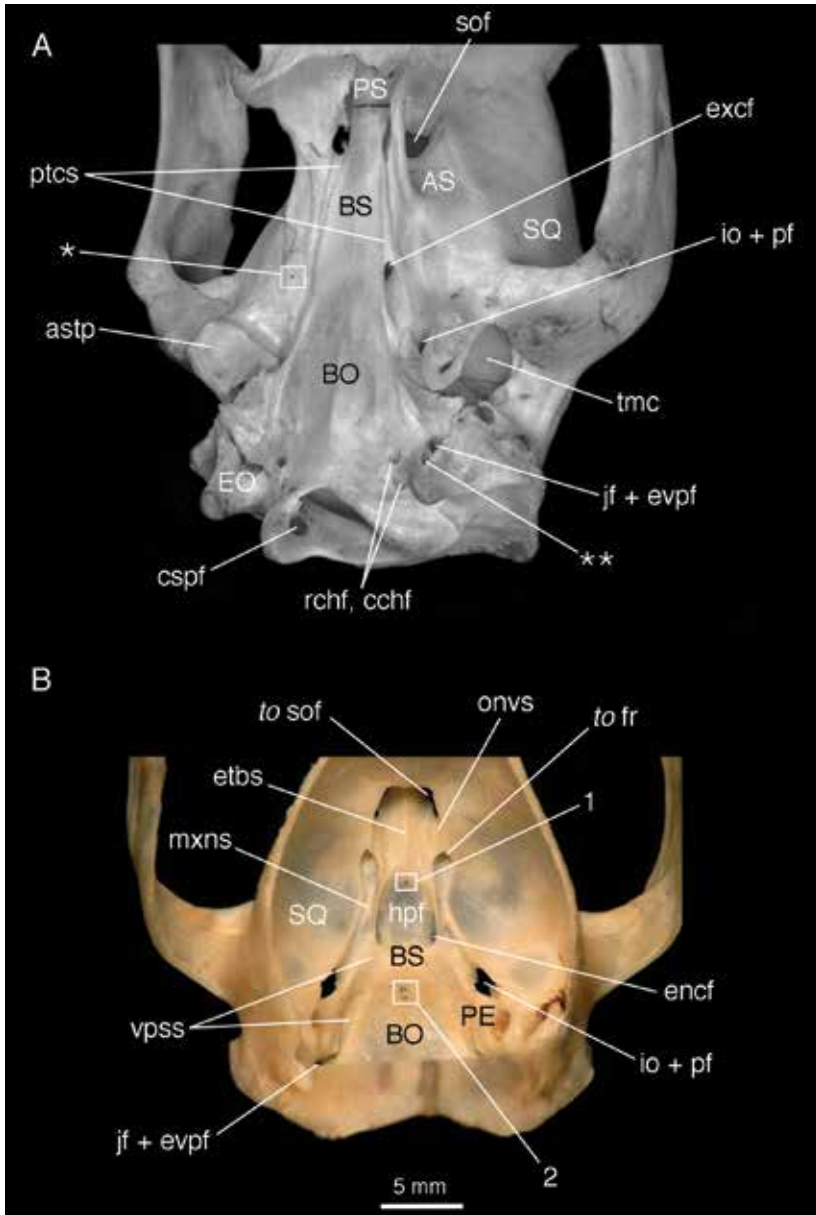


FIG. 8. **A**, *Caluromys derbianus* AMNH M-18910 (Didelphidae, Didelphimorphia), adult caudal cranium in oblique caudoventral view. **B**, *Caluromys* sp. AMNH M-184599 (Didelphidae, Didelphimorphia), adult caudal cranium in endocranial view. Although transverse canal foramen is usually scored as completely absent in the short-tailed opossum group, in **A** a tiny dimple (single asterisk) lateral to exocranial opening of right carotid canal may represent vestige of vein's trackway, assuming it differentiated but did not persist. Equivalent opening is not seen on left side or in **B**. There is no swelling or eminence for transverse canals on endocranial floor, consistent with rostral branch tubes not being present. Endocranial carotid grooves contain only one aperture, for internal carotid neurovascular bundle, indicating caudal branch of transverse canal vein is also absent in this taxon. Note well marked foramina for craniopharyngeal (feature 1) and notochord (feature 2) canals.

emissary vein,” traveling in an open sulcus on the mesocranium, “is connected medially to the pericarotid vein [i.e., ICV], and laterally, to an anterior vein of the pterygoid plexus.” This emissarium was therefore conducted through the carotid canal, which is different from the usual CBTC pathway through an independent TCF. Aplin (1990) did not address this issue further, evidently assuming that lack of a separate foramen and passage through the carotid canal did not affect vessel homology.

The TCF is also said to be absent in another acrobatid that Aplin examined, *Distoechurus pennatus*. We found that a pseudoforamen occurs at the TCF’s usual site in *D. pennatus* AMNH M-105938. This feature is created by a partly calcified or ossified ligament (?sphenopetrosal ligament) that walls off a groove directly connected to the carotid canal (fig. 23). This suggests, but does not settle, whether the carotid canal is the exit foramen for the putative TCV as well as the ICV. As in the case of *Trichosurus*, determining the junction pattern of *Distoechurus* is problematic and placement must be provisional (see table 4).

**VOMBATUS** (VOMBATIFORMES, VOMBATIDAE) (figs. 24, 25). According to Sánchez-Villagra and Wible (2002: 30), wombats and koalas are the only diprotodontians known to exhibit intramural union of right and left transverse canals (i.e., RBTCs of this paper). Aplin (1990: plate 4.12a) pointed to additional PCVN-related similarities between *Vombatus* and *Phascolarctos*, and commented on the great size of the TCFs (frequently multiple) found in both (Aplin, 1990: 255).

Wegner (1964: 33) stated that the transverse canals are missing in vombatids, but they are illustrated in his figure 22. In the common wombat *V. ursinus* TMM M-2953 the rostral branches of the transverse canals produce a conspicuous midline junction, visible endocranially (figs. 24C, 25A–C) as in *Didelphis* (figs. 2C, 5C). These taxa differ, however, in that the opossum lacks caudal branches (simple pattern), while in the wombat they are present and large (complex pattern; fig. 25C–G).

The rostral and caudal portions of the TBS are extensive, with areas of trabecularization as well as rarefaction, as would be expected in a large-bodied taxon like the common wombat (table 2). However, TBS communication with either set of transverse canal branches appears negligible, consisting only of small interstitial canaliculi. There is a patent craniopharyngeal canaliculus that joins the transverse canal junction (fig. 25C, D), but as in other cases its vascular role, if any, is not known. Foramina for the EVPS and IJV are well separated and the basijugular sulcus is deeply etched.

#### DASYUROMORPHIA

**DASYURUS** (DASYURIDAE) (figs. 26, 27). A scanned adult of the northern quoll *Dasyurus hallucatus* TMM M-6921 was accessed for this study, along with intact specimens of this species in the AMNH collection. Archer (1976: 252), who examined a number of species in this genus, explicitly described the transverse canal as bifurcated in most specimens, one branch (CBTC) communicating with the carotid foramen (=

← Extracranial continuation of ventral petrosal sinus does not cross external aspect of exoccipital; vessel passes instead directly into an intramural canal (double asterisks) linked to condylohypoglossal canals. Basijugular sulcus barely represented. Compare small size of jugular foramen to that of craniospinal foramen. **Key:** **AS**, alisphenoid; **astp**, tympanic process of alisphenoid; **BO**, basioccipital; **BS**, basisphenoid; **cchf**, caudal condylohypoglossal foramen; **cspf**, craniospinal venous foramen; **enfc**, endocranial carotid foramen; **EO**, exoccipital; **etbs**, eminence of transverse basisphenoid sinus; **excf**, exocranial carotid foramen; **fr**, foramen rotundum; **hpf**, hypophyseal fossa; **io + pf**, combined incisura ovalis and piriform fenestra; **jf + evpf**, joint aperture formed by jugular foramen and extracranial continuation of ventral petrosal sinus; **mxns**, sulcus for maxillary nerve; **onvs**, sulcus for ophthalmic neurovascular array; **PE**, petrosal; **PS**, presphenoid; **ptcs**, sulcus for nerve of pterygoid canal; **rchf**, rostral condylohypoglossal foramen; **sof**, sphenoorbital fissure; **SQ**, squamosal; **tmc**, tympanic cavity; **vpss**, sulcus for ventral petrosal sinus.

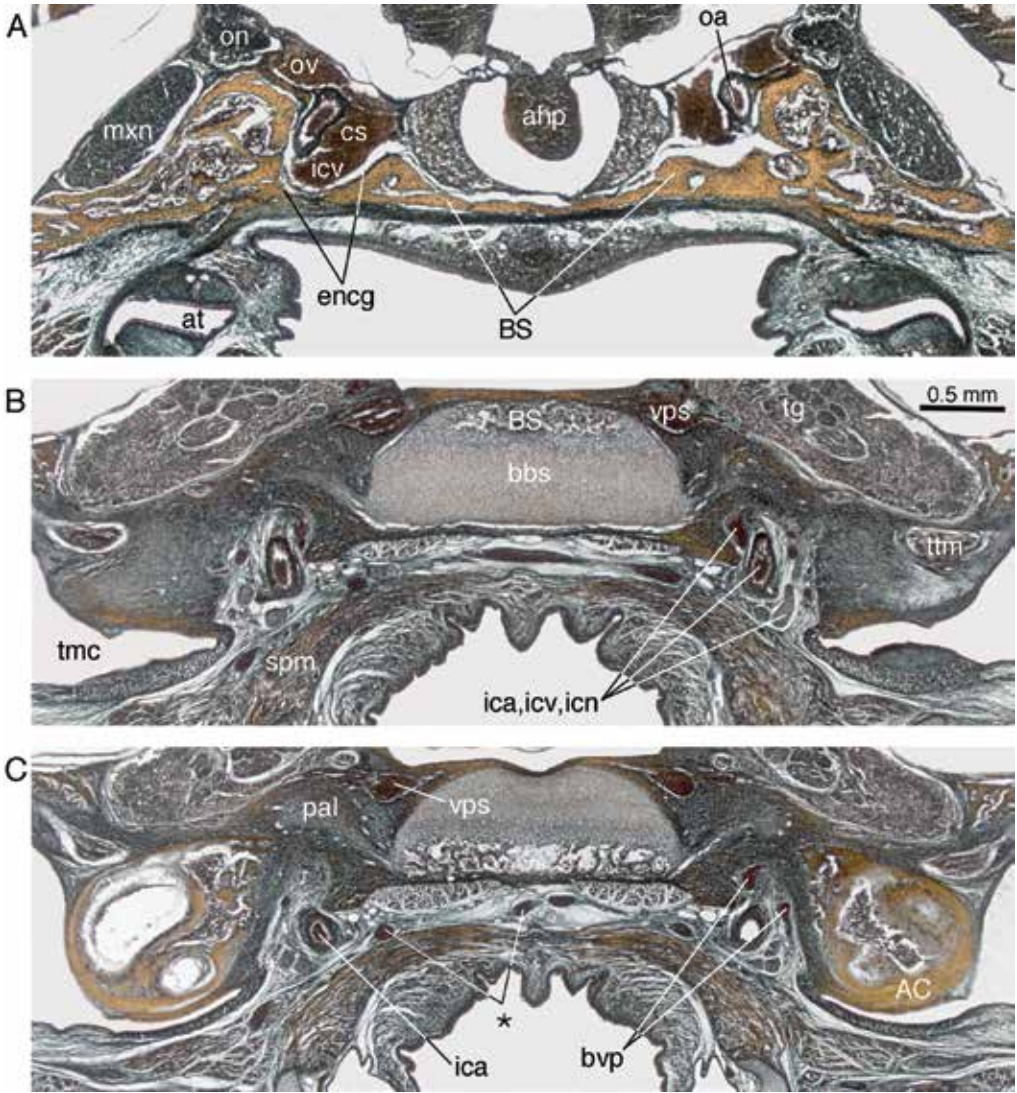
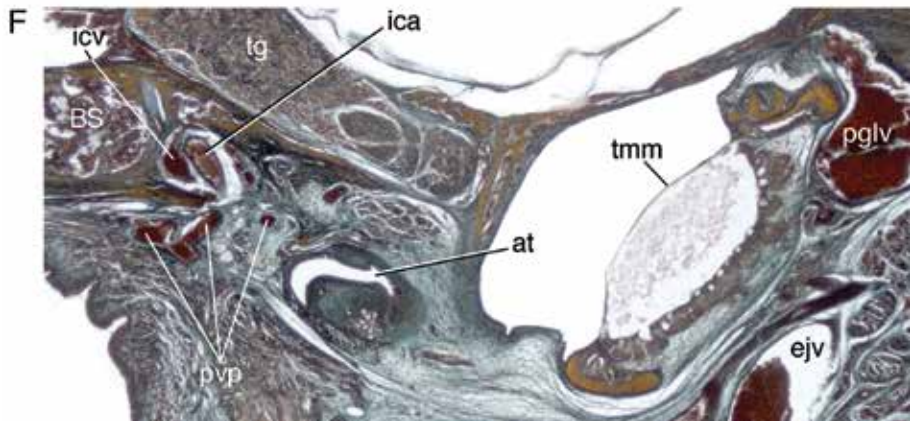
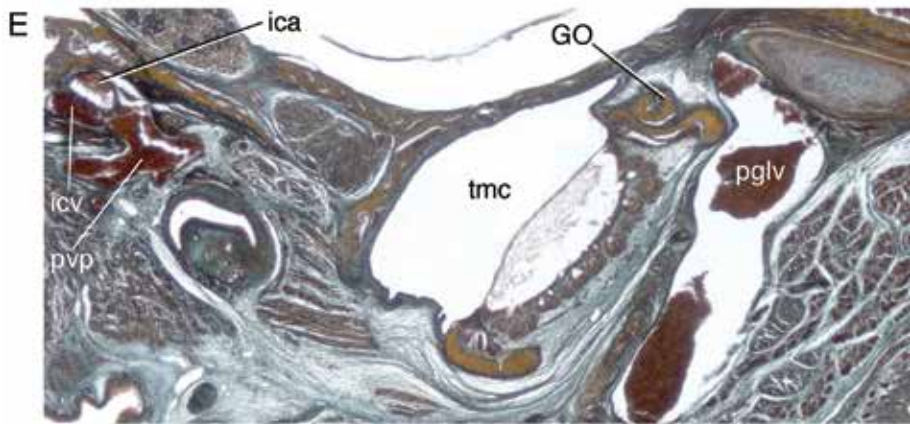
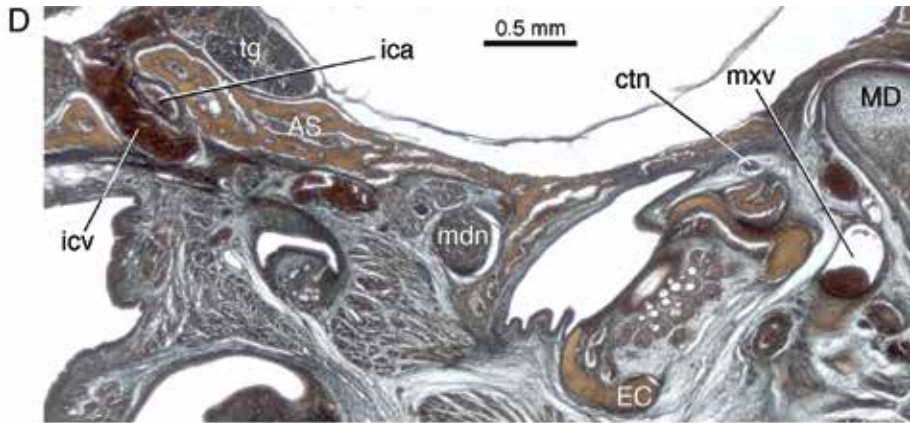
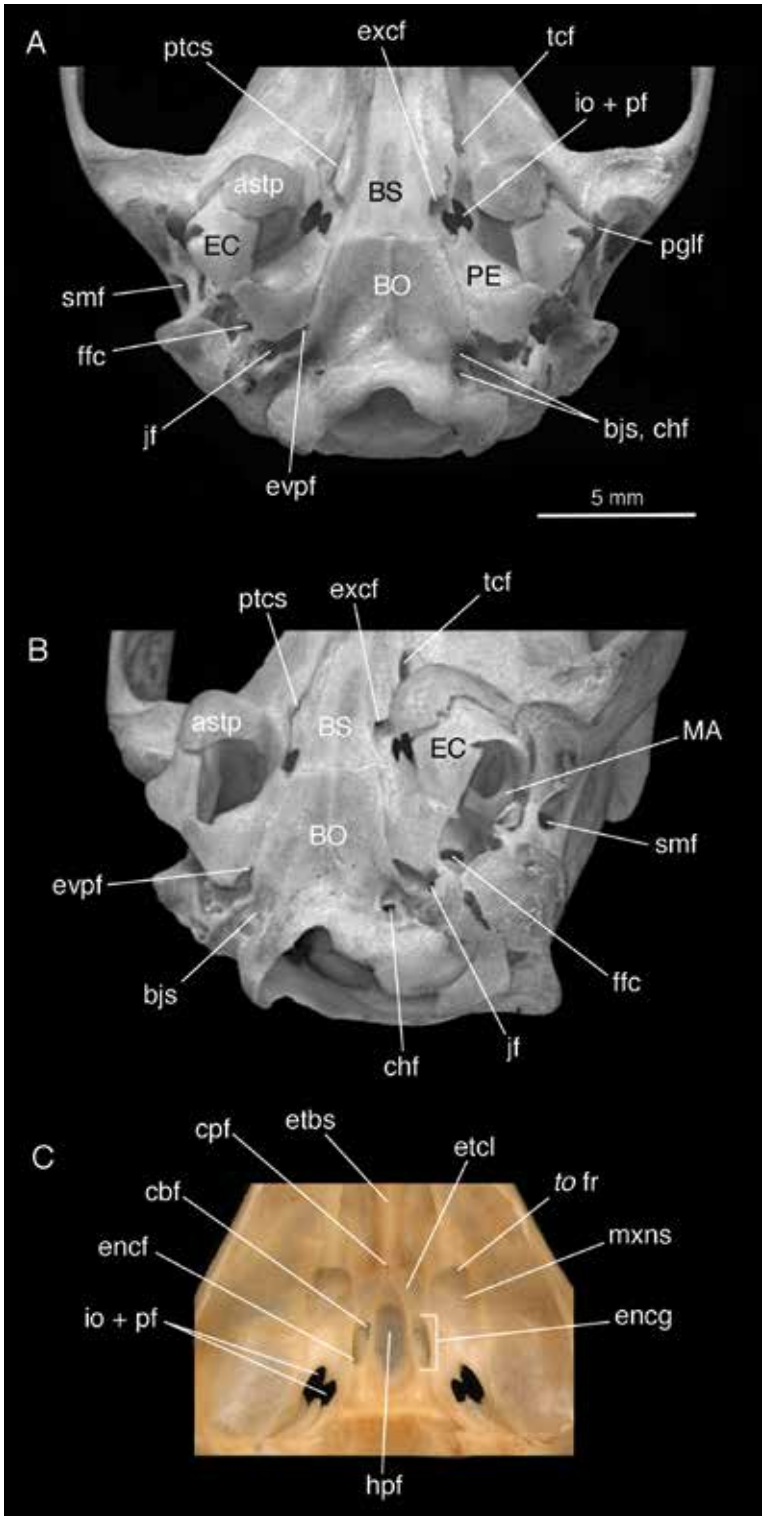


FIG. 9. *Caluromys* sp. ZIUT PND 77 (Didelphidae, Didelphimorphia), postnatal specimen, stained coronal sections in rostrocaudal order. A–C, sections through rostral portion of transverse basisphenoid sinus (ss. 71.02.02, 78.03.02, 79.03.02); D–F, sections through rostral end of tympanic cavity and carotid canal, showing rapid diminution of internal carotid vein (ss. 76.03.03, 77.02.03, 77.03.01). There is no evidence of trunk of transverse canal vein or its branches in expected positions. Internal carotid artery and vein still fill endocranial carotid grooves, even though shrinkage occurred during histological processing. Asterisk, branches of pharyngeal and pterygoid plexuses. **Key:** AC, auditory capsule; ahp, adenohypophysis; AS, alisphenoid; at, auditory tube; bbs, basisphenoid-basioccipital synchondrosis; BS, basisphenoid; bvp, basicranial venous plexus; cs, cavernous sinus; ctn, chorda tympani nerve; EC, ectotympanic; ejv, external jugular vein; encg, endocranial carotid groove; GO, goniale; ica, internal carotid artery; icn, internal carotid nerve; icv, internal carotid vein; MD, mandible; mdn, mandibular nerve; mxn, maxillary nerve; mxv, maxillary vein; oa, ophthalmic artery; on, ophthalmic nerve; ov, ophthalmic vein; pal, processus alaris; pglv, postglenoid vein; pvp, pterygoid venous plexus; spm, stylopharyngeus muscle; tg, trigeminal ganglion; tmc, tympanic cavity; tmm, tensor tympani muscle; vps, ventral petrosal sinus.





endocranial carotid groove), the other branch (RBTC) joining the “cellular sinus in anterior midline of basisphenoid” (= TBS). The CBTC pathway is not distinct in our scanned specimen, but the large opening on the rostral wall of each carotid groove confirms that the CBV was present in life (arrows, fig. 27D). Endocranially, the rostral TBS exhibits modest relief and forms a junction with the RBTCs (fig. 27A–C). The position of the hypophyseal fossa is not marked by any special feature, but is assumed to lie as usual between the endocranial carotid foramina (fig. 27E).

Exocranially, there is an appreciable distance between the TCF and the undivided piriform fenestra/incisura ovale (fig. 26), which appears to be the case in most dasyuromorphians. As is especially obvious in the segment series, *Dasyurus* (fig. 27) is very similar to *Monodelphis* (fig. 12) for the characters under consideration, but quite different in body size (1000–1500 g and (60–100 g, respectively). Both are considered to exhibit the complex pattern (table 4).

*SARCOPHILUS* (DASYURIDAE) (fig. 28). The only published study that includes empirical information on the cephalic vascular system of the Tasmanian devil *S. harrisi* is that of Shah and Nichol (1989). In their paper, principal cephalic veins are identified on a venogram and accompanying interpretative diagram (Shah and Nichol, 1989: fig. 2; partly reproduced here as fig. 28D). Neither Archer (1976) nor Sánchez-Villagra and Wible (2002) present any specific information on PCVN components in this species.

From Shah and Nichol’s venogram it is possible to infer that the TCV, labelled as “PS” (pterygoid sinus), is of substantial size in this taxon. This accords with the large caliber of the TCFs on the skull (fig. 28B), but does not provide the details necessary for assigning a junction pattern.

The top of the skull of an adult no-data specimen (AMNH M-35535) was removed in order to gain access to the cranial interior (fig. 28C). A point of interest is the condition of the endocranial carotid grooves in this specimen, which are notably asymmetric. On the left side, the large carotid groove exhibits both the carotid canal and a large foramen on its rostral wall, which by its position must be the CBF. By contrast, the right groove is considerably shallower, especially rostrally, and lacks a CBF. Yet there is an external TCF on the right side, which means that there was a functional TCV in life. Probing is of little help: when inserted into the specimen’s right TCF, it always emerges through the CBF, which gives no indication whether a rostral pathway is also present, as in the majority of investigated dasyuromorphians (see Archer, 1976; Sánchez-Villagra and Wible, 2002). The endocranial evidence is similarly ambiguous: there is no convincing eminence for the RBTCs rostral to the hypophyseal fossa, but in large-bodied species a discernible ridge is not always present. The large bilateral “pterygoid sinus” veins illustrated in the venogram do not show the slight arching of the RBTC at the point of their junction as seen in *Didelphis* or *Caenolestes*; instead, they run in

←  
 FIG. 10. *Monodelphis domestica* AMNH-M 133247 (Didelphidae, Didelphimorphia), adult caudal cranium in **A**, ventral, **B**, oblique caudoventral, and **C**, endocranial views. In investigated didelphids, foramen ovale (or incisura ovalis) is relatively displaced caudomedially in comparison to its position in most other marsupial taxa, and is not distinctly separated from piriform fenestra in adult. There is only a single condylohypoglossal foramen in this specimen. Suprameatal foramen is substantially larger than slitlike postglenoid incisure. **Key:** **astp**, tympanic process of alisphenoid; **bjs**, basijugular sulcus; **BO**, basioccipital; **BS**, basisphenoid; **cbf**, caudal branch foramen; **chf**, condylohypoglossal foramen; **cpf**, craniopharyngeal foramen; **EC**, ectotympanic; **encf**, endocranial carotid foramen; **encg**, endocranial carotid groove; **etbs**, eminence of transverse basicranial sinus; **etcl**, eminence of transverse canals; **evpf**, foramen for extracranial continuation of ventral petrosal sinus; **excf**, exocranial carotid foramen; **ffc**, fossula fenestrae cochleae; **fr**, foramen rotundum; **hpf**, hypophyseal fossa; **io** + **pf**, incisura ovalis and piriform fenestra; **jf**, jugular foramen; **MA**, malleus; **mxns**, maxillary nerve sulcus; **PE**, petrosal; **pglf**, postglenoid foramen; **ptcs**, sulcus for nerve of pterygoid canal; **smf**, suprameatal foramen; **tcf**, transverse canal foramen.

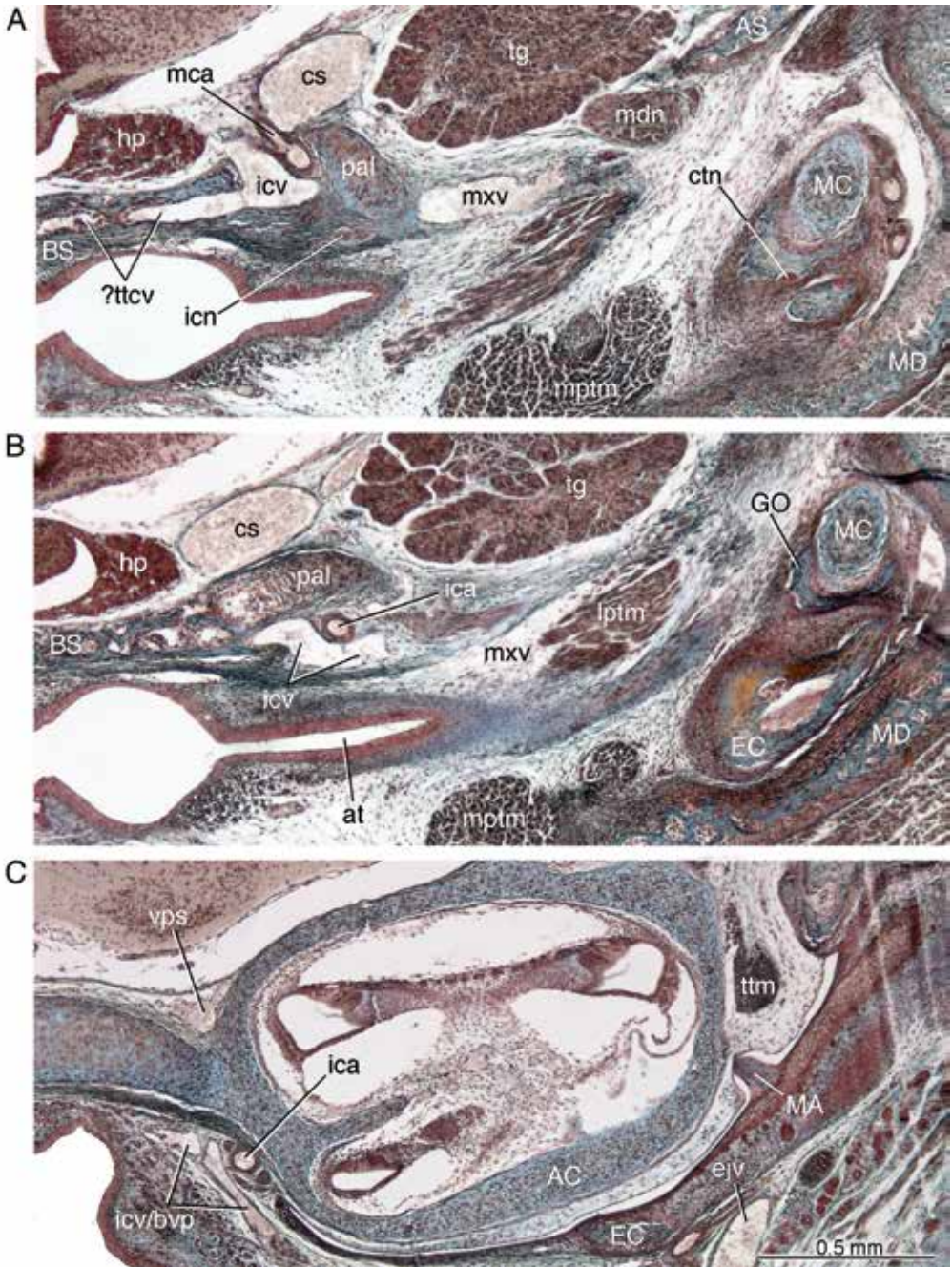
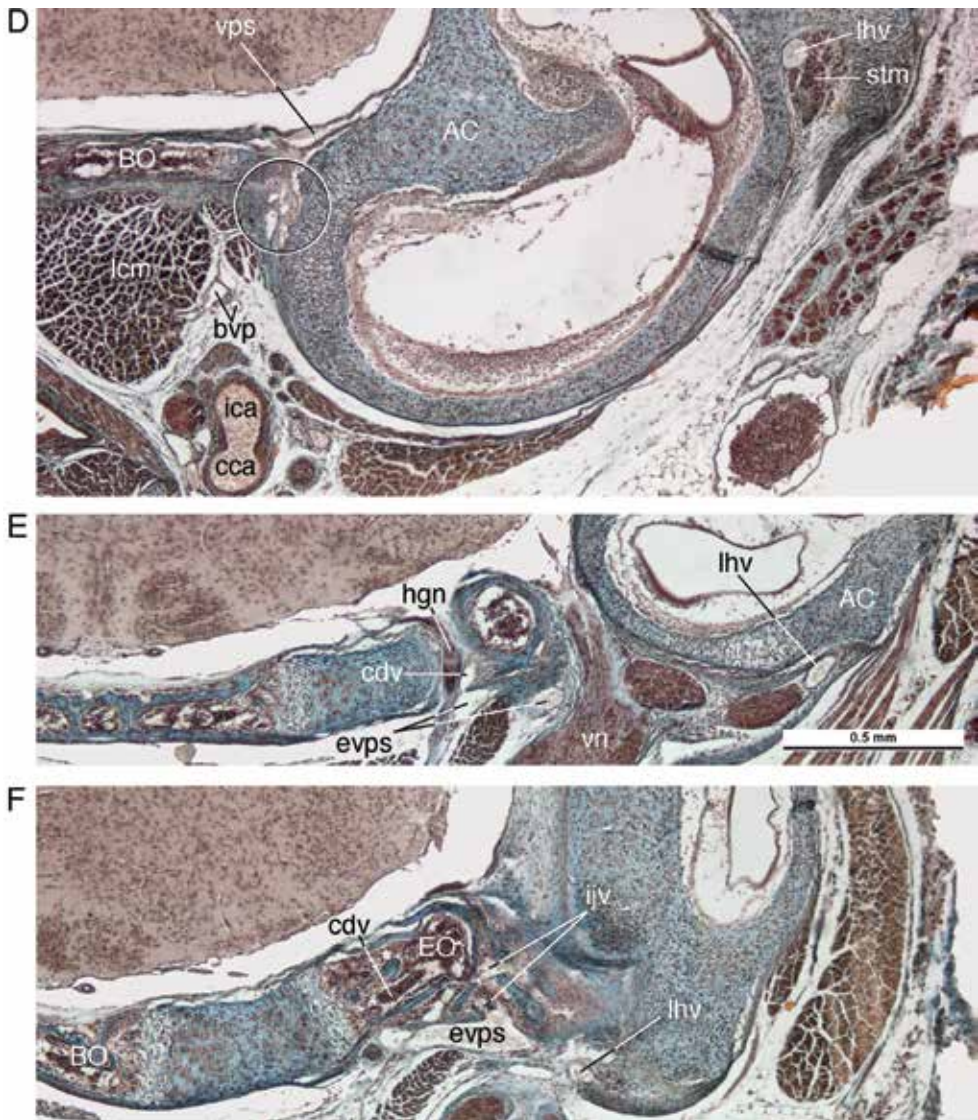


FIG. 11. *Monodelphis domestica* ZIUT PND 12, HL 8.5 (Didelphidae, Didelphimorphia), young postnatal specimen, stained coronal sections in rostrocaudal order. In **A** and **B**, note anastomotic link between internal carotid vein and presumptive trunk of transverse canal vein (ss. 22.03.03, 23.02.01). In **C**, note internal carotid vein/basicranial venous plexus lying medial to auditory capsule (s. 25.04.02); size diminished compared to appearance in **A**. In **D**, unnamed emissaria from ventral petrosal sinus (circled) passing through basicapsular



fenestra (s. 29.04.04. In E and F, complex of anastomoses involving condylar emissary vein, internal jugular vein, and extracranial continuation of ventral petrosal sinus; note also persistent lateral head vein (ss. 26.05.0, 32.04.02). **Key:** AC, auditory capsule; AS, alisphenoid; at, auditory tube; BO, basioccipital; BS, basisphenoid; **bvp**, basicranial venous plexus; **cca**, common carotid artery; **cdv**, condylar vein; **cs**, cavernous sinus; **ctn**, chorda tympani nerve; **EC**, ectotympanic; **ejuv**, external jugular vein; **EO**, exoccipital; **evps**, extracranial continuation of ventral petrosal sinus; **GO**, goniale; **hgn**, hypoglossal nerve; **hp**, hypophysis; **ica**, internal carotid artery; **icn**, internal carotid nerve; **icv**, internal carotid vein; **icv/bvp**, internal carotid vein and basicranial venous plexus; **ijv**, internal jugular vein; **lcm**, longus capitis muscle; **lhv**, lateral head vein; **lptm**, lateral pterygoid muscle; **MA**, malleus; **MC**, meckelian cartilage; **mca**, middle cerebral carotid artery; **MD**, mandible; **mdn**, mandibular nerve; **mptm**, medial pterygoid muscle; **mxv**, maxillary vein; **pal**, processus alaris; **stm**, stapedius muscle; **tg**, trigeminal ganglion; **?ttcv**, ?presumptive trunk of transverse canal vein anastomosing with internal carotid vein vein; **ttn**, tensor tympani muscle; **vn**, vagus nerve; **vps**, ventral petrosal sinus.

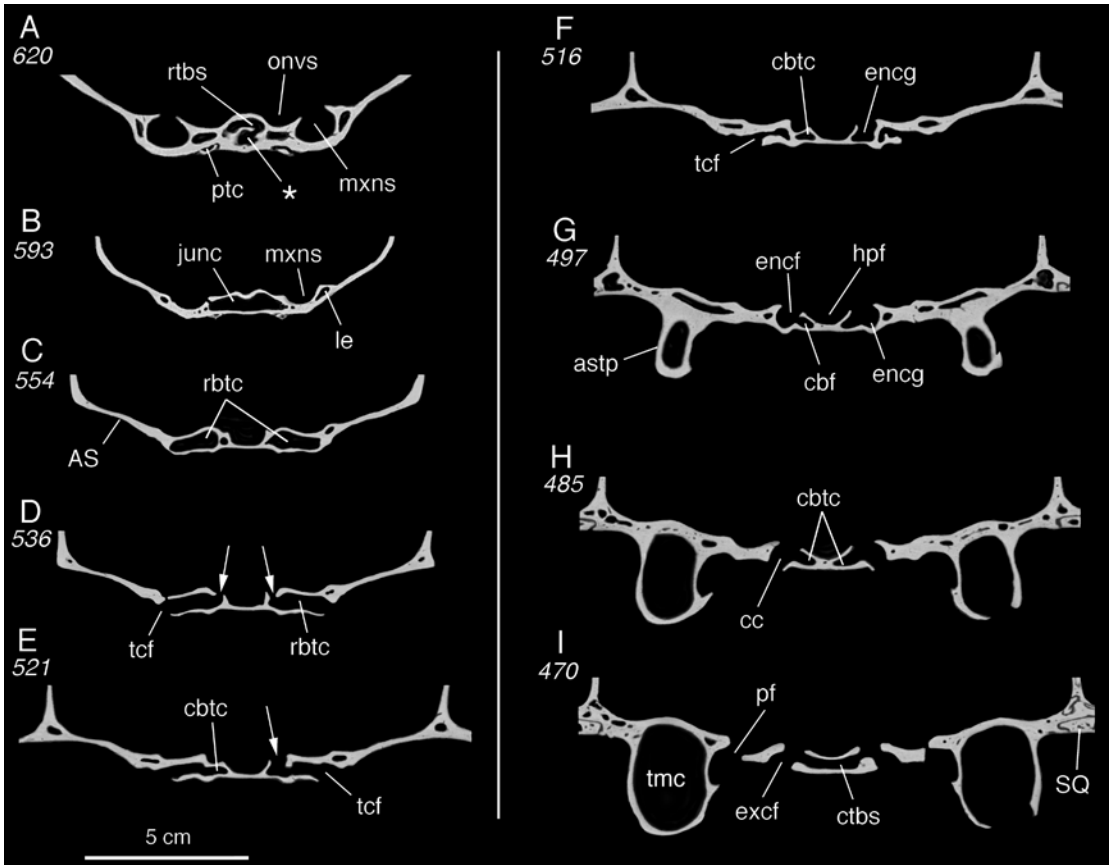


FIG. 12. *Monodelphis domestica* NMB c. III.777 (Didelphidae, Didelphimorphia), adult caudal cranium, selected coronal segments in rostrocaudal order (data source, table 2). In A–E, note general resemblance to *Caenolestes* in mesocranial organization (figs. 13A; 14A, B), with prominent transverse canals and basisphenoid sinus, multiple openings in endocranial floor. Asterisk identifies either an internal compartment within transverse basisphenoid sinus, or an improbably large craniopharyngeal canal. In D–G, note partial tubes or grooves for caudal branches of transverse canal, absent in *Didelphis* (fig. 5), leading to caudal branch foramen (arrow). **Key:** AS, alisphenoid; **astp**, alisphenoid tympanic process; **cbtc**, caudal branch of transverse canal; **cc**, carotid canal; **ctbs**, caudal portion of transverse basisphenoid sinus; **encf**, endocranial carotid foramen; **encg**, endocranial carotid groove; **excf**, exocranial carotid foramen; **hpf**, hypophyseal fossa; **junc**, junction of transverse canals; **le**, lateral extension of transverse basisphenoid sinus; **mxns**, sulcus for maxillary nerve; **onvs**, sulcus for ophthalmic neurovascular array; **pf**, piriform fenestra; **ptc**, pterygoid canal; **rbtc**, rostral branch of transverse canal; **rtbs**, rostral portion of transverse basisphenoid sinus; **SQ**, squamosal; **tcf**, transverse canal foramen; **tmc**, tympanic cavity.

a transverse direction, directly to the CS (fig. 28D). The venogram shows other veins in the vicinity, but none resembles a likely RBV. On this evidence all that can be said is that the CBTC is evidently dominant in *Sarcophilus*; if there is a functional rostral branch, it must be highly reduced. At least in this respect, *Sarcophilus* is

similar to *Thylacinus*, although the former lacks the union of transverse and carotid canals seen in the latter. In light of these uncertainties we omit *Sarcophilus* from the junction pattern framework (table 4).

OTHER EXTANT DASYURIDS. Archer (1976) described conditions in dry skulls of several

dasyuromorphians (principally *Thylacinus*, *Sarcophilus*, *Dasyurus*, *Dasyercus*, *Dasyuroides*, *Myrmecobius*). Although PCVN components were not investigated in detail, his data reveal that many dasyurid taxa possess the RBV (as inferred from the presence of the RBTC intramural pathway). The survey by Sánchez-Villagra and Wible (2002) supports this conclusion, although the authors also reported some polymorphisms, especially for *Dasyurus*, and were not able to investigate Archer's (1976) remarks on variation in *Planigale* (see below). The status of *Myrmecobius* in this regard is uncertain: Archer (1976: 246) presented evidence that the numbat possesses both anterior and posterior pathways, but also stated that the intramural condition does not exist in this taxon.

As noted in Anatomical Structures, Archer (1976: figs. 2–4) provided schematic drawings of cephalic venation in injected specimens of several dasyurid species, but overlaps and apparent disparities make them difficult to interpret. In regard to the sminthopsine *Planigale*, Archer (1976: 265) stated:

When transverse canal foramina are present they are often not connected by canal, but rather open directly into endocranium. In other specimens where they are present, they do lead to canal which opens into endocranium via internal sulcus for entocarotid foramen. In no instance observed, does transverse canal cross basicranium to link both foramina via basisphenoid sinus.

This description is consistent with the trunk of the TCV receiving only the CBV in *Planigale*, with the RBV evidently being absent. This may also apply to the related *Sminthopsis* and the dasyurine *Antechinus*, although the relationship of the TCVs to the midline “transverse canal sinus” (= transverse basisphenoid sinus) implies that rostral rather than caudal branches are present. Whether dasyurids are as morphologically disparate as this is an interesting problem that could be resolved with appropriate data.

*THYLACINUS* (THYLACINIDAE) (figs. 29–31). *Thylacinus cynocephalus*, the only extinct Quaternary marsupial to be reviewed here, exhibits a

mesocranial region that is interesting but complicated. Our treatment is based on two specimens: NMB c.2526a, an intact skull for which a scan is available, and AMNH M-144316, a coronally hemisected skull (table 1). Although several soft-tissue and perinatal specimens of *Thylacinus* exist in collections (Sleightholme and Ayliffe, 2013; Newton et al., 2018), to our knowledge there are no published sources on intracranial venation in this species.

The apparent complexity of the PCVN in *Thylacinus*, as reflected in our endocast reconstruction, is fundamentally due to the elaborate connections between the carotid and transverse canals. All four canals briefly coalesce just distal to the endocranial carotid foramina, something that is difficult to properly show in 2D ventral views (fig. 30A, D), but that can be better appreciated by viewing the successive segments illustrated in figure 31. An additional complication for illustration is that digitally filling the sulci for the endocranial carotid groove and hypophyseal fossa, as required by our method (see Illustrations), results in a continuous isoshape for these features. This is insufficiently realistic. We correct for this in figure 30F by depicting the fossa's shape in a different color and removing enough of the vasculature to reveal the position of the carotid grooves.

Although there are no indicia to indicate how the veins in the conjoined canals would have interacted, their basic routes can be inferred from conditions in other taxa. In our interpretation, the veins connecting the contents of the hypophyseal fossa with the trunk of the TCV would have been homologous with CBVs, not RBVs. The basis for this inference is that their osteological pathways start at the hypophyseal fossa, suggesting that they emerged at this point from the CS/ICV before descending into their respective canals. Furthermore, as there is no indication of a pathway rostral to the fossa, there is no basis for inferring the presence of RBTCs. This constitutes a major difference from the simple, complex, and compound junction patterns, but it accords in principle with the hybrid pat-

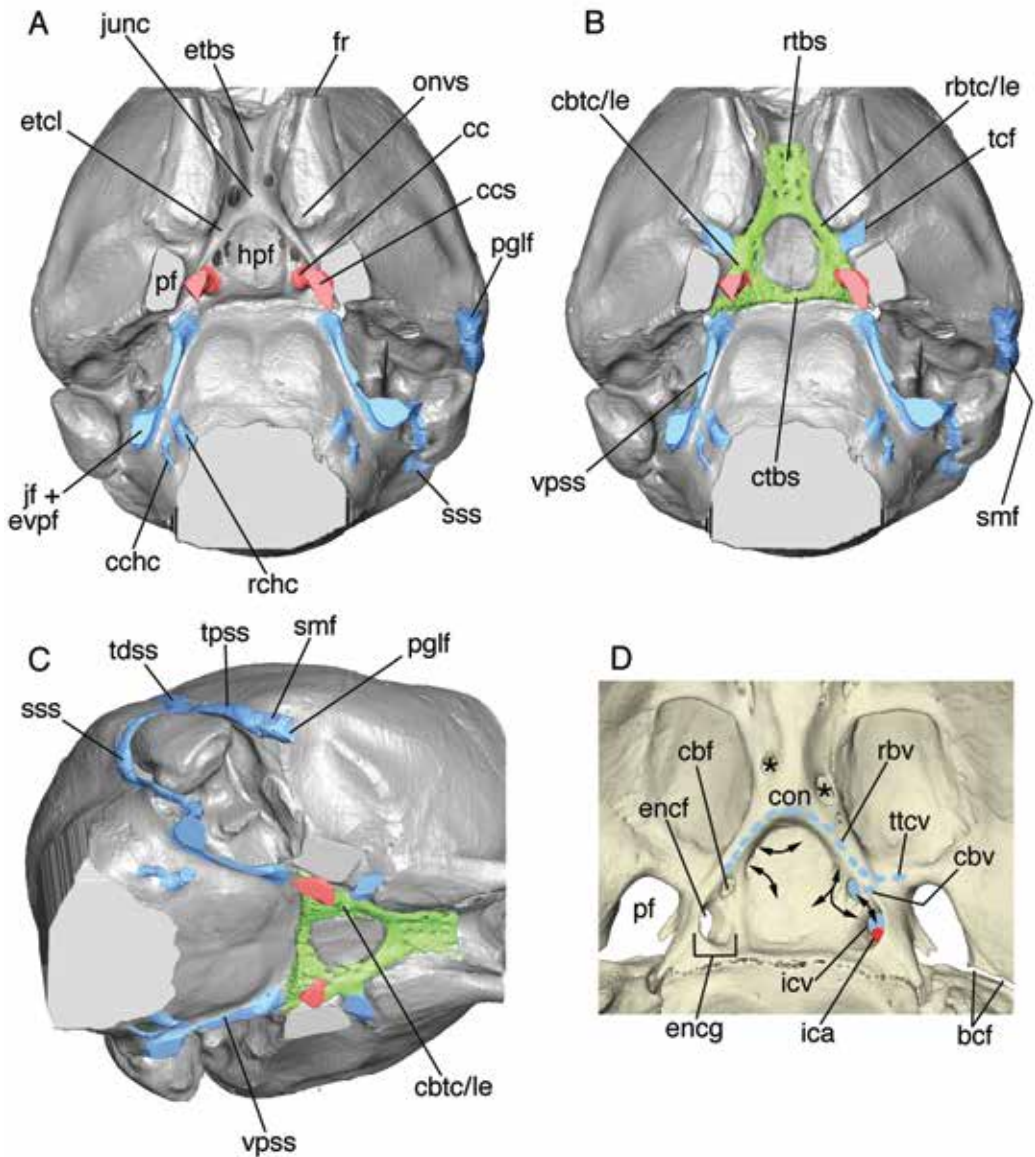
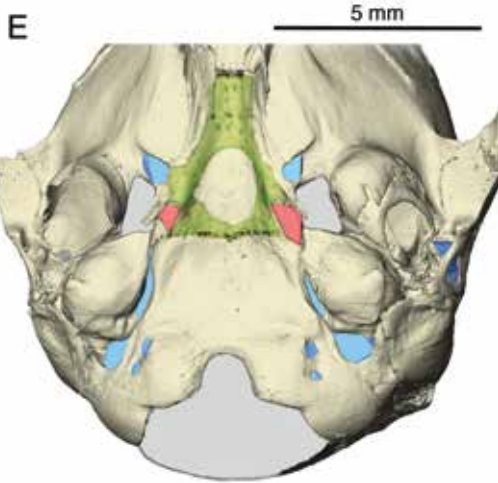


FIG. 13. *Caenolestes* sp. IANIGLA uncatalogued (Caenolestidae, Paucituberculata), adult specimen, endocast reconstruction showing osteological features associated with pericarotid venous network and related vasculature (data source, table 2; color key, fig. 4). Views: **A**, ventral; **B**, same, with transverse basisphenoid sinus superimposed; **C**, oblique left lateral (rev.); **D**, endocranial floor, based on **A** (rev.); **E**, intact caudal cranium, reconstructed trackways of transverse canal branches superimposed on ventral surface. In **D**, note small apertures (hypophyseal canaliculi) on periphery of hypophyseal fossa in addition to caudal branch foramen. Inferred streamlines (small black arrows) suggest communication between caudal branch vein, internal carotid veins, and cavernous sinus. Large apertures opening into rostral portion of transverse basisphenoid sinus (asterisks) are of unknown function but may relate to track of nearby ophthalmic veins rather than cranio-pharyngeal canal (cf. *Perameles*, fig. 32C). **Key:** **bcbf**, basicapsular fenestra; **cbf**, caudal branch foramen; **cbtc/le**, caudal branch of transverse canal inside lateral extension of transverse basisphenoid sinus; **cbv**, caudal



branch vein; **cc**, carotid canal; **ccs**, sulcus leading to carotid canal; **cchc**, caudal condylohypoglossal canal; **con**, confluence of rostral branch veins; **ctbs**, caudal portion of transverse basicranial sinus; **encf**, endocranial carotid foramen; **encg**, endocranial carotid groove; **etbs**, eminence of transverse basisphenoid sinus; **etcl**, eminence of transverse canal; **fr**, foramen rotundum; **hpf**, hypophyseal fossa; **ica**, internal carotid artery; **icv**, internal carotid vein; **jf + evpf**, joint aperture formed by jugular foramen and extracranial continuation of ventral petrosal sinus; **junc**, junction of transverse canals; **onvs**, sulcus for ophthalmic neurovascular array; **pf** piriform fenestra; **pglf**, postglenoid foramen; **rbtc/le**, rostral branch of transverse canal inside lateral extension of transverse basisphenoid sinus; **rbv**, rostral branch vein; **rhc**, rostral condylohypoglossal canal; **rtbs**, rostral portion of transverse basicranial sinus; **smf**, suprameatal foramen; **sss**, sulcus for sigmoid sinus; **tcf**, transverse canal foramen; **tdss**, sulcus for transverse dural sinus; **tpss**, sulcus for temporal sinus; **ttcv**, trunk of transverse canal vein; **vpss**, sulcus for ventral petrosal sinus.

tern as seen, in a differently derived format, in macropodids (see above and fig. 18C).

Archer (1976: 238), however, came to a different set of conclusions. He noted that, depending on the direction in which he probed a transverse canal, a hair might pass from one TCF to the other through the basisphenoid (indicating that, in our terminology, the RBTC pathway was present), or it might simply go into the endocranium

(suggesting that the CBTC pathway was also present). He found that most of the thylacine specimens that he examined (N = 8) showed evidence of “two partly divergent canals or paths through basisphenoid” (p. 238), which would imply the existence of a junction pattern resembling the complex or compound arrangement rather than the hybrid. However, it is pertinent to note that he also mentioned some other features that he thought might represent individual variation: for example, a sagittally sectioned skull appeared to have only one pathway, while another skull showed “just mesial to entrance of transverse foramen, [a] fork in [?]transverse] canal with bony median wall” (p. 238). These differences were not analyzed further, except to observe in conclusion that *Thylacinus* might be significantly polymorphic for mesocranial traits. Sánchez-Villagra and Wible (2002: 30) were unable to replicate Archer’s results, as they found no intramural pathway in their material.

The CT scan of NMB c.2526a sheds some light on possible reasons for these conflicting interpretations:

(1) Archer was correct in pointing to a caudally directed pathway (“fork”) that branches off from the transverse canal immediately medial to the location of the TCF (fig. 30D: feature a). But this pathway, which originates in the TBS, does not qualify as a CBTC, at least as defined in this paper, because it communicates with the proximal part of the canal for the accessory VPS, not the CS. The pathway in question is, in effect, a greatly enlarged interstitial canaliculus. Consistent with the variability associated with such features, on the specimen’s right side the canaliculus is large; but on the left side, the accessory VPS is highly reduced, and so is the fork that joins it (fig. 30D: feature d).

(2) Having a candidate for the CBTC in the shape of the fork, Archer (1976) evidently concluded that the other branch that he had detected was an RBTC. Our definition of the rostral branch pathway requires that it should run intramurally from the trunk of the TCV to meet its partner rostral to the position of the hypophyseal

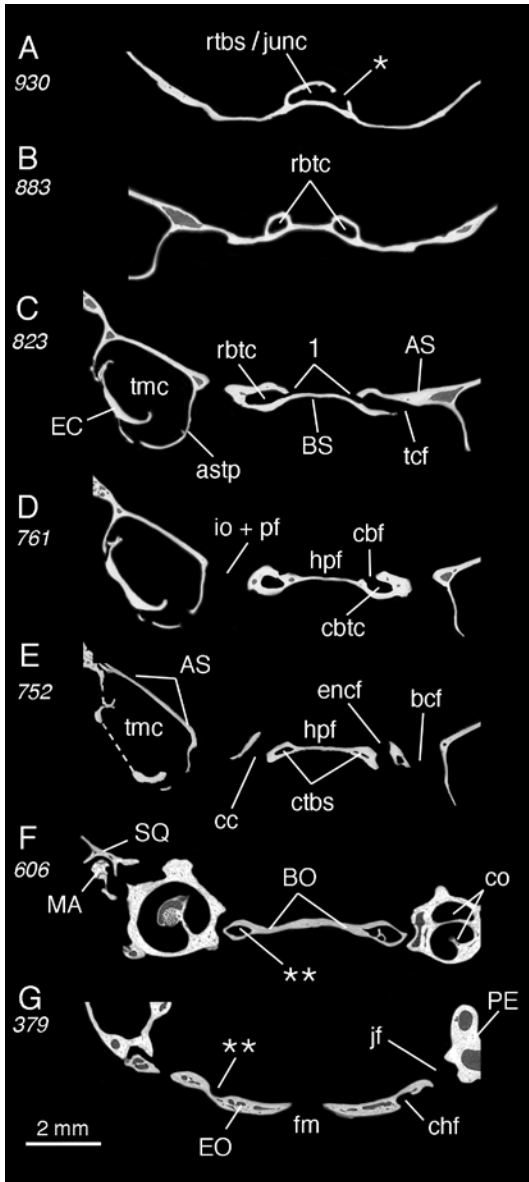


FIG. 14. *Caenolestes* sp. IANIGLA uncatalogued (Caenolestidae, Paucituberculata), adult caudal cranium, selected coronal segments in rostrocaudal order (data source, table 2). In A and B, rostral branches of transverse canals and rostral portion of transverse basisphenoid sinus raise separate eminences on dorsal surface of bony endocranial floor. Large aperture (single asterisk), possibly related to a vessel communicating with ophthalmic veins, opens into rostral portion of sinus. In C and D, hypophyseal canaliculi (feature 1) communicate with cavernous sinus (hypophyseal fossa). In F and G, double asterisks identify trackways for vessels apparently associated with ventral petrosal sinus. **Key:** AS, alisphenoid; **astp**, tympanic process of alisphenoid; **bcf**, basicapsular fenestra; **BO**, basioccipital; **BS**, basisphenoid; **cbf**, foramen of caudal branch of transverse canal; **cbtc**, caudal branch of transverse canal; **cc**, carotid canal; **chf**, condylohypoglossal foramen (nonspecific); **co**, cochlea; **ctbs**, caudal portion of transverse basisphenoid sinus; **EC**, ectotympanic; **encl**, endocranial

fossa, communicating with the TBS along the way but displaying little or no contact with the CS/ICV. No branch of this type was found in NMB c.2526a.

(3) As Archer (1976) noted, it took careful maneuvering to pass a probe from one TCF to the other. But the reason that it was possible to do at all was not because *Thylacinus* skulls exhibit a rostral pathway like that of *Didelphis* or *Caenolestes*, but because the merger of all four of the major mesocranial canals creates a continuous space linked on either side to the TCFs via the transverse canals (fig. 31C–G). Merger, however, occurs caudal to the position of the hypophyseal fossa and involves a different TCV pathway (CBTC) than the one found in *Didelphis* (i.e., RBTC). In short, the result is what might be called a false intramural passage, which blind probing cannot differentiate from the real thing. Archer (1976: 238) also noted that, with different maneuvering, his probe would “appear inside cranium in sulcus for internal carotid artery,” but he did not state that it emerged through a separate foramen.

Because the conformation of the hypophyseal fossa plays a role in how mesocranial vasculature is to be interpreted in *Thylacinus cynocephalus*, a few more details concerning its osteological appearance are worth exploring. Archer (1976) remarked that he could not locate the hypophyseal fossa in his material with certainty, but the segmental data establish that the fossa in NMB c.2526a is located as usual on the same coronal plane as the endocranial carotid foramina. However, in this case the fossa does not conform to the simple broad depression seen in most other

members of the comparative set, but is instead a deep, flask-shaped pocket (fig. 31A, B). An extension of the fossa that projects rostr dorsally toward the likely position of the optic chiasma on the endocast (fig. 30D) is apparently an ossified sheath for the hypophyseal stalk or infundibulum. Obviously, how closely the endocast conforms to the shape of the pituitary body or the CS cannot be ascertained.

Archer (1976) noted the presence of a midline aperture on the basioccipital, which he called the median basioccipital foramen and thought that it might have carried a nutrient vessel. This feature is seen in NMB c. 2526a (fig. 31I: feature 3), but there is nothing at the equivalent place in AMNH M-144316 (fig. 29A). In NMB c.2526a the feature communicates with the left accessory VPS (fig. 30D). We consider it to be either a remnant of the notochord canal or an unpaired transclival venous foramen.

Proceeding rostrocaudally through the segments presented in figure 31, it may be seen that the trackway for the VPS after it leaves the vicinity of the hypophyseal fossa becomes, successively, a deep sulcus and then a canal (= internal jugular canal of Archer, 1976) (fig. 31J). The VPS canal continues onward to penetrate the exoccipital, where it coalesces with a series of continuous channels related to the passage of the VV, SS, transverse dural sinus, and condylar veins (fig. 31K, L). On the external surface of the basicranium, the short but wide basijugular sulcus connects the large foramen for the EVPS to the caudal condylohypoglossal foramen (fig. 29A–C), as in other marsupials and many placentals. The true jugular foramen is smaller than the foramen for the EVPS, also as in many extant marsupials. The postglenoid foramina are comparatively large, signifying the importance of the PGLVN in this species. Other features connected with mesocranial circulation, including several

additional sites where the TBS is connected to the transverse canals by interstitial canaliculi, are presented in figure 30D (asterisks).

Ultimately, we cannot specify from osteological evidence alone how the mesocranial veins (i.e., TCV trunk, CBTC, and ICV) would have interacted while running through the merged carotid and transverse canals. Our assumption, however, is that the ICV would not have been lost to anastomosis, but would have instead remained independent up to the point of its departure from the exocranial carotid foramen (cf. similar assumption for *Osphranter*, fig. 20). In this scenario the TCV trunk would have likewise remained intact, leaving the skull through its proper port. A good analogy would be plexiform vertebral veins, which share branches and anastomoses at different vertebral levels but retain their longitudinal identity (MacPhee, 1994: fig. 23).

#### PERAMELEMORPHIA

*PERAMELES* (PERAMELIDAE) (figs. 32, 33). The auditory capsule of *Perameles* sp. ZIUT HL 17.5 mm (table 1) is partly ossified, particularly in the region of the fenestra cochleae. A particularly valuable feature of this specimen is that it provides direct evidence of the confluence of the RBVs, represented by the thin-walled vessel seen in the midline in figure 33A. Confluence occurs within the large chamber formed by the fusion of the rostral TBS and transverse canal junction immediately rostral to the root of the ossifying processus alaris. The chamber's internal walls exhibit rows of osteoclasts and osteoblasts on opposing trabecular surfaces, indicating that intensive bone remodeling was in progress at the time of death. Although Azan is not a conventional hematological stain, abundant erythrocytes can be identified by their shape within the chamber. Other erythroid cells in various stages

---

← carotid foramen; **EO**, exoccipital; **fm**, foramen magnum; **hpf**, hypophyseal fossa; **io + pf**, incisura ovalis and piriform fenestra; **jf**, jugular foramen; **MA**, malleus; **PE**, petrosal; **rbtc**, rostral branch of transverse canal; **rtbs/junc**, junction of transverse canals with rostral portion of transverse basisphenoid sinus; **SQ**, squamosal; **tcf**, transverse canal foramen; **tmc**, tympanic cavity.

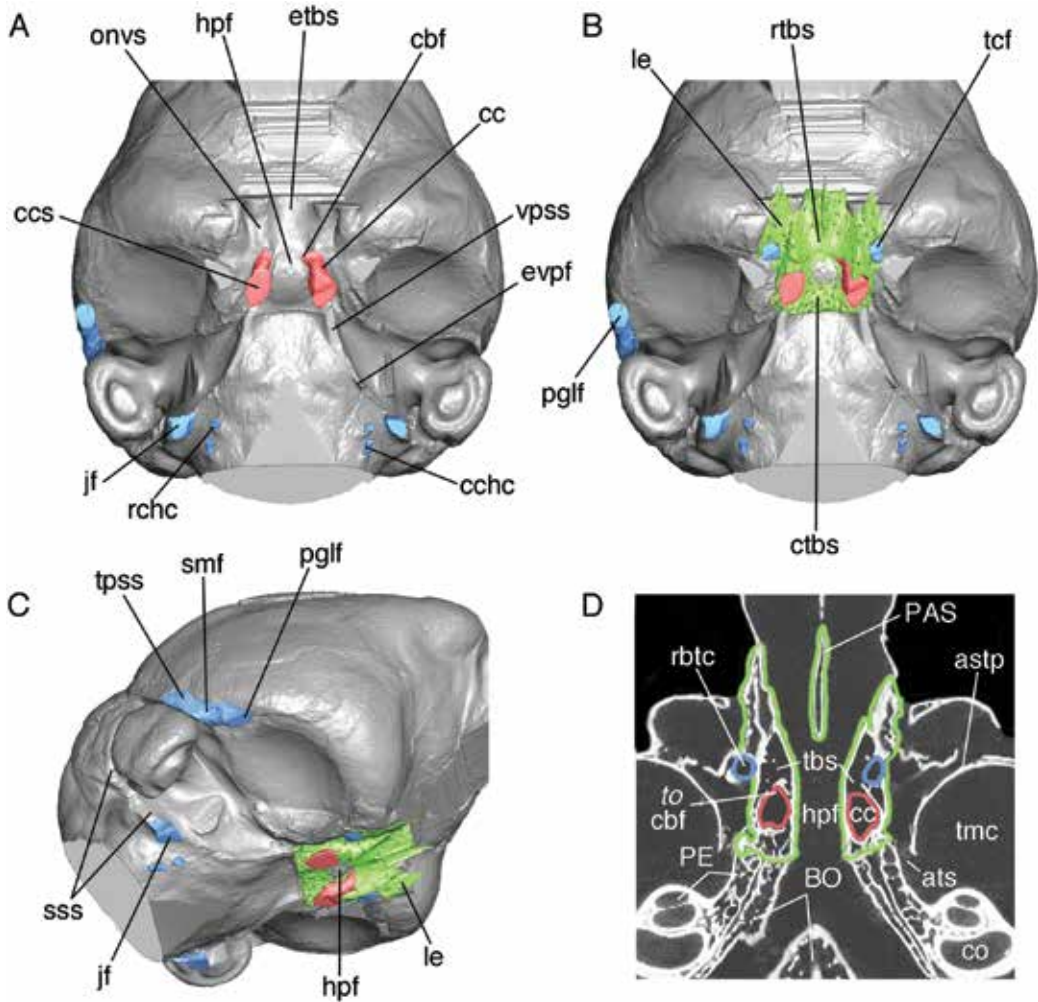
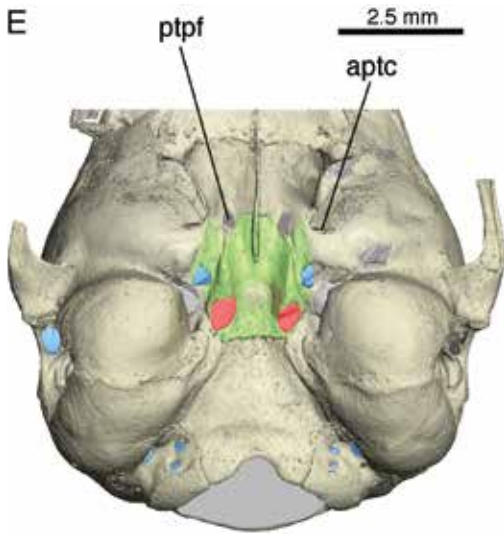


FIG. 15. *Dromiciops gliroides* MACN Ma-23607 (Microbiotheriidae, Microbiotheria), near-adult specimen, endocast reconstruction showing osteological features associated with pericarotid venous network and related vasculature (data source, table 2; color key, fig. 4). Skull is slightly damaged (e.g., left carotid canal). Views: **A**, ventral; **B**, same, with transverse basisphenoid sinus superimposed; **C**, oblique right lateral; **D**, horizontal segment through mesocranium; and **E**, ventral surface, intact caudal cranium. In **C**, sulcus for sigmoid sinus shallow and discontinuous; if internal jugular vein functionally present in adult, vessel probably small. In **D**, fingerlike projection from carotid canal leads to caudal branch foramen; transverse canals are continuous with transverse basicranial sinus, and rostral branches run through large compound space (cf. fig. 17A). **Key:** **aptc**, anterior pterygoid canal (= ?anterior pterygoid foramen of Beck et al., 2023: char. 50); **astp**, tympanic process of alisphenoid; **ats**, sulcus for auditory tube; **BO**, basioccipital; **cbf**, caudal branch foramen; **cc**, carotid canal; **ccs**, sulcus leading to carotid canal; **cchc**, caudal condylohyoglossal canal; **co**, cochlea; **ctbs**, caudal portion of transverse basicranial sinus; **etbs**, eminence of transverse basisphenoid sinus; **evpf**, extracranial continuation of ventral petrosal sinus; **hpf**, hypophyseal fossa; **jf**, jugular foramen; **le**, lateral extension of transverse basisphenoid sinus; **onvs**, sulcus for ophthalmic neurovascular array; **PAS**, parasphenoid; **PE**, petrosal; **pglf**, postglenoid foramen; **ptpf**, pterygopalatine fissure; **rbtc**, rostral branch of transverse canal; **rchc**, rostral condylohyoglossal foramen; **rtbs**, rostral portion of transverse basicranial sinus; **smf**, suprameatal foramen; **sss**, sulcus for sigmoid sinus; **tbs**, transverse basicranial sinus; **tcf**, transverse canal foramen; **tmc**, tympanic cavity; **tpss**, sulcus for temporal sinus; **vpss**, sulcus for ventral petrosal sinus.



of differentiation can be seen, as well as darker-staining cells that may be megakaryocytes (see Fawcett, 1986; Old et al., 2004; Young et al., 2014; see Discussion).

In the stained sections, the RBV and CBV communicate with the TCV trunk medial to the TCF (fig. 33B–D, H). The CBV, which is extremely short, passes from the ICV through the CBF to directly join the trunk. The CBF can be made out on the damaged mesocranium of AMNH M-154403 by obliquely tilting the skull (fig. 32C, D). In this specimen there is also a small hypophyseal canaliculus on the specimen's left side that opens into the carotid groove. The right and left RBVs meet in the compound vacuity formed by the rostral TBS and transverse canals. As usual, because RBVs travel intramurally they are not seen on the endocranial floor, although there is a slight swelling marking their presence (eminence of the transverse canals).

In the sectioned specimen the intracranial ICV is significantly larger than the internal carotid artery (fig. 33A–D). As usual the BVP is plexiform and small in caliber relative to the VPS (fig. 33E). By contrast, the anastomosis formed by the SS and VV is very substantial (fig. 33J). If also true of the adult, this would imply that encephalic return is mostly dis-

charged into the CSVS rather than the IJV in this marsupial.

In the adult skull of *Perameles nasuta* AMNH M-160199, the osteological foramen ovale is subdivided into daughter apertures by a bony bridge (fig. 32A: feature b). The lateral aperture is possibly for the large emissary vein (v.e. foraminis ovalis) seen issuing from this location in company with the mandibular nerve in the perinatal specimen (fig. 33H: asterisk). The specimen exhibits a large TCF on its left side, but the foramen on the right side is much smaller (fig. 32A, B), despite the size of the fossa in which it is located. In *P. gunnii* AMNH M-106102 (not illustrated), both TCFs are larger than the exocranial foramina of the carotid canals. Some taxa are known to display a significant degree of variation in TCF dimensions (Aplin, 1990; Sánchez-Villagra and Wible, 2002), but whether this is particularly the case in *Perameles* has not been reported.

One of the very few published mentions of PCVN components in *Perameles* is Cords's (1915: 40) observation that the carotid canal contains a vein (i.e., ICV) as well as an artery. Cords (1915: 22) also argued that the IJV of *Perameles* is possibly not homologous with that of "higher" mammals. The basis for her observation was that she noticed a vein that she took to be the IJV passing through a foramen situated well rostral to the track of the glossopharyngeal and vagus nerves, as in nonmammals like the chicken *Gallus*. A more likely interpretation is that Cords mistook the EVPS for the true (and notably smaller) IJV, and incorrectly assumed that the former's exit aperture was the jugular foramen (see fig. 32).

#### NOTORYCTEMORPHIA

*NOTORYCTES* (NOTORYCTIDAE) (figs. 34, 35). The dry skull of a single adult specimen, *Notoryctes typhlops* AMNH M-202103, was available for study and scanning. Compared with other taxa in the comparative set, the skull of *Notoryctes* is rostrocaudally telescoped, with the result

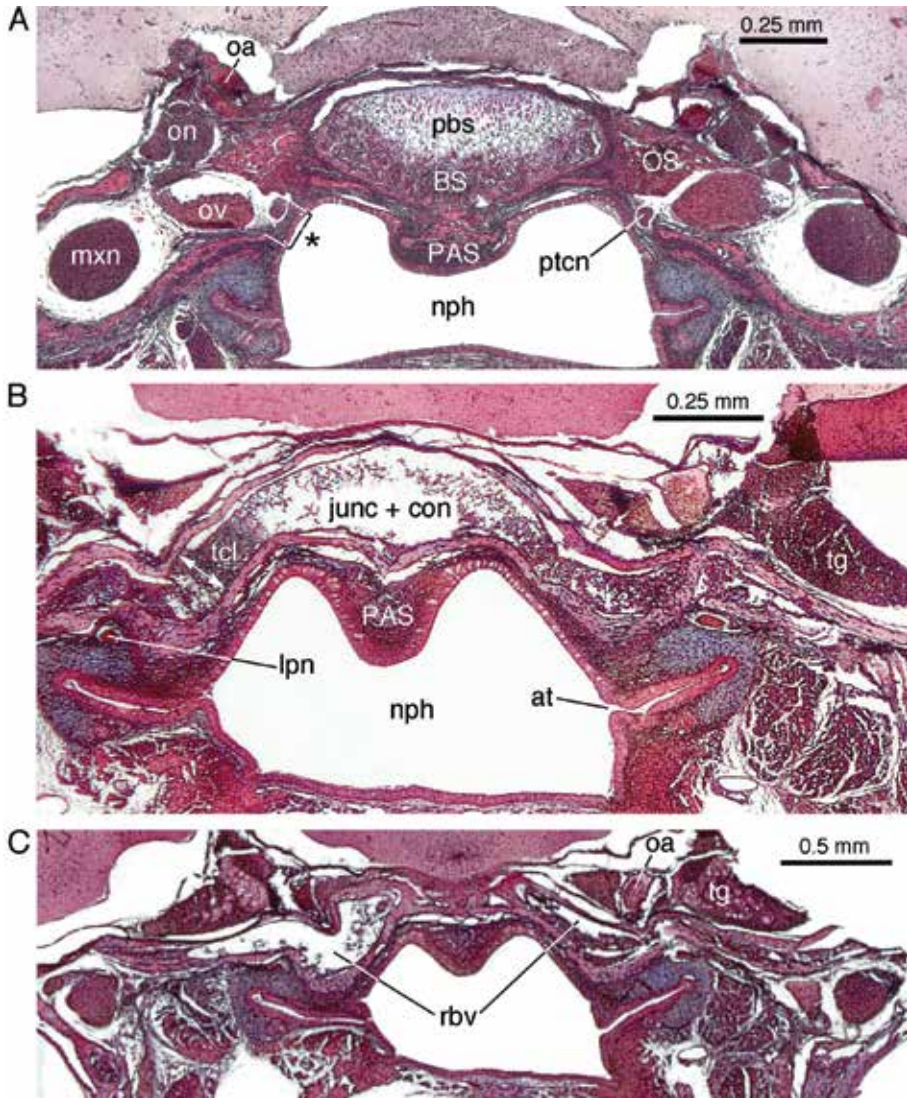
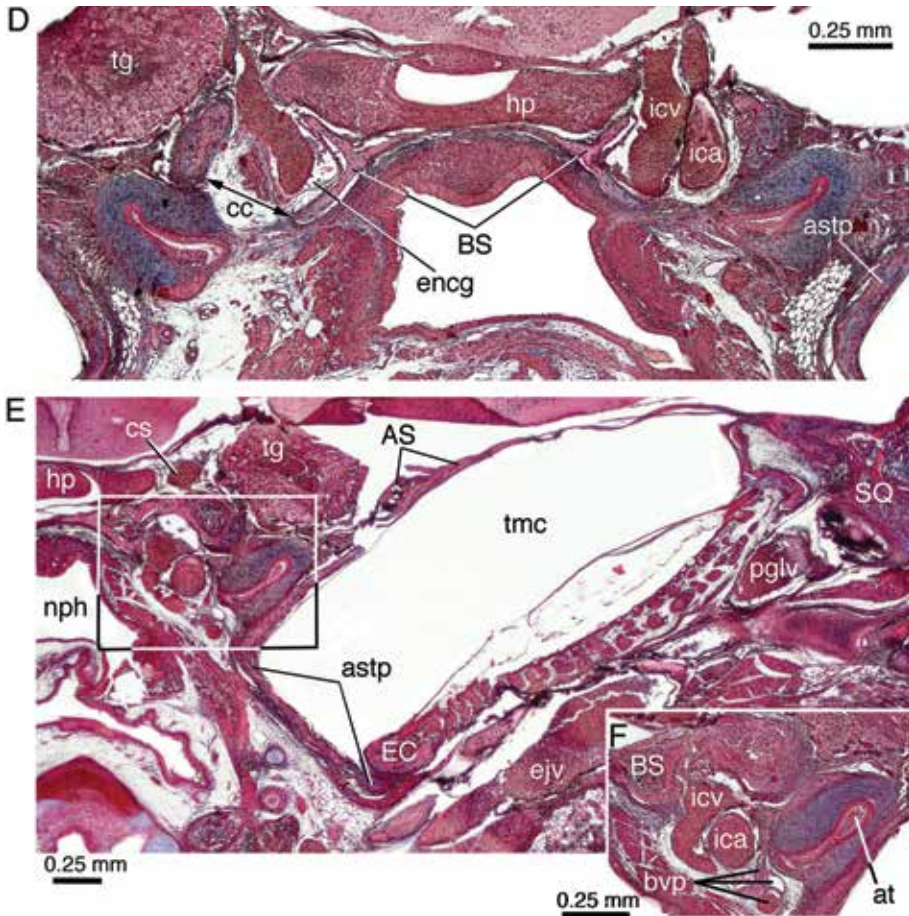


FIG. 16. *Dromiciops gliroides* ZIUT HL 19 mm (Microbiotheriidae, Microbiotheria), juvenile specimen, stained coronal sections in rostrocaudal order. Effects of shrinkage during histological processing obvious (e.g., size of maxillary nerve relative to its sulcus) **A**, Presphenoid-basisphenoid synchondrosis, large pterygopalatine fissure provides passage for nerve of pterygoid canal (asterisk) (s. 25.02.02). **B**, Veins of rostral branches of transverse canals form confluent, with canals largely incorporated into rostral portion of transverse basicranial sinus. Cells within sinus nondiagnosable but probably erythroid (s. 28.03.01; cf. fig. 33A). **C**, Rostral branches of transverse canals present and large (s. 29.01.03). **D**, Entrance to carotid canal (double-headed arrow) (s. 30.04.01). **E**, Anastomosis of internal carotid vein with basicranial venous plexus (s. 31.01.01). **F**, Same anastomosis in closeup, typical plexiform arrangement (s. 31.03.02). **Key**: AS, alisphenoid; **astp**, tympanic process of alisphenoid; **at**, auditory tube; **BS**, basisphenoid; **bvp**, basicranial venous plexus; **cc**, carotid canal; **cs**, cavernous sinus; **EC**, ectotympanic; **eju**, external jugular vein; **encg**, endocranial carotid groove; **hp**, hypophysis; **ica**, internal carotid artery; **icv**, internal carotid vein; **junc + con**, junction containing confluence; **lpn**, lesser petrosal nerve; **mxn**, maxillary nerve; **nph**, nasopharynx; **oa**, ophthalmic artery; **on**, ophthalmic nerve;

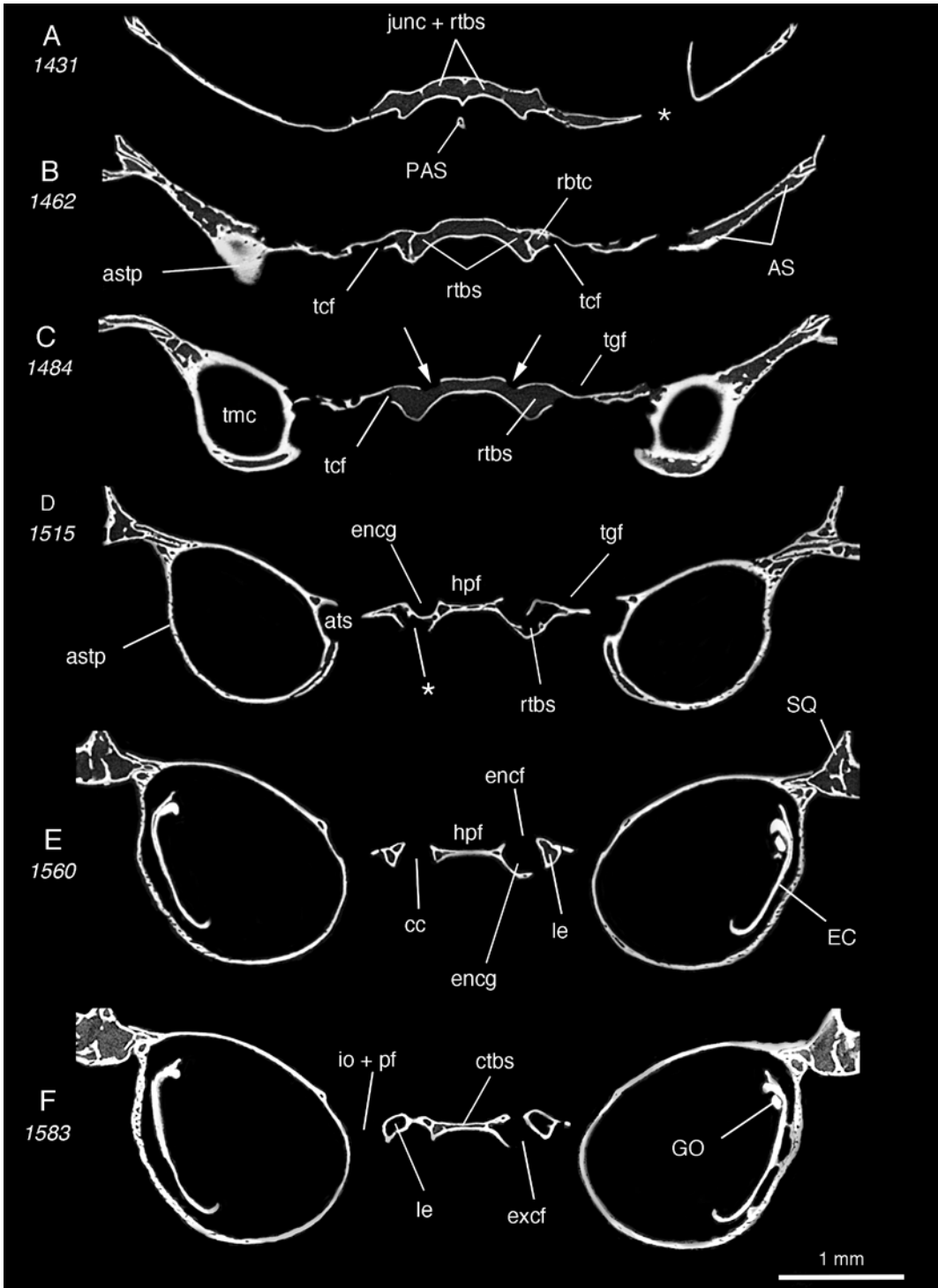


OS, orbitosphenoid; ov, ophthalmic vein; PAS, parasphenoid; pbs, presphenoid-basisphenoid synchondrosis; pglv, postglenoid vein; ptcn, nerve of pterygoid canal; rbv, rostral branch vein; SQ, squamosal; tcl, transverse canal (for rostral branches); tg, trigeminal ganglion; tmc, tympanic cavity.

that the caudal end of the nasal cavity extends over part of the rostral TBS when seen in coronal section (fig. 35A–C). Archer (1976: 270) states that in *Notoryctes* the “transverse canal involves large mesial external foramen ovale. Transverse canal, as in many dasyurids, connects with entocarotid canals within body of basisphenoid.” In our specimen the foramen ovale and TCF are quite distinct, with no indication of internal merger (fig. 34B). Archer’s (1976) mention of a pathway connected with the carotid canal is, in other contexts, a reference to the CBTC of this paper. The carotid groove is, unusually, partly subdivided by a septum (fig. 34A, 35G: asterisk),

interpreted here as a plate between separate pathways for the internal carotid neurovascular bundle and the CBTC. The short conduit leading away from the carotid groove is assumed to have carried the CBV (fig. 35F). Unfortunately, this channel cannot be traced further rostrally.

There is unquestionably a RBTC pathway in *Notoryctes* as well, which Archer (1976) did not separately mention. Its canal runs rostral to the hypophyseal fossa and a junction exists in the expected place, confirming its identity (fig. 35A, B). Possession of both branches constitutes a nonexclusive resemblance to *Dasyurus* (fig. 27). The RBTCs are fully integrated into



the large rostral TBS (compound pattern, fig. 35A–E), another nonexclusive resemblance to *Dasyurus*. Apart from one aperture in a relatively rostral position (fig. 35D: double asterisks), there is little osteological evidence of communication between the TBS and the endocranium. The basijugular sulcus is inconspicuous and the two condylohypoglossal foramina are recessed within a joint aperture on the ventral surface of the exoccipital.

### Placentalia

As mentioned in the Introduction, emissarial elements of the PCVN are arguably present in placentals, but are almost always underdeveloped compared to their apparent marsupial equivalents. Although they provide little insight into character history, the few placentals in which parts of the pericarotid network are quite well developed have considerable morphological interest. Some representative cases, pro and con, are interpreted in the following sections. As it is not known whether transverse canal veins found in placentals exhibit consistent branching patterns like those of many marsupials, in this section all conditions will be referred to as TCVs without further qualification.

### RODENTIA

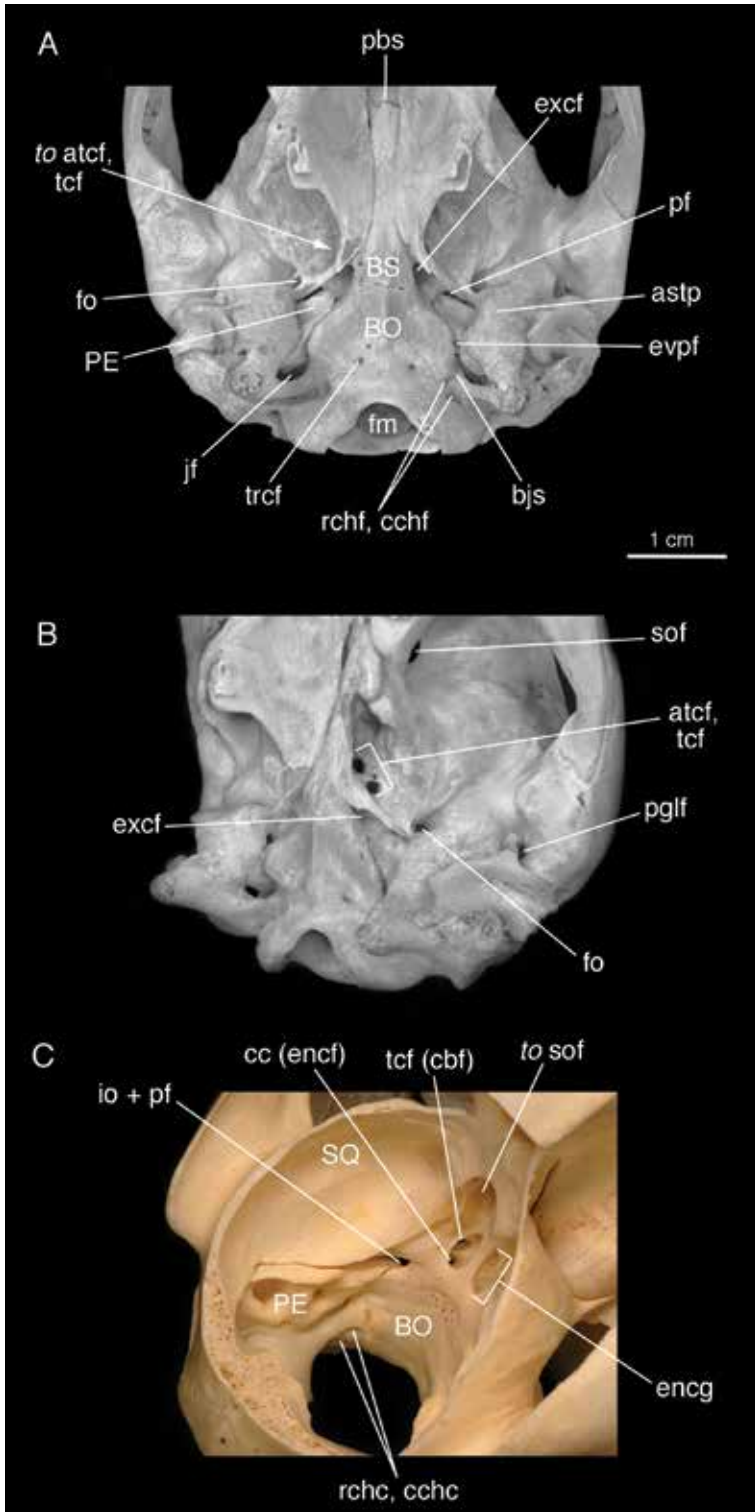
*DIPDOMYS* (HETEROMYIDAE, DIPODOMYINAE) (fig. 36A, B). In his detailed monograph

on the banner-tailed kangaroo rat (*Dipodomys spectabilis*), Howell (1932: 480) noted that on each side of the ventral midline of the skull there is a large mesocranial foramen. This “foramen pterygoideus” released an equally large vein which, “emerging from between the external and internal pterygoid muscles and extending laterally to the base of the ear... joins with the facial and temporal veins to form the external jugular.” According to Howell (1932), similarly positioned but smaller foramina occur in myomorph dipodoids (*Allactaga*, *Stylodipus*, etc.), indicating that, although infrequent, they are not restricted to a single major clade of rodents.

Wahlert (1985) added some important new details concerning this feature, based on his dissection of a related species, Ord’s kangaroo rat (*D. ordii*) as well as comparisons with other extant and extinct geomyoids. Borrowing terminology from Hill (1935), he used the names sphenopterygoid vein and sphenopterygoid canal for the mesocranial vessel and its channel. Wahlert (1985) verified Howell’s observation that a large vein passes through the sphenopterygoid canal, but also noted that the medial pterygoid muscle invades the canal and partly arises from its walls.

Neither Howell nor Wahlert conducted an intracranial investigation of *Dipodomys* and therefore did not observe whether the sphenopterygoid veins actually drain the CS, although given their location this seems practically certain. (Char. 111 of Meng et al. [2003], which

←  
FIG. 17. *Dromiciops gliroides* MACN Ma-23607 (Microbiotheriidae, Microbiotheria), subadult caudal cranium, selected coronal segments in rostrocaudal order (data source, table 2). In **A** and **B**, rostral portion of transverse basisphenoid sinus is a single vacuity, extending bilaterally from level of carotid canal to junction and incorporating rostral branches of transverse canals. In **C**, arrows indicate foramina for caudal branch veins, although pathway to transverse canal not distinctly marked. In **D–F**, note diminutive caudal portion of transverse basisphenoid sinus, connection with lateral extensions. Asterisks indicate artificial gaps or breakage. **Key:** **AS**, alisphenoid; **astp**, tympanic process of alisphenoid; **ats**, groove for auditory tube; **cc**, carotid canal; **ctbs**, caudal portion of transverse basicranial sinus; **EC**, ectotympanic; **encf**, endocranial carotid foramen; **encg**, endocranial carotid groove; **excf**, exocranial carotid foramen; **GO**, gonial; **hpf**, hypophyseal fossa; **io + pf**, incisura ovalis and piriform fenestra; **junc + rtbs**, junction of rostral branches of transverse canals incorporated within rostral portion of transverse basicranial sinus; **le**, lateral extension of transverse basisphenoid sinus; **PAS**, parasphenoid; **rbtc**, rostral branch of transverse canal; **rtbs**, rostral portion of transverse basicranial sinus; **SQ**, squamosal; **tcf**, transverse canal foramen; **tgf**, trigeminal ganglion fossa; **tmc**, tympanic cavity.



summarizes various literature references to the sphenopterygoid foramen in rodents and their relatives, states that the sphenopterygoid foramen gives passage to the internal maxillary artery; this suggests that in some cases it has been conflated with the alisphenoid canal.) Howell (1932) speculated that these veins might actually be the main channels for encephalic drainage in *Dipodomys*, given that the IJV was apparently either small or absent in his specimens. Brylski's (1990) investigation was concerned with cephalic arteries rather than veins, but there is no indication in his vascular reconstruction that the sphenopterygoid foramen also transmits an artery in *Dipodomys*.

Howell (1932) made no mention of the fact that the sphenopterygoid veins are at least positionally similar to PMDs of marsupials, and it may not have occurred to him that such a comparison could be usefully made. Indeed, he avoided discussing the possible homologies of the sphenopterygoid vein, allowing only that "in primitive Mammalia it may possibly occur as a small vessel and this, if of aid in draining the blood sinuses at the base of the brain (as inferior petrosal or cavernous sinuses) could easily, if the need arose, develop to assume the entire duty of a true internal jugular" (Howell, 1932: 480). Whether he meant by this statement that the sphenopterygoid veins might functionally replace the IJVS and its major tributaries, such as the VPS, is unclear. The suprameatal foramen and postglenoid incisure are both relatively large

in the kangaroo rat, suggesting that large transverse dural sinuses must contribute significantly to encephalic return.

Wahlert (1985) concluded that a large sphenopterygoid canal counts as a shared derived feature of Heteromyidae and Geomyidae, and it would be of interest to know whether versions of these canals (and their contents) were more widespread in the larger clade, Castorimorpha, to which these families belong. Wahlert (1985) additionally identified, as the "transverse foramen," a small hole variably situated in the caudolateral wall of the sphenopterygoid canal or in the medial wall of the alisphenoid canal. This feature was said to be lacking in some geomyid and most heteromyid specimens. The thin bone of the basisphenoid portion of the keel lacks a sphenoid sinus of any sort, and there is nothing corresponding to the lateral extensions of the TBS. The much smaller size, inconstant location, and low incidence of such apertures outside of geomyoids places their homology in question, although these veins would still qualify as emissaria.

An equivalent to the ICV is not mentioned in Howell's study, and in any case the route of the internal carotid artery in *Dipodomys* (see Wahlert, 1985; Brylski, 1990) is so different from the one characteristic of most other mammals that their homology is questionable. The basicapsular fenestra is widely open in *Dipodomys* and there are no obvious indicia marking the external route of the VPS or the precise location of the internal jugular vein's exit.

←  
 FIG. 18. **A** and **B**, *Notamacropus eugenii* AMNH M-197003 (Macropodidae, Diprotodontia), adult caudal cranium in ventral and oblique lateral views. **C**, *Osphranter robustus* AMNH M-80171, juvenile, in oblique endocranial view. In **A**, note accessory transverse canal foramen. In **C**, large apertures for transverse canal and carotid canal punctuate floor of endocranial carotid groove, creating a large common space osteologically. **Key:** **astp**, tympanic process of alisphenoid; **atcf**, accessory transverse canal foramen; **bjs**, basijugular sulcus; **BO**, basioccipital; **BS**, basisphenoid; **cc (encf)**, carotid canal, including endocranial carotid foramen; **cchc**, rostral condylohypoglossal canal; **cchf**, caudal condylohypoglossal foramen; **encg**, endocranial carotid groove; **evpf**, foramen for extracranial continuation of ventral petrosal sinus; **excf**, exocranial carotid foramen; **fm**, foramen magnum; **fo**, foramen ovale; **io + pf**, incisura ovalis and piriform fenestra; **jf**, jugular foramen; **pbs**, presphenoid-basisphenoid synchondrosis; **PE**, petrosal; **pf**, piriform fenestra; **pglf**, postglenoid foramen; **rhc**, rostral condylohypoglossal canal; **rchf**, rostral condylohypoglossal foramen; **sof**, sphenoorbital fissure; **SQ**, squamosal; **tcf**, transverse canal foramen; **tcf (cbf)**, coterminous transverse canal foramen and caudal branch foramen; **trcf**, transclival foramen.

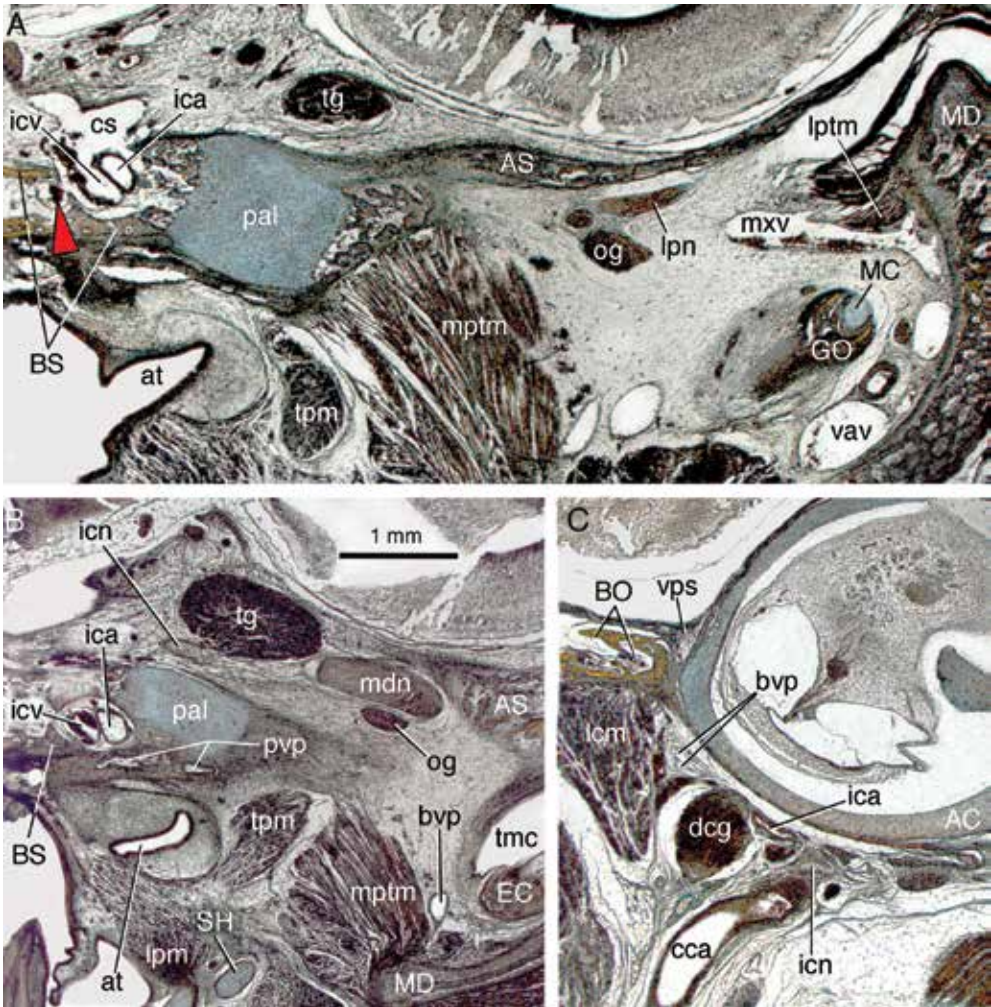


FIG. 19. *Notamacropus eugenii* ZIUT HL 29 mm (Macropodidae, Diprotodontia), perinatal specimen, stained coronal sections in rostrocaudal order. **A**, Carotid canal, showing internal carotid artery enveloped by cavernous sinus/internal carotid vein (s. 182.02.02); **B**, Pharyngeal and pterygoid venous plexuses, internal carotid vein (s. 184.04.03) **C**, Midcochlear region, showing plexiform basicranial venous plexus (s. 196.03.03). In **A**, inside basisphenoid note anastomosis of internal carotid vein with a vein possibly representing caudal branch of transverse canal vein (red pointer). **Key:** AC, auditory capsule; AS, alisphenoid; at, auditory tube; BO, basisphenoid; BS, basisphenoid; bvp, basicranial venous plexus; cca, common carotid artery; cs, cavernous sinus; dca, dorsal cervical ganglion; EC, ectotympanic; GO, gonial; ica, internal carotid artery; icn, internal carotid nerve; icv, internal carotid vein; lcm, longus capitis muscle; lpm, levator veli palatini muscle; lptm, lesser petrosal nerve; lptm, lateral pterygoid muscle; MC, meckelian cartilage; MD, mandible; mdn, mandibular nerve; mptm, medial pterygoid muscle; mxv, maxillary vein; og, otic ganglion; pal, processus alaris; pvp, pterygoid venous plexus; SH, stylohyal; tg, trigeminal ganglion; tmc, tympanic cavity; tpm, tensor veli palatini muscle; vav, ventral alveolar vein; vps, ventral petrosal sinus.

## PRIMATES

*GALAGO* (LORISIFORMES, GALAGIDAE) AND *MICROCEBUS* (LEMURIFORMES, CHEIROGALEIDAE) (figs. 36C, 37A–D). Unlike other primates, lorisiforms, and cheirogaleid lemuriforms exhibit well developed transcranial venous channels in the mesocranial region. In these strepsirhines a venous plexus surrounds the ascending pharyngeal artery as it enters the carotid foramen (Saban, 1963; Cartmill, 1975; MacPhee, 1981). (The internal carotid artery, reduced to a thread in these taxa, is functionally replaced by an anastomosis between the ascending pharyngeal artery and the circulus arteriosus [Cartmill, 1975]; this anastomosis is not known to occur in marsupials [Aplin, 1990].) The plexus is found where the PVP and BVP occur in other mammals and presumably incorporates them in whole or in part. The plexus is connected to the cavernous sinus by a large emissarium, regarded here as a primary homolog of the ICV (= sinus carotidien of Saban, 1963) (fig. 37A). Other primates do not exhibit ICV hypertrophy of this kind, and likely possess only a small internal carotid venous plexus along the lines of the one in *Homo*.

In *Galago* both the ascending pharyngeal artery and the ICV are retiform and intertwined (fig. 37A), which may mean that they function as a counter-current heat-exchange mechanism (see Cartmill, 1975; Caputa, 2004). However, in *Microcebus* the artery is a single tube, not a rete, and the function of this arrangement in mouse lemurs is obscure (fig. 37D). According to Saban (1963: fig. 36), two emissaria leave the rostral carotid foramen in *Cheirogaleus* (a close relative of *Microcebus*) to anastomose with the maxillary vein or EJV. Indicators are ambiguous regarding whether these qualify as TCVs; their destinations are similar to those of marsupial TCVs, but separate TCFs are absent. Both the ICV/BVP (= sinus pétro-occipital of Saban, 1963) and IJV are depicted as rather small in this lemur, but Saban's figure is impressionistic and actual dimensions are not provided.

## MACROSCELIDEA

*ELEPHANTULUS* (MACROSCELIDIDAE) (fig. 37E). In the macroscelidean afrothere *Elephantulus fuscipes* the carotid foramen transmits a large vein in addition to the internal carotid artery (MacPhee, 1981: fig. 46c). Although it might be assumed that this vessel is a version of the ICV, its morphological relations in sengis are quite different from those seen in marsupials. Homology is therefore unlikely; however, showing this in developmental terms illustrates how ontogeny can help inform character analysis.

The vein departs from the temporal (= prootic) sinus on the interior sidewall of the skull and crosses the tympanic roof to enter the intratympanic carotid foramen, where it merges with the CS. The vessel never leaves the skull and therefore does not conform to either an emissarial CBV or emissarylike RBV as seen in marsupials. The vein may be a remnant of a portion of the prootic sinus that is lost in most placentals, but this needs to be corroborated. Van der Klaauw's (1929) paper on the development of the macroscelidean bulla includes section drawings that show a vein that is unidentified but positionally like the one described here for *E. fuscipes*. Something similar may occur in the chrysochlorid *Eremitalpa granti*: Roux (1947: fig. 41) depicts a large unidentified vein passing between the ossifying basisphenoid and the location of the trigeminal ganglion in a 45 mm embryo, but does not discuss its relations. If this vein is widespread in afrotheres—which is completely unknown—it may mark a shared retention, perhaps lost in adult stages of other placental clades.

## OTHER PLACENTALS

TCFs/TCVs large enough to be recognizable as such may be uncommon in extant placentals, but they are also rarely searched for. TCFs have been explicitly identified in the rodent *Rattus* (Greene, 1935; Wible and Shelley, 2020), the lipotyphlan

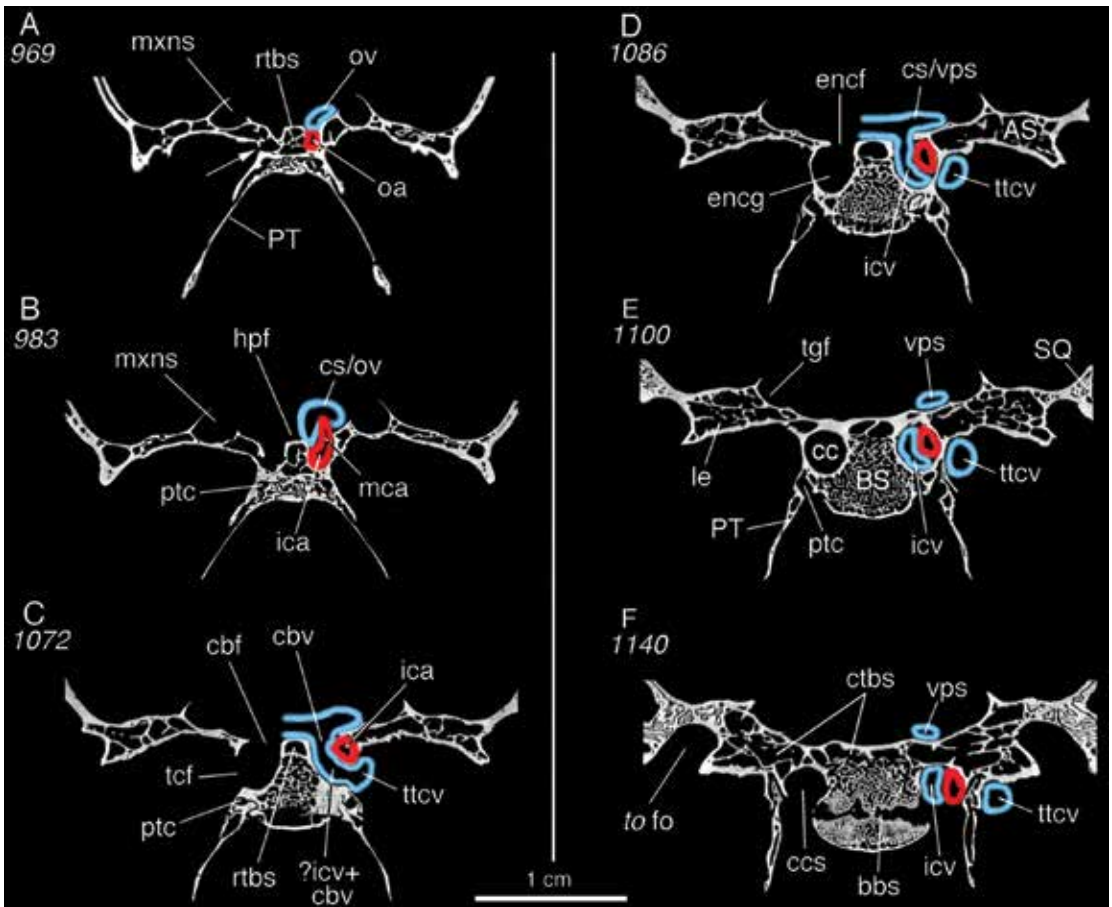


FIG. 20. *Osphranter robustus* AMNH M-80171 (Macropodidae, Diprotodontia), juvenile caudal cranium, selected coronal segments in rostrocaudal order (data source, table 2). A–F, Conjectured arrangement of mesocranial blood vessels (red, arterial only; blue, venous only), sizes exaggerated for clarity. Macropodids often have multiple transverse canal foramina (e.g., *Notamacropus*, fig. 18B). In this specimen, accessory foramina (arrow in A) are tiny and open into cancellous tissue, but do not form recognizable junction or communicate directly with endocranium or much larger main foramen (cf. *Trichosurus*, fig. 22A, B). Nevertheless, they may qualify as RBTCs. In C–E, external apertures for main transverse canal and carotid canal can be seen passing through floor of endocranial carotid groove, where their pathways merge. As a result there is no separate caudal branch foramen because entire trunk consists of caudal branch vein. Whether it retains its separate identity or anastomoses with internal carotid vein in carotid groove as suggested in C (?icv + cbv) is unknown. In any case, in this reconstruction internal carotid vein is shown as departing as a separate vessel through main transverse canal foramen, as in other taxa. **Key:** AS, alisphenoid; bbs, basisphenoid-basioccipital synchondrosis; BS, basisphenoid; cbf, caudal branch foramen; cbv, caudal branch vein; cc, carotid canal; cs/ov, ophthalmic vein entering cavernous sinus; cs/vps, cavernous sinus releasing ventral petrosal sinus; ctbs, caudal portion of transverse basisphenoid sinus; encf, endocranial carotid foramen; encg, endocranial carotid groove; fo, foramen ovale; hpf, hypophyseal fossa; ica, internal carotid artery; icv, internal carotid vein; ?icv + cbv, possible anastomosis of caudal branch vein of transverse canal and internal carotid vein; le, lateral extension of transverse basisphenoid sinus; mca, middle cerebral artery; mxns, suclus for maxillary nerve; oa, ophthalmic artery; ov, ophthalmic vein; PT, pterygoid; ptc, pterygoid canal; rtbs, rostral portion of transverse basisphenoid sinus; SQ, squamosal; tcf, transverse canal foramen; tgf, trigeminal ganglion fossa; ttcv, trunk transverse canal vein; vps, ventral petrosal sinus.

*Solenodon* (Wible, 2008), the carnivorans *Nandinia*, *Felis*, and *Genetta* (Wible and Spaulding, 2013), and a number of xenarthrans including *Dasypus*, *Euphractus*, vermilinguans, and glyptodonts (Wible and Gaudin, 2004; Le Verger et al., 2021). However, even in the case of the extant taxa, in only a few cases has there been verification of the actual presence of the TCV (as opposed to its purported foramen). One such is *Solenodon* (Wible, 2008): in addition to possessing a definite TCV and TCF, it also exhibits pneumatic sinuses in the basisphenoid and presphenoid bones. Wible (2008) also found that several venous channels communicate with the sphenoid sinus, including one situated on the dorso-lateral aspect of the basisphenoid. This suggests that *Solenodon* may possess features of PCVN organization also seen in marsupials.

#### RECONSTRUCTING PERICAROTID VENOUS NETWORKS IN EXTINCT SPARASSODONTAN METATHERIANS

In this section we present interpretations of structures related to the PCVN in two Miocene sparassodontans, *Sipalocyon gracilis* AMNH VP-9254 and *Prothylacynus patagonicus* YPM VPPU-15700, chosen because they exhibit markedly different junction patterns (see figs. 38–42). The species selected for analysis represent two main clades, Hathliacynidae and Borhyaenoidea. They differ in estimated body size by a factor of 10 (table 2), with the estimate for *P. patagonicus* lying within adult ranges recorded for the largest marsupial species included in the present study. The morphological question of interest is whether the main components of the PCVN found in extant marsupials were already present and arguably similar functionally in these stem metatherians (see Marshall, 1976, 1978; Muizon and Ladevèze, 2020).

On any given marsupial skull it is usually possible to ascertain by simple inspection whether the TCF is present. As the TCV is the only recorded occupant of this foramen, identifying the foramen in a fossil is tantamount to acknowledging the

vein's existence during life. However, identification has proven to be a contentious topic in nonmarsupial metatherian studies, partly because of disagreements about acceptable criteria for inferring TCF presence, as the following survey illustrates.

In Sparassodonta, the TCF is reported to be either absent or inapparent in *Borhyaena tuberata*, *Arctodictis munizi*, *A. sinclairi*, *Thylacosmilus atrox*, *Callistoe vincei*, *Sallacyon hoffstetteri*, *Acyon myctoderos*, *Cladosictis patagonica*, and *Hondadelphys fieldsi* (Archer, 1976; Marshall, 1976, 1978; Muizon, 1999; Babot et al., 2002; Forasiepi, 2009; Forasiepi et al., 2019). In *Prothylacynus patagonicus* (Archer 1976; Forasiepi, 2009; Forasiepi et al., 2019), *Lycopsis longirostris* (Marshall, 1977; but see Forasiepi et al., 2019), and at least some specimens of *Cladosictis patagonica* (Muizon, 1999; see also Archer 1976; Babot et al., 2002) and *Sipalocyon gracilis* (Archer, 1976), TCFs have been described as present. The situation is less clear in some other taxa, such as *Notogale mitis* (Muizon, 1999; Babot et al., 2002), although in this last taxon the TCF is clearly bilaterally present in some specimens (R. Beck, personal commun.)

Our position is that identification of the TCF and other PCVN components in metatherian fossils ought to be based, wherever possible, on well-tested recognition criteria like those used for extant taxa. Tomography has helped in defining such criteria, and in this section we show how scanning provides new opportunities for assessing the existence of PCVN vasculature and improving interpretations of character evolution in early South American metatherians.

#### SIPALOCYON (HATHLIACYNIDAE)

##### Figures 38, 39

Archer (1976), who described AMNH VP-9254 under one of its synonyms, *Thylacodictis*, was able to trace only surface details in the mesocranial area. Our scan of this specimen clears up several points that were previously in doubt.

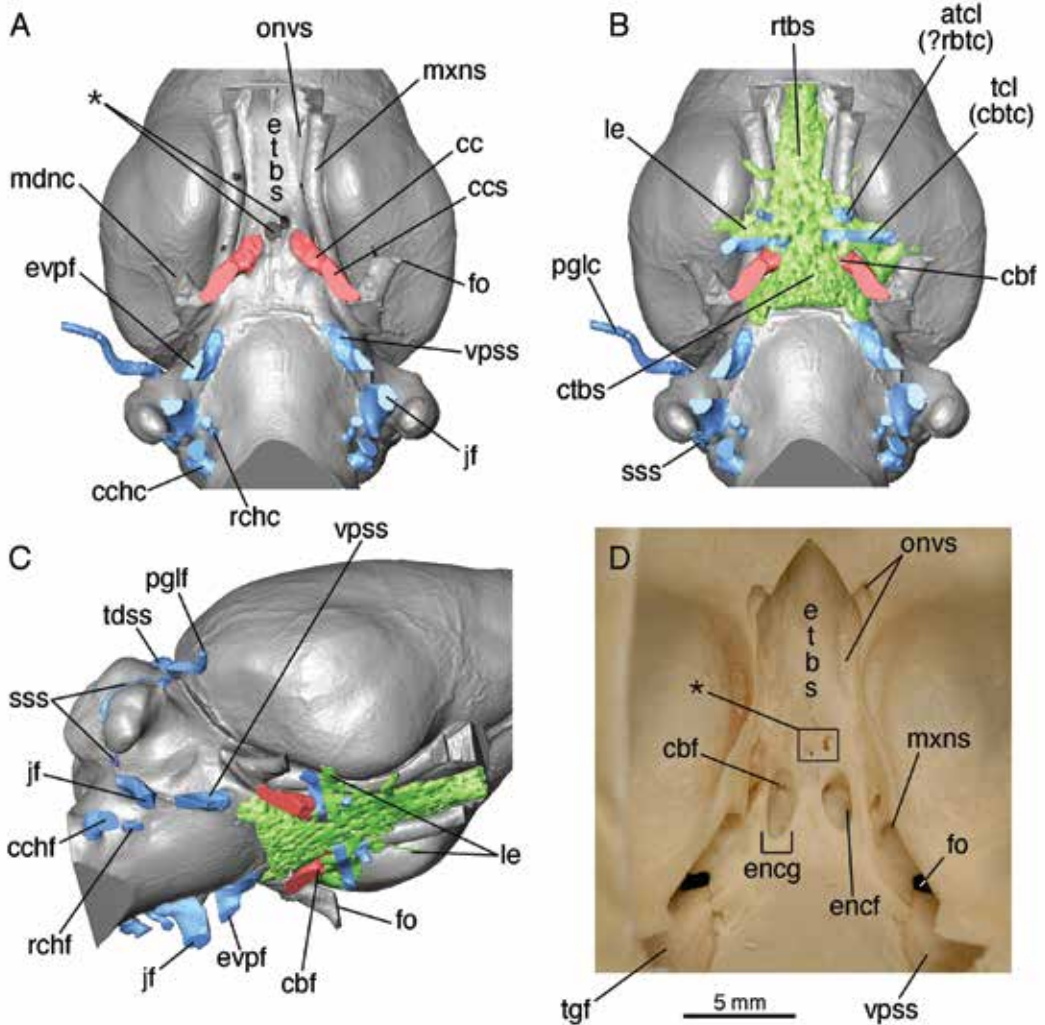
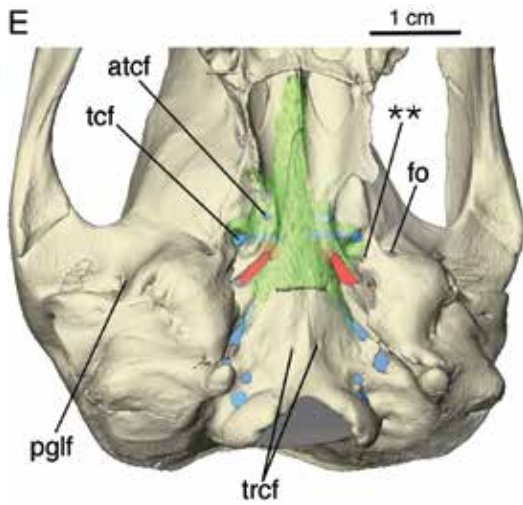


FIG. 21. *Trichosurus vulpecula* TMM M-849 (Phalangeridae, Diprotodontia), adult specimen, endocast reconstruction showing osteological features associated with pericarotid venous network and related vasculature (data source, table 2; color key, fig. 4). Views: **A**, ventral; **B**, same, with transverse basisphenoid sinus superimposed; **C**, oblique right lateral; **D**, closeup of mesocranial osteological features in *T. vulpecula* AMNH 48055; and **E**, oblique caudoventral surface, intact caudal cranium. In **B** and **C**, endocast of caudal branch foramen projecting from carotid groove (cf. *Dromiciops*, fig. 15A, D). In **A** and **D**, in addition to caudal branch foramen, note foramina (single asterisk, box) perforating endocranial floor, linking hypophyseal fossa to transverse canals by means of hypophyseal canaliculi (cf. fig. 22C, D). Separate craniopharyngeal foramen not identifiable. In **E**, note foramen (double asterisks) medial to position of foramen ovale (see text). **Key:** **atcf**, accessory transverse canal foramen; **atcl (?rbtc)**, accessory transverse canal (?rostral branch of transverse canal); **cbf**, caudal branch foramen; **cc**, carotid canal; **cchc**, caudal condylohypoglossal canal; **cchf**, caudal condylohypoglossal canal; **ccs**, sulcus leading to carotid canal; **ctbs**, caudal portion of transverse basisphenoid sinus; **encf**, endocranial carotid canal; **encg**, endocranial carotid groove; **etbs**, eminence of transverse basisphenoid sinus; **evpf**, extracranial continuation of ventral petrosal sinus; **fo**, foramen ovale; **jf**, jugular foramen; **le**, lateral extension of transverse basisphenoid sinus; **mdnc**, canal for mandibular nerve; **mxns**, sulcus for maxillary nerve; **onvs**, sulcus for



ophthalmic neurovascular array; **pglc**, postglenoid canal; **pglf**, postglenoid foramen; **rhc**, rostral condylohypoglossal canal; **rhc**, rostral condylohypoglossal canal; **rhc**, rostral condylohypoglossal canal; **rtbs**, rostral portion of transverse basisphenoid sinus; **sss**, sulcus for sigmoid sinus; **tcf**, (primary) transverse canal foramen; **tcl (cbtc)**, (primary) transverse canal (caudal branch of transverse canal); **tdss**, sulcus for transverse dural sinus; **tgf**, fossa for trigeminal ganglion; **trcf**, transclival foramina; **vpss**, ventral petrosal sinus.

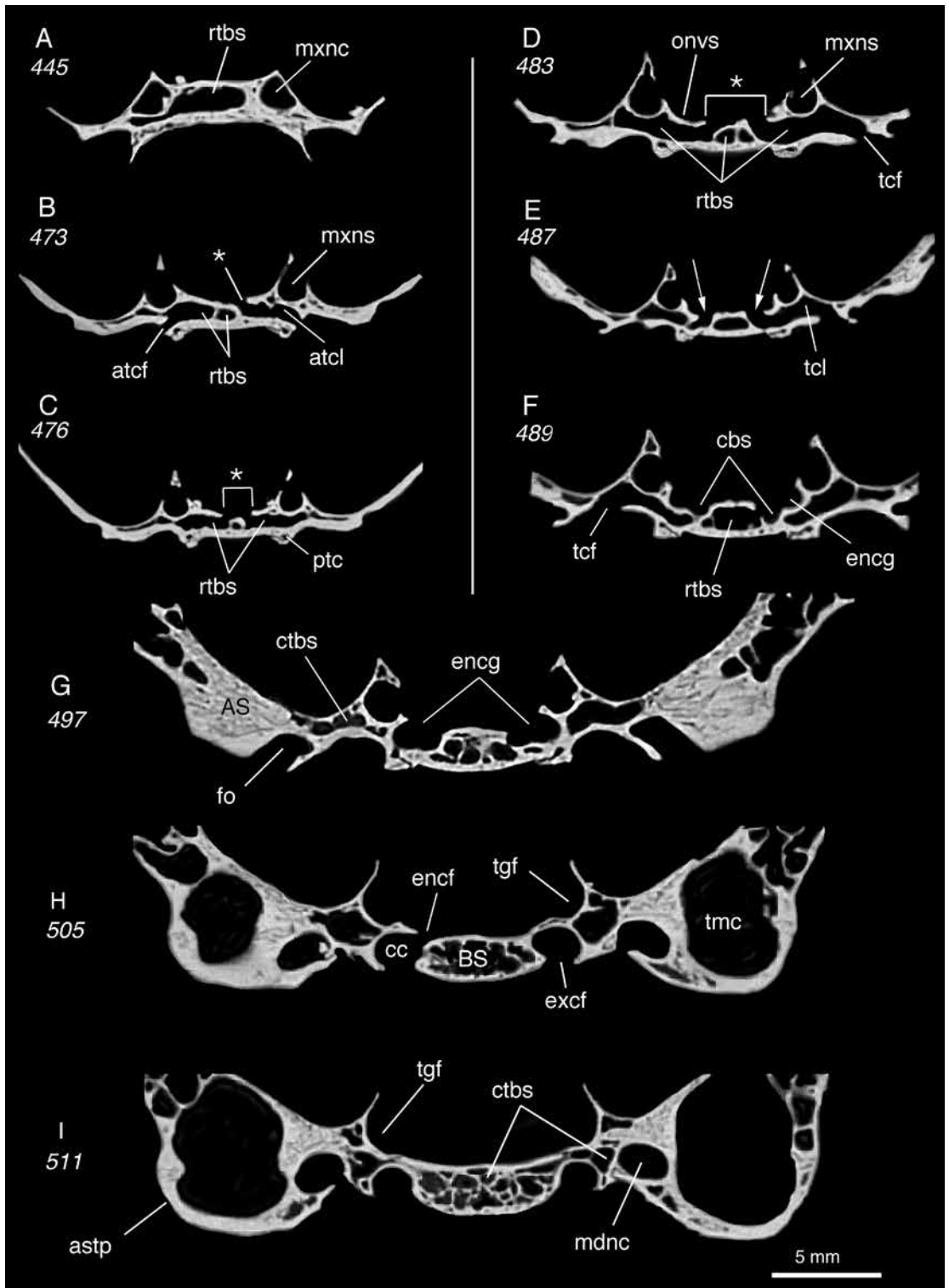
Archer (1976: 289, 307) wondered whether one or the other of two small foramina or notches (fig. 39: features 1, 2) seen on the lateral margin of each carotid foramen in AMNH VP-9254 could have accommodated true TCVs. Our CT evidence indicates that this is unlikely in both cases. Feature 2 ends abruptly and cannot be traced further rostrally along the skull (fig. 39C–E). Its nature remains uncertain, but in being directed away from the basicranial keel its routing is not that of a typical TCV as seen in marsupials. Feature 1, situated more medially (fig. 39A–F), is bordered by pterygoid material; it continues rostrally as either a canal (specimen's left side) or sulcus (right side), to terminate in a tiny aperture located in the infratemporal fossa immediately caudal to the foramen rotundum (location indicated in fig. 38E). In this case the relations of the aperture are consistent with its being a rostral foramen for the nerve of the pterygoid canal, not a port for the TCV.

Aplin (1990) showed that in several extant marsupials the postganglionic sympathetic fibers composing the deep petrosal nerve often pass out of the carotid canal through a separate foramen, rather than adhering closely to the internal carotid artery as in many placentals (MacPhee, 1981). The equivalent of this foramen could be represented in *Sipalocyon* by the small gap (feature 1) in the wall of the carotid canal seen in figure 39F. If so, the gap marks the trackway not of the transverse canal, as Archer (1976) thought, but rather that of a component of the nerve of the pterygoid canal.

It is of course possible that the TCV started to develop embryonically in *Sipalocyon*, but failed to persist after an early stage. In such circumstances all that can be said is that an identifiable TCF would not be expected in the adult, and that is the case here: there is nothing in the organization of the mesocranium that would suggest the presence of the TCV trunk or its branches in adult *Sipalocyon*.

As expected, the carotid canals pass into the endocranium lateral to the probable location of the hypophyseal fossa. Within the body of the basisphenoid the right and left carotid canals communicate with a small intramural space that positionally conforms to the caudal TBS (figs. 38B, D; 39D: feature 3), although organizationally it differs appreciably from anything seen in extant marsupials. Conceivably, this space could have permitted flow between bilateral ICVs (fig. 38D: double-headed arrow), although what purpose would be served thereby is obscure. Feature 4, a short tube that occupies the midline, could be another connector or alternatively a remnant of the notochord canal (cf. *Thylacinus*, fig. 30D). The TBS is not extensively developed, especially as compared with *Prothylacynus* (fig. 40B), and the lateral extensions only weakly connect its rostral and caudal portions.

The basijugular sulcus on the caudal basicranial surface is strongly marked in *Sipalocyon* and other sparassodontans (e.g., *Thylacosmilus*, *Lycopsis*; Forasiepi et al., 2019; see also Archer, 1976: 290). It is continuous, via the caudal condylo-



hypoglossal foramen, with the craniospinal foramen on the interior lip of the foramen magnum. This implies that the vessel that occupied the basijugular sulcus—presumably the EVPS, as in marsupials—anastomosed directly with the VVs, as well as with the highly reduced IJV and local emissaria (see vascular reconstruction for *Thylacosmilus* by Forasiepi et al., 2019: fig. 26). In addition to the foregoing, prominent craniospinal foramina are also seen, as in *Prothylacynus*, *Cladosictis*, and *Borhyaena*.

#### PROTHYLACYNUS (BORHYAENOIDEA)

##### Figures 40, 41

The caudal cranium of YPM VPPU-15700 shows considerable damage in the vicinity of the right carotid canal and basioccipital surface. Another skull, *P. patagonicus* MACN A-5931, was examined to corroborate surface details not well preserved on the Yale specimen.

Scanning reveals a complicated arrangement of internal vascular channels in the rostral part of the mesocranial region. These channels are comparable to the rostral branches (RBTCs) seen in extant marsupials, and they are designated as such here. However, there are some important differences that need to be acknowledged. In the Yale specimen the RBTCs are connected to two sets of similar-sized TCFs (features 1–4, fig. 40A, D). The canals into which they feed are situated in advance of the carotid canals, and present cross-sectional widths that are approximately

half that of the latter. From these canals, groups of interstitial canaliculi extend into the TBS (fig. 40E–F), or invade the alisphenoid where they continue as far as the latter's sutural contact with the frontal. There is nothing in their position or relations to suggest that nerves were transmitted through these conduits. In MACN A-5931 only a single TCF is distinctly present on each side, but additional cleaning or scanning might reveal more (see Forasiepi et al., 2019: fig. 15).

The doubling of rostral branches in this manner recalls conditions in some extant diprotodonts, especially petauroids (*Dactylopsila*, *Dactylonax*, and *Gymnobelideus*) in which typical TCFs exist alongside large anterior pterygoid foramina according to Beck et al. (2022: char. 50). Given the close proximity of all these vessels in the petauroids, they probably anastomose within the mesocranium. However, whether it would be meaningful to call all of them transverse canals is a different problem. We recognize that *Prothylacynus* presents the same nomenclatural issue.

The rostral branches join across the midline and communicate with the carotid canals by means of tubes functionally similar to the caudal branches (CBTCs) of marsupials, but there are differences. No potential sites of communication between these branches and any likely location for the hypophyseal fossa were identified. The left tube exhibits a particularly large interstitial connector that directly communicates with the TBS (fig. 40D: asterisk). Another (fig. 40E: double

FIG. 22. *Trichosurus vulpecula* TMM M-849 (Phalangeridae, Diprotodontia), adult caudal cranium, coronal segments in rostrocaudal order (data source, table 2). In **A** and **B**, rostral portion of transverse basisphenoid sinus inflates endocranial floor of basisphenoid and receives accessory transverse canal. In **C–E**, main transverse canals directly communicate with hypophyseal fossa via endocranial floor apertures (single asterisk with bracket) and caudal branch foramina (arrows). In **F–H**, note endocranial carotid groove, carotid canal, and possible sulcus for caudal branch of transverse canal. Junction pattern provisionally regarded as hybrid (see text). **Key:** **AS**, alisphenoid; **astp**, tympanic process of alisphenoid; **atcf**, accessory transverse canal foramen; **atcl**, accessory transverse canal (?rostral branch of transverse canal); **BS**, basisphenoid; **cbs**, sulcus for caudal branch of transverse canal; **cc**, carotid canal; **ctbs**, caudal portion of transverse basisphenoid sinus; **enccf**, endocranial carotid foramen; **encg**, endocranial carotid groove; **excf**, exocranial carotid foramen; **fo**, foramen ovale; **mdnc**, canal for mandibular nerve; **mxnc**, canal for maxillary nerve; **mxns**, sulcus for maxillary nerve; **onvs**, sulcus for ophthalmic neurovascular array; **ptc**, pterygoid canal; **rtbs**, rostral portion of transverse basisphenoid sinus; **tcf**, (primary) transverse canal foramen; **tcl**, (primary) transverse canal (caudal branch of transverse canal); **tgf**, fossa for trigeminal ganglion; **tmc**, tympanic cavity.

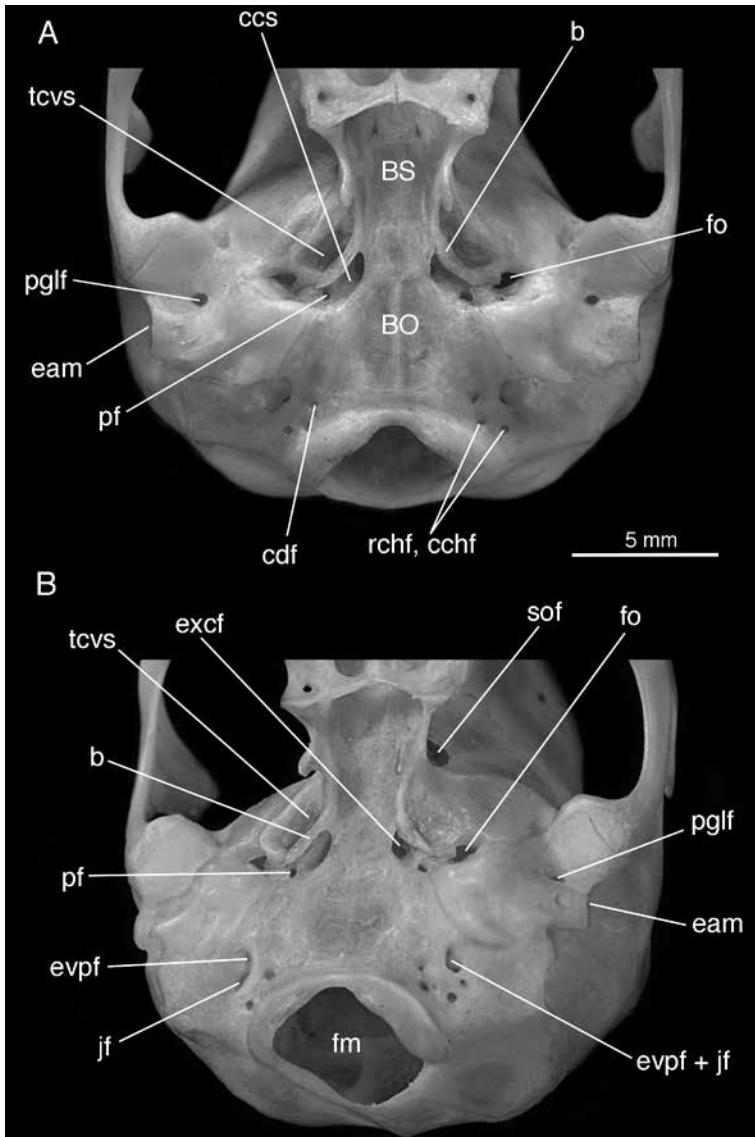


FIG. 23. *Distoechurus pennatus* AMNH M-105938 (Acrobatidae, Diprotodontia), adult caudal cranium in **A**, ventral, and **B**, oblique caudoventral views. Two sulci, incompletely separated by a bridge (**b**) formed by a calcified ligament, converge on a single aperture identified as exocranial carotid foramen. As there is no separate transverse canal foramen, transverse canal vein is thought to share carotid canal with internal carotid neurovascular bundle (Aplin, 1990). Basijugular sulcus not prominent; jugular foramen and extracranial continuation of ventral petrosal sinus are separate, but open into common external aperture. **Key:** **b**, bridge (calcified ?sphenopetrosal ligament); **BO**, basioccipital; **BS**, basisphenoid; **cchf**, caudal condylohypoglossal foramen; **ccs**, sulcus leading to carotid canal; **cdf**, condylar foramen additional to **rchf** and **cchf**; **eam**, external acoustic meatus; **evpf**, extracranial continuation of ventral petrosal sinus; **evpf + jf**, common external aperture for jugular foramen and extracranial continuation of ventral petrosal sinus (left side only); **excf**, exocranial carotid foramen; **fm**, foramen magnum; **fo**, foramen ovale; **jf**, jugular foramen; **pf**, piriform fenestra; **pglf**, postglenoid foramen; **rchf**, rostral condylohypoglossal foramen; **sof**, sphenoorbital fissure; **tcvs**, sulcus for transverse canal vein.

asterisks) is pointed toward the sphenoorbital fissure, suggesting a more extensive drainage field.

In *Prothylacynus* (fig. 40E) the carotid canals are much smaller in caliber relative to endocast width than in *Sipalocyon* (fig. 38E), or indeed in most of the marsupials investigated in this paper. This difference, which is the opposite of expected, is of uncertain significance but cannot be attributed to specimen damage.

## DISCUSSION

### MORPHOLOGICAL SUMMARY AND CONCLUSIONS

We are conscious of the fact that our descriptions are based on one or a few specimens for each highlighted taxon. Intrataxon variability, which certainly exists in marsupial cephalic venous systems, is therefore not adequately addressed. This is a first effort to combine traditional techniques as well as modern visualization technology to bring out the complexity of these systems. It has yielded dividends such as the discovery of erythroid activity in the mesocranium of young stages, and the previously underappreciated significance of circulation patterns in the same area. At the same time, it is important not to be overly optimistic that the specimens examined in detail here are representative of conditions throughout Metatheria.

**PERICAROTID VENOUS NETWORK IN MARSUPIALS.** On the basis of the investigations reported in this paper, we propose that in extant marsupials the transverse canal vein (TCV), the only occupant of the transverse canal foramen (TCF), is formed, in most but not all investigated species, by the union of two tributaries or source vessels: a rostral branch vein (RBV) which does not directly enter the endocranium and is therefore best described as only emissarylike, and a caudal branch vein (CBV), which has a clear emissarial role involving the cavernous sinus (CS). The TCV and the internal carotid vein (ICV) are the chief pericarotid mesocranial distributaries (PMDs) of the pericarotid venous network (PCVN). In adult marsupials these vessels are almost always of considerable size, in

contrast to their diminutive equivalents in most placentals. Although it is likely that in all extant therians the PMDs provide some venous drainage for the CS, their role in this regard is usually minor compared to that of the petrosal sinuses, particularly the ventral petrosal sinus (VPS) which ultimately communicates with the sigmoid sinus (SS) and other large caudal veins. On leaving the skull the TCV terminates in the pterygoid venous plexus (PVP) and maxillary vein of the external jugular venous system (EJVS). Although the ICV is also in anastomotic contact with the TCV and local plexuses, its most significant linkage is with the basicranial venous plexus (BVP), forming the compound vessel designated as the ICV/BVP.

Some features of the PCVN can be consistently identified on dry skulls and fossils using osteological criteria. Bony canals for rostral branches of the transverse canal (RBTCs), which carry the RBVs, characteristically terminate in a junction within a pneumatized structure, the transverse basisphenoid sinus (TBS), immediately rostral to the hypophyseal fossa. The junction contains the mesocranial confluence of right and left RBVs. By contrast, the caudal branches of the transverse canal (CBTCs), which carry the CBVs, tend to be much shorter. The osteological indicium for the presence of a CBV is normally the caudal branch foramen (CBF), situated within the endocranial carotid groove that also houses the endocranial carotid foramen. The CBV is the only tributary of the TCV trunk in taxa lacking detectable RBTCs, in which case the CBF will have a caliber resembling that of the transverse canal foramen. CBVs always communicate with the CS/ICV, from which they originate. They do not form a confluence, as right and left veins do not cross the midline, but instead follow separate courses within the basisphenoid to their respective transverse canals. Their origins are in the same coronal plane as the hypophyseal fossa, and thus caudal to the junction of the RBTCs.

Although many extant marsupial taxa confirmably possess both RBTCs and CBTCs, some have

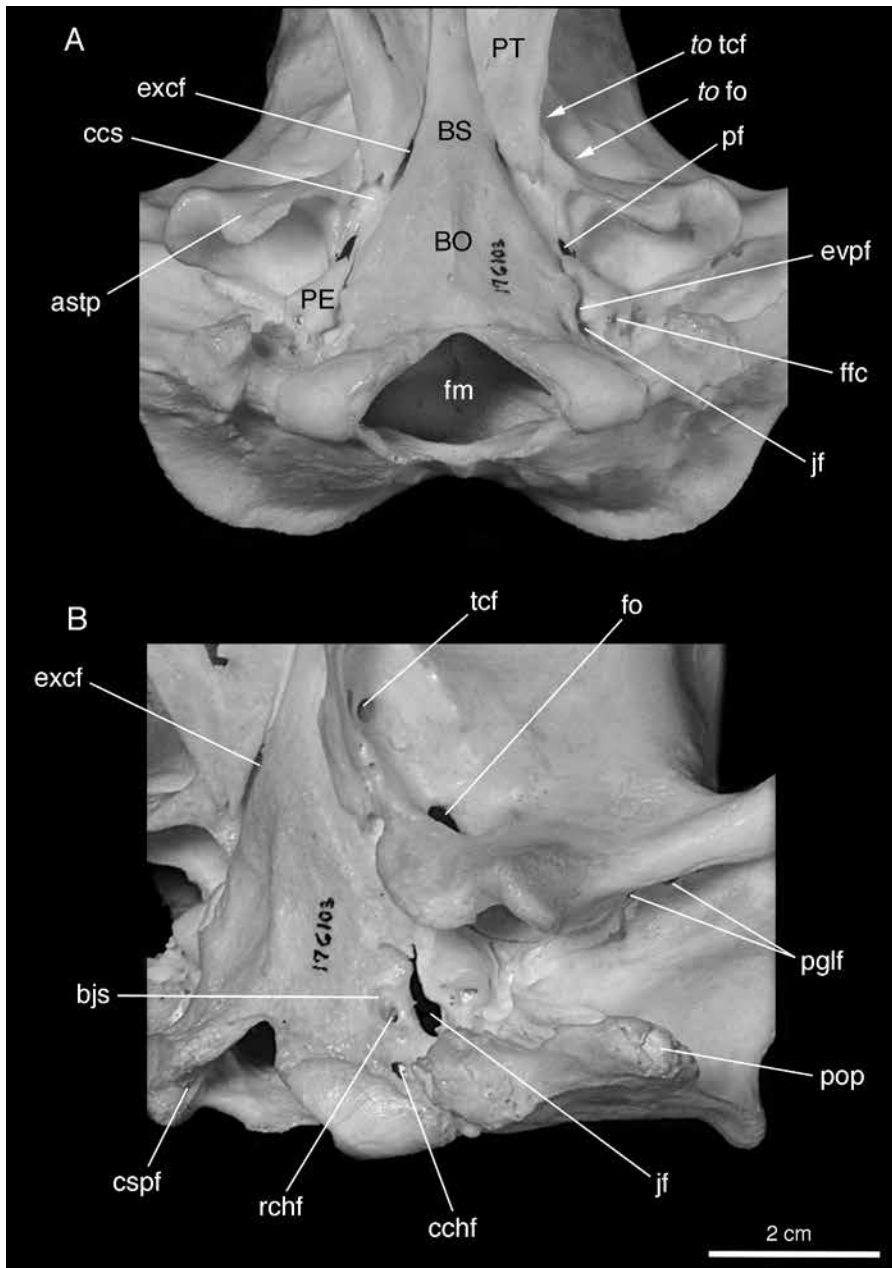
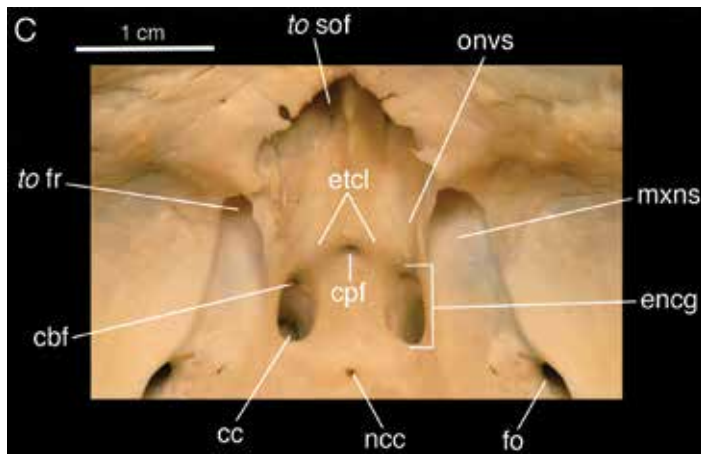


FIG. 24. *Vombatus ursinus* AMNH M-176103 (Vombatidae, Diprotodontia), adult caudal cranium in **A**, ventral; **B**, oblique caudolateral, and **C**, endocranial aspects. In **C**, RBTC canals are notably large (fig. 25B) and sharply define rostral border of deep hypophyseal fossa. **Key:** *astp*, tympanic process of alisphenoid; *bjs*, basi-jugular sulcus; *BO*, basioccipital; *BS*, basisphenoid; *cbf*, foramen for caudal branch of transverse canal vein; *cc*, carotid canal; *ccs*, exocranial sulcus leading to carotid canal; *cchf*, caudal condylohyoglossal foramen; *cpf*, craniopharyngeal foramen; *cspf*, craniospinal foramen; *encg*, endocranial carotid groove; *etcl*, eminence formed by junction of rostral branches of transverse canals; *evpf*, foramen for extracranial continuation of



ventral petrosal sinus; **excf**, exocranial carotid foramen; **ffc**, fossula fenestrae cochleae; **fm**, foramen magnum; **fo**, foramen ovale; **fr**, foramen rotundum; **jf**, jugular foramen; **mxns**, sulcus for maxillary nerve; **ncc**, notochord canal; **onvs**, sulcus for ophthalmic neurovascular array; **PE**, petrosal; **pf**, piriform fenestra; **pglf**, postglenoid foramina (double); **pop**, paracondylar process; **PT**, pterygoid; **rchf**, rostral condylohyoglossal foramen; **tcf**, transverse canal foramen.

only one set, and a few lack TCVs entirely, at least in the adult stage. *Thylacinus* appears to lack even a vestige of the RBTC pathway, at least in the material available to us. The situation in phalangeridans is less clear; small RBTCs may persist into the adult stage, but they do not form a recognizable junction or a continuous, side-to-side canal.

An unresolved morphological problem is whether marsupials (individuals or species) that lack a discrete TCF nonetheless have a vein that plays the part of the TCV, but one which leaves the endocranium through another aperture such as the exocranial carotid foramen or foramen ovale/piriform fenestra (= foramen pseudovalve; see Archer [1976] and Sánchez-Villagra and Wible [2002] for possible examples). Such arrangements are not implausible, although the emissaries involved would presumably be different in a homological sense. In any case, verification of their nature awaits appropriate investigation. The transverse canals also communicate with the CS by means of small hypophyseal canaliculi. Their number and position appear to fluctuate greatly within and across taxa (Beck et al., 2022), suggesting that variation is strong. Their possible physiological importance is that they may act as a hedge against major-vessel

failure due to malformation, disease, or other factors, as well as providing the raw material for evolutionary change (as in the case of caudal vs. rostral dominance between branches of the TCV).

Our combined histological and CT data on extant marsupials support the following additional generalizations:

(1) The ICV is always present in young stages as a morphologically differentiated part of the CS that travels with the internal carotid artery out of the mesocranium. Thereafter it passes into the pharyngeal region, where it anastomoses with the BVP. Empirical observations on adult marsupials are few, but they support the conclusion that the ICV persists as a CS effluent throughout marsupial ontogeny (see Archer, 1976; Aplin, 1990).

(2) TCV branch connections with the CS vary from direct and extensive via CBVs (e.g., *Osphranter*, fig. 20) to negligible or even absent in the case of RBVs (e.g., *Didelphis*, fig. 4D). Connections may be supplemented by hypophyseal canaliculi, but their number and contribution are probably always small (e.g., *Caenolestes*, figs. 13D). In a very few taxa the TCV is known to be highly reduced or lost in the adult (e.g., *Caluromys*, fig. 8A; *Tarsipes*, Aplin, 1990).

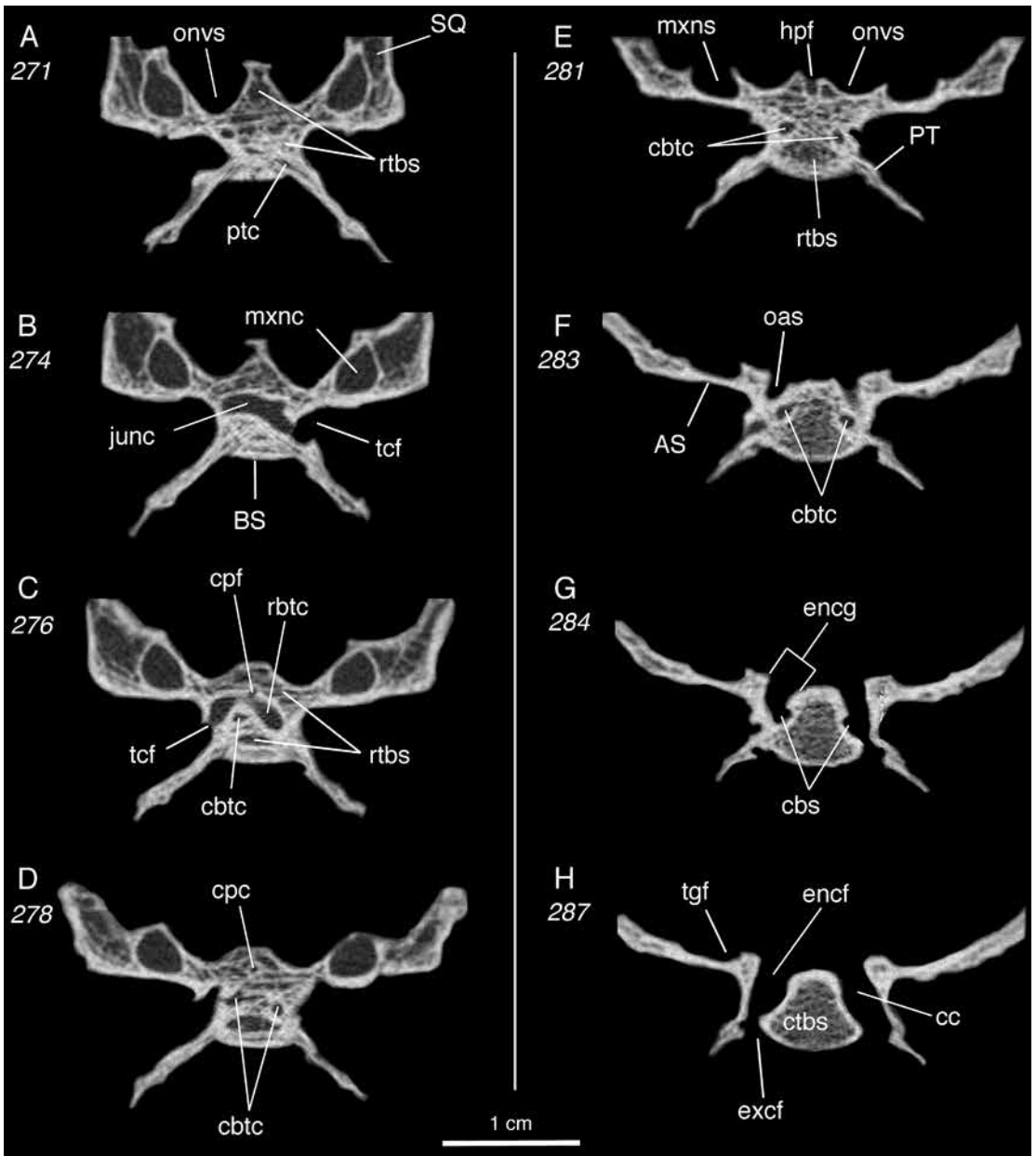


FIG. 25. *Vombatus ursinus* TMM M-2953 (Vombatidae, Diprotodontia), adult caudal cranium, selected coronal segments in rostrocaudal order (data source, table 2). In A–C, large transverse canals meet in midline junction (cf. *Phascolarctos*, Aplin, 1990: 255). In D–G, note large right and left conduits for caudal branches of transverse canal, traceable bilaterally from caudal branch foramen in endocranial carotid groove to terminus in transverse canal trunk. **Key:** AS, alisphenoid; BS, basisphenoid; cbs, sulcus for caudal branch, leading into caudal branch foramen; cbtc, canal for caudal branch of transverse canal; cc, carotid canal; cpc, cranio-pharyngeal canal; cpf, craniopharyngeal foramen; ctbs, caudal portion of transverse basisphenoid sinus; encf, endocranial carotid foramen; encg, endocranial carotid groove; excf, exocranial carotid foramen; hpf,

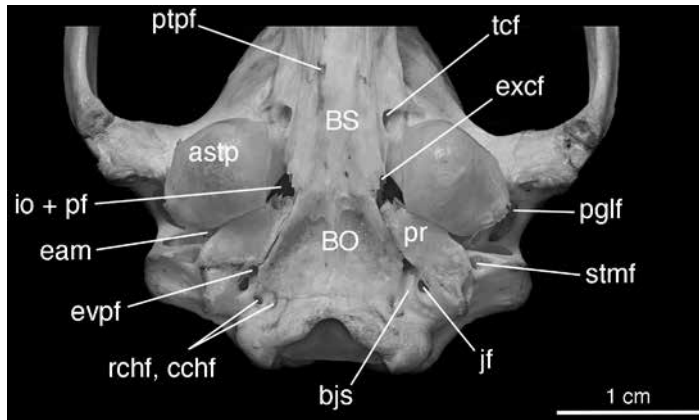


FIG. 26. *Dasyurus hallucatus* AMNH M-16033 (Dasyuridae, Dasyuromorphia), adult caudal cranium in ventral view. Note large size of piriform fenestra, acting as exit aperture for mandibular nerve in absence of separate foramen ovale. Exocranial aperture of carotid canal cannot be seen adequately in this perspective. **Key:** **astp**, tympanic process of alisphenoid; **bjs**, basijugular sulcus; **BO**, basioccipital bone; **BS**, basisphenoid; **cchf**, caudal condylohypoglossal foramen; **eam**, external acoustic meatus; **evpf**, foramen for extracranial continuation of ventral petrosal sinus; **excf**, exocranial carotid foramen; **io + pf**, incisura ovalis and piriform fenestra (undivided); **jf**, jugular foramen; **pglf**, postglenoid foramen; **pr**, promontorium of petrosal; **ptpf**, pterygopalatine fissure; **rchf**, rostral condylohypoglossal foramen; **stmf**, stylomastoid foramen; **tcf**, transverse canal foramen.

In the case of *Didelphis*, having a large RBV does not directly compensate for the absence of the CBV because these veins drain different areas (coverage is nonredundant). But this is unlikely to matter much, given the major roles of the ICV and petrosal sinuses. As the physiological functions of the RBV are uncertain (see Functional Considerations), the effect of its absence is unknown. Investigated macropodids exhibit the reverse case, in which the CBV is the only significant tributary of the TCV trunk.

Loss of a functional TCV trunk and both branches, as in *Caluromys* and *Tarsipes*, seems like a radical reduction, but in a way it is not. As far as can be ascertained, in *Caluromys* the drainage of the CS is almost exclusively accomplished by the ICV in concert with the petrosal sinuses. This arrangement is therefore similar to the near-universal pattern found in placentals,

but it should be considered secondarily derived within Marsupialia.

(3) TCVs are notably robust in marsupials, no matter which branch is dominant or the degree of communication that the TCV has with the CS. This is a strong hint that TCVs mediate vascular functions not directly related to the CS, and perhaps have always done so during metatherian evolution (see Functional Considerations).

(4) The TBS has a vascular-related function, but it is poorly investigated. This pneumatic space is considered an integral part of the PCVN not only because it may communicate with the PMDs to varying degrees in different taxa, but also because of its previously unrecognized role in extramedullary blood cell production (which also takes place in the homologous sphenoid sinus of placentals).

(5) Among extant marsupials only a few substantive differences can be detected in the basic

hypophyseal fossa; **junc**, junction of rostral branch canals; **mxnc**, canal for maxillary nerve; **mxns**, sulcus for maxillary nerve; **oas**, sulcus for ophthalmic artery; **onvs**, sulcus for ophthalmic neurovascular array; **PT**, pterygoid; **ptc**, pterygoid canal; **rbtc**, rostral branch of transverse canal; **rtbs**, rostral portion of transverse basisphenoid sinus; **SQ**, squamosal; **tcf**, transverse canal foramen; **tgf**, fossa for trigeminal ganglion.

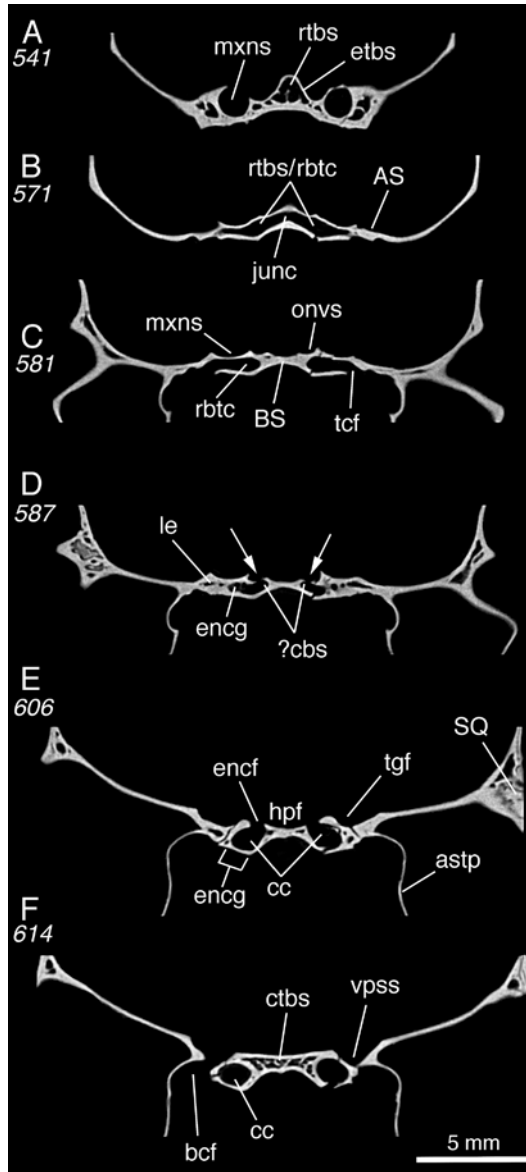


FIG. 27. *Dasyurus hallucatus* TMM M-6921 (Dasyuridae, Dasyuromorphia), adult caudal cranium, selected coronal segments in rostrocaudal order (data source, table 2). In A–C, rostral transverse basisphenoid sinus inflates endocranial surface of basisphenoid, forms compound junction with rostral branches of transverse canals. In D, caudal branch foramina open into endocranium on rostral margin of carotid grooves (arrows). However, as no definite trackway for this vein can be detected, actual course not certain. **Key:** AS, alisphenoid; **astp**, tympanic process of alisphenoid; **bcf**, basicapsular fenestra; **BS**, basisphenoid; **?cbs**, assumed track of caudal branch of transverse canal; **cc**, carotid canal; **ctbs**, caudal portion of transverse basisphenoid sinus; **encf**, endocranial carotid foramen; **encg**, endocranial carotid groove; **etbs**, eminence of transverse basisphenoid sinus; **hpf**, hypophyseal fossa; **junc**, junction of transverse canals; **le**, lateral extension of transverse basisphenoid sinus; **mxns**, sulcus for maxillary nerve; **onvs**, sulcus for ophthalmic neurovascular array; **rbtc**, rostral branches of transverse canal; **rtbs**, rostral portion of trans-

organization of the transverse canals and other PCVN elements (Archer, 1976: 307), which accords with the overall conservatism of their cephalic vascular systems (Aplin, 1990). Differences correlated with distinctive osteological features can be summarized in the form of junction patterns (see figs. 1C, 42; table 4). The complex pattern is widespread among extant marsupials, occurring among representatives of four orders. The complex as well as the compound patterns are found in both New World and Sahulian marsupials, but the hybrid pattern has not been encountered in the Neotropical marsupial fauna. Taxa in which TCVs are not functionally present in the adult are rare but occur in both major areas of marsupial distribution.

**PERICAROTID VENOUS NETWORK IN NONMARSUPIAL METATHERIANS.** Although we confirm that some sparassodontan taxa are polymorphic for TCF presence (see Archer, 1976; Beck et al., 2022), apart from *Prothylacynus*, *Sipalocyon*, and several Tiupampan taxa (e.g., Muizon et al., 2018; Muizon and Ladevèze, 2020), the situation in most nonmarsupial metatherians awaits study using modern methods. This topic is treated in greater detail in the next section.

**VENOUS PATHWAY DOMINANCE AND THE PERICAROTID VENOUS NETWORK.** The concept of competition between cephalic venous pathways serving the same or similar areas (Padgett, 1957) should apply to the development of the intracranial VPS and the extracranial ICV/BVP, with the predictable result that the growth of the one should slow or stop as the other gains dominance during the ontogeny of the individual. Our limited data indicate that the ICV/BVP does not increase in relative size in postnatal life, perhaps because it has few distal tributaries. It usually joins the IJVS, which is itself frequently reduced in didelphids (Shindo, 1915; Toeplitz, 1920; Dom et al., 1970) and at least some Sahulian taxa (Archer, 1976; Aplin, 1990). By contrast, the VPS is part of a

major pipeline that involves the transverse dural sinus and SS, which drain the developing brain. A strong anastomotic connection between the VPS and the cerebrospinal venous system (CSVS), involving the extracranial continuation of the ventral petrosal sinus (EVPS) and condylar veins, is apparent in most investigated marsupials.

With regard to the CS, it is important to note that there is no documented case in which the drainage function of the VPS is superseded by that of the PCVN. Osgood's (1921) speculation that the sphenopterygoid veins (= ?TCVs) drain most of the braincase in *Dipodomys* needs corroboration, especially with respect to the role of the IJV and VPS. Similarly, when enlargement of certain PMDs occurs in placentals as a normal feature of their development, as in the case of the ICVs of some strepsirrhine primates, it is correlated with other vascular specializations (e.g., reduction or obliteration of internal carotid artery, extracranial retia). These have not been recorded in any metatherians.

Caudal and rostral branches of the TCVs drain different areas and are presumably not in competition during ontogeny. Their loss or great reduction in different taxa have to be accounted for on other grounds.

#### CHARACTER ANALYSIS AND PHYLOGENY

Topics discussed in this section necessarily cover a much broader range of issues and taxa than those solely concerned with metatherian systematics. However, their joint purpose is to provide justifications for many of our inferences, such as those regarding the probable junction pattern of the last common ancestor of Marsupialia, or how junction patterns might have been transformed during the course of metatherian evolution (tables 4, 5). These treatments are followed by remarks regarding whether mesocranial character states can be correlated with specific divergences

---

←  
 verse basisphenoid sinus; **rtbs/rbtc**, compound junction, rostral portion of transverse basisphenoid sinus and rostral branches of transverse canal; **SQ**, squamosal; **tcf**, transverse canal foramen; **tgf**, fossa for trigeminal ganglion; **vpss**, sulcus for ventral petrosal sinus.

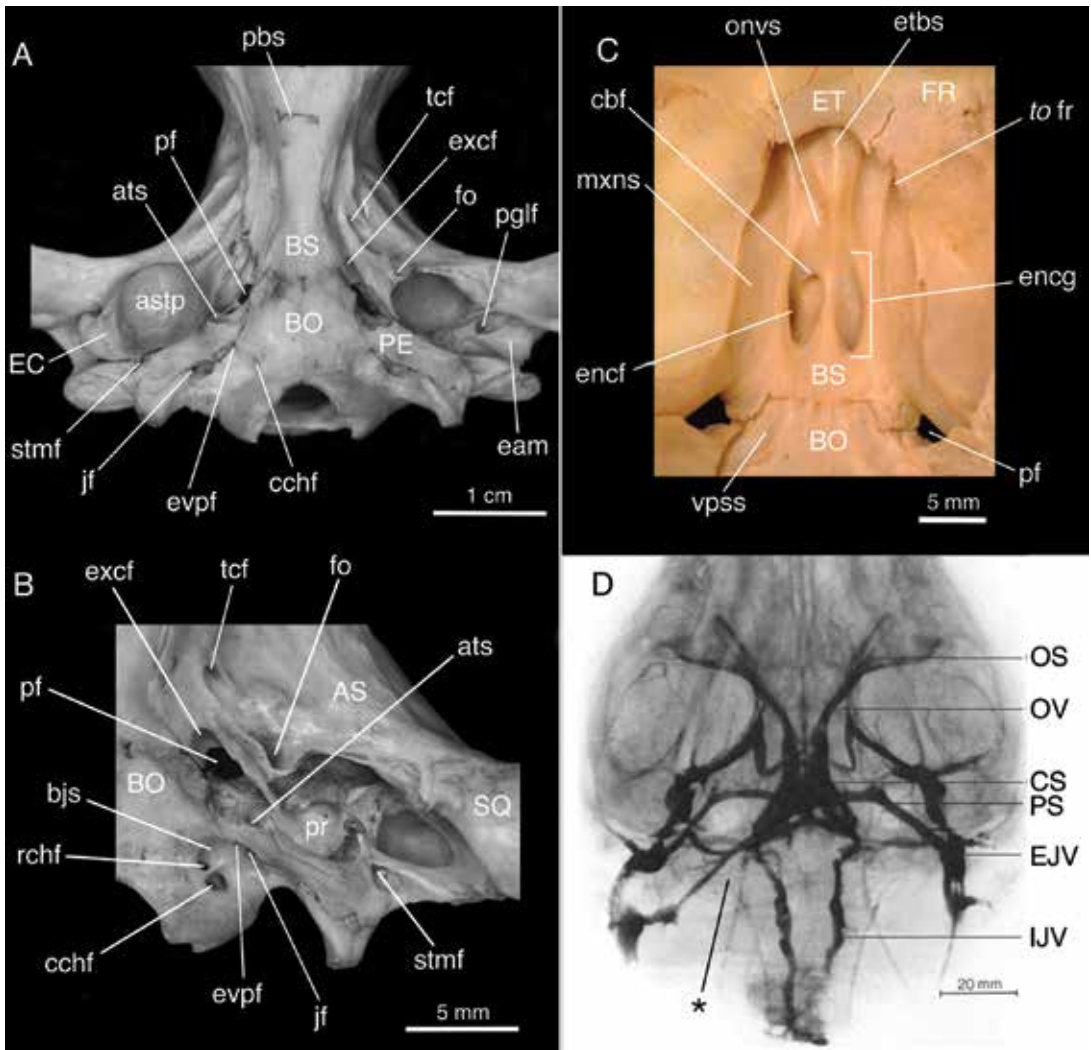


FIG. 28. *Sarcophilus laniarius* AMNH M-65673 (Dasyuridae, Dasyuromorphia), adult caudal cranium in **A**, ventral, **B**, oblique lateral, and **C**, oblique endocranial aspects; and **D**, *S. harrisii*, venogram (after Shah and Nicol, 1989: fig. 2). (Although catalogued as *S. laniarius*, usually regarded as an extinct taxon, AMNH M-65673 came to the AMNH in 1913 from New York Zoological Society, and is therefore more likely *S. harrisii*.) Note asymmetry within endocranial carotid grooves—caudal branch present on left side only. Plexiform nature of vessels identified in original venogram as internal jugular veins, as well as their apparent medial convergence, suggest that they may instead represent ventral petrosal sinus and its extracranial continuation, seen in anastomotic union with internal vertebral venous plexus. True internal jugular veins are probably situated more laterally (asterisk). **Key:** **A–C:** **AS**, alisphenoid; **astp**, tympanic process of alisphenoid; **ats**, sulcus for auditory tube; **bjs**, basijugular sulcus; **BO**, basioccipital; **BS**, basisphenoid; **cbf**, caudal branch foramen; **cchf**, caudal condylohyoglossal foramen; **eam**, external acoustic meatus; **EC**, ectotympanic; **ET**, ethmoid; **encf**, endocranial carotid foramen; **encg**, endocranial carotid groove; **etbs**, eminence of transverse basicranial sinus; **evpf**, foramen for extracranial continuation of ventral petrosal sinus; **excf**, exocranial carotid foramen; **fo**, foramen ovale; **fr**, foramen rotundum; **FR**, frontal; **jf**, jugular foramen; **onvs**, sulcus for ophthalmic neurovascular array; **mxns**, sulcus for maxillary nerve; **pbs**, presphenoid-basisphenoid synchondrosis; **PE**, petrosal;

among marsupial crown clades: Didelphimorphia vs. other Marsupialia; Paucituberculata vs. Australidelphia; Agreodontia vs. Microbiotheria + Diprotodontia, and Macropodiformes + Phalangeriformes vs. Vombatiformes.

**PERICAROTID CHARACTERS IN THERIAN EVOLUTION.** Although the cephalic venous systems of marsupials and placentals are very similar in an overall sense, Aplin (1990: 126) argued that marsupials display certain features not found in the latter. These include the late persistence of the intratympanic portion of the lateral head vein and the presence of a substantial pericarotid vein accompanying the internal carotid artery. Both of these are better viewed as retained primitive features. A persistent lateral head vein, for example, has since been documented or suspected in a number of therians, extant and extinct (see Ekdale et al., 2004; Wible, 2008; Wible and Rougier, 2017; Muizon et al., 2015; MacPhee et al., 2021; this paper). Like PMDs, the lateral head vein is a retained developmental feature that variably persists into the adult stage, but determining whether it is consistently functional or merely vestigial in individual taxa requires individual study.

In regard to the pericarotid vein—the ICV of this paper—Aplin (1990: 99) thought that it might be a diagnostic feature of Marsupialia, but a more basal position for its appearance in mammals seems much more likely. In addition to the therian evidence discussed earlier, according to Hochstetter (1896: 226) in *Ornithorhynchus* a vein emanating from the CS accompanies the internal carotid artery within the carotid canal and terminates in the IJV. The same feature is illustrated, but not identified, by Zeller (1989: fig. 45). The echidna *Tachyglossus* is probably similar to the platypus, as Gaupp (1908: pl. 73) portrayed a vessel labelled as “Sin. Cavernos.” projecting into the carotid canal in a hatchling. Thus in both extant monotreme

clades there is an enlarged mesocranial distributary that corresponds to the ICV of extant marsupials and the internal carotid venous plexus of placentals, which is consistent with its presence as a symplesiomorphy of the mammalian crown group. Whether the ICV was once more important in mammalian evolution as a drainage route for the CS is an interesting but possibly unanswerable question, given that the vein travels coaxially with the internal carotid artery and rarely correlates with any determinative osteological indicia of its own.

Marsupials and sparassodonts exhibit shared osteological correlates related to the EVPS, which suggests that it was present and comparatively large in their last common ancestor. This vessel is well attested in placentals (albeit under various names), and the likeliest conclusion is that it too is a retained mammalian symplesiomorphy.

Giannini et al. (2021) have demonstrated that body size as well as phylogeny may have a major effect on the positioning of skull attributes in marsupial morphospace. Although body size may correlate with the expression of some characters associated with junction patterns, the associations do not appear to be very strong and much larger sample sizes would be required to meaningfully explore any such relationships.

**TRANSVERSE CANAL FORAMEN IS A MARSUPIAL SYMPLESIOMORPHY, NOT A SYNAPOMORPHY.** The proposal that the TCF may be a synapomorphy of crown-group Marsupialia (see Sánchez-Villagra and Wible, 2002; Horovitz and Sánchez-Villagra, 2003) was largely based on the assumption that it was lacking in most early metatherians. However, alternative interpretations have stressed the opposite view: because the TCF is in fact present in some nonmarsupial metatherians, it is better interpreted as a primitive feature retained in the crown group (e.g., Marshall, 1977). As shown in

---

←  
**pf**, piriform fenestra; **pglf**, postglenoid foramen; **pr**, promontorium of petrosal; **rchf**, rostral condylohypoglossal foramen; **SQ**, squamosal; **stmf**, stylomastoid foramen; **tcf**, transverse canal foramen; **vpss**, sulcus for ventral petrosal sinus; **D**: (Key from Shah and Nichol, 1989) **CS**, cavernous sinus; **EJV**, external jugular vein; **IJV**, “internal jugular vein” (see above); **OS**, ophthalmic sinus; **OV**, ophthalmic vein; **PS**, pterygoid sinus (= transverse canal vein, probably enlarged caudal branch vein).

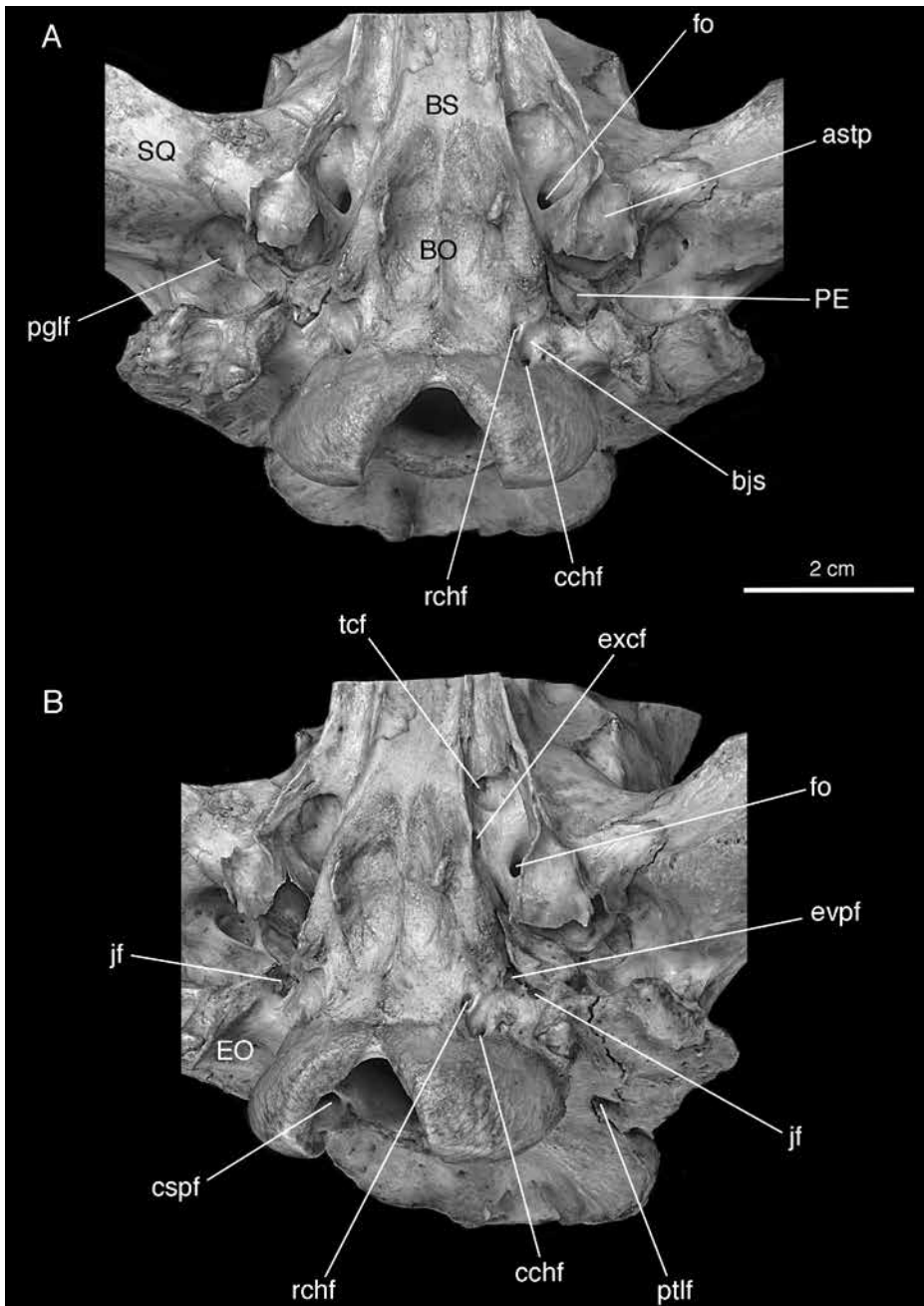
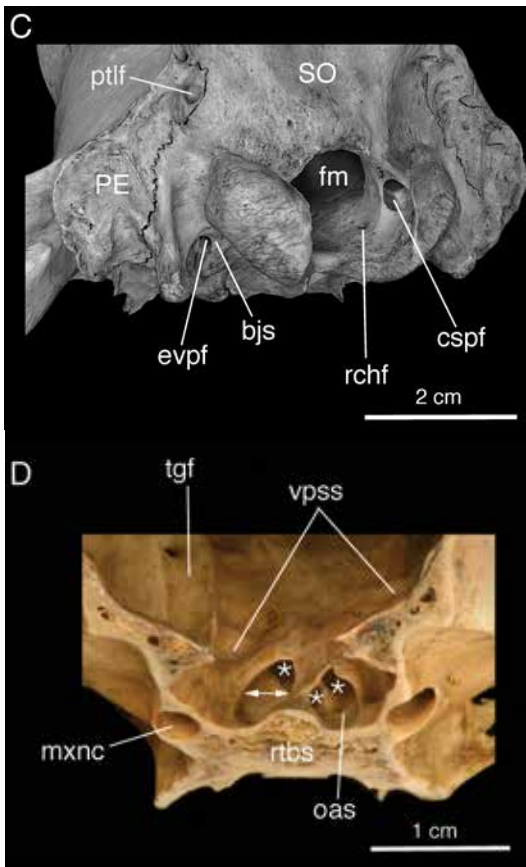


FIG. 29. *Thylacinus cynocephalus* AMNH M-144316 (Thylacinidae, Dasyuromorphia), adult specimen, coronally hemisected skull. Views: **A**, ventral; **B**, oblique ventrolateral; **C**, oblique dorsocaudal; and **D**, coronal section through mesocranium, caudal aspect, closeup of endocranial carotid grooves. Asterisks mark union of carotid and transverse canals in base of carotid grooves (see fig. 31). In this version of hybrid configuration, interpretation is that enlarged caudal branch vein arising from cavernous sinus shares carotid groove with internal carotid sinus neurovascular bundle before separating and departing through transverse canal to join trunk. For this reason,



joint foramen completely fills each carotid groove (double-headed arrow). In D, edge of coronal cut passes through position equivalent to segments of scanned specimen depicted in figure 31A, B. Although cut is slightly caudal to rostral end of hypophyseal fossa, there is no sign of intramural RBTC pathways on other half of hemisected skull, which is consistent with RBV absence. **Key:** *astp*, alisphenoid tympanic process; *bjs*, basijugular sulcus; *BO*, basioccipital; *BS*, basisphenoid; *cchf*, caudal condylohypoglossal foramen; *cspf*, craniospinal foramen; *EO*, exoccipital; *evpf*, foramen for extracranial ventral petrosal sinus; *excf*, exocranial carotid foramen; *fo*, foramen ovale; *fm*, foramen magnum; *jf*, jugular foramen; *mxnc*, canal of maxillary nerve; *oas*, ophthalmic artery sulcus; *PE*, petrosal; *pglf*, postglenoid foramen; *ptlf*, posttemporal foramen; *rchf*, rostral condylohypoglossal foramen; *rtbs*, rostral portion of transverse basi-sphenoid sinus; *SO*, supraoccipital; *SQ*, squamosal; *tcf*, transverse canal foramen; *tgf*, trigeminal fossa; *vpss*, sulcus of ventral petrosal sinus.

the following paragraphs, the situation is more complicated than a simple presence/absence distinction would imply.

The distribution of TCF occurrence in several nonmarsupial metatherians is unclear, usually because poor preservation of the mesocranium and lack of information concerning internal osteological conditions prevents unambiguous determination. The TCF has been reported as absent in an undescribed metatherian skull from the Late Cretaceous Nemegt Formation of Mongolia (informally named the “Gurlin Tsav skull” [Rougier et al., 1998]), but as present in *Asiatherium reshetovi*, also from the Late Cretaceous of Mongolia from levels correlated with the Barum Goyot Formation (Szalay and Trofimov, 1996; see also Rougier et al., 1998; Muizon and Ladevèze, 2020). It should be noted that preservation of the only known skull of *A. reshetovi* is poor and consequently TCF presence should be accepted with caution until better substantiated (Sánchez-Vilagra and Wible, 2002).

*Pucadelphys* and *Andinodelphys* are members of Pucadelphyidae, a clade recently proposed as a monophyletic group distinct from sparassodontans (see Muizon et al., 2018; Muizon and Ladevèze, 2020). These taxa are variable for TCF presence/absence. A polymorphic condition of the TCF has also been recorded for *Pucadelphys andinus*, from the same locality and age. The foramen, absent in most specimens (Marshall and Muizon, 1995; Ladevèze et al., 2011), is present in two of several recently discovered examples described by Muizon and Ladevèze (2020). The TCF also occurs in *Andinodelphys cochabambensis* according to the same authors. Left and right transverse canals, definitely present in MHNC 8308, communicate with the ipsilateral carotid canals and hypophyseal fossa. In MHNC 8264, another specimen of the same species, the transverse canals were found to communicate with each other inside the basisphenoid. These findings imply that both of the TCV branch pathways (CBTC and RBTC) found in extant marsupial skulls may exist in pucadelphyids. TCF absence has been claimed

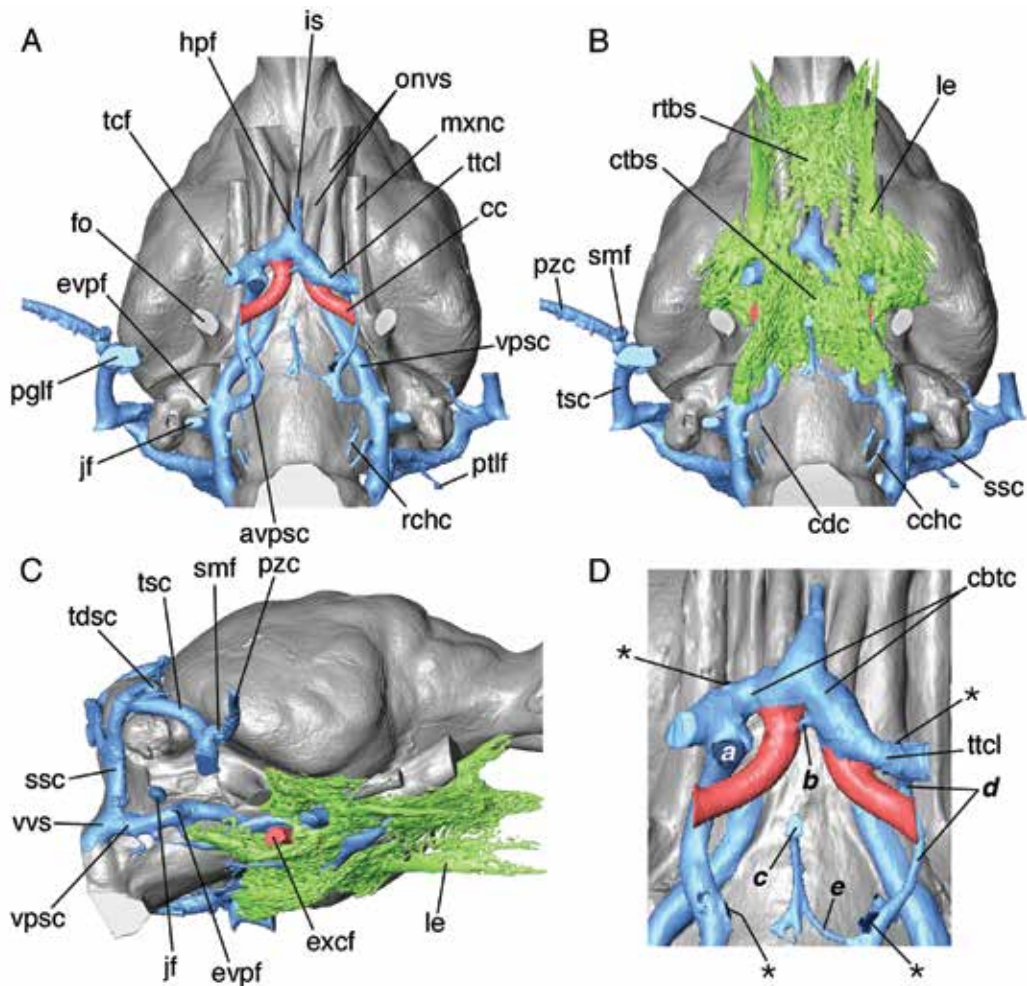
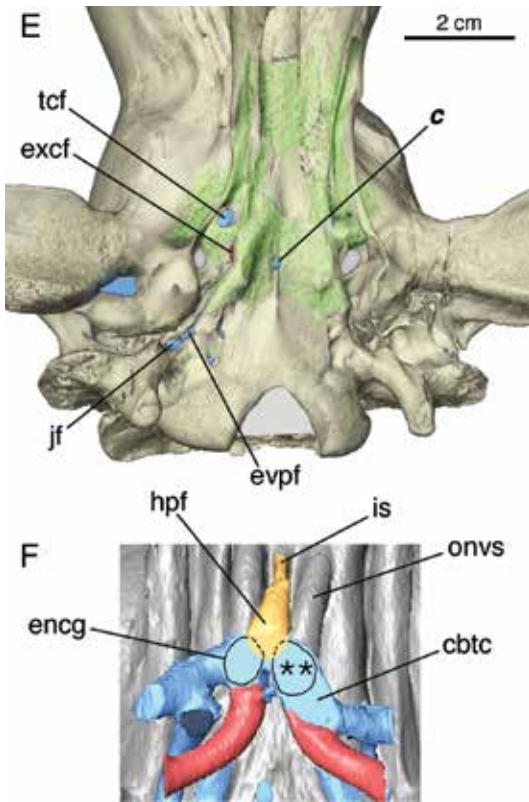


FIG. 30. *Thylacinus cynocephalus* NMB c.2526 (Thylacinidae, Dasyuromorphia), adult specimen, endocast reconstruction showing osteological features associated with pericarotid venous network and related vasculature (data source, table 2; color key, fig. 4). Views: **A**, ventral; **B**, same, with transverse basisphenoid sinus superimposed; **C**, oblique right lateral; **D**, closeup of mesocranial vascular features; **E**, ventrolateral surface, intact caudal cranium; **F**, as in **D**, but with shape of hypophyseal fossa (yellow) separately depicted and resected to show position of endocarotid foramina. In **A** and **B**, carotid and transverse canals form complicated multiple union; see text and also figures 29 and 31. In **C**, no sulcus is in evidence to connect jugular foramen with sigmoid sinus trackway (which instead exclusively joins sulcus for vertebral vein), consistent with internal jugular vein reduced or absent. In **D**, single asterisks indicate small openings in transverse canals and other features, mostly representing connection points (interstitial canaliculi) with transverse basisphenoid sinus. In **E**, communication between caudal branch veins, cavernous sinus, and internal carotid vein is suggested but its actual soft-tissue form cannot be reconstructed. Because both CRVs originate from CS/ICV they are not considered to form a confluence like that of RBVs. Internal carotid artery would have passed rostrally out of endocranial carotid foramen as ophthalmic artery. Other features in **D**: **a**, large connector joining transverse canal to accessory ventral petrosal sinus; **b**, intercanal branch, significance unknown; **c**, notochord (or transclival canal); **d**, reduced left accessory ventral petrosal sinus, partly hidden by carotid canal (compare right side); **e**, canaliculus linking **c** and **d**. **Key**: **avpsc**, canal for right accessory ventral petrosal sinus; **cbtc**, caudal branch of transverse canal (pathway); **cc**, carotid canal; **cchc**, caudal condylohypoglossal



canal; **cdc**, canal for condylar vein; **ctbs**, caudal portion of transverse basicranial sinus; **encg**, endocranial carotid groove; **evpf**, foramen for extracranial extension of ventral petrosal sinus; **excf**, exocranial carotid foramen; **fo**, foramen ovale; **hpf**, hypoglossal fossa; **is**, infundibular sulcus; **jf**, jugular foramen; **le**, lateral extension of transverse basisphenoid sinus; **mxnc**, canal for maxillary nerve; **onvs**, sulcus for ophthalmic neurovascular array; **pglf**, postglenoid foramen; **ptlf**, posttemporal foramen; **pzc**, postzygomatic canal; **rchc**, rostral condylohypoglossal canal; **rtbs**, rostral portion of transverse basicranial sinus; **smf**, suprameatal foramen; **ssc**, sulcus for sigmoid sinus; **tcf**, transverse canal foramen; **tdsc**, sulcus for transverse dural sinus; **tsc**, sulcus for temporal sinus; **ttcl**, trunk of bony transverse canal; **vpsc**, sulcus for (main) ventral petrosal sinus; **vvs**, sulcus for vertebral vein. Other features in D: **a**, large connector joining transverse canal to accessory ventral petrosal sinus; **b**, intercanal branch, unknown significance; **c**, notochord (or transclival canal); **d**, reduced left accessory ventral petrosal sinus, partly hidden by carotid canal (compare right side); **e**, canalculus linking **c** and **d**.

for well-preserved skulls of *Mayulestes ferox* and *Allqokirus australis* from the Early Paleocene Santa Lucía Formation (Bolivia) (Muizon, 1998; Muizon et al., 2018), whether these taxa are placed close to (e.g., Muizon et al., 2018) or within (e.g., Forasiepi, 2009) Sparassodonta.

Polydolopimorphians have been considered as variously related to Paucituberculata, Microbiotheria, or Diprotodontia (e.g., Goin et al., 2016 and references therein), but some authors consider them to be nonmarsupial metatherians (e.g., Beck, 2017). The polydolopimorphian *Epidolops ameghinoi* from the Early Eocene of Itaboraí (Brazil) exhibits a minute aperture in the area in which the TCF is normally found in marsupials (Beck, 2017), but whether an associated canal is present is unknown.

TCF presence has also been noted for the peradectid *Mimoperadectes houdei* from the Early Eocene Willwood Formation (Horovitz et al., 2009). This taxon has been regarded as either close to didelphids within Marsupialia (e.g., Horovitz et al., 2009) or as a stem taxon outside Marsupialia (Muizon and Ladevèze, 2020; Beck et al., 2022). *Herpetotherium* sp. from the Late Eocene White River Formation, which also has a recognizable TCF, has been interpreted in a similar way, as either a didelphimorphian (e.g., Gabbert, 1998) or a stem marsupial (e.g., Beck et al., 2022).

The most recent investigation relevant to metatherian PCVN interpretation is that of Beck et al. (2022: char. 51, fig. 31). In their dated total evidence tree, TCF presence did not appear as a synapomorphy of either Marsupialia or Marsupialia + *Herpetotherium*, although its absence did emerge as an unambiguous autapomorphy of one monotypic clade (i.e., Tarsipedidae). While this determination removes the TCF from consideration as a marsupial synapomorphy, there is still much to learn about the distribution and significance of PCVN components in Metatheria. TCF presence in *Epidolops* and *Herpetotherium* implies that they possessed functional TCVs, but nothing is yet known about connections with other PCVN components or their junction character states.

POSSIBLE TRANSVERSE CANAL FORAMEN OCCURRENCE IN OTHER MAMMALIAFORMS. The fact that apparently homologous PMDs exist at all in extant placentals and marsupials suggests that some form of encephalic drainage involving these vessels is basal for Theria. Unlike ICVs, TCVs have not been recognized in extant monotremes, at least under that name (e.g., Hochstetter, 1896; van Bemmelen, 1901; Kesteven and Furst, 1929; Simpson, 1938; Kuhn, 1971), and it may be that a different emissarium is involved in CS drainage in that group. In *Ornithorhynchus* a large vein runs from the endocranium to the apparent equivalent of the PVP and maxillary vein according to Hochstetter (1896: 226). This author did not state whether it communicated with the CS, but given that the vein passed through the foramen ovale it is reasonable to conclude that communication did occur, and that it is therefore comparable to the v.e. foraminis ovalis (= peritrigeminal vein of Aplin, 1990). Whether an equivalent vessel is present in tachyglossids has not been ascertained.

Other possibilities for the contents of mesocranial apertures in nonplacental eutherians and multituberculates have also been proposed (e.g., for *Asioryctes*, Kielan-Jaworowska, 1981; *Kamptobaatar*, Hurum et al., 1996). Examples include foramina in the infratemporal fossa lateral to the exocranial carotid foramen, speculatively regarded as ports for the passage of divisions of the mandibular nerve or the vidian artery (e.g., Kielan-Jaworowska, 1971; Kielan-Jaworowska et al., 1986). Although divided foramina for the sensory and motor roots of the mandibular nerve are occasionally found in Theria, including some macropodids according to Aplin (1990: 183), in most clades this condition is uncommon or absent (see Starck, 1967; Moore, 1981). The vidian artery is always diminutive when identifiable at all in therians (e.g., some lipotyphlans, MacPhee, 1981; *Tarsipes*, Aplin, 1990).

In our view it seems rather more likely than not that apertures like the ones just mentioned would have transmitted enlarged PMDs in these and other noncrown taxa. Wible (1986: 319)

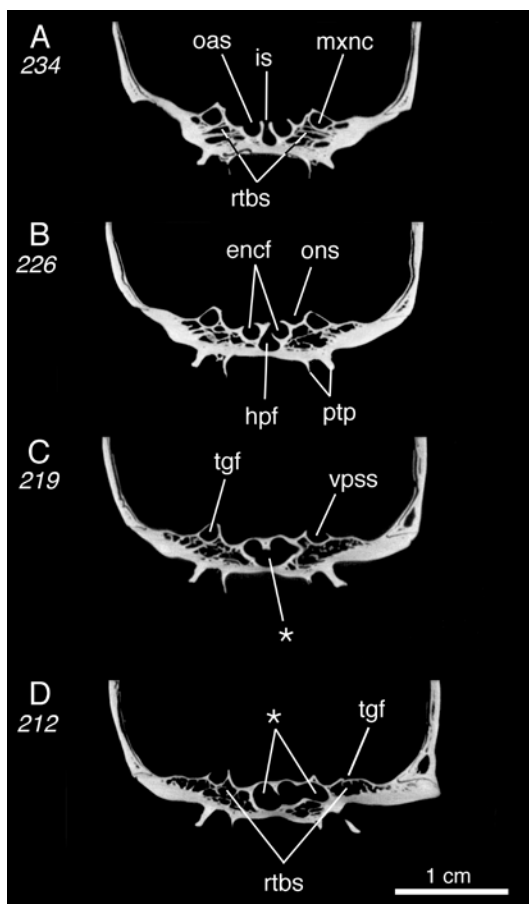
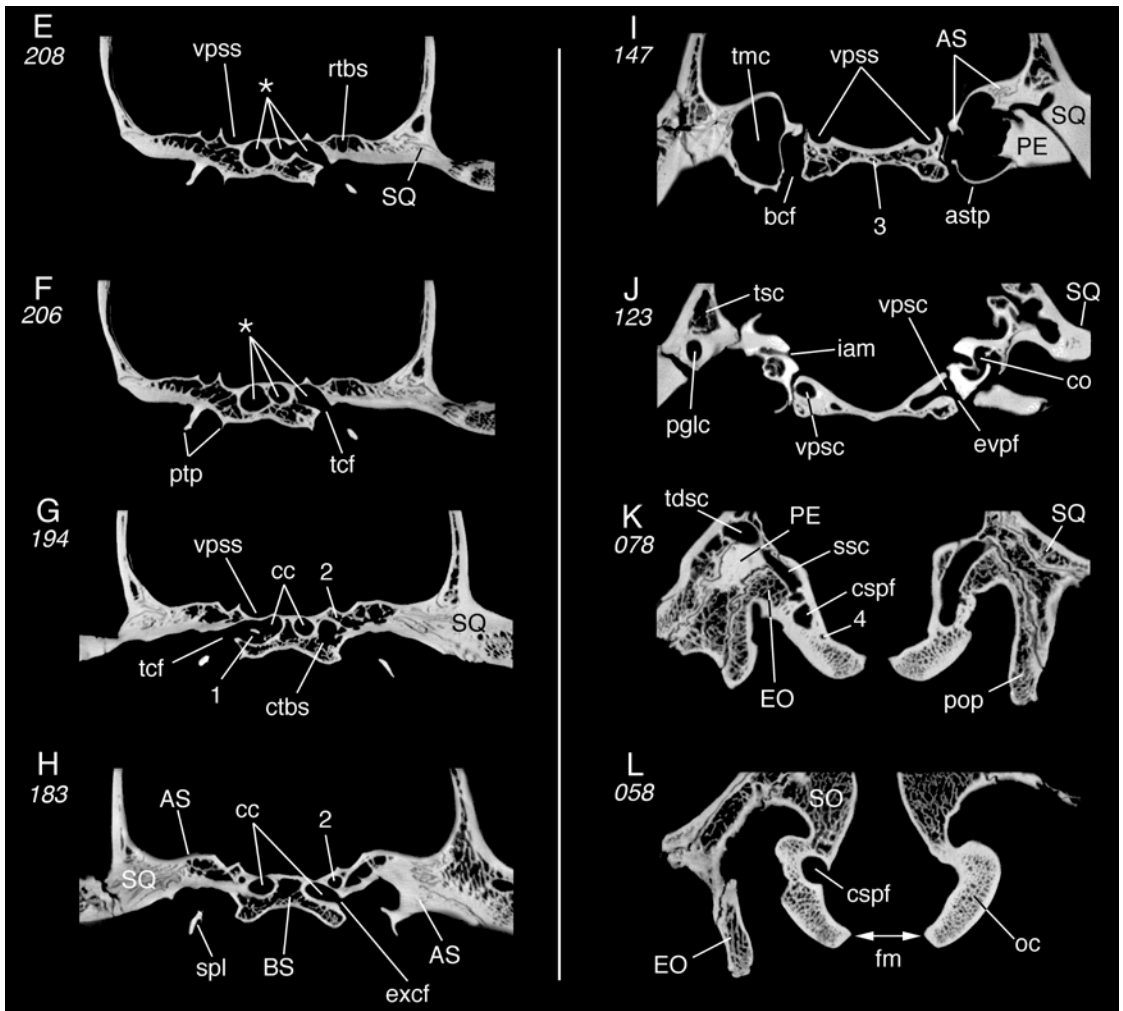


FIG. 31. *Thylacinus cynocephalus* NMB c.2526 (Thylacinidae, Dasyuromorphia), adult caudal cranium, selected coronal segments in rostrocaudal order (data source, table 2). In A and B, apart from endocranial apertures of carotid canals, there are no additional openings in endocranial floor and no evidence of transverse canal junction rostral to hypophyseal fossa. These facts are consistent with rostral branch of transverse canal vein being absent, and caudal branch sharing foramen with internal carotid neurovascular bundle. In C–E, two carotid and two transverse canals briefly coalesce to form composite space (asterisk). Whether this coalescence occurs in other thylacine skulls is likely but poorly documented. **Key:** AS, alisphenoid; **astp**, tympanic process of alisphenoid; **bcbf**, basicapsular fenestra; **BS**, basisphenoid; **cc**, carotid canal; **co**, cochlea; **cspf**, craniospinal foramen; **ctbs**, caudal portion of transverse basisphenoid sinus; **encf**, endocranial carotid foramen; **EO**, exoccipital; **evpf**, foramen for extra-



cranial continuation of ventral petrosal sinus; **excf**, exocranial carotid foramen; **fm**, foramen magnum; **hpf**, hypophyseal fossa; **iam**, internal acoustic meatus; **is**, infundibular sulcus; **mxnc**, canal for maxillary nerve; **oas**, sulcus for ophthalmic artery; **oc**, occipital condyle; **ons**, sulcus for ophthalmic nerve; **PE**, petrosal; **pglc**, postglenoid canal; **pop**, paracondylar process; **ptp**, medial and lateral pterygoid processes; **rtbs**, rostral portion of transverse basisphenoid sinus; **SO**, supraoccipital; **spl**, sphenopterygoid lamina; **SQ**, squamosal; **ssc**, canal for sigmoid sinus; **tcf**, transverse canal foramen; **tdsc**, canal for transverse dural sinus; **tgf**, trigeminal ganglion fossa; **tmc**, tympanic cavity; **tsc**, sulcus for temporal sinus; **vpsc**, canal for ventral petrosal sinus; **vpss**, sulcus for ventral petrosal sinus; **1**, strut in confluence of carotid and transverse canals; **2**, reduced left accessory ventral petrosal sinus; **3**, notochord (or possibly transclival) canal; **4**, canal for condylar emissary vein.

stated that, in the Triassic–Jurassic mammaliaform *Morganucodon*, small foramina near the midline are possibly equivalent to the transverse canals of some modern marsupials, although their positioning is different. More recently, Wible and Rougier (2000) specifically identified

a transverse canal in the basicranial floor of *Kryptobaatar* and another unnamed multituberculate. A good case for TCF presence can also be made for the Paleocene ?dryolestoid *Peligrotherium* (Páez Arango, 2008: 36, fig. 17), in which a foramen located just behind the pterygoids is as

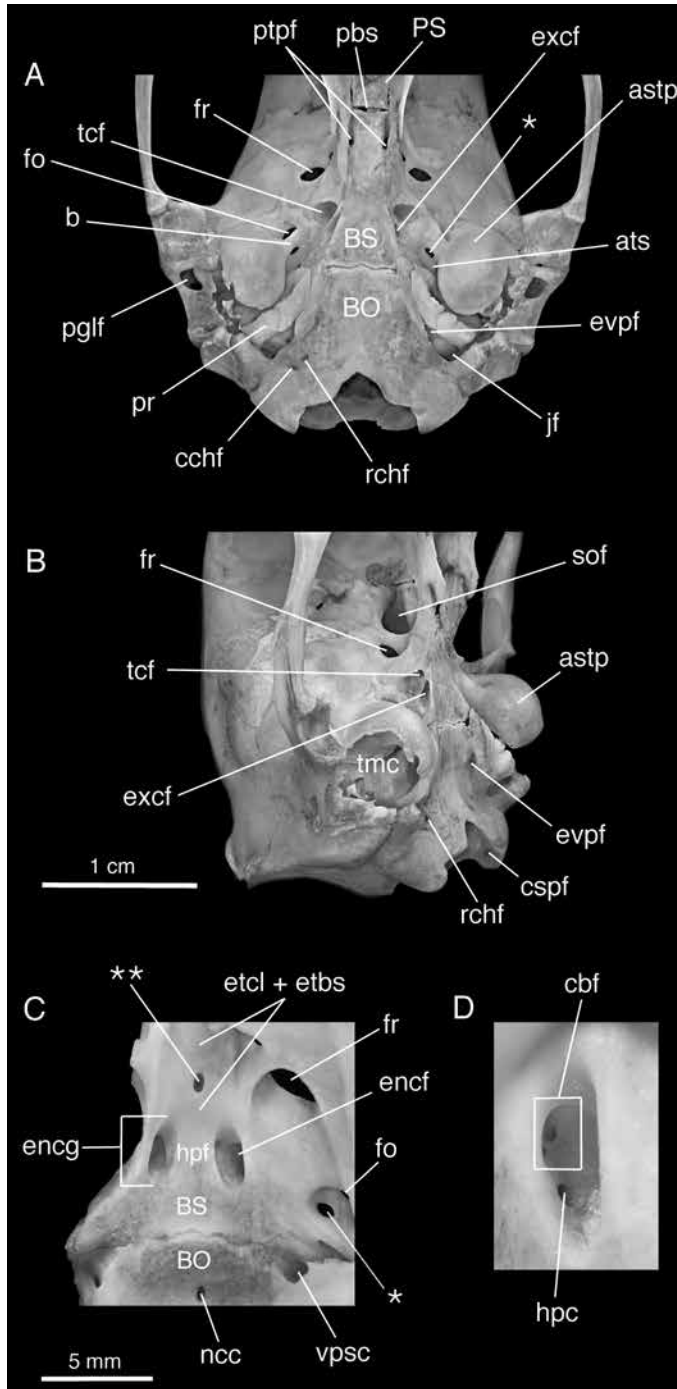


FIG. 32. **A** and **B**, *Perameles nasuta* AMNH M-160199 (Peramelidae, Peramelemorphia), adult caudal cranium in (respectively) ventral and right oblique lateral views. **C** and **D**, *Perameles nasuta* AMNH M-154403, damaged adult caudal cranium, showing (respectively) endocranial floor and closeup of left carotid groove. In A

large as the external aperture of the carotid canal. Of course, just because (for example) early eutherians probably developed PMDs during ontogeny does not mean that these vessels were retained into adulthood or were functionally consequential. TCFs, for example, have not been found or recognized as such in nonplacental Eutheria (e.g., *Zalambdalestes*, Wible et al., 2004; see also O’Leary et al., 2013: chars. 443–445). Yet it is clear that the possible presence of enlarged mesocranial distributaries in mammals lying cladistically outside Theria has been underappreciated in the past, and that this problem deserves closer study using modern methods.

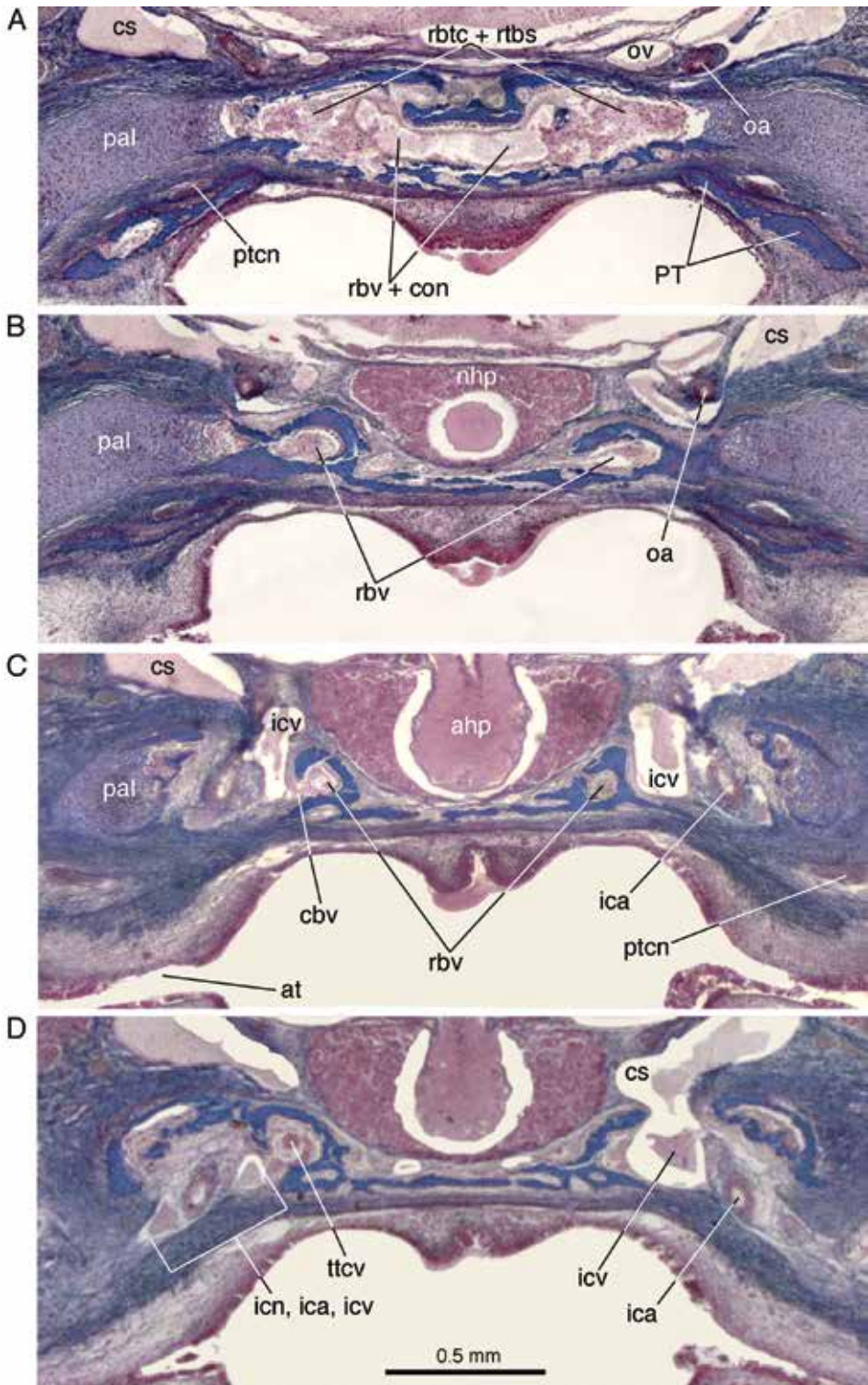
**TRANSFORMATIONS IN JUNCTION PATTERNS: PLESIOMORPHIC CONDITION IN MARSUPIALIA.** With regard to PCVN vasculature, there are four TCN configurations in the comparative set. In addition to the trunk of the TCN, which is common to all, these include: RBV only; CBV only, both veins present; and neither vein present. Assuming that differing expressions of these veins are homologous across Marsupialia, it is parsimonious to infer that the last common ancestor of extant marsupials exhibited both branches of the TCN. In the comparative set, both are demonstrably present in taxa exhibiting the complex and compound junction patterns, which suggests that one of these arrangements should be primitive for Marsupialia. Although they are quite similar, the complex pattern is more widespread: it occurs in

members of four orders, including both Sahulian and New World clades, as well as the stem taxon *Prothylacynus*. Other patterns (simple, hybrid, and indeterminate) can be logically excluded as basal because each of them involves the loss of something judged as primitively present. For all these reasons the complex pattern, which includes both the “intramural” and the “endocranial” pathways, is currently the best choice for the primitive condition.

**TRANSFORMATIONS IN JUNCTION PATTERNS: PNEUMATIZATION.** The most distinctive character state related to the TBS concerns the degree of its integration with the RBTCs. Strong integration is most apparent in the compound pattern, in which the TBS and transverse canals are expanded into a large vacuity, as exemplified by *Perameles* (fig. 33A). This degree of TBS pneumatization may be viewed as a correlate of increased blood cell production, leading to character transformation. For example, the complex pattern, characterized by fairly narrow communication between the TBS and transverse canals, could be transformed into the compound pattern primarily by enhanced pneumatization of the rostral TBS, and possibly influence other features thereby.

It is more difficult to visualize how the conformation of the mesocranium in sparasodontans could be antecedent to any of the patterns typical of extant marsupials, but part of the difficulty may lie with a lack of obvious

and B, bony bridge (**b**) subdivides foramen ovale into lateral port for mandibular nerve, and a smaller medial aperture (remnant of piriform fenestra), through which passes unidentified emissarium to maxillary vein (single asterisk). In C and D, extremely short caudal branch foramen opens into large trabeculated chamber formed by integration of rostral branch of transverse canal and rostral portion of transverse basisphenoid sinus (compound pattern) (cf. fig. 33A, B). Foramen (double asterisks) penetrating eminence of transverse basisphenoid sinus is positionally comparable to apertures in specimen of *Caenolestes* (fig. 13D); in both cases, these apertures seem too far rostral to represent craniopharyngeal foramen. **Key:** **astp**, tympanic process of alisphenoid; **ats**, sulcus for auditory tube; **b**, bridge (derived from alisphenoid); **BO**, basioccipital; **BS**, basisphenoid; **cbf**, caudal branch foramen; **chf**, caudal condylohypoglossal foramen; **cspf**, craniospinal foramen; **encf**, endocranial carotid foramen; **encg**, endocranial carotid groove; **etcl + etbs**, combined eminence of transverse canals and transverse basisphenoid sinus; **evpf**, foramen for extracranial continuation of ventral petrosal sinus; **excf**, exocranial carotid foramen; **fo**, foramen ovale; **fr**, foramen rotundum; **hpc**, hypophyseal canaliculus; **hpf**, hypophyseal fossa; **jf**, jugular foramen; **ncc**, notochord canal; **pbs**, presphenoid-basisphenoid synchondrosis; **pglf**, postglenoid foramen; **pr**, promontorium of petrosal; **PS**, presphenoid; **ptpf**, pterygopalatine fissure; **rchf**, rostral condylohypoglossal foramen; **sof**, sphenoorbital fissure; **tcf**, transverse canal foramen; **tmc**, tympanic cavity; **vpsc**, canal for ventral petrosal sinus.



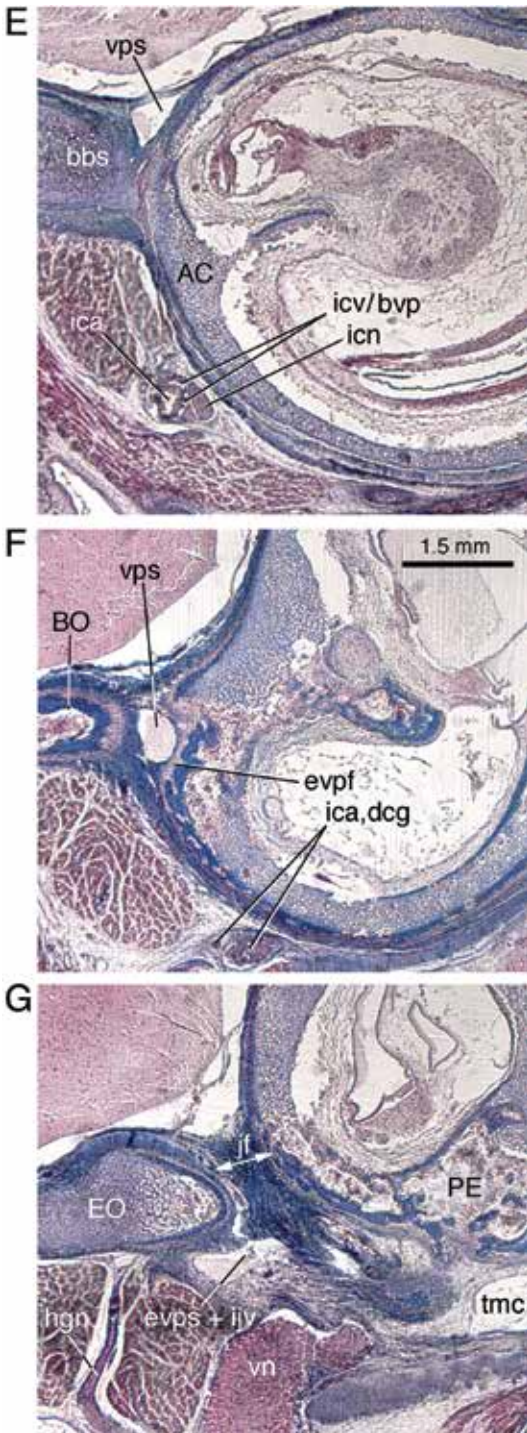
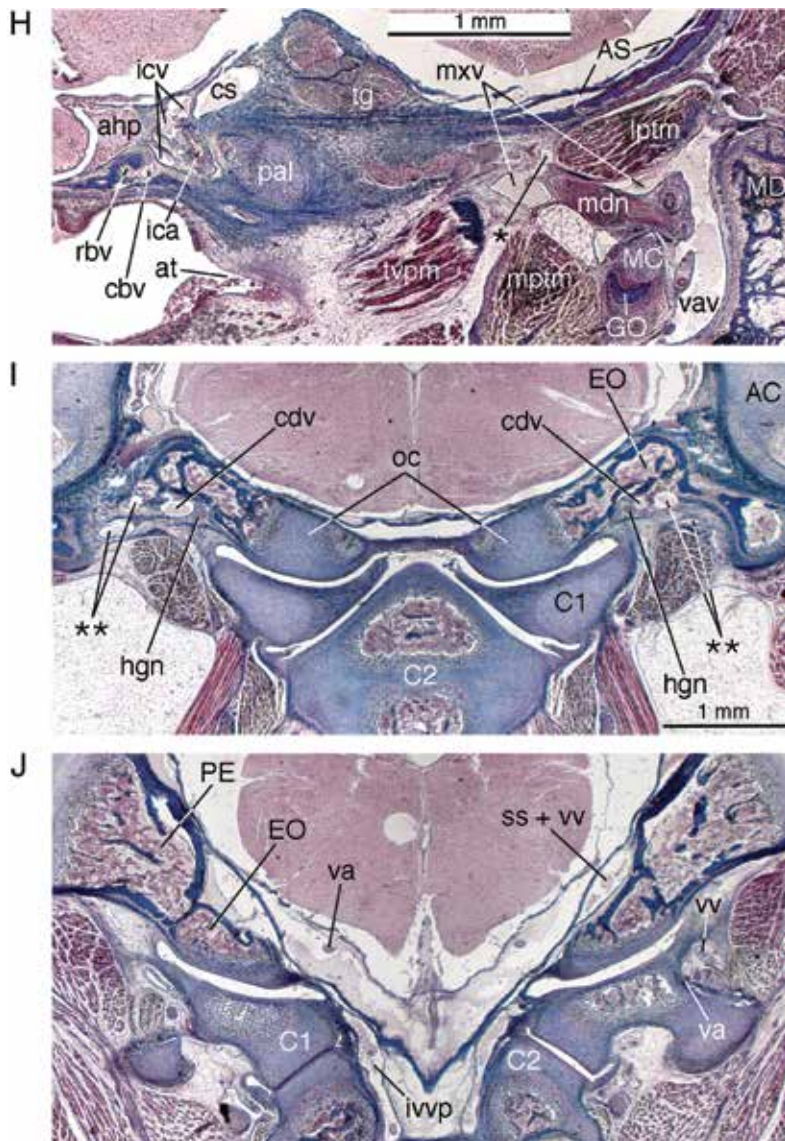


FIG. 33. *Perameles* sp. ZIUT HL 17.5 mm (Perame-  
lidae, Peramelemorphia), perinatal specimen,  
stained coronal sections in rostrocaudal order. **A**,  
Rostral branch veins forming mesocranial conflu-  
ence; active signs of hematopoiesis in compound  
structure with rostral portion of transverse basicra-  
nial sinus (ss. 39.03.02, 40.03.03). **B–D**, Trunk of  
transverse canal vein successively receiving its source  
vessels—caudal and rostral branch veins (s. 40.03.03,  
42.03.04, 43.02.04). **E**, Notable size difference  
between basicranial venous plexus and ventral petro-  
sal sinus (s. 51.01.04). **F**, Ventral petrosal sinus  
descending into its extracranial foramen (s.  
59.01.02). **G**, Anastomosis of extracranial contin-  
uation of ventral petrosal sinus with internal jugular  
vein, ventral to jugular foramen (s. 62.02.02). **H**,  
Caudal branch of transverse canal vein joining inter-  
nal carotid vein, and possible example of peritri-  
geminal emissarium (as defined by Aplin, 1990)  
running from foramen ovale to maxillary vein (single  
asterisk, s. 41.04.03). **I, J**, Condylar plexus includ-  
ing extracranial continuation of ventral petrosal  
sinus (double asterisks), internal vertebral venous  
plexus inside vertebral canal, sigmoid sinus/verte-  
bral vein anastomosis, vertebral artery passing  
through foramen transversarium of atlas and travel-  
ling beneath brainstem (ss. 67.01.02, 70.02.02). In **A**,  
left side of confluent’s lumen slightly enhanced in  
order to differentiate it from background. Cells  
within confluent include differentiating erythro-  
cytes; those populating walls of bony canal are  
osteoclasts and osteoblasts. Other cell types in lumen  
are consistent with active hematopoiesis in highly  
cellular bone marrow (cf. Cline and Maronpot, 1985;  
Young et al., 2014). **Key:** **AC**, auditory capsule; **ahp**,  
adenohypophysis; **AS**, alisphenoid; **at**, auditory tube;  
**bbs**, basisphenoid-basioccipital synchondrosis; **BO**,  
basioccipital; **CL**, atlas vertebra; **C2**, axis vertebra;  
**cbv**, caudal branch of transverse vein; **cdv**, condylar  
emissary vein (not specific); **cs**, cavernous sinus;  
**dcg**, dorsal cervical ganglion; **EO**, exoccipital; **evpf**,  
foramen for extracranial continuation of ventral  
petrosal sinus; **evps + ijv**, extracranial continuation  
of ventral petrosal sinus joining internal jugular  
vein; **GO**, goniale; **hgn**, hypoglossal nerve; **ica**, inter-  
nal carotid artery; **icn**, internal carotid nerve; **icv**,  
internal carotid vein; **icv/bvp**, internal carotid vein/  
basicranial venous plexus; **ivvp**, internal vertebral  
venous plexus; **jf**, jugular foramen; **lptm**, lateral  
pterygoid muscle; **MC**, meckelian cartilage; **MD**,  
mandible; **mdn**, mandibular nerve; **mptm**, medial



pterygoid muscle; **mxv**, maxillary vein; **nhp**, neurohypophysis; **oa**, ophthalmic artery; **oc**, occipital condyle; **ov**, ophthalmic vein; **pal**, processus alaris; **PE**, petrosal; **PT**, pterygoid; **ptcn**, nerve of pterygoid canal; **rbtc** + **rtbs**, merged rostral branch of transverse canal + rostral portion of transverse basicranial sinus (compound junction pattern); **rbv**, rostral branch of transverse vein; **rbv** + **con**, rostral branch veins in midline confluence; **ss + vv**, sigmoid sinus/vertebral vein anastomosis; **tg**, trigeminal ganglion; **tmc**, tympanic cavity; **ttcv**, trunk of transverse canal vein; **tvpm**, tensor veli palatini muscle; **va**, vertebral artery; **vav**, ventral alveolar vein; **vn**, vagus nerve; **vps**, ventral petrosal sinus; **vv**, vertebral vein.

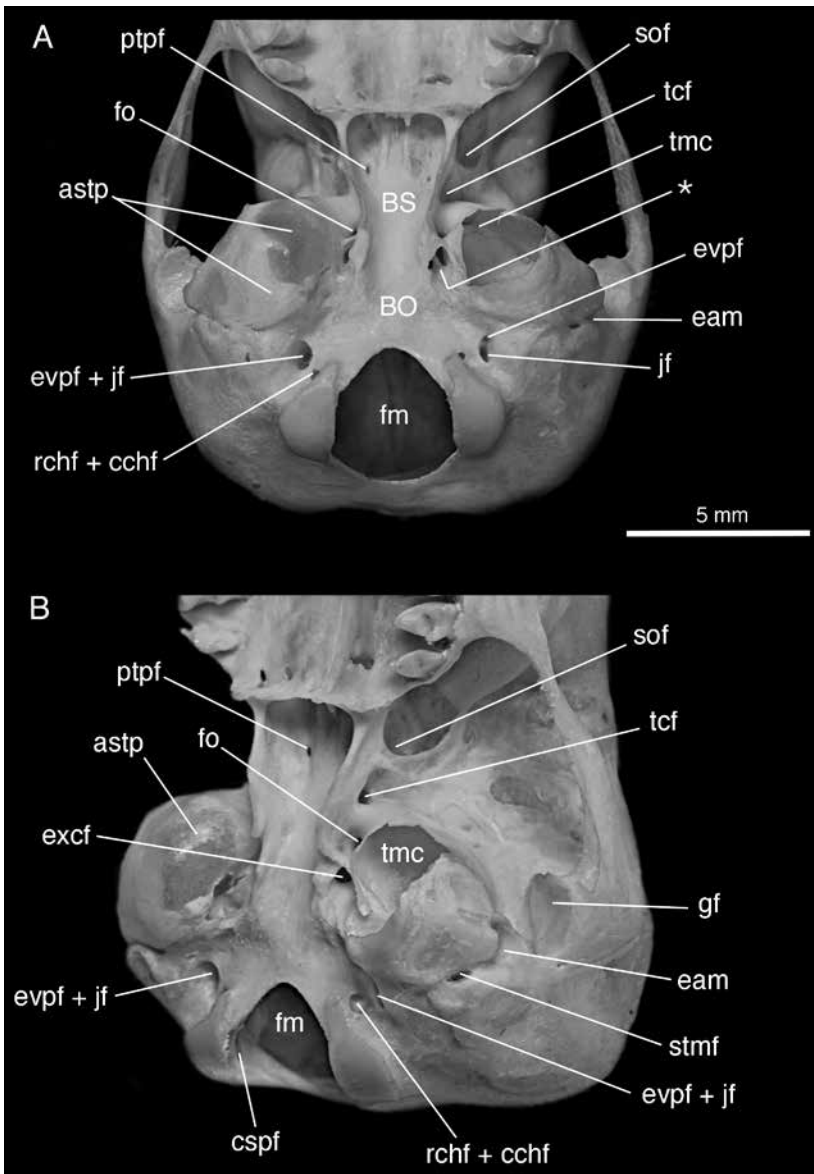


FIG. 34. *Notoryctes typhlops* AMNH M-202103 (Notoryctidae, Notoryctemorphia), adult caudal cranium in **A**, ventral, and **B**, oblique lateral views. In **A**, note internal subdivision within carotid groove (asterisk), assumed to separate internal carotid neurovascular bundle from channel for caudal branch of transverse canal. **Key:** **astp**, tympanic process of alisphenoid; **BO**, basioccipital; **BS**, basisphenoid; **cspf**, craniospinal foramen; **eam**, external acoustic meatus; **evpf**, extracranial extension of ventral petrosal sinus; **evpf + jf**, joint aperture for extracranial extension of ventral petrosal sinus and internal jugular vein; **excf**, exocranial carotid foramen; **fm**, foramen magnum; **fo**, foramen ovale; **gf**, mandibular fossa; **jf**, jugular foramen; **ptpf**, foramen for nerve of pterygoid canal; **rchf + cchf**, joint aperture for rostral and caudal condylohypoglossal foramina; **sof**, sphenooccipital fissure; **stmf**, stylomastoid foramen; **tcf**, transverse canal foramen; **tmc**, tympanic cavity.

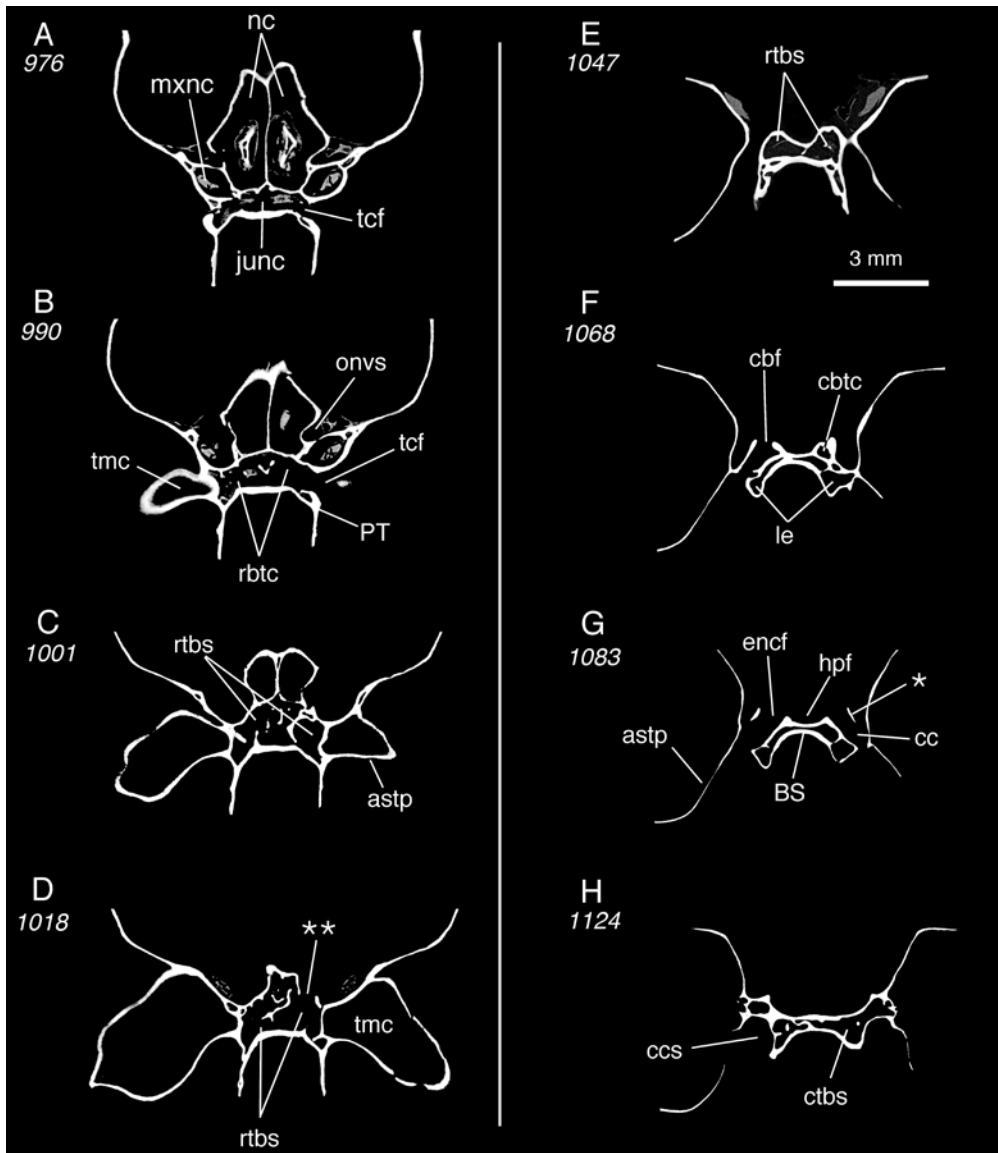


FIG. 35. *Notoryctes typhlops* AMNH M-202103 (Notoryctidae, Notoryctemorphia), adult caudal cranium, selected coronal segments in rostrocaudal order (data source, table 2). In **A** and **B**, rostral portion of transverse basisphenoid sinus and transverse canal are fully integrated. In **C** and **D**, roof of transverse basisphenoid sinus bears a large opening (double asterisks), presumably for a venous connection, although given its rostral location it is probably not related to hypophyseal fossa. In **E** and **F**, transverse basicranial sinus continues caudally as a pair of semidistinct large pneumatic chambers. On right side a small tube for caudal branch, originating from carotid canal, opens into ipsilateral chamber, but ends quickly. In **G**, partition (single asterisk) within carotid canal defines two channels; lateral one leads into small tube in **F**, medial one into endocranial carotid foramen. **Key:** *astp*, tympanic process of alisphenoid; *BS*, basisphenoid; *cbf*, caudal branch foramen; *cbtc*, possible conduit for caudal branch of transverse canal; *cc*, carotid canal; *ccs*, sulcus leading into carotid canal; *ctbs*, caudal portion of transverse basisphenoid sinus; *encf*, endocranial carotid foramen; *hpf*, hypophyseal

intermediates and our limited understanding of mesocranial ontogeny in stem metatherians. Certainly, aspects of the complex and compound junction patterns are exhibited to some extent in *Prothylacynus*, as both TCV branches are arguably present and communicate with the rostral portion of the TBS. However, the integration of their canals with the TBS is different and communication with the hypophyseal fossa (CS) cannot be verified at present. *Sipalocyon* lacks transverse foramina and canals altogether, and its TBS organization differs from that of *Prothylacynus* (and all extant marsupials, except Caluromyinae and Tarsipedidae in a purely convergent sense).

**TRANSFORMATIONS IN JUNCTION PATTERNS: MERGER.** Another form of integration among PCVN components concerns the osteological merger of the carotid and transverse canals. *Thylacinus* and the closely related macropodids *Notamacropus* and *Osphranter* are classed as having a hybrid pattern according to our criteria, although they are otherwise divergent for pattern features, especially with regard to the extent of canal mergers. Their point of strongest similarity may simply be the absence or great reduction of RBTCs coupled with robust CBTCs, a result surely achieved convergently.

Whether the hybrid pattern, or something like it, exists in phalangeriforms is not completely settled. We allow for this possibility in table 4 with regard to the phalangerid *Trichosurus* and the acrobatid *Distoechurus*, dry skulls of which we have personally examined, but more specific observations are needed. The major contrast between these two taxa in mesocranial architecture is that *Trichosurus* preserves separate carotid and transverse foramina and canals, whereas *Distoechurus* merges them, apparently completely (Aplin, 1990). The only direct observation on the vascular consequences of canal

fusion in phalangeriforms is Aplin's (1990: 326) report on a sectioned *Acrobates* (see above, description of *Trichosurus*). His description implies that the only vein exiting the carotid canal in this specimen is the ICV (his pericarotid vein), which may mean that the TCV trunk has been lost or, possibly, taken over by the former as a result of pathway dominance interactions during ontogeny. In any case, in terms of character analysis, the vascular connection between the CS/ICV and CBTC has been derivedly simplified in *Acrobates*. As there is no acknowledged RBTC candidate, there is no second source vessel requiring preservation of the TCV trunk. Macropodids are well on their way to this form of simplification, but if Aplin's (1990) remarks are correctly interpreted, among diprotodonts only certain phalangeriforms have fully achieved it. Note that Beck et al. (2022) have challenged some of Aplin's assessments, and the scenario presented here does not replace the need for actual observation.

#### PHYLOGENETIC IMPLICATIONS

Our data set is not adequate for a quantitative optimization of PCVN character states across Metatheria (see also table 5). In lieu of this we present our current understanding of the distribution and significance of certain PCVN-related features in Marsupialia using, for discussion purposes, an edited version of the dated total evidence tree recently published by Beck et al. (2022). The icons adjacent to taxon names in the tree depicted in figure 42 are the same as the junction patterns illustrated in figure 1C. Exemplar taxa are the same as the ones mentioned in the systematic descriptions, but we have excluded species for which information is insufficient.

**DIDELPHIMORPHIA VS. OTHER MARSUPIALIA.** In their morphology-based analyses, Beck

---

fossa; **junc**, junction of rostral branches of transverse canals; **le**, lateral extension of transverse basicranial sinus; **mxnc**, sulcus for maxillary nerve; **nc**, nasal cavity; **onvs**, sulcus for ophthalmic neurovascular array; **PT**, pterygoid; **rbtc**, rostral branch of transverse canal; **rtbs**, rostral portion of transverse basisphenoid sinus; **tcf**, transverse canal foramen; **tmc**, tympanic cavity.

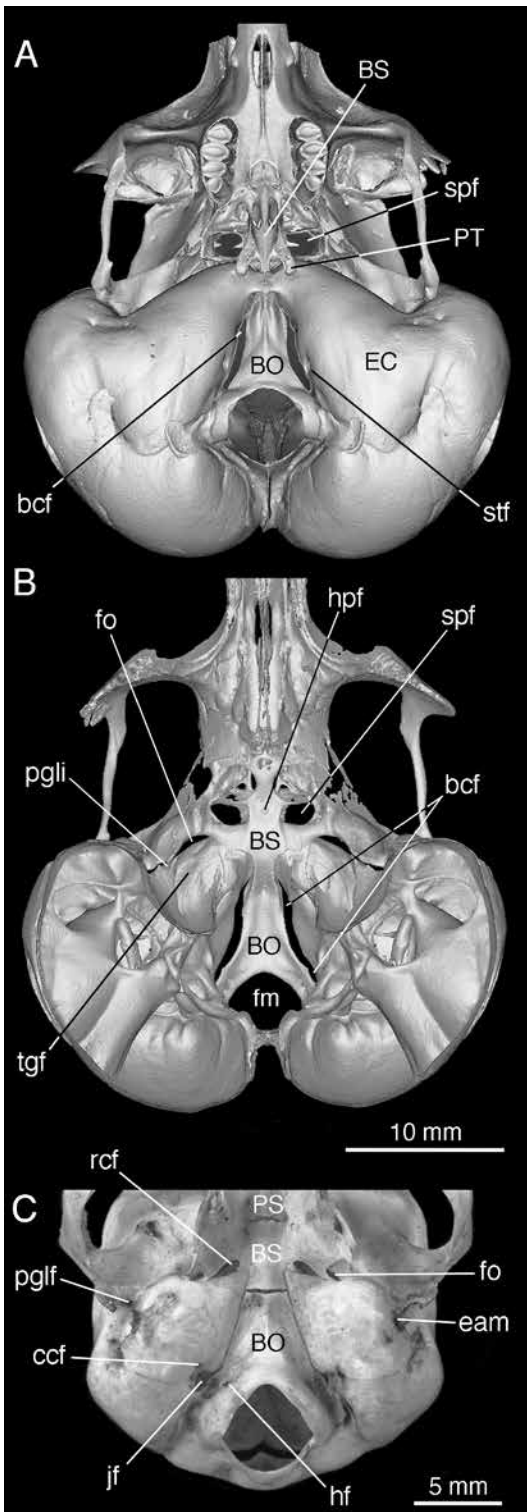


FIG. 36. **A** and **B**, *Dipodomys deserti* AMNH M-182081 (Dipodomysinae, Heteromyidae, Rodentia), adult caudal cranium in ventral and endocranial aspects; **C**, *Galago demidovii* AMNH M-89605 (Galagidae, Primates), adult caudal cranium in ventral aspect. Despite highly derived aspect of kangaroo rat skull, mesocranial position of foramina for sphenopterygoid veins suggests that latter may arise from emissaria comparable to those giving rise to transverse canal veins in marsupials. In *Galago* and other lorisiforms, in addition to ascending pharyngeal artery, rostral carotid foramen transmits large vein with same relations as internal carotid vein. **Key:** **bcf**, basicapsular fenestra (includes piriform fenestra and carotid foramen; see Brylski, 1990); **BO**, basioccipital; **BS**, basisphenoid; **ccf**, caudal carotid foramen; **eam**, external acoustic meatus; **EC**, ectotympanic; **fm**, foramen magnum; **fo**, foramen ovale; **hf**, hypoglossal foramen; **hpf**, hypophyseal fossa; **jf**, jugular foramen; **pglf**, postglenoid foramen; **pgli**, postglenoid incisure; **PS**, presphenoid; **PT**, pterygoid; **rcf**, rostral carotid foramen; **spf**, sphenopterygoid foramen (= ?transverse canal foramen); **stf**, stapedial foramen (according to Howell, 1932; Brylski, 1990); **tgf**, fossa for trigeminal ganglion.

et al. (2022: 188) did not recover a monophyletic clade Didelphimorphia (stem age, 56 mya). They attributed this outcome to the lack of resolution at the base of Marsupialia plus the general plesiomorphic aspect of didelphimorphians compared to other marsupial clades. They were, however, able to detect several dental synapomorphies that serve to define the extant clade, Didelphidae. Unfortunately, no PCVN-related character can be added to this list, as didelphids are internally disparate. *Didelphis* itself displays the least elaborate PCVN architecture found in the comparative set: the CBTC pathway is not present, the CS/ICV does not connect in any substantial way with either the transverse canals or the TBS, and the caudal and rostral portions of the TBS are poorly developed and discontinuous. In line with our other inductions (see above), this suggests derived loss rather than primitive retention on the part of *Didelphis*. The complex junction pattern verified for *Monodelphis*, *Philander*, and (possibly) *Marmosa* differs

from the simple pattern of *Didelphis* in that CBVs are present and communicate with the CS/ICV in the hypophyseal fossa. In these regards these last taxa are broadly similar and plesiomorphic, leaving *Didelphis* as an outlier within examined Didelphinae. None of our admittedly small sample of didelphids expresses the compound or hybrid patterns.

The other pattern found in the didelphid sample is the one expressed by the caluromyines *Caluromys* and *Caluromysiops* (fide Sánchez-Villagra and Wible, 2002), here defined as indeterminate because the TCF and its associated vasculature are functionally completely absent. The fact that TCV/TCF absence also occurs in acrobatids and many phalangerids according to Aplin 1990; but see Beck et al., 2022: 65), as well as among individuals in other taxa, may imply that loss of the TCV/TCF is developmentally not infrequent.

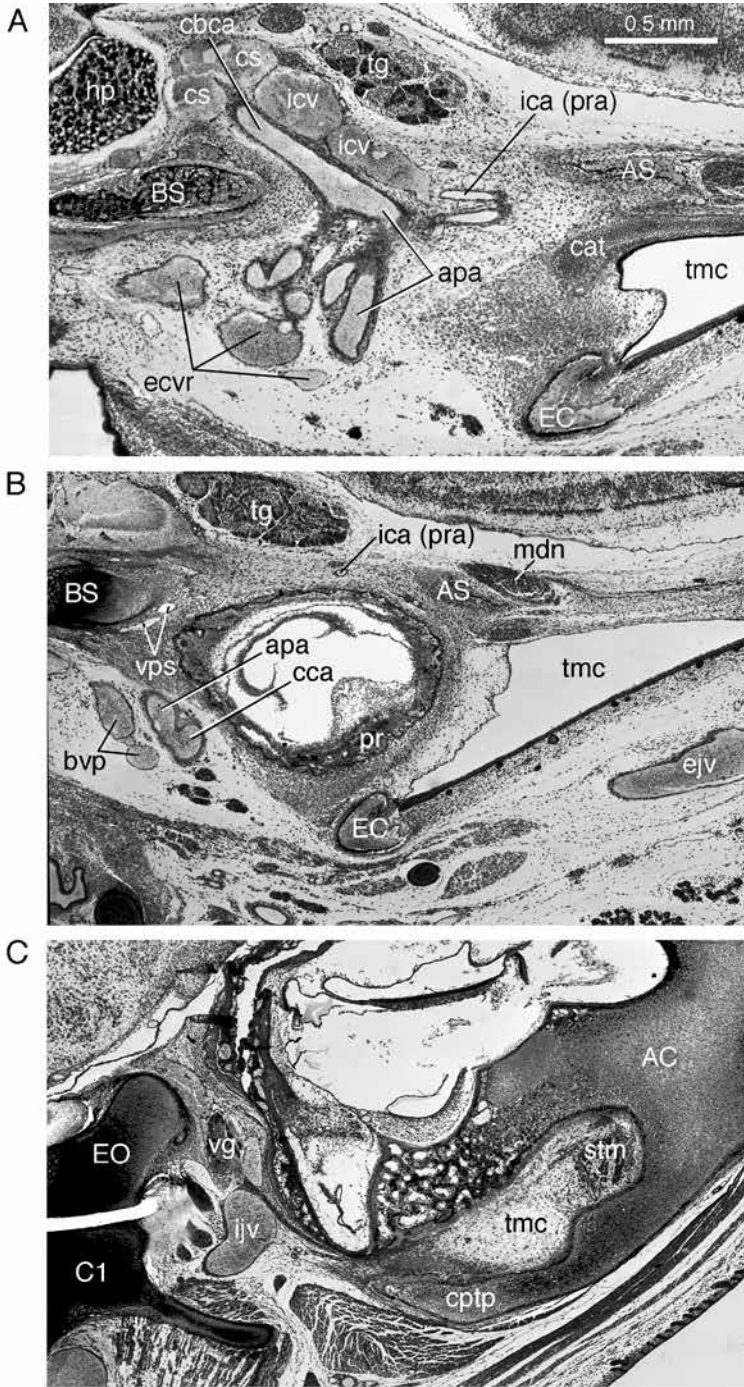
Although both caluromyines and *Didelphis* exhibit structural simplification of PCVN components, they do not do so in the same way. An interesting question regarding caluromyines concerns the condition of the junction pattern in its ancestral lineage: did it more closely resemble that of *Didelphis* or of *Monodelphis*? The first option implies only one branch-loss event, the other two.

**PAUCITUBERCULATA VS. AUSTRALIDELPHIA.** Extant *Caenolestes* and its close kin are generally considered to be sister to Australidelphia (Amrine-Madsen et al., 2003; Horovitz and Sánchez-Villagra, 2003; Luo et al., 2003; Asher et al., 2004; Nilsson et al., 2004, 2010; Beck et al., 2022). Alternative views link these paucituberculatans with didelphimorphians (= Ameridelphia sensu Szalay, 1982, 1994), or place them at the root of Marsupialia (e.g., Meredith et al., 2009; Mitchell et al., 2014; May-Collado et al., 2015). The divergence between Paucituberculata and Australidelphia is placed near the Paleocene-Eocene boundary by Beck et al. (2022).

No unambiguous craniodental synapomorphies linking Paucituberculata and Australidelphia were recovered by Beck et al. (2022: 206). In their view, the difficulty in identifying synapo-

morphies in this case stems from “the fact that the ancestral australidelphian probably had a relatively generalized cranium and dentition that was little different from the plesiomorphic marsupial condition and that different lineages within Australidelphia subsequently evolved very disparate apomorphies of the dentition, cranium, or both.” In our sample, *Caenolestes* exhibits the complex junction pattern, as does *Monodelphis* and probably most other non-*Didelphis* didelphids. Two nonspeciose agreodontian clades express variations in the compound junction pattern, but the complex pattern appears in *Dasyurus* (and probably other dasyuromorphs judging from Archer’s [1976] descriptions). This is also the case in *Vombatus*, and probably *Phascolarctos* as well (see Aplin, 1990). Phalangeridans are quite different in displaying several potential (but unconfirmed) versions of the hybrid pattern. Better information on fossil taxa, to clarify conditions in ancestral australidelphians, is needed for PCVN characters to be of help in testing this superordinal relationship.

*Yalkaparidon* may be briefly mentioned here, as it has been aligned with both Australidelphia and Paucituberculata, among other possibilities (Beck et al., 2014, 2022; Abello and Candela, 2019; Zimicz and Goin, 2020). Beck et al. (2014) demonstrated a plausible TCF in this taxon as well as a connected TCV pathway, using transmitted light to determine its route through the thin basicranial floor. (The authors described the foramen’s position as posterior to the exocranial carotid foramen, but in illustrations it appears to be more lateral than caudal, not radically different from conditions in many extant marsupials.) The pathway thus exposed appears to directly communicate with the hypophyseal fossa, which is a strong similarity to the track of the CBTC. Whether a second pathway, consistent with the presence of the RBTC, exists in this taxon has not been explored and there is no information on junction pattern. Two pathways would be consistent but not dispositive of a relationship with Paucituberculata, as this is judged to be the primitive condition.



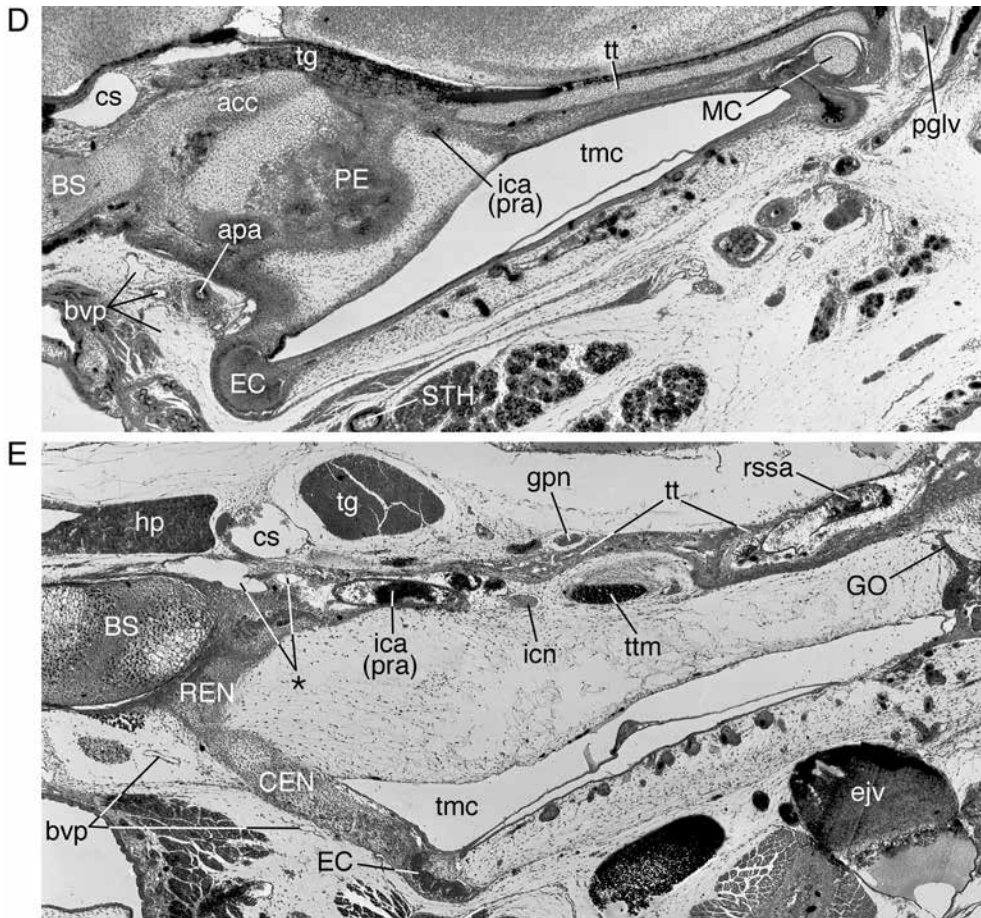


FIG. 37. A–C, *Galago demidovii* MPIH 120 (Galagidae, Primates), near-term fetus; D, *Microcebus murinus* MPIH 1962/57 (Cheirogaleidae, Primates), fetus; and E, *Elephantulus fuscipes* MPIH 311/E1 (Macroscelididae, Macroscelidea), fetus. Coronal sections, all to same scale. In A and B (ss. 961, 979, sides rev.), rete mirabile with ascending pharyngeal artery, internal carotid vein, and basicranial venous plexus. In C and D (ss. 1285; 91/2/3), relatively large internal jugular vein, typical of strepsirhines, receives multiply branching basicranial venous plexus. In E (s. 1558), mesocranial vascular arrangements in sengis are quite different from those seen in strepsirhines: vein (asterisk) running across tympanic roof to accompany internal carotid artery into endocranium originates from prootic sinus, therefore not homologous with internal carotid vein. **Key:** AC, auditory capsule; acc, alicochlear commissure; apa, ascending pharyngeal artery; AS, alisphenoid; BS, basisphenoid; bvp, basicranial venous plexus; C1, atlas vertebra; cat, cartilage of auditory tube; cbca, cerebral carotid artery; cca, common carotid artery; CEN, caudal entotympanic; ctp, caudal tympanic process of petrosal; cs, cavernous sinus; EC, ectotympanic; ecvr, extracranial arterial rete; ejv, external jugular vein; EO, exoccipital; GO, gonial; gpn, greater petrosal nerve; hp, hypophysis; ica (pra), internal carotid artery (promontorial artery); icn, internal carotid nerve; icv, internal carotid vein (= internal carotid venous plexus); ijv, internal jugular vein; MC, meckelian cartilage; mdn, mandibular nerve; PE, petrosal; pglv, postglenoid vein; pr, promontorium; REN, rostral entotympanic; rssa, ramus superior of stapedial artery; STH, stylohyal; stm, stapedius muscle; tg, trigeminal ganglion; tmc, tympanic cavity; tt, tegmen tympani; ttm, tensor tympani muscle; vg, vagus ganglion; vps, ventral petrosal sinus.

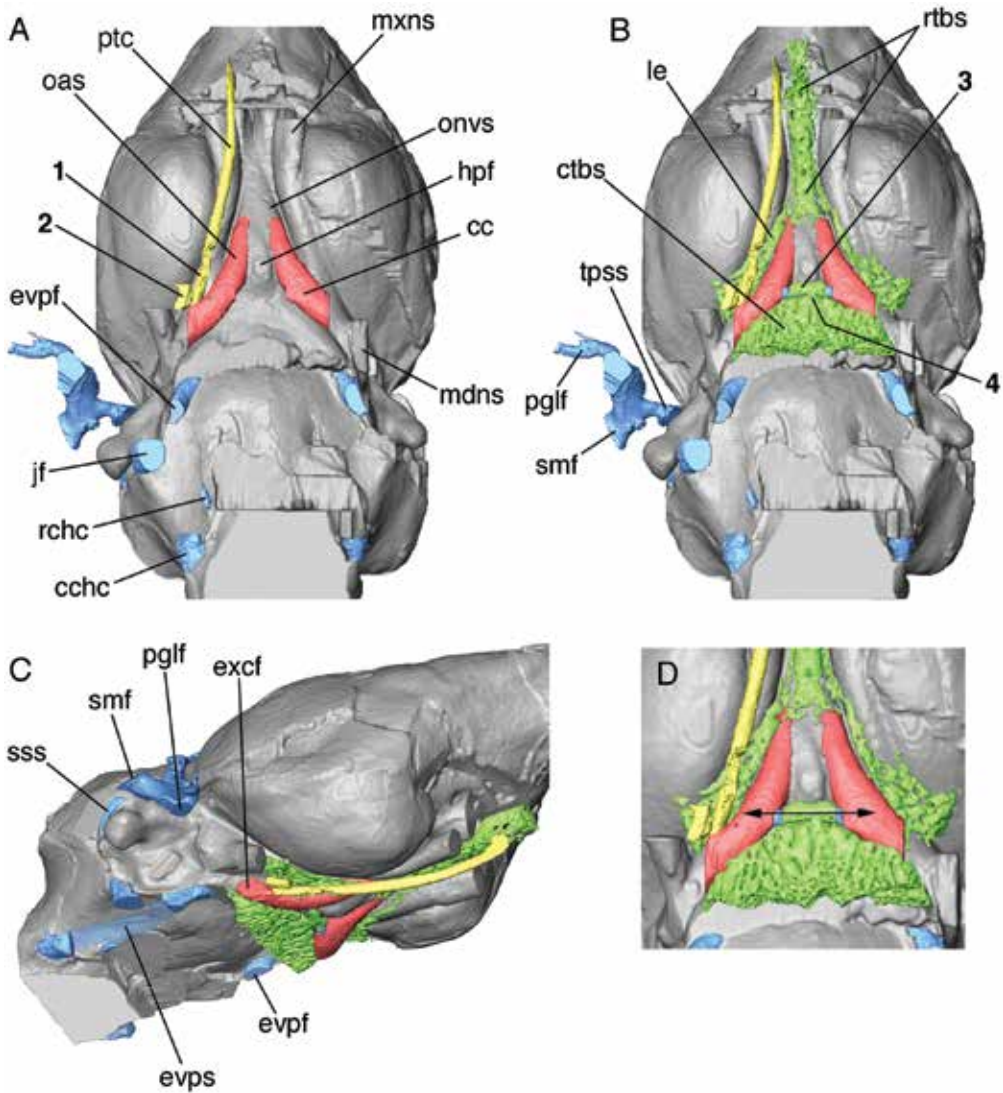
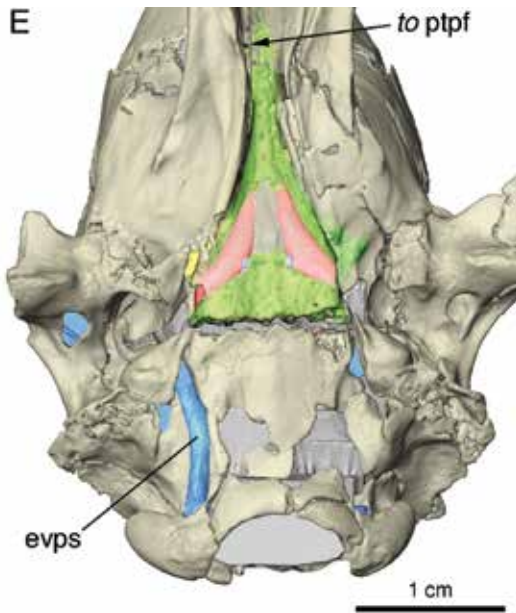


FIG. 38. *Sipalocyon gracilis* AMNH VP-9254 (Hathliacynidae, Sparassodonta), adult specimen, endocast reconstruction showing osteological features associated with pericarotid venous network and related vasculature (data source, table 2; color key, fig. 4). Views: **A**, ventral; **B**, same, with transverse basisphenoid sinus superimposed; **C**, oblique right lateral; **D**, closeup of endocranial surface of mesocranial region; and **E**, caudoventral surface, intact caudal cranium showing extracranial continuation of ventral petrosal sinus. In A–C, rostral portion of transverse basicranial sinus lacks identifiable intramural connections with carotid canals or cavernous sinus. Feature 1, identified by Archer (1976) as a possible transverse canal in *Sipalocyon*, is more likely a channel for nerve of pterygoid canal. Feature 2 is a sulcus of unknown function, unrelated to either nerve of pterygoid canal or typical transverse canal. Feature 3, small channel within basisphenoid sinus tissue, presumably venous, passes between bilateral carotid canals (double-headed arrow in D) caudal to hypophyseal fossa. Arrangement is different from that of CBTC of investigated marsupials. Feature 4, another small canaliculus, either interstitial or remnant of notochord canal, connects feature 3 with rest of sinus. **Key:** cc, carotid canal; cchc, caudal condylohyoglossal canal; ctbs, caudal portion of



transverse basisphenoid sinus; **evpf**, foramen for extracranial continuation of ventral petrosal sinus; **evps**, extracranial continuation of ventral petrosal sinus (reconstructed in E, passing along basijugular sulcus on external surface); **excf**, exocranial carotid foramen; **hpf**, hypophyseal fossa; **jf**, jugular foramen; **le**, lateral extension of transverse basisphenoid sinus; **mdns**, sulcus for mandibular nerve (to foramen ovale); **mxns**, sulcus for maxillary nerve; **oas**, sulcus for ophthalmic artery; **onvs**, sulcus for ophthalmic neurovascular array; **pglf**, postglenoid foramen; **ptc**, pterygoid canal; **ptpf**, rostral foramen for nerve of pterygoid canal and pterygopalatine fissure (latter in orbital floor, not visible); **rchc**, rostral condylohypoglossal canal; **rtbs**, rostral portion of transverse basisphenoid sinus; **smf**, supra-meatal foramen; **sss**, sulcus for sigmoid sinus; **tpss**, sulcus for temporal sinus.

**AGREODONTIA VS. MICROBIOTHERIA + DIPROTODONTIA.** The initial split within Australidelphia, yielding Agreodontia (Notoryctemorphia + Peramelemorphia + Dasyuromorphia) and Microbiotheria + Diprotodontia, occurred about 48 Mya according to the divergence estimate of Beck et al. (2022). In Agreodontia, the transition from the ancestrally complex pattern to the derived compound pattern must have occurred

at least once, to account for similar conditions in peramelids, notoryctids, and some dasyurids.

Of interest here is the proposal, mostly based on retrotransposon data, that Microbiotheria is sister to all the Sahulian diversity (Nilsson et al., 2010; Gallus et al., 2015; Feng et al., 2022), rather than exclusively to Diprotodontia. *Dromiciops* exhibits a version of the compound junction pattern, together with both TCV branches; this same pattern is inferred for *Notoryctes* and *Perameles*, representing two of the three major extant clades of agreodontians (and is probably present in some members of the third, Dasyuromorphia). As noted, this combination is not seen in the very few diprotodontians studied so far.

Assuming that the compound pattern is a synapomorphy of the total group (i.e., Microbiotheria + Agreodontia + Diprotodontia), taxa lacking this derived state can be interpreted as follows. Dasyuromorphia, a large clade, is known to differ internally: *Dasyurus* possesses both TCV branches in the complex pattern, while *Thylacinus* resembles Macropodiformes in lacking the RBV in a version of the hybrid pattern. In these cases, an acceptable topology would require that the lineage of *Dasyurus* reverted to the basal condition (complex pattern), while that of *Thylacinus* convergently developed a resemblance to the derived pattern of Macropodiformes. Obviously, many more taxa in their respective groups, including fossils, need to be investigated to establish the likelihood of this scenario.

**MACROPODIFORMES + PHALANGERIFORMES VS. VOMBATIFORMES.** As *Notamacropus*, *Osphranter*, *Trichosurus*, and *Vombatus* constitute our entire diprotodontian sample, out of a total of at least 40 extant genera, interpretation has to be cautious. All extant nonvombatiform diprotodontians can be grouped in the clade Phalangerida (Beck et al., 2022), and certainly the macropodids and *Trichosurus* are much more like each other than either is to *Vombatus*. Indeed, their particular mesocranial attributes are not seen in that combination in any other Holocene marsupial investigated to date, adding to their distinctiveness. The partial merger of the carotid and transverse canals seen in the macro-

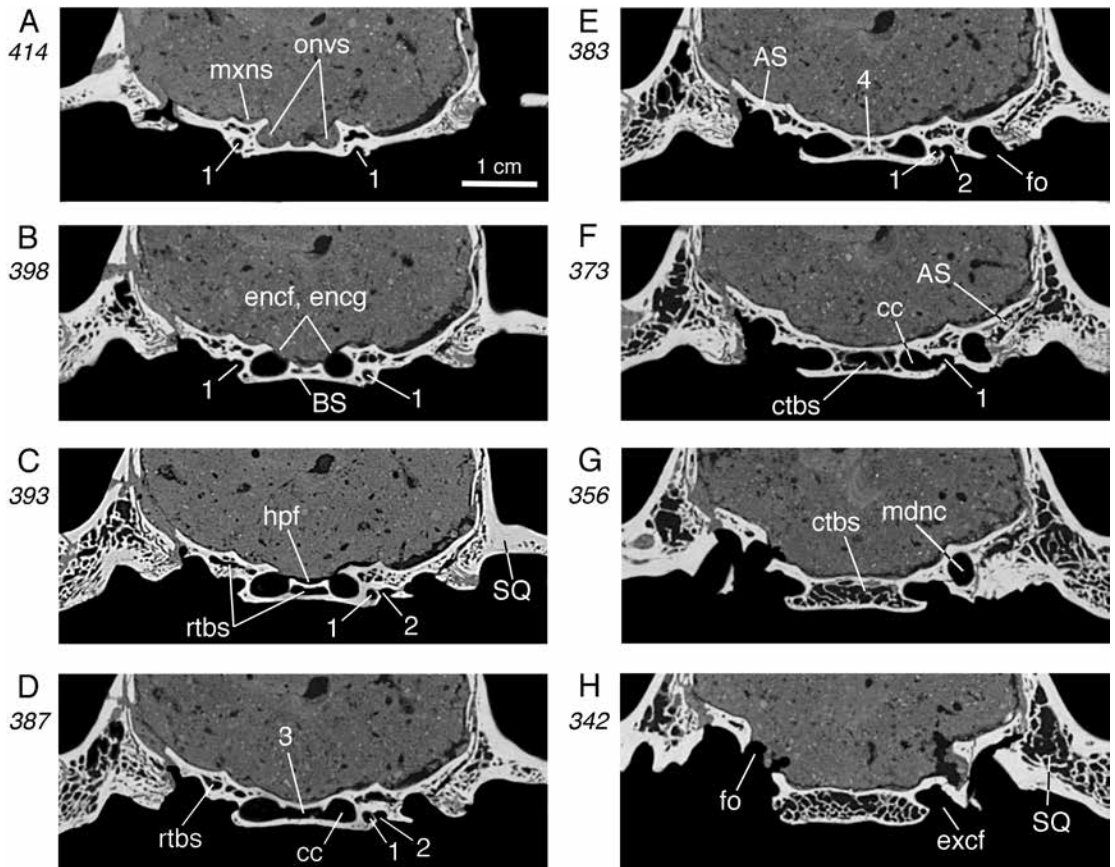


FIG. 39. *Sipalocyon gracilis* AMNH VP-9254 (Hathliacynidae, Sparassodonta), adult caudal cranium, selected coronal segments in rostrocaudal order (data source, table 2). As in extant marsupials, large carotid canals probably carried internal carotid vein as well as artery. However, channels for transverse canal veins resembling those of most marsupials or *Prothylacynus* (fig. 40A) are not in evidence. Small channels on lip of extracranial carotid foramen, thought by Archer (1976) to be possible transverse foramina, are for components of nerve of pterygoid canal and another structure that cannot be securely identified (features 1, 2; cf. fig. 38). Right and left internal carotid veins could have interacted with each other and with caudal portion of transverse basisphenoid sinus via features 3 and 4 (cf. fig. 38D). **Key:** AS, alisphenoid; BS, basisphenoid; cc, carotid canal; ctbs, caudal portion of transverse basisphenoid sinus; encf, endocranial carotid foramen; encg, endocranial carotid groove; excf, exocranial carotid foramen; fo, foramen ovale; hpf, hypophyseal fossa; mdnc, canal for mandibular nerve (to foramen ovale); mxns, sulcus for maxillary nerve; onvs, sulcus for ophthalmic neurovascular bundle; rtbs, rostral portion of transverse basisphenoid sinus; SQ, squamosal; 1, pterygoid canal; 2, sulcus of unknown function; 3, small canaliculus joining right and left carotid canals (presumably venous, for anastomosis between internal carotid veins); 4, small connector between 3 and rest of caudal transverse basisphenoid sinus; possibly retained portion of notochord canal.

podids is less advanced in *Trichosurus*. The two also differ in that *Trichosurus* may retain a small RBTC in the form of the accessory transverse canal (fig. 22B), whereas the similarly positioned conduit in the macropodids appears to vary greatly in both size and incidence (figs. 18, 20).

As outlined in the systematic descriptions, *Trichosurus* could be regarded as displaying a morphologically intermediate condition between the hybrid version as typified by *Notamacropus* and *Osphranter* and the compound pattern seen in most agrodontians and *Dromiciops*. Other phalangeriforms have not been studied in sufficient detail, but the possibility that some of them derivedly recruit other emissaries, such as the ICV, needs to be considered. This is of interest because it once again underlines the importance of basicranial characters: all five features that optimize as unambiguous craniodental synapomorphies of Phalangerida in the dated total-evidence analysis of Beck et al. (2022) are located in the basicranium. Equally important from an analytical perspective, the PCVNs of Vombatiformes (including *Phascolarctos*, based on Aplin's [1990] description) bear no unique derived mesocranial resemblances to Macropodiformes or Phalangeriformes.

#### FUNCTIONAL CONSIDERATIONS

**DRAINAGE OF CAVERNOUS SINUS.** Overall, our evidence is consistent with the view that PMDs function in most marsupials just as they do in placentals, i.e., they act as ancillary drainage channels for the CS. However, there is acknowledged variation, and one of the PMDs, the RBV, does not directly perform that particular task to any important extent in the taxa investigated here. This suggests that PMDs may have other tasks to perform, as yet poorly characterized; some possibilities are outlined in the following paragraphs.

**CORRELATION WITH SUCKLING.** The oropharyngeal pump mechanism seen in infant marsupials is one of the adaptational hallmarks of the clade (Tyndale-Biscoe, 2005; Fabre et al., 2021).

Routing blood from the CS directly to the EJV via enlarged PMDs could be part of a vascular adaptation related to the pump's precocious development. The muscles of the infratemporal fossa are supplied by the maxillary artery and drained in part by the pterygoid and related plexuses, which are tributary to the maxillary vein. We speculate that maximizing blood flow through this region via maxillary vasculature might facilitate local muscular pumping action and contribute to efficient suckling. A functional relationship between an enlarged PCVN and precocial suckling might also correlate with certain pervasive cranial adaptations in marsupials that are absent, or nearly so, in placentals, such as early ossification of the secondary palate (see Maier, 1993; Smith, 1997, 2001). This last development is crucial for separating the oral and nasal cavities in order to permit breathing while suckling. Although the correlation is worth examining further, it is recognized that the CS lies well outside the oral cavity and pharyngeal region and any functional relationship with suckling and blood flow may be incidental.

**CUSHIONING OF INTERNAL CAROTID ARTERY.** In *Homo* the CS and the internal carotid venous plexus surround the internal carotid artery as it passes through the carotid canal to enter the endocranium. It has been suggested that this arrangement provides protection for the artery under conditions of increased intravascular pressure or dampens pulsations within the canal that might be transmitted to, and thus affect, cochlear function (Moreira, 1998; Young et al., 2006). The plexus has also been implicated in stabilization of intracranial pressure during postural changes (Cironi et al., 2022). Such functions seem plausible enough in the case of *Homo* because of the relatively enormous size of the internal carotid artery, but in marsupials this vessel travels far from the cochlea, especially in taxa with inflated middle ears. If protection of the artery within the carotid canal were important in mammals generally, then one would expect to see the equivalent of a well-developed ICV in more placental clades.

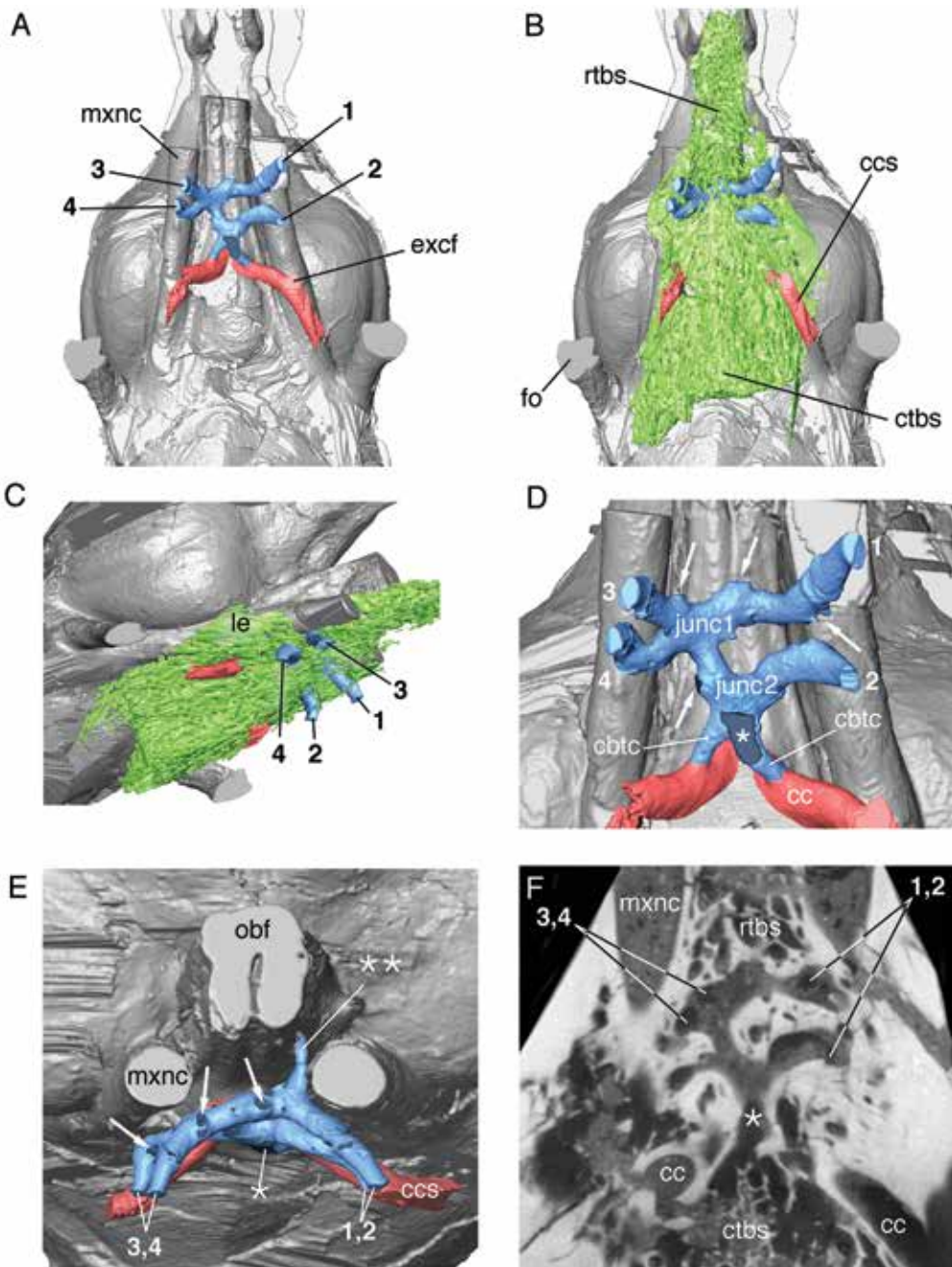
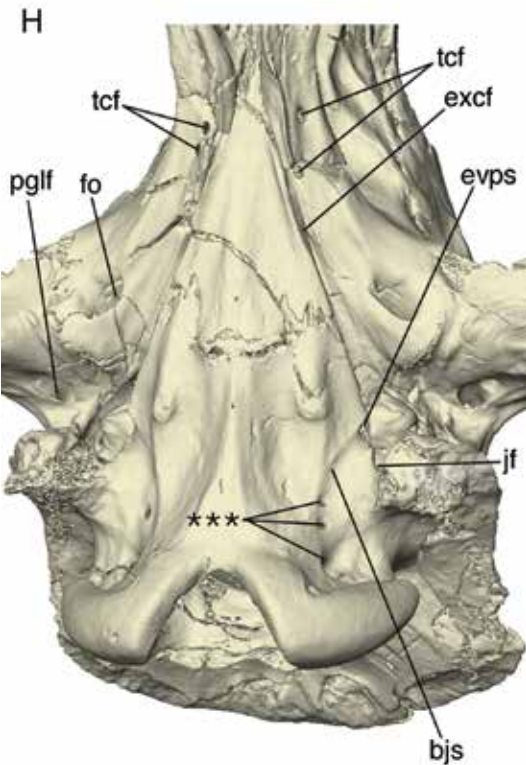
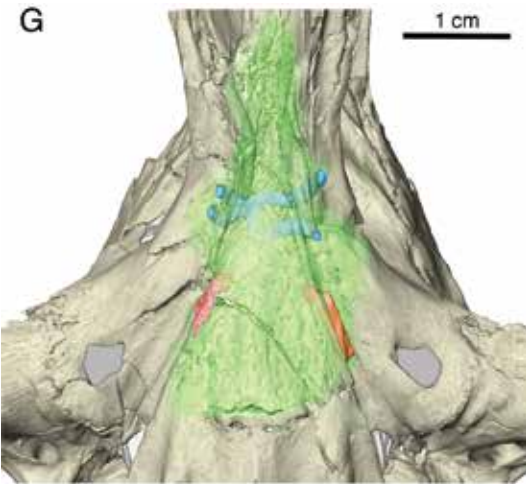


FIG 40. *Prothylacynus patagonicus* YPM VPPU-15700 (Borhyaenoidea, Sparassodonta), adult specimen, endocast reconstruction showing osteological features associated with pericarotid venous network and related vasculature (data source, table 2; color key, fig. 4). Views: **A**, ventral; **B**, same, with transverse basisphenoid sinus superimposed; **C**, oblique right lateral; **D**, closeup of transverse canals, ventral aspect; **E**, closeup of transverse canals, rostral aspect; **F**, horizontal section through transverse canals and mesocranium; **G**, ventral and **H**, left ventrolateral surfaces of intact caudal cranium. In A–F, features 1–4



are transverse canal foramina and associated rostral branches. In D and E, these are connected by caudal branches to carotid canals and by interstitial canaliculi to transverse basisphenoid sinus (arrows). Single asterisk identifies especially large, ventrally directed interstitial canaliculus joining transverse basisphenoid sinus. Double asterisks

identify canaliculus directed toward sphenoorbital fissure. In H, triple asterisks identify condylar (i.e., vascular only) foramina. **Key:** **bjs**, basijugular sulcus; **cbtc**, caudal branch of transverse canal; **cc**, carotid canal; **ccs**, sulcus leading to carotid canal; **ctbs**, caudal portion of transverse basisphenoid sinus; **evps**, extracranial continuation of ventral petrosal sinus; **excf**, exocranial carotid foramen; **fo**, foramen ovale; **jf**, jugular foramen; **junc1**, **junc2**, junctions of rostral branches of transverse canals; **le**, lateral extension of transverse basisphenoid sinus; **mxnc**, canal for maxillary nerve; **obf**, fossa for olfactory lobes; **pglf**, postglenoid foramen; **rtbs**, rostral portion of transverse basicranial sinus; **tcf**, transverse canal foramina (features 1–4).

**RETIAL FORMATION.** In certain placentals, homologs of the ICV/PVP are incorporated into a highly distinctive functional arrangement of vessels, the extracranial “carotid” rete (Barnett et al., 1958), exemplified in this study by the loriform *Galago demidovii* (fig. 37A). Although ICV/PVP formations may be more extensive in some marsupials than others (e.g., *Caluromys*, fig. 9D–F), the result does not compare with the elaborate extracranial venous retia seen in *Galago* and *Felis*, for example (e.g., Daniel et al., 1953; du Boulay and Verity, 1973; Kier et al., 2019). In the few placentals exhibiting relatively substantial TCVs (e.g., *Solenodon*, Wible, 2008), retial formations in the mesocranial area are unknown. Hypotheses regarding the functional significance of extracranial retia include selective brain cooling (e.g., Cartmill, 1975; Caputa, 2004). At present there is no conclusive evidence for inferring the existence of true retial structures, extracranial or intracranial, in any marsupial, although such claims have been made in the past (Shah et al., 1986; but see Shah and Nicol, 1989; Rose et al., 2017).

**HEMATOPOIESIS.** Although it is often assumed that the purpose of pneumatization in cranial bones is to reduce their mass by creating “air” spaces within them, coterminous functions may also exist (see Sharp, 2016). One of these is blood cell production. In young stages of placental mammals, hematopoiesis typically occurs

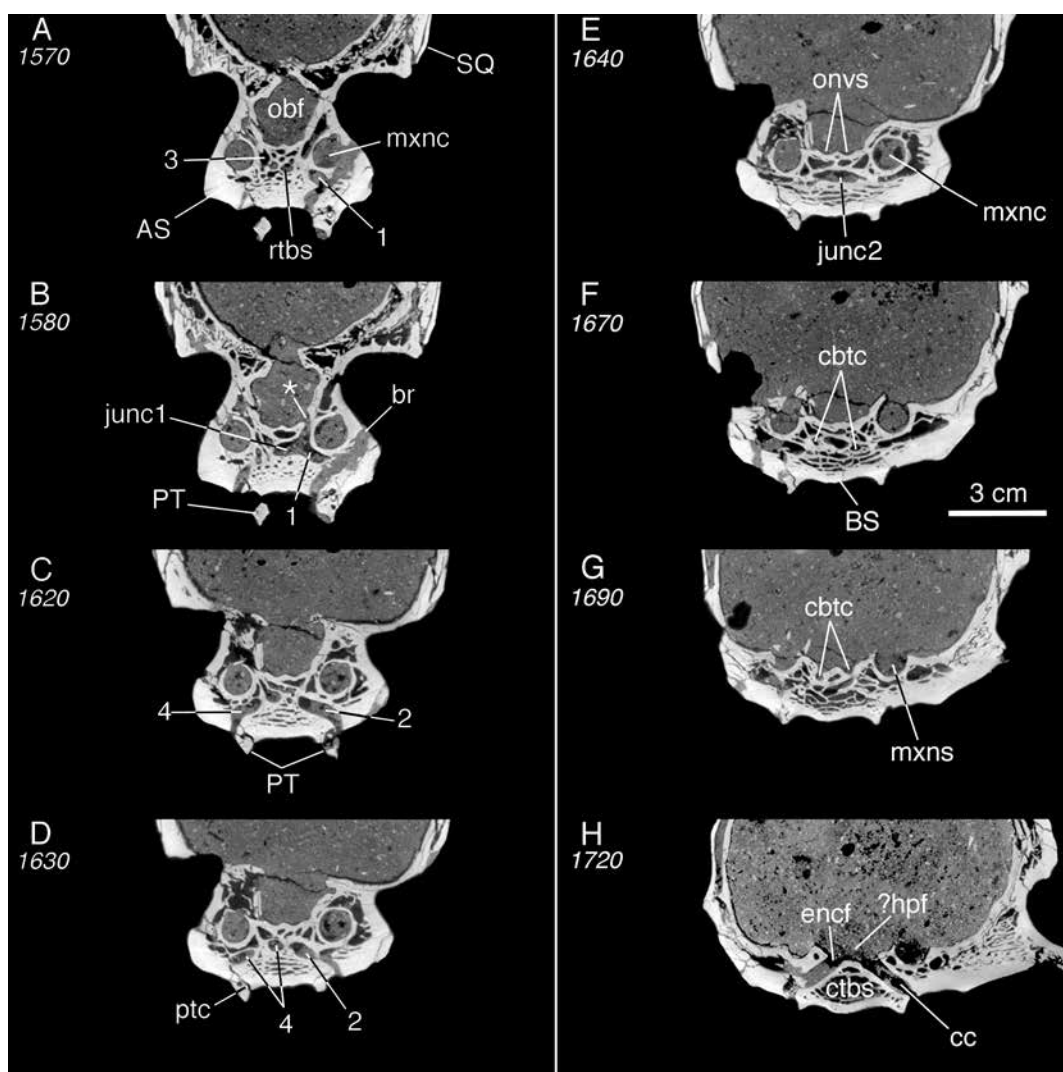


FIG. 41. *Prothylacynus patagonicus* YPM VPPU-15700 (Borhyaenoidea, Sparassodonta), adult caudal cranium, selected coronal segments in rostrocaudal order (data source, table 2). Rostral branches of transverse canals (features 1–4, cf. fig. 40A, D) are situated relatively more rostrally than in extant marsupials. However, they connect with transverse basisphenoid sinus and carotid canals via caudal branches as well as interstitial canaliculi, similar to conditions in certain marsupials. In B, asterisk indicates dorsally directed interstitial canaliculus originating from transverse canal. **Key:** AS, alisphenoid; br, breakage; BS, basisphenoid; cbtc, caudal branch of transverse canal; cc, carotid canal; ctbs, caudal portion of transverse basisphenoid sinus; encf, endocranial carotid foramen; ?hpf, hypophyseal fossa; junc1, junc2, junctions of rostral branches of transverse canals; mxnc, canal for maxillary nerve; mxns, sulcus for maxillary nerve; obf, fossa for olfactory lobes; onvs, sulcus for ophthalmic neurovascular array; PT, pterygoid; ptc, pterygoid canal; rtbs, rostral portion of transverse basisphenoid sinus; SQ, squamosal.

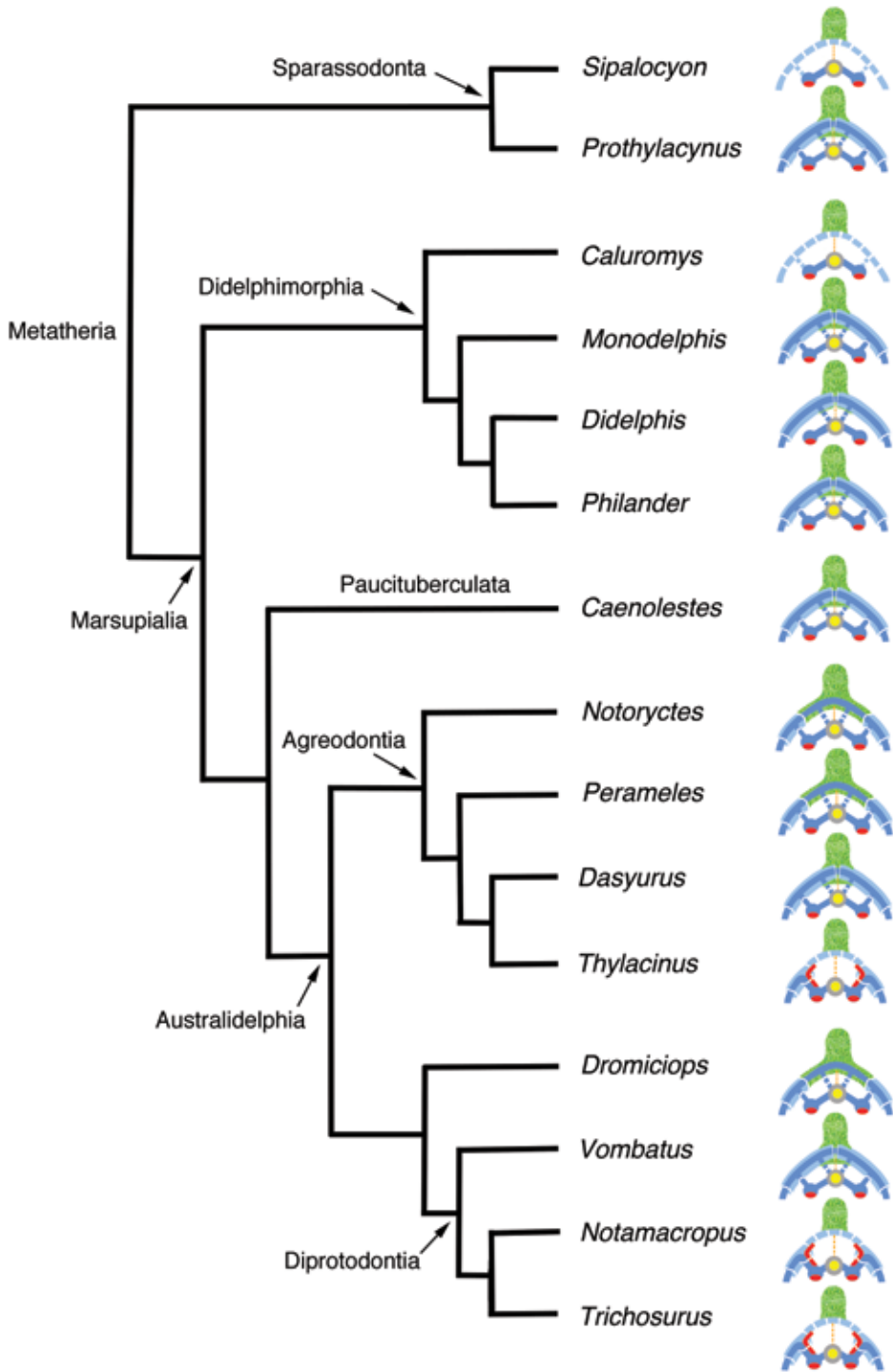
TABLE 5  
**Inferred Basal Mesocranial Characters of Marsupialia**

Plesiomorphies	Supporting Evidence
1. PMDs act as significant drainage route for CS (a, b)	(a) All adequately investigated extant marsupials possess ICV; also present in placentals (as internal carotid venous plexus) and monotremes, but generally unenlarged. (b) Most adequately investigated extant marsupials possess well-developed TCV (trunk and branches) in adult stage, but rare as significant vessel in placentals. Other PMEs (emissaries of foramen ovale and of piriform fenestra) probably present developmentally in all therian taxa, although almost never enlarged.
2. TCF present (b, c)	(c) Almost all adequately investigated extant marsupials as well as some nonmarsupial metatherians possess TCF (one or more).
3. TBS present in basisphenoid portion of keel (d)	(d) “Pneumatic” sinuses, functioning as centers of extramedullary blood cell production (at least in young stages); generally present in basicranial keel elements in extant therians.
4. TCV/ICV communication present via caudal branch of transverse canal (e)	(e) Except in <i>Didelphis</i> , caudal branch present or suspected in most sampled extant marsupial taxa. Anastomosis of ICV and TCV probable but unconfirmed in hybrid pattern. Caudal branch present in some sparassodonts ( <i>Prothylacynus</i> , this paper; <i>Andinodelphys</i> , Muizon and Ladevèze, 2020).
5. TCV/CS communication present via hypophyseal canaliculi (f)	(f) Apertures in walls of transverse canals opening into endocranial floor in vicinity of hypoglossal fossa are frequent but variable in sampled taxa.

in red marrow within the basicranial and calvarial diploe, as has been extensively documented in animal models and human clinical studies (e.g., Cline and Maronpot, 1985; Zollikofer and Weismann, 2008; Johns and Christopher, 2012). During human cranial development, this function eventually declines: fatty marrow replaces red marrow, and blood cell production moves to the spleen and medullary cavities of long bones. In the adult human the basisphenoid sinus is occupied by fatty marrow and has no persisting functional relationship with the vascular system, unless so-called extramedullary hematopoiesis develops as a pathological process (“arrested pneumatization”; Park and Hwang, 2021). However, in some mammals blood cell formation in cranial bones may continue into maturity, where it is plainly non-pathological (see Cline and Maronpot, 1985). Although active blood-cell formation is indicated in the sectioned perinatal specimen of *Perameles* (fig. 33A), whether it continues into later ontogeny in this taxon (or any other marsupial) has not been investigated.

PMDs may be implicated in distributing new erythrocytes to the systemic circulation, but they are probably not required for this purpose. Ordinary interstitial canaliculi, linked to successively larger drainage zones, are the means by which erythrocytes produced in the calvarial diploe are eventually moved to larger systemic veins (see Tubbs et al., 2020), and the same kind of routing should apply to blood cells produced in the skull base. What, then, is the need for large vessels like the TCVs to pass through the mesocranium? This hints at one other function that these vessels may have, to which we shall now turn.

REGULATION OF VASCULAR PRESSURE. Aplin (1990: 255) speculated that the real job of the large TCVs characteristic of most marsupials was to influence the movement of blood passing bilaterally between the PVPs, to ensure “regulation of vascular pressure during venous shunting in other parts of the system.” This is in line with the proposal that emissaries generally function to equalize intracranial pressure (Curé et al., 1994; Tubbs et al., 2020). However, as far as we are aware the possibility that TCVs are



involved in regulating blood pressure in the head region of marsupials has never been pursued as a research question in mammalian vascular physiology. Among other issues it should be noted that, for the PCVN to work as a regulator, the blood passing through the mesocranial confluence would have to be easily transmitted in both directions across the midline. In *Homo* and presumably most other mammals, the PVPs are valved, which would be inhibitory (but see Watanabe et al., 2013). Whether marsupial TCVs are valveless, like diploic veins (García-González et al., 2009), or valved, like systemic veins, should be easy to determine. How presence or absence of valves in TCVs would affect pressure regulation is more complicated, but it might finally answer a question that has lingered for well over a century: what, exactly, is the transverse canal vein for?

#### ACKNOWLEDGMENTS

We extend our grateful thanks to colleagues who arranged access to specimens in their care, particularly Wolfgang Maier (University of Tübingen), Marcelo Sánchez-Villagra (University of Zürich), Chris Norris and Vanessa Rhue (Yale Peabody Museum), Meng Jin (American Museum of Natural History), Georg Schulz (Bio-

materials Science Center, University of Basel), Loïc Costeur (University of Basel), Jorge Domingo Carrillo Briceño and Gabriel Aguirre (University of Zürich), and Pablo Teta (Museo Argentino de Ciencias Naturales “Bernardino Rivadavia”). The specimen of *Dromiciops* utilized for this study was donated to MACN by Guillermo Amico.

For our use of open-access CT scans of TMM M-2517, 6921, 849, and 2953 (see tables 1 and 2), we thank Ted Macrini and DigiMorph.org, administered by The University of Texas High-Resolution X-ray CT Facility with support from National Science Foundation (NSF) grants NSF IIS-0208675, NSF IIS-9874781, and DEB-0309369. We also acknowledge Morphosource.org, administered by Duke University, and Roger Benson and the European Research Council (ERC, starting grant TEMPO (ERC-2015-STG-677774). Lorraine Meeker (American Museum of Natural History) produced the illustrations with her usual skill and attention to detail. Ross MacPhee and Ben Sulser wish to thank the staff of the AMNH Imaging Facility and the Department of Mammalogy for their assistance. This study is a contribution to the projects PICT 2019-2874 (National Agency for Scientific and Technological Promotion, Argentina) and SNSF SPIRIT (Swiss Programme for

FIG. 42. Distribution of PCVN-related features in selected marsupials and sparassodontans, framed against a depiction of their phylogenetic relationships as assessed in dated total evidence tree of Beck et al. (2022). Coverage is limited to taxa described in our systematic descriptions. (*Osphranter* and *Notamacropus* do not significantly differ for features considered, so only latter taxon is referenced.) Icons accompanying individual taxa are meant to summarize main differences in transverse canal junction patterns, and are based on cartoons illustrating PCVN components in fig. 1C (see also text and table 4). This is a first attempt at interpreting mesocranial disparities across Marsupialia (and Sparassodonta). *Monodelphis*-like complex pattern is regarded as basal for Marsupialia. Compound pattern is found in nondiverse taxa Notoryctemorph (Notoryctes) and Peramelemorphia (*Perameles*) as well as Microbiotheria (*Dromiciops*). Substantially more speciose dasyuromorphians are underinvestigated: there is definitely more than one junction pattern in extant diversity (*Dasyurus*, complex pattern; *Thylacinus*, hybrid pattern). Sparse evaluations in previous literature are hard to convert into detailed system used in this paper, and need to be restudied before incorporation. Representative diprotodontians are sharply divided into those expressing hybrid pattern (macropodiforms and ?some phalangeriforms) and complex pattern (*Vombatus*, probably *Phascolarctos*). Didelphimorphians as a group also exhibit less elaborate patterns (simple and complex). Indeterminate pattern exemplified by *Caluromys* is a result of loss (involution of all of transverse canal vein) and may occur convergently in other groups, particularly phalangerids, although nature and degree of loss is disputed. Sparassodontan patterns are somewhat comparable to those found in extant marsupials, but are otherwise distinct.

International Research Projects by Scientific Investigation Teams, Switzerland). Finally, we are indebted to our two reviewers, John Wible and Robin Beck, for their close reading of this paper and many useful suggestions for improving it.

## REFERENCES

- Abele, T.A., K.L. Salzman, H.R. Harnsberger, and C.M. Glastonbury. 2014. Craniopharyngeal canal and its spectrum of pathology. *American Journal of Neuro-radiology* 35: 772–777.
- Abello, M.A., and A.M. Candela. 2019. Paleobiology of *Argyrolagus* (Marsupialia, Argyrolagidae): an astonishing case of bipedalism among South American mammals. *Journal of Mammalian Evolution* 27: 419–444.
- Amador, L.I., and N.P. Giannini. 2016. Phylogeny and evolution of body mass in didelphid marsupials (Marsupialia: Didelphimorphia: Didelphidae). *Organisms Diversity Evolution*. [doi 10.1007/s13127-015-0259-x]
- Amrine-Madsen, H., et al. 2003. Nuclear gene sequences provide evidence for the monophyly of australidelphian marsupials. *Molecular Phylogenetics and Evolution* 28: 186–196.
- Anders, U., W. von Koenigswald, I. Ruf, and B.H. Smith. 2011. Generalized individual dental age stages for fossil and extant placental mammals. *Paläontologische Zeitschrift* 85: 321–339.
- Anthwal, N., and H. Thompson. 2016. The development of the mammalian outer and middle ear. *Journal of Anatomy* 228: 217–232.
- Aplin, K.P. 1990. Basicranial regions of diprotodontian marsupials: anatomy, ontogeny, and phylogeny. Ph.D. dissertation, School of Biological Sciences, University of New South Wales, Sydney, 389 pp.
- Archer, M. 1976. The basicranial region of marsupicarnivores (Marsupialia), relationships of carnivorous marsupials, and affinities of the insectivorous marsupial peramelids. *Zoological Journal of the Linnean Society* 59: 217–322.
- Arey, L.B. 1950. The craniopharyngeal canal reviewed and reinterpreted. *Anatomical Record* 106: 1–16.
- Arnautovic, K.I., O. Al-Mefty, T.G. Pait, A.F. Krisht, and M.M. Husain. 1997. The suboccipital cavernous sinus. *Journal of Neurosurgery* 86: 252–262.
- Asher, R.J., I. Horovitz, and M.R. Sánchez-Villagra. 2004. First combined cladistic analysis of marsupial-mammal interrelationships. *Molecular Phylogenetics and Evolution* 33: 240–250.
- Babot, M.J., J.E. Powell, and C. de Muizon. 2002. *Calistoe vincei*, a new Proborhyaenidae (Borhyaenoidae, Metatheria, Mammalia) from the Early Eocene of Argentina. *Geobios* 35: 615–629.
- Barnett, C.H., R.J. Harrison, and J.D.W. Tomlinson. 1958. Variations in the venous systems of mammals. *Biological Reviews of the Cambridge Philosophical Society* 33: 442–487.
- Beck, R.M.D. 2017. The skull of *Epidolops ameghinoi* from the Early Eocene Itaboraí Fauna, Southeastern Brazil, and the affinities of the extinct marsupialiform order Polydolopimorphia. *Journal of Mammalian Evolution* 24: 373–414.
- Beck, R.M.D., K.J. Travouillon, K.P. Aplin, H. Godthelp, and M. Archer. 2014. The osteology and systematics of the enigmatic Australian Oligo-Miocene metatherian *Yalkaparidon* (Yalkaparidontidae; Yalkaparidontia; ?Australidelphia; Marsupialia). *Journal of Mammalian Evolution* 21 (2): 127–172.
- Beck, R.M.D., R.S. Voss, and S.A. Jansa. 2022. Craniodental morphology and phylogeny of marsupials. *Bulletin of the American Museum of Natural History* 457: 1–350.
- Broom, R. 1911. On the affinities of *Caenolestes*. *Proceedings of the Linnean Society of New South Wales* 36: 315–320.
- Brylski, P. 1990. Development and evolution of the carotid circulation in geomyoid rodents in relationship to their craniomorphology. *Journal of Morphology* 204: 33–45.
- Bugge, J. 1974. The cephalic arterial system in insectivores, primates, rodents and lagomorphs, with special reference to the systematic classification. *Acta Anatomica* 87 (suppl 62): 1–159.
- Butler, H. 1957. The development of certain human dural venous sinuses. *Journal of Anatomy* 91: 510–526.
- Butler, H. 1967. The development of mammalian dural venous sinuses with especial reference to the post-glenoid vein. *Journal of Anatomy* 102: 33–56.
- Campos Leonel, L.C.P., M. Peris-Celda, S.D. Gonçalves De Sousa, R.G. Haetinger, and E. Aparecido Liberti. 2020. The sphenoidal emissary foramen and the emissary vein: anatomy and clinical relevance. *Clinical Anatomy* 33: 767–781.
- Caputa, M. 2004. Selective brain cooling: a multiple regulatory mechanism. *Journal of Thermal Biology* 29: 691–702.
- Cartmill, M. 1975. Strepsirhine basicranial structures and the affinities of the Cheirogaleidae. *In* W.P.

- Luckett and F.S. Szalay (editors), *Phylogeny of the Primates, a multidisciplinary approach*: 313–354. New York: Plenum Press.
- Celik, M., et al. 2019. A molecular and morphometric assessment of the systematics of the *Macropus* complex clarifies the tempo and mode of kangaroo evolution. *Zoological Journal of the Linnean Society* 186: 793–812.
- Cironi, K., et al. 2022. Anatomical study of the internal carotid venous plexus: new findings with application to skull base surgery. *Acta Neurochirurgica*. [doi: 10.1007/s00701-021-05081-x]
- Cline J.M., and R.R. Maronpot. 1985. Variations in the histologic distribution of rat bone marrow cells with respect to age and anatomic site. *Toxicologic Pathology* 13: 349–355.
- Cook, L.E., A.H. Newton, C.A. Hipsley, and A.J. Pask. 2021. Postnatal development in a marsupial model, the fat-tailed dunnart (*Sminthopsis crassicaudata*; Dasyuromorphia: Dasyuridae). *Communications Biology* 4: 1028.
- Cords, E. 1915. Über das Primordialcranium von *Perameles* spec. unter Berücksichtigung der Deckknochen. *Anatomische Hefte* 52: 1–81.
- Cornillie, P. C. Casteleyn, C. von Horst, and R. Henry. 2019. Corrosion casting in anatomy: visualizing the architecture of hollow structures and surface details. *Anatomia Histologia Embryologia* 48: 591–604.
- Curé, J.K., P. Van Tassel, and M.T. Smith. 1994. Normal and variant anatomy of the dural venous sinuses. *Seminars in Ultrasound, CT, and MRI* 15: 499–519.
- Daniel, P.M., J. D.K. Dawes, and M.M.L. Prichard. 1953. Studies of the carotid rete and its associated arteries. *Philosophical Transactions of the Royal Society, London B*237: 173–204.
- Davis, D.D. 1964. The giant panda: a morphological study of evolutionary mechanisms. *Fieldiana Zoology Memoirs* 3: 5–339.
- De Beer, G.R. 1937. *The development of the vertebrate skull*. Oxford: Clarendon Press.
- Dederer, P.H. 1909. Comparison of *Caenolestes* with Polyprotodonta and Diprotodonta. *American Naturalist* 43 (514): 614–618.
- D'Elía, G., N. Hurtado, and A. D'Anatro. 2016. Alpha taxonomy of *Dromiciops* (Microbiotheriidae) with the description of 2 new species of monito del monte. *Journal of Mammalogy* 97: 1136–1152.
- Díaz, M.M., and D.A. Flores 2008. Early reproduction onset in four species of Didelphimorphia in the Peruvian Amazonia. *Mammalia* 72: 126–130.
- Dom, R., B.L. Fisher, and G.F. Martin. 1970. The venous system of the head and neck of the opossum (*Didelphis virginiana*). *Journal of Morphology* 132: 487–496.
- Du Boulay, G.H., and P.M. Verity. 1973. *The cranial arteries of mammals*. London: Heinemann.
- Dye, J., et al. 2020. Endovascular approaches to the cavernous sinus in the setting of dural arteriovenous fistula. *Brain Sciences* 10: 554.
- Ekdale, E.G., J.D. Archibald, and A.O. Averianov. 2004. Petrosal bones of placental mammals from the Late Cretaceous of Uzbekistan. *Acta Palaeontologica Polonica* 49: 161–176.
- Eldridge, M., R.M.D. Beck, D.A. Croft, K.J. Travouillon, and B.J. Fox. 2019. An emerging consensus in the evolution, phylogeny, and systematics of marsupials and their fossil relatives (Metatheria). *Journal of Mammalogy* 100: 802–837.
- Ercoli, M.D., and F.J. Prevosti. 2011. Estimación de masa de las especies de Sparassodonta (Mammalia, Metatheria) de edad santacrucense (Mioceno temprano) a partir del tamaño del centroide de los elementos apendiculares: inferencias paleoecológicas. *Ameghiniana* 48: 462–479.
- Evans, H.E., and G.C. Christensen. 1979. *Miller's anatomy of the dog*. Philadelphia: Saunders.
- Fabre, A.-C., et al. 2021. Functional constraints during development limit jaw shape evolution in marsupials. *Proceedings of the Royal Society B*288: 20210319.
- Fawcett, D.W. 1986. *Bloom and Fawcett, a textbook of histology*, 11th ed. New York: Chapman & Hall.
- Feng, S., et al. 2022. Incomplete lineage sorting and phenotypic evolution in marsupials. *Cell* 185 (10): 1646–1660.
- Forasiepi, A.M. 2009. Osteology of *Arctodictis sinclairi* (Mammalia, Metatheria, Sparassodonta) and phylogeny of Cenozoic metatherian carnivores from South America. *Monografías del Museo Argentino de Ciencias Naturales* 6: 1–174.
- Forasiepi, A.M., R.D.E. MacPhee, and S. Hernández Del Pino. 2019. Caudal cranium of *Thylacosmilus atrox* (Mammalia, Metatheria, Sparassodonta), a South American predaceous sabertooth. *Bulletin of the American Museum of Natural History* 433: 1–64.
- Frazer, E.J. 1911. Pharyngeal end of Rathke's pouch. *Journal of Anatomy* 45: 190–96.
- Gabbert, S. 1998. Basicranial anatomy of *Herpetotherium* (Marsupialia: Didelphimorphia) from the Eocene of Wyoming. *American Museum Novitates* 3235: 1–13.

- Gallus, S., A. Janke, V. Kumar, and M.A. Nilsson. 2015. Disentangling the relationship of the Australian marsupial orders using retrotransposon and evolutionary network analyses. *Genome Biology and Evolution* 7: 985–992.
- García-González, U., et al. 2009. The diploic venous system: surgical anatomy and neurosurgical implications. *Neurosurgical Focus* 27: E2.
- Gaupp, E. 1908. Zur Entwicklungsgeschichte und vergleichen Morphologie des Schädels von *Echidna aculeata* var. typical. *Denkschriften der Medicinisch-Naturwissenschaftlichen Gesellschaft zu Jena* 6: 539–788.
- Giannini, N.P., et al. 2021. The cranial morphospace of extant marsupials. *Journal of Mammalian Evolution* 28: 1145–1160.
- Gignac, P.M., et al. 2016. Diffusible iodine-based contrast-enhanced computed tomography (diceCT): an emerging tool for rapid, high-resolution, 3-D imaging of metazoan soft tissues. *Journal of Anatomy* 228: 889–909.
- Goin, F.J., M.O. Woodburne, A.N. Zimicz, G.M. Martin, and L. Chornogubsky. 2016. A brief history of South American metatherians: Evolutionary contexts and intercontinental dispersals. Dordrecht: Springer.
- Goin, F.J., N. Zimicz, M. De Los Reyes, and L. Soibelson. 2009. A new large didelphid of the genus *Thylorphops* (Mammalia: Didelphimorphia: Didelphidae), from the late Tertiary of the Pampean Region (Argentina). *Zootaxa* 2005 (1): 35–46.
- García-González, U., et al. 2009. The diploic venous system: surgical anatomy and neurosurgical implications. *Neurosurgical Focus* 27: E2.
- Greene, 1935. Anatomy of the rat. *Transactions of the American Philosophical Society* 27: 1–370.
- Gregory, W.K. 1910. The orders of mammals. *Bulletin of the American Museum of Natural History* 27: 3–524.
- Hayashi, S., et al. 2020. Vena capitis prima and the cavernous sinus in human embryos and fetuses. *Annals of Anatomy* 229: 151467.
- Herrick, C.J. 1921. The brain of *Caenolestes obscurus*. *Publications of the Field Museum of Natural History, Zoological Series* 14: 157–162.
- Hill, J.E. 1935. The cranial foramina in rodents. *Journal of Mammalogy* 16: 121–129.
- Hochstetter, F. 1896. Beiträge zur Anatomie und Entwicklungsgeschichte des Blutgefäßsystems der Monotremen. In R. Semon (editor), *Zoologische Forschungsreisen in Australien und den Malayischen Archipel*, vol. 2, Monotremen und Marsupialier. *Denkschriften der Medicinisch-Naturwissenschaftlichen Gesellschaft zu Jena* 5: 191–243. Jena: Gustav Fischer.
- Horowitz, I., and M.R. Sánchez-Villagra. 2003. A morphological analysis of marsupial mammal higher-level phylogeny relationships. *Cladistics* 19: 181–212.
- Horowitz, I., et al. 2009. Cranial anatomy of the earliest marsupials and the origin of opossums. *PLoS One* 4. [doi:10.1371/journal.pone.0008278]
- Howell, A.B. 1932. The saltatorial rodent *Dipodomys*: the functional and comparative anatomy of its muscular and osseous systems. *Proceedings of the American Academy of Arts and Sciences* 67: 377–536.
- Hurum, J.H., R. Presley, and Z. Kielan-Jaworowska. 1996. The middle ear in multituberculate mammals. *Acta Palaeontologica Polonica* 41: 253–275.
- James, T.M., R. Presley, and F.L.D. Steel 1980. Foramen ovale and sphenoidal angle in man. *Anatomy and Embryology* 160: 93–104.
- Johns, J.L., and M.M. Christopher. 2012. Extramedullary hematopoiesis: a new look at the underlying stem cell niche, theories of development, and occurrence in animals. *Veterinary Pathology* 49: 508–523.
- Kesteven, H.L., and H.C. Furst. 1929. The skull of *Ornithorhynchus*, its later development and adult features. *Journal of Anatomy* 63: 447–472.
- Kielan-Jaworowska, Z. 1971. Skull structure and affinities of the Multituberculata. *Palaeontologia Polonica* 25: 4–41.
- Kielan-Jaworowska, Z. 1981. Evolution of the therian mammals in the Late Cretaceous of Asia. Part IV. Skull structure in *Kennalestes* and *Asioryctes*. *Acta Palaeontologica Polonica* 42: 25–78.
- Kielan-Jaworowska, R. Presley, and C. Poplin, 1986. The cranial vascular system in taenolabidoid multituberculate mammals. *Philosophical Transactions of the Royal Society B* 313: 525–602.
- Kier, E.L., C.J. Conlogue, and Z. Zhuang. 2019. High-resolution computed tomography imaging of the cranial arterial system and rete mirabile of the cat (*Felis catus*). *Anatomical Record* 302: 1958–1967.
- Kuhn, H.-J. 1971. Die Entwicklung und Morphologie des Schädels von *Tachyglossus aculeatus*. *Abhandlungen der Senckenbergischen Naturforschenden Gesellschaft* 528: 1–192.
- Ladevèze S., C. de Muizon, R.M.D. Beck, D. Germain, and R. Céspedes-Paz. 2011. Earliest evidence of mammalian social behaviour in the basal Tertiary of Bolivia. *Nature* 474: 83–86.
- Lake, A.R., I.J. Van Niekerk, C.G. Le Roux, T.R. Trevor-Jones, and P.D. De Wet. 1990. Angiology of the

- brain of the baboon *Papio ursinus*, the vervet monkey *Cercopithecus pygerrithrus* [sic] and the bushbaby *Galago senegalensis*. *American Journal of Anatomy* 187: 277–286.
- Lang, J. 1983. Clinical anatomy of the head: neurocranium, orbit, craniocervical regions. New York: Springer-Verlag. [Translated from the German by R.R. Wilson and D.P. Winstanley]
- Le Verger, K., González Ruiz, L., Billet, G. 2021. Comparative anatomy and phylogenetic contribution of intracranial osseous canals and cavities in armadillos and glyptodonts (Xenarthra, Cingulata). *Journal of Anatomy*. [doi:10.1111/joa.13512ff.fhal-03291344]
- Luo, Z.-X., and J.R. Wible. 2005. A Late Jurassic digging mammal and early mammalian diversification. *Science* 308: 103–107.
- Luo, Z.-X., Q. Ji, J.R. Wible, and C.-X. Yuan. 2003. An Early Cretaceous tribosphenic mammal and metatherian evolution. *Science* 302: 1934–1940.
- MacPhee, R.D.E. 1981. Auditory regions of primates and eutherian insectivores: morphology, ontogeny, and character analysis. *Contributions to Primatology* 18: 1–282.
- MacPhee, R.D.E. 1994. Morphology, adaptations, and relationships of *Plesiorycteropus*, and a diagnosis of a new order of eutherian mammals. *Bulletin of the American Museum of Natural History* 220: 1–213.
- MacPhee, R.D.E., and A.M. Forasiepi. 2022. Re-evaluating cranial pathways of the internal carotid artery in Notoungulata (Mammalia, Panperissodactyla). *Ameghiniana* 59: 141–161.
- MacPhee, R.D.E., A.M. Forasiepi, A. Kramarz, S. Hernandez Del Pino, M. Bond, and R.B. Sulser. 2021. Cranial morphology and phylogenetic relationships of *Trigonostylops*, an Eocene South American native ungulate. *Bulletin of the American Museum of Natural History* 449: 1–183.
- Maier, W. 1987. The ontogenetic development of the orbitotemporal region in the skull of *Monodelphis domestica* (Didelphidae, Marsupialia), and the problem of the mammalian alisphenoid. In H.J. Kuhn and U. Zeller (editors), *Morphogenesis of the mammalian skull*: 71–90. Hamburg: Verlag Paul Parey.
- Maier, W. 1993. Cranial morphology of the therian common ancestor, as suggested by the adaptations of neonate marsupials. In F.S. Szalay, M.J. Novacek, and M.C. McKenna (editors), *Mammal phylogeny: Mesozoic differentiation, multituberculates, monotremes, early therians, and marsupials*: 165–181. New York: Springer-Verlag.
- Marshall, L.G. 1976. Evolution of the Thylacosmilidae, extinct saber-tooth marsupials of South America. *PaleoBios* 23: 1–30.
- Marshall, L.G. 1977. A new species of *Lycopsis* (Borhyaenidae, Marsupialia) from the La Venta fauna (Miocene) of Colombia, South America. *Journal of Paleontology* 51: 633–642.
- Marshall, L.G. 1978. Evolution of the Borhyaenidae, extinct South American predaceous marsupials. University of California Publications in Geological Sciences 117: 1–89.
- Marshall, L.G., and C. de Muizon. 1995. The skull. In C. de Muizon (editor), *Pucadelphys andinus* (Marsupialia, Mammalia) from the Early Paleocene of Bolivia, Part II. *Mémoires du Muséum National d'Histoire Naturelle* 165: 21–90.
- Matthes, E. 1921. Neuere Arbeiten über das Primordialekranium der Säugetiere. *Ergebnisse der Anatomie und Entwicklungsgeschichte* 23: 669–912
- May-Collado, L.J., C.W. Kilpatrick, and I. Agnarsson. 2015. Mammals from ‘down under’: a multi-gene species-level phylogeny of marsupial mammals (Mammalia, Metatheria). *PeerJ* 3: e805.
- Meng, J., Y. Hu, and C. Li. 2003. The osteology of *Rhombomylus* (Mammalia, Glires): implications for phylogeny and evolution of Glires. *Bulletin of the American Museum of Natural History* 275: 1–247.
- Meredith, R.W., C. Krajewski, M. Westerman, and M.S. Springer. 2009. Relationships and divergence times among the orders and families of Marsupialia. *Museum of Northern Arizona Bulletin* 65: 383–406.
- Mitchell, K.J., et al. 2014. Molecular phylogeny, biogeography, and habitat preference evolution of marsupials. *Molecular Biology and Evolution* 31: 2322–2330.
- Moore, W.J. 1981. *The mammalian skull*. Cambridge: Cambridge University Press.
- Moreira, M.B. 1998. Physiological importance of the conjugation of the internal carotid artery and cavernous sinus. *Medical Hypotheses* 50: 389–91.
- Mortazavi, M.M., et al. 2011. Anatomy and pathology of the cranial emissary veins: a review with surgical implications. *Neurosurgery* 70: 1312–1319.
- Muizon, C. de. 1998. *Mayulestes ferox*, a borhyaenoid (Metatheria, Mammalia) from the Early Paleocene of Bolivia. *Phylogenetic and palaeobiologic implications*. *Geodiversitas* 20: 19–142.
- Muizon, C. de. 1999. Marsupial skulls from the Deseadan (late Oligocene) of Bolivia and phylogenetic analysis of the Borhyaenoidea (Marsupialia, Mammalia). *Geobios* 32: 483–509.

- Muizon, C. de, and S. Ladevèze. 2020. Cranial anatomy of *Andinodelphys cochabambensis*, a stem metatherian from the Early Palaeocene of Bolivia. *Geodiversitas* 42: 597–739.
- Muizon, C. de, G. Billet, C. Argot, S. Ladevèze, and F. Goussard. 2015. *Alcidedorbignya inopinata*, a basal pantodont (Placentalia, Mammalia) from the Early Palaeocene of Bolivia: anatomy, phylogeny and palaeobiology. *Geodiversitas* 37: 397–634.
- Muizon, C. de, Ladevèze S., Selva C., Vignaud R., and Goussard F. 2018. *Allqokirus australis* (Sparassodonta, Metatheria) from the Early Palaeocene of Tiupampa (Bolivia) and the rise of the metatherian carnivorous radiation in South America. *Geodiversitas* 40: 363–459.
- Nathoo, N., E.C. Caris, J.A. Wiener, E. Mendel. 2011. History of the vertebral venous plexus and the significant contributions of Breschet and Batson. *Neurosurgery* 69: 1007–14.
- NAV [International Committee on Veterinary Gross Anatomical Nomenclature]. 2017. *Nomina anatomica veterinaria*, 6th ed. Online resource (<http://www.wava-amav.org/wava-documents.html>).
- Newton, A.H., F. Spoutil, J. Prochazka, J.R. Black, K. Medlock, R.N. Paddle, M. Knitlova, C.A. Hipsley, and A.J. Pask. 2018. Letting the “cat” out of the bag: pouch young development of the extinct Tasmanian tiger revealed by X-ray computed tomography”. *Royal Society Open Science* 5: 171914.
- Nilsson, M.A., U. Arnason, P.B.S. Spencer, and A. Janke. 2004. Marsupial relationships and a timeline for marsupial radiation in South Gondwana. *Gene* 340: 189–196.
- Nilsson, M.A., et al. 2010. Tracking marsupial evolution using archaic genomic retroposon insertions. *PLoS Biology* 8 (7): e1000436.
- Old, J.M., L. Selwood, and E.M. Deane. 2004. A developmental investigation of the liver, bone marrow and spleen of the stripe-faced dunnart (*Sminthopsis macroura*). *Developmental and Comparative Immunology* 28: 347–355.
- O’Leary, M.A., J.I. Bloch, J.J. Flynn, T.J. Gaudin, A. Giallombardo, N.P. Giannini, S.L. Goldberg, B.P. Kraatz, Z.X. Luo, J. Meng, X. Ni, M.J. Novacek, F.A. Perini, Z.S. Randall, G.W. Rougier, E.J. Sargis, M.T. Silcox, N.B. Simmons, M. Spaulding, P.M. Velazco, M. Weksler, J.R. Wible, and A.L. Cirranello. 2013. The placental mammal ancestor and the post-K-Pg radiation of placentals. *Science* 339: 662–667.
- Osgood, W.H. 1921. A monographic study of the American marsupial, *Caenolestes*. Publications of the Field Museum of Natural History, Zoological Series 14: 1–156.
- Padgett, D.H. 1956. The cranial venous system in man in reference to development, adult configuration, and relation to the arteries. *American Journal of Anatomy* 98: 307–355.
- Padgett, D.H. 1957. The development of cranial venous system in man: from the viewpoint of comparative anatomy. *Contributions to Embryology* 36: 79–140.
- Páez Arango, N. 2008. Dental and craniomandibular anatomy of *Peligrotherium tropicalis*: the evolutionary radiation of South American dryolestoid mammals. M.Sc. thesis, University of Louisville, Louisville, KY.
- Park, S.-H., and J.-H. Hwang. 2021. Arrested pneumatization of the sphenoid sinus in the skull base. *Brain Tumor Research and Treatment* 9: 40–43.
- Patterson, B. 1965. The auditory region of the borhyaenid marsupial *Cladosictis*. *Breviora* 217: 1–9.
- Porter, W.R., and L.M. Witmer. 2015. Vascular patterns in iguanas and other squamates: blood vessels and sites of thermal exchange. *PLoS One* 10 (10): e0139215.
- Prince, J.H., E.D. Diesem, I. Eglitis, and G.L. Ruskell. 1960. *Anatomy and histology of the eye and orbit in domestic animals*. Springfield, IL: Charles C Thomas.
- Rager L., L. Hautier, A.M. Forasiepi, A. Goswami, and M.R. Sánchez-Villagra. 2014. Timing of cranial suture closure in placental mammals: phylogenetic patterns, intraspecific variation, and comparison with marsupials. *Journal of Morphology* 275: 125–140.
- Raybaud, C. 2010. Normal and abnormal embryology and development of the intracranial vascular system. *Neurosurgery Clinics of North America* 21: 399–426.
- Reinhard, K.R., M.E. Miller, and H.E. Evans. 1962. The craniovertebral veins and sinuses of the dog. *American Journal of Anatomy* 111: 67–87.
- Rose, R.K., D.A. Pemberton, N.J. Mooney, and M.E. Jones. 2017. *Sarcophilus harrisii* (Dasyuromorphia: Dasyuridae). *Mammalian Species* 49 (942): 1–17.
- Rougier, G.W., J.R. Wible, and M.J. Novacek. 1998. Implications of *Deltatheridium* specimens for early marsupial history. *Nature* 396: 459–463.
- Roux, G.H. 1947. The cranial development of certain Ethiopian “insectivores” and its bearing on the mutual affinities of the group. *Acta Zoologica* 28: 165–397.
- Saban, R. 1963. Contribution à l’étude de l’os temporal des primates. Description chez l’homme et les prosimiens. *Anatomie comparée et phylogénie. Mémoires du Museum National d’Histoire Naturelle (sér. A) Zoologie* 29: 1–377.

- San Millán Ruiz, D., et al. 2002. The craniocervical venous system in relation to cerebral venous drainage. *American Journal of Neuroradiology* 23: 1500–1508.
- Sánchez-Villagra, M.R., and A.M. Forasiepi. 2017. On the development of the chondrocranium and the histological anatomy of the head in perinatal stages of marsupial mammals. *Zoological Letters* 3: 1. [doi: 10.1186/s40851-017-0062-y]
- Sánchez-Villagra, M.R., and J.R. Wible. 2002. Patterns of evolutionary transformation in the petrosal bone and some basicranial features in marsupial mammals, with special reference to didelphids. *Journal of Zoological Systematics and Evolutionary Research* 40: 26–45.
- Schnitzlein, H.N., F.R. Murtagh, J.A. Arrington, and D. Parkinson. 1985. The sinus of the dorsum sellae. *Anatomical Record* 213: 587–589.
- Shah, S.K.H., and S.C. Nicol. 1989. Cephalic vasculature and distribution of blood flow through the cranial arterial circle of the Tasmanian devil, *Sarcophilus harrisii*. *Journal of Mammalogy* 70: 123–131.
- Shah, S.K. H., S.C. Nicol, and R. Swain. 1986. Functional morphology of the cranial vasculature and the nasal passage in the Tasmanian devil, *Sarcophilus harrisii* (Marsupialia: Dasyuridae): a marsupial carotid rete? *Australian Journal of Zoology* 34: 125–133.
- Sharp, A.C. 2016. A quantitative comparative analysis of the size of the frontoparietal sinuses and brain in vombatiform marsupials. *Memoirs of Museum Victoria* 74: 331–342.
- Shindo, T. 1915. Über die Bedeutung des Sinus cavernosus der Säuger mit vergleichend-anatomischer Berücksichtigung anderer Kopfvenen. *Anatomische Hefte* 52: 319–495.
- Simpson, G.G. 1938. Osteography of the ear region in monotremes. *American Museum Novitates* 978: 1–15.
- Sisson, S., and J.D. Grossman. 1953. *The anatomy of the domestic animals*, rev. 4th ed. Philadelphia: Saunders.
- Sleightholme, S.R., and N. Ayliffe. 2013. *International thylacine specimen database*, 5th revision. DVD-ROM on file, Zoological Society of London.
- Smith, K.K. 1997. Comparative patterns of craniofacial development in eutherian and metatherian mammals. *Evolution* 51: 1663–1678.
- Smith, K.K. 2001. Heterochrony revisited: the evolution of developmental sequences. *Biological Journal of the Linnean Society* 73: 169–186.
- Starck, D. 1967. Le crâne des mammifères. In P.-P. Grassé (editor), *Traité de zoologie: anatomie, systématique, biologie*, vol. 16.1, Mammifères, téguments et squelette: 405–549; 1095–1102. Paris: Masson.
- Szalay, F.S. 1982. A new appraisal of marsupial phylogeny and classification. In M. Archer (editor), *Carnivorous marsupials*: 621–640. Mosman, New South Wales: Royal Zoological Society of New South Wales.
- Szalay, F.S. 1994. *Evolutionary history of the marsupials and an analysis of osteological characters*, Cambridge: Cambridge University Press.
- Szalay F.S., and B.A. Trofimov. 1996. The Mongolian Late Cretaceous *Asiatherium*, and the early phylogeny and paleobiogeography of Metatheria. *Journal of Vertebrate Paleontology* 16: 474–509.
- Tandler, J. 1899. Zur vergleichenden Anatomie der Kopfarterien bei den Mammalia. *Denkschriften der Kaiserlichen Akademie der Wissenschaften, Mathematisch-Naturwissenschaftliche Classe, Wien* 67: 677–784.
- Tobinick, E., and C.P. Vega. 2006. The cerebrospinal venous system: anatomy, physiology, and clinical implications. *Medscape General Medicine* 8 (1): 53.
- Toepflitz, C., 1920. Bau und Entwicklung des Knorpelschadels von *Didelphys* [sic] *marsupialis*. *Zoologica* 27 (70): 1–83.
- Towbin, J.A., B. Casey, and J. Belmont. 1999. The molecular basis of vascular disorders. *American Journal of Human Genetics* 64: 678–684.
- Tubbs, R.S., et al. (editors). 2020. *Anatomy, imaging and surgery of the intracranial dural venous sinuses*. New York: Elsevier.
- Tyndale-Biscoe, H. 2005. *Life of marsupials*. Collingwood, Australia: CSIRO Publishing.
- van Bemmelen, J.F. 1901. Der Schädelbau der Monotremen. *Denkschriften der Medicinisch-Naturwissenschaftlichen Gesellschaft zu Jena* 6: 729–798.
- van der Klaauw, C.J. 1929. On the development of the tympanic region of the skull in the Macroscelididae. *Proceedings of the Zoological Society of London* 1929: 491–560.
- van Gelderen, C. 1924. Die Morphologie der Sinus durae matris. Zweiter Teil. Die vergleichende Ontogenie der neurokranialen Venen der Vögel und Säugetiere. *Zeitschrift für Anatomie und Entwicklungsgeschichte* 74: 432–508.
- Verli, F.D., T.R. Rossi-Schneider, F.L. Schneider, L.S. Yurgel, and M.A.L. de Souza. 2007. Vascular corrosion casting technique steps. *Scanning* 29: 128–132.
- Voss, R.S., and S.A. Jansa. 2003. Phylogenetic studies on didelphid marsupials II. Nonmolecular data and new IRBP sequences: separate and combined analyses of didelphine relationships with denser taxon

- sampling. *Bulletin of the American Museum of Natural History* 276: 1–82.
- Voss, R.S., and S.A. Jansa. 2009. Phylogenetic relationships and classification of didelphid marsupials, an extant radiation of New World metatherian mammals. *Bulletin of the American Museum of Natural History* 322: 1–177.
- Wahlert, J. 1985. Skull morphology and relationships of geomyoid rodents. *American Museum Novitates* 2812: 1–20.
- Warwick, R., and P.L. Williams. 1973. *Gray's anatomy* (35th British ed.). Philadelphia: Saunders.
- Watanabe, K., S. Kakeda, R. Watanabe, N. Ohnari, and Y. Korogi. 2013. Normal flow signal of the pterygoid plexus on 3T MRA in patients without DAVF of the cavernous sinus. *American Journal of Neuroradiology* 34: 1232–1236.
- Wible, J.R. 1984. The ontogeny and phylogeny of the mammalian cranial arterial pattern. Ph.D. thesis, Duke University, Durham, NC.
- Wible, J.R. 1986. Transformations in the extracranial course of the internal carotid artery in mammalian phylogeny. *Journal of Vertebrate Paleontology* 6: 313–325.
- Wible, J.R. 2003. On the cranial osteology of the short-tailed opossum *Monodelphis breviceaudata* (Didelphidae, Marsupialia). *Annals of Carnegie Museum* 72: 137–202.
- Wible, J.R. 2008. On the cranial osteology of the Hispaniolan solenodon, *Solenodon paradoxus* Brandt, 1833 (Mammalia, Lipotyphla, Solenodontidae). *Annals of Carnegie Museum* 77: 321–402.
- Wible, J.R. 2022. CT study of the cranial osteology of the short-tailed opossum *Monodelphis domestica* (Wagner, 1842) (Marsupialia, Didelphidae) and comments on the internal nasal skeleton floor. *Annals of Carnegie Museum* 87: 249–289.
- Wible, J.R., and T.J. Gaudin. 2004. On the cranial osteology of the yellow armadillo *Euphractus sexcinctus* (Dasypodidae, Xenarthra, Placentalia). *Annals of Carnegie Museum* 73: 117–196.
- Wible, J.R., and J.A. Hopson. 1995. Homologies of the prootic canal in mammals and non-mammalian cynodonts. *Journal of Vertebrate Paleontology* 15: 331–356.
- Wible, J.R., and G.W. Rougier. 2000. Cranial anatomy of *Kryptobaatar dashzevegi* (Mammalia, Multituberculata), and its bearing on the evolution of mammalian characters. *Bulletin of the American Museum of Natural History* 247: 1–124.
- Wible, J.R., and G.W. Rougier. 2017. Craniomandibular anatomy of the subterranean meridiolestidan *Necrolestes patagonensis* Ameghino, 1891 (Mammalia, Cladotheria) from the Early Miocene of Patagonia. *Annals of Carnegie Museum* 84: 183–252.
- Wible, J.R., and S.L. Shelley. 2020. Anatomy of the petrosal and middle ear of the brown rat, *Rattus norvegicus* (Berkenhout, 1769) (Rodentia, Muridae). *Annals of Carnegie Museum* 86: 1–35.
- Wible, J.R. and M. Spaulding. 2013. On the cranial osteology of the African palm civet, *Nandinia binotata* (Gray, 1830) (Mammalia, Carnivora, Feliformia) *Annals of Carnegie Museum* 82: 1–114.
- Wible, J.R., M.J. Novacek, and G.W. Rougier. 2004. New data on the skull and dentition of the Mongolian Cretaceous eutherian mammal *Zalambdalestes*. *Bulletin of the American Museum of Natural History* 281: 1–144.
- Wible, J.R., G.W. Rougier, M.J. Novacek, and R.J. Asher. 2009. The eutherian mammal *Maelestes gobiensis* from the Late Cretaceous of Mongolia and the phylogeny of Cretaceous Eutheria. *Bulletin of the American Museum of Natural History* 327: 1–123.
- Wible, J.R., S.L. Shelley, and C. Belz. 2021. The element of Paaw in marsupials and the middle ear of *Philander opossum* (Linnaeus, 1758) (Didelphimorphia, Didelphidae). *Annals of Carnegie Museum* 87: 1–35.
- Wortman, J.L. 1901–1903. Studies of Eocene Mammalia in the Marsh Collection, Peabody Museum [published in multiple parts]. *American Journal of Science* 11: 333–348, 437–450; 12: 143–154, 193–206, 281–296, 377–382, 421–432; 13: 39–46, 115–128, 197–206, 433–448; 14: 17–23.
- Young, B., P. Woodford, and G. O'Dowd. 2014. *Wheatler's functional histology: a text and color atlas*. 6th ed. New York: Elsevier.
- Young R.J., D.R. Shatzkes, J.S. Babb, and A.K. Lalwani. 2006. The cochlear-carotid interval: anatomic variation and potential clinical implications. *American Journal of Neuroradiology* 27: 1486–1490.
- Zeller, U. 1989. Die Entwicklung und Morphologie des Schädels von *Ornithorhynchus anatinus* (Mammalia: Prototheria: Monotremata). *Abhandlungen der Senckenbergischen Naturforschenden Gesellschaft* 545: 1–140.
- Zimicz, A.N., and F.J. Goin. 2020. A reassessment of the genus *Groeberia* Patterson, 1952 (Mammalia, Metatheria): functional and phylogenetic implications. *Journal of Systematic Palaeontology* 18: 975–992.
- Zollikofer, C.P.E., and J.D. Weissmann. 2008. A morphogenetic model of cranial pneumatization based on the invasive tissue hypothesis. *Anatomical Record* 291: 1446–1454.

## APPENDIX 1

## COMPARATIVE ANATOMY AND DEVELOPMENT OF COMPONENTS OF THE PERICAROTID VENOUS NETWORK AND RELATED STRUCTURES

These short accounts provide additional information and references regarding structures described in the text, as well as identifying topics warranting further investigation. For abbreviations see Anatomical Acronyms Used in Text (p. 12)

**CAVERNOUS SINUS (CS).** As far as is known, the basic arrangement of CS-related sinuses and emissaria found in placentals also occurs in marsupials (e.g., Shindo, 1915; Dom et al., 1970; Archer, 1976; Shah and Nichol, 1989; Aplin, 1990; this paper), although for most members of the latter clade empirical data are wanting. The definitive CS is situated on the intracranial surface of the basisphenoid, in the same position in all adult therians relative to the hypothalamus. The CS acts as the central collector of venous blood returning from the rostral end of the neurocranium and the orbits. In amniotes generally (e.g., Porter and Witmer, 2015), drainage is mostly from the eyes and orbital adnexa, via ophthalmic venous sinuses and plexuses, but in therians its neural role is proportionately increased to include the large volume of the brain's white matter (via rostral and middle cerebral or sylvian veins) as well as local meninges and diploe (via sphenoparietal sinuses) (Shindo, 1915; Raybaud, 2010; Tubbs et al., 2020; Dye et al., 2020). In humans and presumably other mammals, the CS develops from the medial part of the primary head vein (Padget, 1957: 103; Tubbs et al., 2020: 139; Raybaud, 2010; Hayashi et al., 2020). By stage 7 in the development of fetal *Homo* (Padget, 1957: 113), earlier connections of the CS have begun to disintegrate, to be succeeded by new links with the developing petrosal sinuses (Hayashi et al., 2020). This kind of succession, which probably takes place in all mammals, helps to account for differences among species due to the retention or modification of prior

structures. There is some evidence that in marsupials the CS may receive venous inputs that have not been reported to exist in adult placentals, but these are probably neither numerous nor of great functional significance. For example, Dom et al. (1970: 492) noted that the dorsal sagittal sinus sends a connection to the CS in *Didelphis* immediately rostral to the hypophysis. This connection occurs as an anomaly in *Homo* and represents a holdover from earlier ontogeny (see Tubbs et al., 2020: ch. 2).

**CONDYLOHYPOGLOSSAL FORAMINA/CANALS.** The hypoglossal nerve represents the morphological union of the ventral roots of as many as four precervical spinal nerves (De Beer, 1937). In *Homo*, this composite origin is reflected in the fact that the roots are collected into two bundles that traverse the dura mater separately, then converge to pass through a (typically) single hypoglossal canal (Warwick and Williams, 1973: 1025). In many therians, however, each bundle may travel in its own bony tube (Wible, 2003). Furthermore, in addition to small arteries, these ports also transmit emissaria that may anastomose with local veins. The end result is an intricate tangle of vessels in the suboccipital region that is not well described for any mammal, including *Homo* (see San Millán Ruíz et al., 2002; Mortazavi et al., 2011; Tubbs et al., 2020: ch. 23), and whose individual members cannot be separately discriminated on the basis of osteological markings. Yet in the literature exoccipital apertures situated immediately next to the condyles are frequently described as “condylar,” while ones situated slightly more rostrally (when present) are named “hypoglossal,” even though there is usually no substantive (i.e., soft tissue) reason for stipulating them in this manner (see Kielan-Jaworowska et al., 1986). To avoid rather than solve the problem, we refer to all such conduits as condylohypoglossal canals or foramina.

Marsupials generally display two (and occasionally more) condylohypoglossal openings on their basicrania; these are differentiated in our text as either rostral or caudal according to their relative positions (see Beck et al. 2022: 98–99,

discussion of char. 92). The caudal canal is often, but not always, the larger of the two because it more frequently accommodates the EVPS or a branch thereof. For this reason, Archer (1976: 223) recommended that it be called the “venous condylar foramen,” but this is unhelpful for the reason given above. When there is only one external foramen, the aperture in question can be referred to as “the” condylohypoglossal canal. A third port, in a markedly rostral position well in advance of any likely position for the brain stem, is sometimes found. It may be assumed to be exclusively vascular and can therefore be identified as an explicitly condylar canal (e.g., *Prothylacynus*, fig. 40H).

CRANIOSPINAL FORAMEN AND VERTEBRAL VEIN (VV). The VV is often neglected in osteological descriptions because in many groups it passes freely into the endocranium along the internal aspect of the exoccipital, leaving no more than a shallow sulcus on the sidewall of the foramen magnum to mark its passage. However, from broader comparative considerations it is clear that the VV is often plexiform, and receives input not only from the SS, which is presumably primitive, but also from the EVPS via the latter’s anastomosis with the caudal condylar emissarium. This anastomosis is the last link in the series of conduits that transmits caudally directed blood from the CS to the CSVS. Its connection with the VV may occur intramurally, during its passage through the exoccipital, before it leaves the skull through the caudal condylohypoglossal canal. For its aperture in the foramen magnum’s sidewall, “craniospinal foramen” is preferred to alternatives like “condyloid foramen,” “vertebral foramen,” or “vertebral vein foramen,” because this term differentiates this port unambiguously from apertures in the caudal cranium and cervical spine (cf. Forasiepi et al., 2019: fig. 26C).

EMISSARY AND EMISSARYLIKE VEINS. The equivalent of multiple safety valves that help to equalize intracranial venous pressure, emissaries are a means for regulating encephalic streamlines (Tubbs et al., 2020). They are by definition transcranial, effecting communication between

endocranial dural sinuses or diploic channels and the extracranial systemic circulation. Emissaries do not occur at random but develop in concert with the formation of the chondro- and osteocranium, appearing at specific places and times during development and thereby influencing the location of many foramina in the definitive skull (Padget, 1956, 1957; Butler, 1957, 1967; Towbin et al., 1999; San Millán Ruíz et al., 2002; Tubbs et al., 2020). Their relative positions are notably consistent across large phylogenetic groupings, which supports the contention that an underlying plan for emissarial differentiation (or, better, co-differentiation with interacting nonvascular tissues) is widely shared among developing therians. Although sometimes described as inconstant, it is more likely that in cases of apparent absence the emissaries are initiated, but simply fail to develop past a certain point. Variability is probably correlated with their development from embryonic plexuses. Emissaries are by definition valveless, but whether this applies to the TCV trunk or its rostral branch has never been clarified. For this reason these vessels are here described as “emissarylike.”

EXTRACRANIAL CONTINUATION OF VENTRAL PETROSAL SINUS (EVPS) AND BASIJUGULAR SULCUS. Although in *Homo* the VPS usually terminates morphologically in the IJV, in many mammals its dominant anastomosis is with the SS (e.g., *Ailuropoda*, Davis, 1964: fig. 23). In still others the VPS does not terminate morphologically within the skull, but instead becomes extracranial by passing through an aperture separate from the one transmitting the IJV and the caudal cranial nerves (e.g., *Sarcophilus*, fig. 28A; *Perameles*, fig. 32A), to anastomose with other veins in the suboccipital region (Aplin, 1990: 98).

In the literature, this continuation of the ventral (= inferior) petrosal sinus is traditionally called by the same name as the parent vessel. This is nomenclaturally inconsistent because the extracranial portion obviously does not qualify as a dural sinus. Although we previously identified this extension as the craniovertebral vein (Forasiepi et al., 2019), in the interest of uniformity we follow

Tubbs et al. (2020: 209) in identifying it as the extracranial continuation of the ventral (= inferior) petrosal sinus. The groove for the EVPS, often very marked on the exterior surface of metatherian exoccipitals, was named the basijugular sulcus by Forasiepi et al. (2019) (e.g., *Didelphis*, fig. 2A; *Notamacropus* fig. 18A; *Thylacinus*, fig. 29A). This usage is retained here. Small sulci emanating from the condylohypoglossal foramina pass into the basijugular sulcus, suggesting involvement of an extensive suboccipital plexus comparable to the anterior condylar confluence of *Homo* (see next entry). Judging from the width of the basijugular sulcus, in many taxa the EVPS may be larger than any other venous vessel in the vicinity, including the IJV (see Forasiepi et al., 2019: fig. 26).

Patterson (1965) incorrectly regarded the foramen for the EVPS in *Didelphis* as an aperture for an artery, calling it the “posterior carotid foramen” (see Wible, 1984; Aplin, 1990; MacPhee and Forasiepi, 2022). Archer (1976) named this aperture the “internal jugular foramen” or “foramen of internal jugular canal,” in part because he regarded the VPS as an intracranial extension of the IJV. As conventionally defined, the true IJV originates at, and leaves the skull through, a separate jugular foramen (e.g., *Perameles*, fig. 32A). See also Wible (1984: 309).

**INTERNAL CAROTID VEIN (ICV) AND BASICRANIAL VENOUS PLEXUS (BVP).** Aplin (1990) suggested “pericarotid vein” as an appropriate name for the ICV, but it is preferable to follow the convention of naming members of the same neurovascular bundle in a similar way (in this case, internal carotid artery, vein, and nerve, which cluster together while passing through the carotid canal; see fig. 1A). In older works (e.g., Gaupp, 1908; Toeplitz, 1920), the ICV is not distinguished nomenclaturally from the cavernous sinus, although from a morphological standpoint it certainly qualifies as a distinct entity. Among other functions, the BVP (= prevertebral venous plexus of Aplin, 1990) drains the dorsal wall of the pharynx. It communicates with a number of local veins, including the ICV,

with which it forms the joint feature here called the ICV/BVP.

Although rarely given attention in the comparative literature, the ICV is consistently mentioned or illustrated in all extant marsupial taxa that have been adequately investigated (*Acrobates* and *Didelphis*: Shindo, 1915; *Perameles*: Cords, 1915; *Didelphis*: Toeplitz, 1920; *Monodelphis*: Maier, 1987; various dasyurids: Archer, 1976; various diprotodontians: Aplin, 1990; *Monodelphis*, *Caluromys*, *Philander*, *Dromiciops*, *Perameles*, *Notamacropus*: this paper). Apart from the present paper, none of these works explicitly notes the composition of the ICV/BVP anastomosis or its route. In our perinatal sample, the plexiform ICV/BVP usually comprises a main branch on the dorsomedial side of the internal carotid artery and smaller branches running ventrally to it. In some taxa the CS and ICV may briefly enclose the internal carotid artery in a collar, but without forming a recognizable arteriovenous rete (e.g., *Notamacropus*, fig. 19A). According to Cironi et al. (2022), the homologous internal carotid venous plexus of *Homo* also forms a venous ring around its artery at the carotid canal entrance.

In a sense the BVP’s route duplicates that of the VPS (fig. 1A, B), but unlike the latter, which travels intradurally along the dorsal surface of the basicranial keel (ossified successor of the chondrocranial central stem), the BVP is consistently extradural (see MacPhee et al., 2021). Before terminating in the IJVS or CSVS, the ICV/BVP and VPS may be in contact via additional emissaria, at least in perinatal specimens (e.g., *Monodelphis*, fig. 11D).

In *Homo* and *Rattus*, the embryonic pituitary vein connects the right and left portions of the CS, passing over the internal carotid arteries as it does so (Padget, 1957; Butler, 1967). This close association implies that in placentals the pituitary vein is the precursor of the ICV plexus, which Cironi et al. (2022) describe as concentrated near the junction of the petrous and cavernous parts of the internal carotid artery. It receives tributaries from the inferior petrosal

sinus, basilar venous plexus, and inferior petro-occipital vein, as well as branches from the veins surrounding the foramen ovale. Few of these connections have been described for marsupials, although it is likely that most exist.

Except for apparent homologs in *Homo* and other primates (Saban, 1963; Cartmill, 1975; Dye et al., 2020), the BVP has rarely been described, although it is large in some well-studied domesticants (e.g., *Equus*; see MacPhee et al., 2021: fig. 6) and is probably present in some form in all mammals. Observations on other placentals support this. Thus Reinhard et al. (1962: 70) note that in *Canis* the “ventral petrosal sinus also gives off a vein which traverses the carotid canal,” a routing that resembles to some degree the course of the ICV in marsupials. Similarly, Davis (1964: 281) notes that in *Ailuropoda* a vessel (?ICV) passes from the CS through the piriform fenestra (= foramen lacerum medium of Davis, 1964) to connect with the pharyngeal plexus—which in Davis’s definition extends from the transverse position of the internal nares to the foramen magnum. It is thus the apparent equivalent of, or includes, the BVP of this paper.

Because it typically communicates with the IJV, the BVP itself is presumably a derivative of embryonic plexuses associated with the anterior cardinal vein. In perinatal (and presumably adult) marsupials the caliber of the ICV at its origin from the CS may be larger than that of the internal carotid artery, but it reduces rapidly once it enters the pharyngeal region (e.g., *Philander*, fig. 7A–C; *Monodelphis*, fig. 11A–C; *Notamacropus*, fig. 19A–C). In marsupials there is no morphological need to separately distinguish the caudal part of the BVP as the craniooccipital vein (as seen in *Equus*; MacPhee et al., 2021).

INTERSTITIAL CANALICULI. Frequently seen in many calvarial and basicranial bones are concentrations of short, thin-walled, densely branching conduits that grade into ordinary diploe. In this paper these channels are named interstitial canaliculi. The featured example in this study is the arrangement of interstitial canaliculi in the TBS, which may intersect the

transverse canals or endocranial floor, or extend into marrow-containing areas in other bones (e.g., *Didelphis*, fig. 4D; cf. accessory lacunae of MacPhee et al. [2021]).

LATERAL HEAD VEIN AND PROOTIC SINUS. These terms, each with several synonyms, have been used interchangeably in the literature and have also been understood in different ways in paleontology and comparative anatomy (see Wible and Hopson, 1995). The primary head vein, which is the principal cephalic vein of the embryonic and early fetal period, drains the entire head, including the orbits, through the primitive maxillary vein and terminates in the anterior cardinal vein (future IJV). Its chief tributaries are the medial head vein (= vena capitis medialis), lateral head vein (= vena capitis lateralis), and their variously named ontogenetic derivatives (Tubbs et al., 2020: ch. 1). The medial head vein becomes in part the cavernous sinus (Padget, 1957) as well as the posttrigeminal vein, which joins the prootic sinus derived from embryonic cerebral veins. The prootic sinus contributes to the transverse dural sinus, dorsal petrosal sinus, and probably the sphenoparietal sinus, and is considered to continue caudally as the lateral head vein (Tubbs et al., 2020: ch. 17). The intracranial caudal end of the lateral head vein, seen in fig. 11F in perinatal *Monodelphis*, is known to persist into adulthood in marsupials but is not usually identified (or is simply overlooked) in placentals (for additional information, see Wible, 2003, 2008).

MESOCRANIAL VENOUS CONFLUENCE AND TRANSVERSE CANAL JUNCTION. These terms are considered together because the first (angiological) structure is partly or wholly housed within the second (osteological) feature. In most marsupials, the antimeric rostral branches (RBVs) of the transverse canal vein are thought to anastomose in the midline to form a mesocranial venous confluence as they pass through the bony transverse canals, as they are known to do in *Didelphis* (Dom et al., 1970; see also *Perameles*, fig. 33A). In the configuration most frequently described in the literature, right and left canals

join or pass into the TBS intramurally (i.e., within the basisphenoid). Caudal branch veins (CBVs) follow a different route and do not form a midline confluence. In taxa in which the RBVs are not present, there is of course no junction of transverse canals.

**POSTGLENOID VENOUS NETWORK (PGLVN).** The temporal dural sinus (= prootic sinus *parte*) drains to the EJV or one of its branches (e.g., deep facial vein, maxillary vein) via the emissarium variously called the v.e. sphenoparietalis, v.e. retroarticularis, or simply the postglenoid vein (van Gelderen, 1924; Butler, 1967; Wible and Hopson, 1995). This drainage pattern is very common in adult therians and easily identified when vessel trackways are well marked (e.g., *Thylacinus*, fig. 30). Dom et al. (1970) mention that in *Didelphis virginiana* a small vessel runs between the petrosal sinuses and the prootic sinus/PGLV. To clarify a related issue, Butler's "posterior pro-otic vein" is the same as the lateral head vein; in his terminology it leaves the skull as the "pro-otic emissary vein" (= v.e. foraminis retroarticularis of Dom et al., 1970).

**PTERYGOID VENOUS PLEXUS (PVP) AND EXTERNAL JUGULAR VEIN (EJV).** The PVP (fig. 1A, B) consists of an extensive network of veins, situated in the infratemporal fossa between the temporalis and pterygoid muscles, that are tributary to the maxillary vein. In *Homo* it receives inputs from the pharyngeal plexus and the sphenopalatine, masseteric, ophthalmic, and deep temporal veins (Warwick and Williams, 1973). In marsupials it also receives branches from ICVs and TCVs (e.g., *Monodelphis*, fig. 11A, B).

The EJV, which receives the maxillary vein, has an extensive territory that includes the face, nasal cavity, tongue, and upper and lower jaws (Padget, 1957). In most mammals the EJVS receives a substantial amount of encephalic blood carried by the PGLVN (Butler, 1967). In marsupials both the PGLVN and TCVs are well developed and serve as major EJV tributaries. Also, the PGLVN is seemingly never diminished or involuted to the extent seen in some placentals; a postglenoid foramen or incisure is nor-

mally present in the adult, often in combination with a large suprimeatal foramen.

The PVP develops from deep facial tributaries of the fetal maxillary vein (Padget, 1957: 117), which in turn drains to the EJV by means of the definitive maxillary vein. Other mammals are probably similar, although given its plexiform nature additional links with other vessels may also be involved.

**SIGMOID SINUS (SS), INTERNAL JUGULAR VEIN (IJV), AND CEREBROSPINAL VENOUS SYSTEM (CSVS).** It is well known that in *Homo sapiens* the caudal dural sinuses and their tributaries are the brain's chief drainage channels, and that almost their entire output is transmitted to the IJV via the SS. However, this is not a frequent pattern; in many therians the CSVS dominates the return of encephalic blood to the vena cava (see Kielan-Jaworowska et al., 1986; Wible and Rougier, 2017). For example, among placentals the IJV is known to be hypoplastic in *Canis* (Evans and Christensen, 1979) and *Equus* (Sisson and Grossman, 1953), and may be functionally absent in the adult. In these cases most of the blood transmitted by the SS is diverted to the CSVS by draining through the foramen magnum or craniospinal foramen to the VVs. Something similar probably applies to extant marsupials in which the IJV is known to be small (e.g., *Didelphis virginiana*, *Monodelphis breviceaudata*, *Sminthopsis murina*; Shindo, 1915; Archer, 1976; Aplin, 1990; Wible, 2003), and justifies the conclusion of Dom et al. (1970) that in marsupials the IJVS is the least important of the dural drainage systems. The CSVS is also important for the regulation of intracranial pressure and venous outflow from the brain (Tobinick and Vega, 2006).

**SULCUS FOR OPHTHALMIC NEUROVASCULAR ARRAY.** In therians the endocranial foramen for the internal carotid artery always opens immediately lateral to the hypophysis (Tandler, 1899: 691), at which point the artery releases the rostral cerebral, middle cerebral, and ophthalmic arteries. In marsupial anatomy it is conventional to call the last the (internal) ophthalmic artery

(Tandler, 1899) or the cranial ramus of the internal carotid artery (du Boulay and Verity, 1973). The former term has been retained for this paper.

Because separate pathways for the ophthalmic artery, veins, and nerve cannot usually be discriminated on endocasts, their joint indicium should be called the “sulcus for the ophthalmic neurovascular array” (e.g., *Didelphis*, fig. 4A; *Thylacinus*, fig. 30A), even though the array’s components follow divergent courses and other structures follow them coaxially (e.g., abducens nerve). Osteologically, the sulcus for the ophthalmic artery is easy to discriminate because it usually presents as a direct rostral continuation of the carotid canal in the middle cranial fossa. There it briefly comes into association with the ophthalmic nerve and veins to form the array. On skulls and endocasts the osteological sulcus can usually be traced into the sphenoorbital fissure.

**TRANSVERSE BASISPHENOID SINUS (TBS).** The TBS, also called the “pterygoid sinus” in the literature, occupies the same anatomical position as the sphenoid sinus of placental osteology, but there are some important differences. The intimate connections between the TBS and TCV in some marsupial species is an indication that the sinus has an important role related to the vascular system that may last throughout ontogeny.

In several of the species investigated for this study, total TBS volume consists of networks of small, intercommunicating interstitial channels rather than a single open space. Because these areas are presumed to contain blood-forming marrow (see Discussion)—at least during fetal and early postnatal life, if not longer—it is reasonable to consider the entire feature, whatever its form, as a morphofunctional unit related to the PCVN. Although a large TBS is common in marsupial basicrania, in many cases its volume may be evident only intracranially, where it forms a prominent eminence between the trackways of the maxillary nerves (e.g., *Caenolestes*, fig. 13A; *Perameles*, fig. 32C).

In extant marsupials the TBS consists of two semidistinct portions, a rostral and a caudal, incompletely separated by the hypophyseal fossa

and its contents (e.g., *Thylacinus*, fig. 30B). Usually, the two portions are connected by lateral extensions on either side of the fossa. In some taxa these extensions are tubelike, showing that the two portions are in maintenance contact, but they can be absent or nearly so (*Didelphis*, fig. 4B).

As an intraosseous structure, the TBS obviously cannot begin to form until the basisphenoid begins to ossify. The expansion of the sphenoid sinus during human ontogeny is usually described as the result of pneumatization (e.g., Zollikofer and Weismann, 2008), and at the histological level the sinus’s development closely resembles the kind of remodeling associated with the expansion of nasal and middle ear “air” spaces (see Anthwal and Thompson, 2016). Whether the TBS develops in marsupials without the formation of nasopharyngeal mucosal “buds,” long thought to initiate the pneumatization process in the nose and ear regions (e.g., Lang, 1983: 150), is not known. In the only quasilongitudinal study of TBS development in marsupials, Aplin (1990: ch. 4) emphasized that the sinus is not recognizable in koalas and wombats until very late stages, which agrees with observations in this paper.

Similar pneumatic volumes may occur in adjacent basicranial bones, including those making up the rest of the keel, and presumably have a similar function in young stages. These may or may not communicate with the TBS following ossification of the basicranial synchondroses and progressive pneumatization within the keel. (Synchondrosial ossification is delayed in marsupials compared to placentals [Rager et al., 2014] and is often incomplete even in animals of advanced chronological age.) The nature of intraspecific variation remains largely unknown.

**TRANSVERSE CANAL, VEIN (TCV), AND FORAMEN (TCF).** As these features are obviously related, it is useful to consider them together. The course and connections of the rostral and caudal branches of the TCV (RCV, CBV) are sufficiently explored in the main text. In marsupials the TCF perforates the basisphenoid (or basisphenoid-alisphenoid boundary) in the ventral

part of the infratemporal fossa or the immediately adjacent pterygoid fossa, usually lateral or slightly rostralateral to the foramen ovale (Sánchez-Villagra and Wible, 2002). In this position the TCF might sometimes be confused with the alisphenoid canal for the maxillary artery, and conversely. The difference is that the alisphenoid canal is more superficial and oriented rostrocaudally, because the artery passes into or across the sphenoorbital fissure, and not transversely into the basisphenoid.

The TCF is exclusively venous (i.e., it is never simultaneously an arterial port) and is typically a significant aperture in most marsupials, its diameter often matching or even exceeding that of the carotid foramen (e.g., *Perameles*, fig. 32A). In some individuals or taxa the TCF may be relatively small or even absent on one or both sides. However, the actual prevalence of absence as an individual variation in species that normally exhibit the TCF is uncertain. Beck et al. (2022) take up this problem in relation to their chars. 50 and 51, but it is clear that more work is needed, especially when it comes to determining homologies among putative TCVs that are said to issue from several different ports (TCF, piriform fenestra, anterior pterygoid foramen, carotid canal). Also seen in extant marsupials as well as sparassodontans is multiplication of TCFs (and therefore TCVs). Double and even triple TCFs may be characteristic of some taxa (see Aplin, 1990; Sánchez-Villagra and Wible, 2002; *Notamacropus*, fig. 18B; *Trichosurus*, fig. 21E). Multiplication of effluents implies origin from embryonic plexuses, which probably also accounts for their intercommunication in known cases.

That right and left RBTCs and their veins actually meet and join across the midline has been assumed since the interconnectedness of the TCFs was first investigated using hair probes (Wortman, 1901–1903; Gregory, 1910; see Sánchez-Villagra and Wible, 2002). However, confusion has reigned regarding the reasons that transverse canals seem to be continuous in some taxa but not in others. One reason is that, in

some taxa, RBVs are simply absent, and therefore canals never form. CBVs are different, in that they communicate with the CS/ICVs rather than each other, and there is no bony continuity between TCFs. Even when bony RBTC-bearing transverse canals are present, it may not be possible to force a probe all the way through them because of their orientation with respect to the TBS (e.g., *Caenolestes*, fig. 13D; *Trichosurus*, fig. 21D). Doubtful cases can be easily resolved with CT scanning.

Citing Padget (1957), Dom et al. (1970: 496) stated that the “anastomotic channel” [i.e., TCV] between the CS and PVP “appears similar to the primitive maxillary vein which is present in the development of the human embryo.” A much more likely candidate for a precursor to the TCV is the dorsal pharyngeal vein, seen in stage 7 in human cranial development (Padget, 1957: 117). According to Padget, in later development the dorsal pharyngeal vein becomes “truly emissarial” by anastomosing with the PVP as the (primary) sphenoidal emissary vein or emissary vein of Vesalius (= ?peritrigeminal emissary vein of Aplin [1990: 95]). Although this suggests possible homology (see Homologies of Mesocranial Distributaries), the sphenoidal emissarium usually passes through the foramen ovale. Padget (1957) noted that another vein, the allegedly more variable accessory sphenoidal emissary vein, may have its own aperture (see James et al., 1980). For our purposes it is sufficient to note that the homology question is far from settled, and that the accessory sphenoidal foramen (confusingly, also called the vesalian foramen by some authors) is another possible homological candidate for the TCF in nonmarsupials.

Regarding other placentals, according to Butler (1967: fig. 4) the CS is connected to the maxillary vein (and thus the EJV) by means of an emissarium in embryonic *Rattus*. Whether the TCV has rostral and caudal branches in placentals has not been investigated.

VENOUS PATHWAY COMPETITION AND DOMINANCE. From an ontogenetic perspective, the development of a dominant venous pathway in

a given vascular system is mainly the result of hemodynamic factors enabling the persistence and progressive enlargement of some channels over others (Tubbs et al., 2020: 127). Our brief observations on vessel size in single stages of perinatal specimens are obviously based on nonfinal conditions. This limitation is important to recognize, because cephalic veins achieve their adult size and even aspects of their final configuration much later than the arteries do (Padget, 1957: 82). Given the altricial state in which marsupials are born, it cannot be assumed that venous development was near completion in young specimens like those available for this study.

With particular regard to structures of interest here, Padget (1957: 135) argued that in the late fetal human the CS/VPS connection offered a more direct route for venous return from the orbits to the IJV than did the more laterally positioned prootic sinus of earlier ontogeny, and for that reason the former becomes dominant in *Homo*. She contrasted this result with conditions in most nonhominoid primates, in which the emissarium-enabled anastomosis between the prootic sinus and the EJV persists throughout ontogeny. This arrangement was said to favor PGLVN enlargement and therefore increased perfusion along that route rather than the VPS.

However, matters cannot be that simple, for in many therians the VPS remains important even though there is a large and functional PGLVN. (See Wible and Hopson, 1995, for discussion of marsupial/placental differences in embryonic origin of emissaria linking the PGLVN to the systemic circuit.) The relevance of these points for the present topic is that, if distance to a primary collector were the only factor determining success in interpathway competition, then a well-developed pericarotid network ought to be much more common than

it is in placentals, as this route is the most direct (shortest) of all for returning orbital blood via the CS to the systemic circulation.

VENTRAL PETROSAL SINUS (VPS). Although not considered morphologically part of the PCVN, the VPS is functionally related to it via connections with the ICV/BVP, IJV, and CSVS. As shown in the reconstructions, the osseous trackway for the VPS always emerges from the caudal margin of the hypophyseal fossa (e.g., *Caenolestes*, fig. 13D). It then passes along or through the bones of the basicranial keel or within the interface between the latter and the petrosal bone (called the basicapsular fenestra or petrobasioccipital suture, depending on the degree to which the gap undergoes closure). The VPS tends to increase in size along its pathway in humans, and presumably in other mammals, because it receives blood from the internal auditory vein as well as branches draining the medulla, pons, and cerebellum (Tubbs et al., 2020: 111).

The ontogeny of the VPS in *Homo* is complicated (Padget, 1957: 112; Tubbs et al., 2020: ch. 11) and is likely to be so in other taxa (e.g., *Rattus*, Butler, 1967). We infer that during marsupial ontogeny the EVPS pirates the emissarium of the caudal condylohyphoglossal canal, which in effect becomes a permanent anastomotic link between the EVPS and the VV.

For completeness it should be noted that the dorsal petrosal sinus is variably present (or is not always recognizable) in *Didelphis* (see Shindo, 1915, vs. Dom et al., 1970). Padget (1957: 123) noted that this sinus's connection with the cavernous sinus is produced rather late in ontogeny, and that it is not universally present as a significant branch in adult mammals (for other examples of claimed absence or reduction of this sinus, see Davis, 1964; Lake et al., 1990; MacPhee et al., 2021).

Downloadable files of reconstructions of the following specimens, in 3D PDF and .mpg formats, are available online (<https://doi.org/10.5531/sd.sp.58>): *Caenolestes* sp. IANIGLA uncataloged (fig. 13); *Dromiciops gliroides* MACN Ma- 23607 (fig. 15); *Thylacinus cynocephalus* NMB c.2526 (fig. 29); *Sipalocyon gracilis* AMNH VP-9254 (fig. 38); and *Prothylacynus patagonicus* YPM VPPU-15700 (fig. 40).





**SCIENTIFIC PUBLICATIONS OF THE AMERICAN MUSEUM OF NATURAL HISTORY**

*AMERICAN MUSEUM NOVITATES*

*BULLETIN OF THE AMERICAN MUSEUM OF NATURAL HISTORY*

*ANTHROPOLOGICAL PAPERS OF THE AMERICAN MUSEUM OF NATURAL HISTORY*

PUBLICATIONS COMMITTEE

ROBERT S. VOSS, CHAIR

BOARD OF EDITORS

JIN MENG, PALEONTOLOGY

LORENZO PRENDINI, INVERTEBRATE ZOOLOGY

ROBERT S. VOSS, VERTEBRATE ZOOLOGY

PETER M. WHITELEY, ANTHROPOLOGY

MANAGING EDITOR

MARY KNIGHT

Submission procedures can be found at <http://research.amnh.org/scipubs>

All issues of *Novitates* and *Bulletin* are available on the web (<https://digitallibrary.amnh.org/handle/2246/5>). Order printed copies on the web from:  
<https://shop.amnh.org/books/scientific-publications.html>

or via standard mail from:

American Museum of Natural History—Scientific Publications  
Central Park West at 79th Street  
New York, NY 10024

Ⓢ This paper meets the requirements of ANSI/NISO Z39.48-1992 (permanence of paper).

*ON THE COVER: RECONSTRUCTED PERICAROTID VENOUS NETWORK AND RELATED VASCULATURE IN THYLACINUS CYNOCEPHALUS.*